MORPHOSTRUCTURAL EVOLUTION OF ACTIVE MARGIN BASINS: THE EXAMPLE OF THE HAWKE BAY FOREARC BASIN, NEW ZEALAND

A thesis submitted in fulfilment of
the requirements for the degree of

Doctor of Philosophy in Geology

at the University of

Canterbury by

FABIEN PAQUET

University of Canterbury
2007

-

Ph.D. thesis realized in co-tutelle with the
University of Rennes 1, Rennes, France

N° ordre : 3563

THESE

présentée

DEVANT L'UNIVERSITE DE RENNES 1

pour obtenir

le grade de **DOCTEUR DE L'UNIVERSITE DE RENNES 1**

Mention Sciences de la Terre

PAR

Fabien PAQUET

Equipe d'accueil: Géosciences Rennes

Ecole Doctorale Sciences de la Matière

Composante universitaire: UFR Structure et Propriétés de la Matière

Morphostructural evolution of active subduction margin basins: The example of the Hawke Bay forearc basin, New Zealand.

Thèse réalisée en co-tutelle avec l'Université de Canterbury, Christchurch, Nouvelle-Zélande.

Soutenue le 9 novembre 2007 devant la commission d'examen composée de

Directeurs de thèse	Jean-Noël Proust	Géosciences Rennes - CNRS
	Jarg Pettinga	University of Canterbury
Rapporteurs	Jean-Yves Collot	IRD Géosciences Azur
	Michel Lopez	Université de Montpellier 2
Examinateurs	François Guillocheau	Université Rennes 1
	Philip Barnes	NIWA

Avant Propos :

Ce travail a été réalisé dans le cadre d'une thèse en cotutelle entre les universités de Rennes 1 (Rennes, France) et de Canterbury (Christchurch, New Zealand). Il a été encadré par Jean-Noël Proust (Géosciences Rennes), Jarg Pettinga (University of Canterbury) et co-encadré par Philip Barnes (NIWA, New Zealand).

Les financements de ce projet sont multiples : Allocation de recherche ministérielle ; CNRS-INSU Intérieur de la Terre ; PICS France / Nouvelle-Zélande ; MAE – Ambassade de France (NZ) ; CNRS-INSU Mission Marion-Dufresne MD152 ; Géosciences Rennes – UMR CNRS 6118 ; Université de Rennes 1 (dont bourse d'aide à la mobilité) ; University of Canterbury – 'Active tectonic and Earthquake Hazards Research Group' ; and NIWA.

La cotutelle a permis de créer des collaborations avec différents intervenants, un échange de connaissance et un accès facilité aux données et aux moyens techniques (logistique et personnels scientifiques et techniques du NIWA pour l'acquisition, le traitement et la mise à disposition des données ; et University of Canterbury pour logistique de la mission de terrain).

L'essentiel du travail présenté dans ce mémoire est le fruit d'un investissement personnel : interprétations stratigraphiques du jeu de données sismiques ; élaboration des cartes d'isopaques et calcul des volumes et masses préservées ; élaboration des plans de positionnement des lignes TAN0412 et GSR 05103 et des carottes MD152 ; participation aux campagnes à la mer TAN0313, GSR 05103 et MD152 ; cartographie et levés de coupes dans le Kidnappers Group et la vallée de la Makaroro ; analyse de Modèles Numériques de Terrain ; préparation d'échantillons pour analyses micropaléontologiques et isotopiques. Certains aspects résultent de contributions, notamment en ce qui concerne la cartographie des structures en mer par Philip Barnes et la pleine collaboration de Nicola Litchfield (IGNS, New Zealand) pour le partage de ses résultats et avis concernant les terrasses fluviatiles. Martin P. Crundwell et Alan G. Beu (IGNS - Institute of Geological and Nuclear Science) ont également participé en effectuant les analyses micro-paléontologiques de plusieurs échantillons. Bruce Hayward (Geomarine Research), Phil A. R. Shane (University of Auckland, NZ) and Brent Alloway (IGNS) sont intervenus dans l'identification des foraminifères et des tephras des carottes Marion-Dufresne MD152, et Gilles Ruffet (Géosciences Rennes) a pris en charge les analyses $^{40}Ar/^{39}Ar$ des échantillons prélevés sur le terrain.

Remerciements – Acknowledgements :

Ce travail, mené dans le cadre d'une co-tutelle entre l'Université de Rennes 1 – Géosciences Rennes, l'Université de Canterbury – Department of Geological Sciences et d'une étroite collaboration avec le NIWA, fut l'occasion de rencontrer un grand nombre de personnes, qui ont contribué, de près ou de loin, à sa réalisation.

Je tiens tout d'abord à te remercier, Jean-Noël, pour m'avoir proposé ce projet alors que je me débattais, avec plaisir, dans un enchevêtrement de filons islandais. Il m'aura fallu assez peu de temps pour me remettre dans la « boue tiède » et pour y prendre goût. Merci donc, pour ce sujet que tu as subtilement dirigé, en me laissant libre d'explorer telle ou telle voie et en m'aiguillant de temps à autre (parfois même sans que je m'en rende compte ?). J'ai vraiment apprécié travailler en ta compagnie. Merci enfin pour avoir développé cette co-tutelle avec Jarg et permis la collaboration avec Phil et le NIWA.

I would like to thank you, Jarg, for having accepted the co-tutelle of this Ph.D. thesis and welcomed me at the University of Canterbury, for the help and advises on the field and during the several discussions we had, and also for the technical and financial support. But, beyond these aspects, I have to say that I met a great person, friendly, available. Finally, thank you and Margaret for the very pleasant stays I have spent at your place.

Thank you Phil for the time and efforts you spent on this project. You were of great support for the planning of the multiple surveys, for providing access to a large set of seismic data and for the help in seismic interpretation. It was a real pleasure to work with you and I have appreciated the few constructive meeting we had all together in New Zealand, France and Austria.

Je tiens à remercier Jean-Yves Collot (IRD - Géosciences Azur) et Michel Lopez (Université de Montpellier 2 - Géosciences Montpellier) pour avoir accepté de juger ce travail. Merci également à François Guillocheau pour avoir examiné le manuscrit et présidé le jury de soutenance.

In New Zealand, I would like to thanks people at NIWA for the great help they provide all along this work, especially Geoffroy Lamarhe, Miles and Soaz Dunkin, Mike Stevens, Lionel Carter, Lisa Northcote, Stéphane Popinet and Vanessa Sherlock, John Mitchell, Richard Garlick, Steve Wilcox, Helen Neill and of course, Cathy Joanne, Arne Pallentin, Sébastien Delaux and Cédric Simon. At the University of Canterbury, I would like to thank Jim Cole, Steve Weaver Kate Bodger and David Shelley as well as the department and student administration staff. I would like to thank Phil Shane from the University of Auckland for

tephra identification and discussion, at IGNS-Lower Hutt: Nicola Litchfield for a nice trip along the Hawke's Bay rivers and terraces, Martin Crundwell and Alan Beu for fossil indetification. Brent Alloway and Bruce Hayward provided identification of tephras and foraminifers on board Marion Dufresne. Finally, I would like to thank Simon Alderdice for his friendship – "profite bien!" – as well as his brothers Matthew and James & Caroline; Geoff and Di from the Tikokino Hotel, Craig and Anne Preston for welcoming me at their place, Tasha, Heath and Trina Locke for spending good time at Napier, the people of the DOC at Napier and Onga Onga, Angus Gordon (Clifton Station), Alec Tuanui (Kidnappers Station) for allowing access to their land and Bryce Wright for the access to the Gwavas Forest.

En France, un merci général aux personnes du laboratoire de Géosciences Rennes - CAREN et à l'équipe bassin sédimentaire, où j'ai passé pas mal de ces dernières bonnes années. Parmi elles, Olivier, Erwan et Frédérique pour l'année de DEA et un petit tour sur une autre jolie Île ; Stéphane B et Alain C, qui m'auront aider à déchiffrer et comprendre les paysages néo-zélandais, Delphine R, Cécile R, Pete C, François G, Jean B, Jean VDD, Gilles R, Yves Q, Annick B et Yann L pour leur aide. Mes remerciements iront tout droit à la troupe de thésards, post-docs, ATER et autres M2 qui auront égayé le quotidien, l'hebdomadaire et le mensuel pendant toutes ces années : à Elise, pour m'avoir aidé et accompagné dans les ultimes instants, Nico, Ben, Flo, Chrys, Nol, Erwan, Thierry, Yul, Djé, Xav, Oliv, Gosia, Fabien, Caro, Jérôme, Cécile A, Julie P, Nat, Aude, Nuno, Seb, Cécile, Stéphane, Rico, Seb « Mr Rohais », Lolo, Gégé, Cédric, Pipo, Nico et Carine, Laure, Adrien, Manu, Mathieu, Yannick, Guilhem, Céline, Camille, Morgan, Martine, Christelle, Romain, Vincent G, François, Catherine, Antoine, Olivier G, Ju, Charles, Pat et Erwan (merci pour la cheville), Castor, César, Blaise, Vincent P, Marie, Céline, Katia (j'en oublie)… mais aussi les autres collègues, les Gobios et les amis d'ici et d'ailleurs qui auront comptés pendant cette thèse : Julie et François (merci pour les vacances), Elsa, Marion, Julie J, Alex, Mathieu… (j'en oublie encore)… et bien évidemment à ma famille pour son soutien indéfectible.

Merci à tous !

Résumé :

La croissance des reliefs et les flux sédimentaires associés à la dynamique des marges actives en subduction sont des processus encore mal connus. Les archives géologiques sont souvent difficiles d'accès ou bien simplement mal préservées à cause de déformations importantes. Le bassin avant arc d'Hawke Bay de la marge Hikurangi en Nouvelle-Zélande constitue un objet d'étude privilégié. En effet, il est peu déformé, partiellement émergé et actif pendant le Pléistocène, période au cours de laquelle l'âge des séries sédimentaires et certains facteurs comme le climat et l'eustatisme sont bien contraints. Une étude pluridisciplinaire, intégrant l'interprétation de données sismiques marines et terrestres, l'analyse de puits, de carottes et de coupes de terrain et l'observation des bassins versants a permis d'établir l'architecture stratigraphique à très haute résolution sur le dernier 1.1 Ma de ce domaine avant arc. Cette stratigraphie montre une organisation en un empilement complexe de 11 séquences de dépôt d'origine climato-eustatique (20, 40 et 100 ka) préservées dans des sous bassins contrôlés par les structures chevauchantes actives. Ces séquences sont caractérisées par des changements paléogéographiques profonds qui évoluent entre deux états extrêmes à chaque maximum glaciaire et optimum interglaciaire. Ainsi, le domaine avant arc d'Hawke Bay montre une segmentation en sous bassins isolés par des rides tectoniques émergeantes pendant les bas niveaux marins et submergées lors des hauts niveaux marins. Aux échelles de temps supérieures à 100 ka, ces structures actives sont à l'origine, dans chacun des bassins, d'une migration progressive vers l'arc des dépocentres des séquences sous l'influence combinée de la tectonique et la charge sédimentaire. Le calcul des volumes de sédiments préservés dans chacune des séquences de dépôt, depuis les sources les plus en amont jusqu'au pied des systèmes sédimentaires les plus profonds à l'aval, permet d'estimer des flux sédimentaires qui ont transité à travers le domaine avant arc au cours de Pléistocène supérieur. Ces flux varient de ~3 à ~6 Mt.a-1. Les variations de flux à long terme (100 ka à 1 Ma) correspondent à des changements de configuration tectonique (distribution de la déformation sur les structures) du domaine avant arc et traduisent la capacité des bassins à stocker des sédiments. Les variations enregistrées à plus court terme (<100 ka) sont corrélées aux importants changements climatiques Pléistocènes, qui modifient les taux d'érosion dans le bassin versant et par conséquent, le flux sédimentaire. Cette observation montre la forte sensibilité et réactivité du domaine amont aux variations environnementales, également illustrée par le doublement des valeurs de flux sédimentaires depuis l'arrivée des européens sur le territoire néo-zélandais au 18ème siècle et le déboisement intensif qui lui a succédé.

Abstract:

Topography growth and sediment fluxes in active subduction margin settings are poorly understood. Geological record is often scarce or hardly accessible as a result of intensive deformation. The Hawke Bay forearc basin of the Hikurangi margin in New Zealand is well suited for studying morphstructural evolution. It is well preserved, partly emerged and affected by active tectonic deformation during Pleistocene stage for which we have well dated series and well-known climate and eustasy.

The multidisciplinary approach, integrating offshore and onshore seismic interpretations, well and core data, geological mapping and sedimentological sections, results in the establishment of a detailed stratigraphic scheme for the last 1.1 Ma forearc basin fill. The stratigraphy shows a complex stack of 11 eustasy-driven depositional sequences (20, 40 and 100 ka periodicity). These sequences are preserved in sub-basins that are bounded by active thrust structures. Each sequence is characterized by important changes of the paleoenvironment that evolves between the two extremes of the glacial maximum and the interglacial optimum. Thus, the Hawke Bay forearc domain shows segmentation in sub-basins separated by tectonic ridges during sea level lows that become submerged during sea level highs.

Over 100 ka timescale, deformation along active structures together with isostasy are responsible of a progressive migration of sequence depocenters towards the arc within the sub-basins.

Calculation of sediment volumes preserved for each of the 11 sequences allows the estimation of the sediment fluxes that transit throughout the forearc domain during the last 1.1 Ma. Fluxes vary from c. 3 to c. 6 $Mt.a^{-1}$. These long-term variations (100 ka to 1 Ma timescale ranges) are attributed to changes in the forearc domain tectonic configuration (strain rates and active structure distribution). They reflect the ability of sub-basin to retain sediments. Short-term variations of fluxes (<100 ka) observed within the last 150 ka are correlated to drastic Pleistocene climate changes that modified erosion rates in the drainage area. This implies a high sensitiveness and reactivity of the upstream area to environmental changes in terms of erosion and sediment transport. Such behaviour of the drainage basin is also illustrated by the important increase of sediment fluxes since the European settlement during the 18^{th} century and the following deforestation.

TABLE DES MATIERES – TABLE OF CONTENT :

Introduction :

Scientific question - goals - means and site – memoir organization.

-

Problématique - objectifs - méthode et site - organisation du manuscrit.

INTRODUCTION

Scientific question:

The Earth surface or relief is shaped by tectonic climatic and hydrological processes over its both submerged and immerged parts. At the interface between lithosphere, atmosphere and hydrosphere, the Earth surface and its evolution witnesses the evolution of these three domains and their interactions - the geodynamic.

Present day relief and its short-terme evolution (10^0 to 10^2 years) are accessible and can be accurately quantified using *in situ* methodology. On the contrary, long-term evolution of the relief (10^3 to 10^8 years) is more difficult to describe and quantify because of its poor preservation due to erosion processes. This is even more problematic within active tectonic contexts (orogens) where topography gowth (mountain ranges) goes with intense erosion that rapidly erases paléotopographies.

One way used to investigate paleoreliefs and their evoltion is the estimation of sédiment fluxes. Actually, sediment fluxes represent the amount of sediment (volume or mass) that transits from areas dominated by erosion (*e.g.* mountain ranges) to areas dominated by sedimentation (*e.g.* basins). This way, considering the volumes of sediments deposited in basins by time-intervals as an equivalent of eroded rock volumes in mountains, it is possible to estimate erosion rates of the source areas. Sediment fluxe study is therefore a mean to evaluate relief dynamic and consequently geodynamic.

Active tectonic areas such as active subduction margins, collisions and rift escarpments are well suited for studying relief evolution because growth and wear of topographies are intensified by geodynamic processes. This generally resluts in high sediment fluxes and consequently, better recording and reading of tectonic and climatic processes in sedimentary archives.

Nevertheless, several limitations exist about the signification of results obtained from deposited volume incremental quantification in areas of convergence and shortening. Sedimentary record is often altered by deformation, erosion, recycling and losses. The complex three-dimensional geometry of the basin fill and the lack of accuracy in the chronostratigraphic schemes induce additional bias that limit the representativeness of sediment flux values in terms of relief dynamics. It results a lack of reliable data on sediment fluxes for the 100 ka to 1 Ma timescale range that limitates the understanding the impact of geodynamic processes relief evolution in active margin context.

Goals:

The present work aims to (i) describe and quantify the morphostructural evolution of a drainage basin/sedimentary basin system, (2) to estimate sediment fluxes by calculating preserved sediment volumes and (3) to discuss spatial and temporal variations of this fluxes for the 10^4 to 10^6 timescale range, within a tectonically active domain. The timing of control processes such as tectonic climat, hydrology and lithology need to be well constrained. It is also proposed to discuss the signification of sediment fluxes and their variations within an active margin setting in order to understand the impact of each of control parameters at different timescales.

Means and study site:

The study of a drainage basin/sedimentary basin system requires an integrated approach coupling stratigraphic and geomorphologic analyses. These analyses should provide a detailed knowledge of the basin fill including the stratigraphy with the depositional sequences and their three-dimensional geometry, the sedimentary facies and the depositional environment determination and a reliable chonostratigraphic scheme. Onshore, the geomorphologic analysis concentrates on paleotopography remnants in order to reconstruct the relief and its evolution. In addition, a structural analysis is required to establish the style, the timing of activity and rates of displacement for each major structure. The detailed knowledge of both contemporaneous climate and eustasy variations are essential for constraining the geodynamic setting prior to any discussion on morphostructural evolution, sediment fluxes and control parameters.

The study site selected for this study is the Hawke Bay forearc domain on the Hikurangi active subduction margin, along the east coast of north Island, in New Zealand. The Hawke Bay forearc basin presents many advantages to handle such work: its location inside a tectonically active area where building mountain ranges are intensively eroded and where products of this erosion are deposited in structurally controlled basins. Due to its topography, the basin is both submerged and emerged. Basin fill is eventually accessible along coastal cliff outcrops and can provide useful information for the detailed stratigraphic study. In addition, several geological and geophysical studies provide a large amount of useful data. Structurally controlled sub-marine ridges located on the outer limit of the forearc limit sediment losses out of the study site. Finally, the period considered for this work covers approximately the last one million years, from the early Mid Pleistocene Transition (MPT) to present day. Besides its duration that cover the suitable timescale ranges, this period presents several advantages

including the best possible controls on climate ad eustasy changes and a relatively well preserved sedimentary record.

Memoir organization:

The manuscript is organize in five main chapters. The first one proposes a state of art on sediment fluxes and on ocean-continent subduction zones. The second chapter briefly presents the Hikurangi subduction margin of New Zealand. The third chapter describes the scientific approach used in this study, he geological and regional settings of the Hawke Bay forearc domain and finally presents the data set. The forth chapter presents, in an article format, the main results obtained from the study of the last 100 ka-type depositional sequence study ad their implication in terms of paleogeographic and sediment flux variations (10 ka timescale) in respect to climate, eustasy and tectonic settings. The fifth chapter focused on the interpretation of the stacking pattern of 100 ka-type depositional sequences for the last 1 Ma and proposes an interpretation for the morphostructural evolution of the basin and for the sediment flux variations for longer timescale (100 ka). The last part includes the conclusion of this study of the Hawke Bay forearc domain with a synthesis of the results obtained on the stratigraphic architecture, the morphostructural evolution and the sediment fluxes for average and long timescales (100 ka and 1 Ma). It is the opportunity to discuss the influence of control parameters from a regional and a global point of view.

INTRODUCTION

La problématique :

Le relief de la Terre, qu'il soit émergé ou immergé, est une surface dont l'état est principalement fonction des processus tectoniques, climatiques et hydrologiques. En tant qu'interface entre la lithosphère, l'atmosphère et l'hydrosphère, son évolution témoigne de l'évolution de ces trois domaines, de leurs interactions et donc de la géodynamique. Si l'état actuel du relief et son évolution sur le court terme (de 10^0 à 10^2 ans) sont accessibles et quantifiables avec précision, le relief passé et son évolution sur le long terme (de 10^3 à 10^8 ans) sont plus difficiles à décrire et quantifier à cause du problème de préservation lié à l'érosion. Ceci est encore plus problématique dans les zones tectoniquement actives (orogènes), où la croissance de la topographie (chaînes de montagne) générée par la déformation est accompagnée d'une intense érosion qui efface rapidement les traces des reliefs passés. Une des voies d'investigation utilisée pour approcher les états passés des reliefs et leur évolution est la mesure des flux sédimentaires anciens. En effet, le flux sédimentaire représente la quantité de sédiment (volume ou masse) transitant au sein d'un système entre des zones en érosion (sources) et des zones en dépôt (bassin). Ainsi, en considérant, par incrément de temps, les volumes déposés dans les bassins comme représentatifs des volumes érodés dans les zones sources, il est possible d'estimer les taux d'érosion des reliefs et donc leur évolution. L'étude des flux sédimentaires passés est donc un moyen d'approcher la dynamique des reliefs et par conséquent, de la géodynamique.

Les zones tectoniquement actives comme les marges en subduction, les collisions et les épaulements de rift, sont des régions privilégiées pour l'étude des reliefs car la croissance et la dégradation des topographies y sont exacerbées par la géodynamique. Ceci a pour conséquence l'augmentation des flux sédimentaires vers les bassins et corrélativement, d'améliorer l'enregistrement et la lecture des processus tectoniques et climatiques dans les archives sédimentaires.

De nombreuses limites existent néanmoins quant à la signification des résultats de quantifications de volumes déposés par incrément de temps, en particulier dans les zones de convergences, où les archives sédimentaires sont souvent rapidement altérées par la déformation, l'érosion, le recyclage et l'exportation. La géométrie tridimensionnelle du bassin, souvent rendue plus complexe du fait de la déformation, ainsi que le manque de précision sur la chronostratigraphie, constituent des biais supplémentaires, pour le calcul de flux sédimentaires représentatifs en terme de dynamique des reliefs et de géodynamique. Il en

résulte un manque de données fiables sur les valeurs de flux sédimentaire pour des intervalles de temps de la centaine de milliers au million d'années, qui permettrait de déterminer la part de chacun des processus géodynamiques dans le contrôle de l'évolution des reliefs dans les marges actives notamment.

Les objectifs :

La présent travail vise, par une étude approfondie d'un système bassin versant / bassin sédimentaire, à décrire de façon qualitative et quantitative son évolution morphostructurale, à quantifier les flux sédimentaires à partir des bilans volumétriques des sédiments préservés et discuter leurs variations spatio-temporelles aux échelles de temps variant de 10^4 à 10^6 ans, au sein d'un domaine tectoniquement actif pour lequel le calendrier des processus de contrôle (tectonique, climat, hydrologie, lithologie…) seront contraints. Il est aussi envisagé de discuter la signification des flux et de leur variations dans un bassin de marge active soumis à des variations environnementales importantes. afin de comprendre l'impact de chacun des processus invoqués pour son contrôle à différentes échelles de temps.

La méthode et le site retenu :

L'étude d'un système bassin versant / bassin sédimentaire requiert une approche pluridisciplinaire mêlant l'analyse du remplissage sédimentaire des zones en dépôt et une analyse de la géomorphologique des zones en érosion. L'objectif de pouvoir fournir des valeurs de flux sédimentaires aux échelles de temps considérées nécessite une connaissance approfondie du remplissage du bassin incluant la stratigraphie, les séquences de dépôts et leur géométrie 3D, la reconstitution des environnements de dépôt et un calage en âge fiable. L'analyse géomorphologique se base essentiellement sur les rémanents des paléotopographies permettant des reconstitutions du relief passé révélant ainsi sa dynamique. En parallèle, une analyse structurale avec l'établissement d'un calendrier d'activité des structures incluant les taux de déformation ainsi qu'une connaissance détaillée des variations climatiques et eustatiques contemporaines du remplissage sont essentielles pour contraindre le cadre géodynamique qui servira de base de réflexion pour discuter de l'évolution des flux sédimentaires et de leurs paramètres de contrôle.

Le site retenu pour cette étude est le domaine avant-arc d'Hawke Bay sur la marge active de la subduction Hikurangi, sur la côte est de l'Île Nord de Nouvelle-Zélande. Le bassin avant-arc d'Hawke Bay présente en effet de nombreux avantages pour entreprendre ce travail. Sa localisation tout d'abord, au sein d'un contexte tectoniquement très actif

responsable de la croissance de chaînes de montagne où une intense érosion s'opère et de la formation de bassins sédimentaires où les produits de l'érosion se déposent. Une particularité de ce bassin est d'être à la fois immergé et émergé, ce qui permet l'existence d'affleurements directement accessibles et fournissant des informations nécessaires au développement de la stratigraphie détaillée. De plus, le domaine avant arc d'Hawke Bay a été l'objet de nombreuses études qui apportent de nombreuses précisions sur son évolution et présente une grande densité de données géologiques et géophysiques utiles à ce travail. La présence de rides sous marines contrôlées par les structures, en bordure du bassin, limite les fuites de matériel sédimentaire hors de la zone d'étude. Enfin, la période d'investigation retenue pour cette étude couvre approximativement le dernier million d'années, de la transition médio Pléistocène à l'actuel. Les avantages de cette période outre sa durée, qui permet de couvrir les échelles de temps désirées, sont la bonne connaissance des variations climatiques et eustatiques et le fait que les archives sédimentaires n'aient pas été profondément altérées par la déformation.

Organisation du manuscrit :

Le manuscrit s'articule en cinq chapitres principaux. Le premier propose un état des connaissances sur les flux sédimentaires d'une part et sur les subductions océan-continent d'autre part. Le second chapitre présente rapidement la subduction Hikurangi de Nouvelle-Zélande. Le troisième chapitre présente la démarche scientifique utilisée dans ce travail, un état des connaissances succint sur Hawke Bay et le jeu de données disponibles utilisé pour mener à bien cette étude. Le quatrième chapitre présente, sous la forme d'un article, les résultats obtenus par l'étude détaillée de la dernière séquence de dépôt élémentaire à 100 ka et les implications en terme d'évolution paléogéographique et de variation du flux sédimentaire en fonction des conditions climatiques, eustatiques et tectoniques. Le cinqième chapitre est focalisé sur l'interprétation de l'empilement des séquences de dépôt à 100 ka au cours du dernier million d'années propose une interprétation de l'évolution morphostructurale du bassin et des variations de flux sur de plus grands incréments de temps (100 ka). Le dernier volet conclue cette étude en synthètisant les résultats obtenus à partir de cette étude du bassin d'Hawke Bay sur le moyen et le long terme (100 ka et 1 Ma) selon trois axes, l'architecture sédimentaire, l'évolution morphostructurale et les variations des flux sédimentaires, en s'attachant plus particulièrement à discuter les influences des paramètres de contrôle au différentes échelles de temps. Ces discussions sont orientées d'un point de vue régionale puis globale.

Chapitre 1 :

L’érosion et les flux sédimentaires / Les subductions océan - continent.

Dès lors que l'on s'intéresse à caractériser l'évolution des reliefs terrestres, le flux sédimentaire revêt un intérêt particulier puisqu'il découle à la fois de l'érosion des zones sources, des capacités de transports des réseaux hydrographiques et participe au remplissage des bassins sédimentaires. La connaissance détaillée des flux sédimentaires et leur quantification au cours du temps au sein d'un couple bassin versant – bassin sédimentaire est cruciale car elle permet d'approcher l'évolution de la surface terrestre au cours du temps et donc, l'évolution morphostructurale du site. Dans les zones tectoniquement actives, comme les marges en subduction océan – continent, le relief est souvent important et soumis à une intense érosion. Il en résulte une disparition progressive et plus ou moins rapide des marqueurs de paléotographies. L'approche de l'évolution de la surface terrestre à long terme (> ka) par la quantification des flux sédimentaires est donc indiquée dans le cas de zones actives.

Dans une première partie, je définirai la notion de flux sédimentaire, et après avoir déterminer les paramètres qui contrôlent son évolution et celle de l'érosion, je présenterai les différentes méthodes de calcul utilisées à différentes échelles de temps. Enfin je discuterai des problèmes de représentativité des valeurs de flux et les limites à son interprétation en terme d'évolution des reliefs.

Dans une seconde partie, je présenterai rapidement les marges actives des subductions continent – océan, leur distribution et leurs caractéristiques morphostructurales.

Enfin, dans une troisième partie, je présenterai un état des connaissances de la marge active Hikurangi en Nouvelle-Zélande et plus particulièrement du domaine avant arc d'Hawke Bay, choisi pour cette étude.

1.1. L'érosion et les flux sédimentaires :

1.1.1. Définitions :

L'érosion est un phénomène naturel qui a pour effet de dégrader une topographie positive née de la déformation tectonique ou du volcanisme. Elle fait intervenir de nombreux processus, parmi lesquels il est possible de distinguer les processus mécaniques (fragmentation, abrasion) et les processus d'altération chimique. Différents facteurs interviennent dans les processus d'érosion :

- L'eau, qu'elle soit solide ou liquide, est considérée comme l'agent d'érosion mécanique le plus efficace sur l'ensemble du globe. A l'état solide, elle forme les glaciers, dont

l'écoulement dans les vallées des chaînes de montagne est responsable de l'arrachement d'importante quantité de roches. A l'état liquide, c'est le ruissellement et l'écoulement chenalisé qui interviennent dans l'érosion des versants des vallées et l'incision fluviatile. En augmentant son volume lors du passage de l'état liquide à l'état glace, l'eau présente dans les fractures favorise la fragmentation des roches (gélifraction).

- Le vent, intervient également dans en transportant les poussières et en abrasant les roches. L'érosion chimique correspond à l'altération des roches (silicates, carbonates) liée principalement à l'acidité naturelle des eaux météoriques.

L'érosion ayant comme effet un abaissement de la topographie, sa quantification de dans le temps est exprimée en $mm.yr^{-1}$. Howard et Kerby (1983) ont montré que la vitesse d'érosion E, au niveau d'une rivière, dépendait de la pente locale S, du flux d'eau Qw (équivalent de l'aire drainée A et du coefficient K d'érodabilité du substrat (lithologie, fracturation…) selon la relation suivante : « stream power law » :

$$E = K\, Qw^m\, S^n$$

$$E = K\, A^m\, S^n$$

(m et n sont des valeurs d'exposants positives)

Cette relation caractérise les systèmes en érosion ou « détachement limité » et est abondamment utilisée, avec ses variantes, dans les modélisations numériques pour simuler l'érosion fluviatile.

Le « flux sédimentaire » correspond à une quantité de sédiment Qs transitant depuis des zones dominées par l'érosion à des zones dominées par la sédimentation, par intervalles de temps. Sa valeur dépend de la quantité de matériel mis à disposition par la fragmentation et l'altération mais surtout de la capacité de transport C du réseau hydrographique, qui fait intervenir le flux d'eau Qw et la pente S (Fig. 1.1). Ainsi, lorsque la capacité de transport est supérieure à la charge sédimentaire, le transport est efficace et l'érosion peut aussi avoir lieu dans le lit, alors que si la capacité de transport est inférieure à l'apport sédimentaire, la sédimentation a lieu. De la même manière que l'érosion, le flux sédimentaire peut être caractérisé par la relation suivante :

$$Qs = K'\, Qw^m\, S^n = K'\, A^m\, S^n$$

(avec K' coefficient incluant la contrainte cisaillante, la taille des grains...)

Néanmoins, suivant l'échelle de temps considérée pour son estimation ou sa mesure ainsi que les méthodes employées, le terme ne revêt pas exactement la même signification. Ainsi, à

court terme (durée des mesures in situ), le flux sédimentaire correspond à la charge sédimentaire transportée par le réseau hydrographique (rivières, glaciers) exprimée en masse par unité de temps (eg. $t.yr^{-1}$). A l'échelle des temps géologiques, les flux sédimentaires correspondent à long terme, soit aux taux d'érosion ou d'exhumation des zones sources, soit aux volumes sédimentaires préservés dans les bassins. Il correspond alors respectivement à un flux sortant des zones sources ou à un flux entrant dans les bassins. Il est exprimé en quantité de matériel produit par érosion par unité de surface et unité de temps – taux de productivité - (eg. $km^3.km^{-2}.yr^{-1}$ ou T. $km^{-2}.yr^{-1}$) ou en volume de sédiment déposé par unité de temps (eg. $km^3.yr^{-1}$). La disharmonie qui existe dans les dimensions et les échelles de temps d'estimation du flux sédimentaire et de l'érosion, résultant des méthodes utilisées, pose le problème de la représentativité de la comparaison de ces valeurs d'érosion ou de flux entre elles et entre différentes échelles de temps.

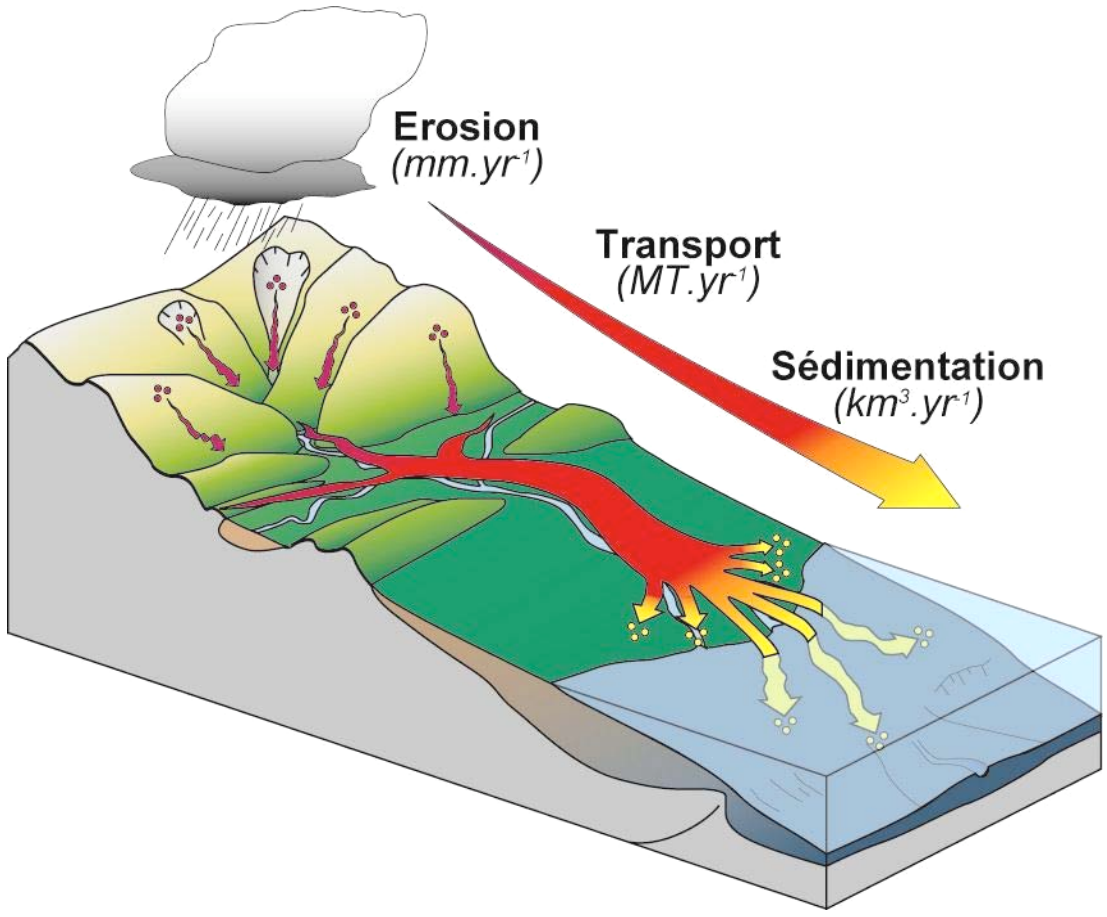

Figure 1.1 : Bloc diagramme schématique montrant les trois processus élémentaires intervenant dans l'évolution des reliefs (érosion, transport et sédimentation) et leur dimensions respectives ($mm.yr^{-1}$, $Mt.yr^{-1}$, $km^3.yr^{-1}$).

1.1.2. Les facteurs de contrôle de l'érosion et du flux sédimentaire :

Les études menées ces quatre dernières décennies sur les systèmes actuels et anciens ont permis de relier le contrôle de l'érosion et des flux sédimentaires à court terme et long terme, aux paramètres géomorphologiques (relief, topographie, aire drainée), aux processus tectoniques et climatiques, à l'eustatisme et à l'impact anthropique.

Les paramètres géomorphologiques :

Milliman et Syvitski (1992) montrent, par l'étude de 288 bassins versants répartis autour du globe, que pour des valeurs d'aire drainée croissantes, la valeur du flux sédimentaire (MT/yr) augmente alors que le taux de productivité (T/km²/yr) diminue (Fig. 1.2). Ahnert (1970) et Pinet et Souriau (1988) montrent l'existence d'une relation de proportionnalité entre la topographie (altitude moyenne) et le taux d'érosion. D'autres études ont confirmé l'importance de la topographie, et surtout du relief (différence d'altitude entre crêtes et vallées), dans le contrôle du taux d'érosion (Pinet et Souriau, 1988 ; Summerfield et Hulton, 1994 ; Hovius, 1997 ; Montgomery and Brandon, 2002). Cette relation est considérée comme linéaire avec une érosion qui croît proportionnellement avec le relief (Ahnert, 1970 ; Summerfield et Hulton, 1994), jusqu'à une valeur seuil de relief pour laquelle la pente de stabilité est dépassée et au-delà de laquelle le mécanisme d'érosion prépondérant est le glissement de terrain (Burbank et al., 1996 ; Montgomery et Brandon, 2002 ; Binnie et al., 2007) (Fig. 1.3). Cette particularité a été observée dans de nombreux domaines orogéniques particulièrement actifs comme l'Himalaya (Burbank et al., 1996 ; Galy et France-Lanord, 2001), Taiwan (Li, 1975 ; Hovius et al., 1997 ; Dadson et al., 2003 ; 2004) ou la Nouvelle-Zélande (Tippett et Kamp, 1993 ; Hovius et al., 1997). L'activité tectonique et notamment la vitesse de surrection semble être décisive dans le contrôle de la topographie et de l'érosion, en offrant un volume disponible à l'érosion (Gunnell, 1998).

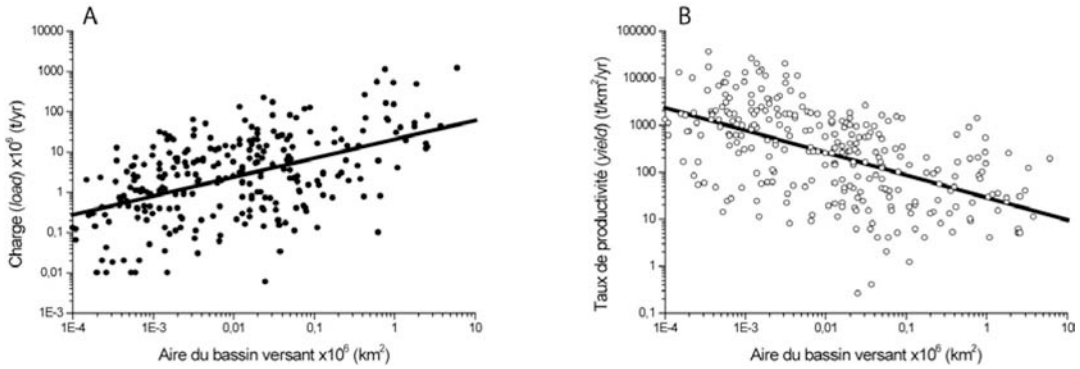

Figure 1.2 : Relations entre aire drainée (surface du bassin versant) et (A) charge sédimentaire, et (B) taux de productivité établie à partir de données recueillies sur 288 rivières réparties à travers le monde (Milliman et Syvitski, 1992 ; d'après Rohais, 2007).

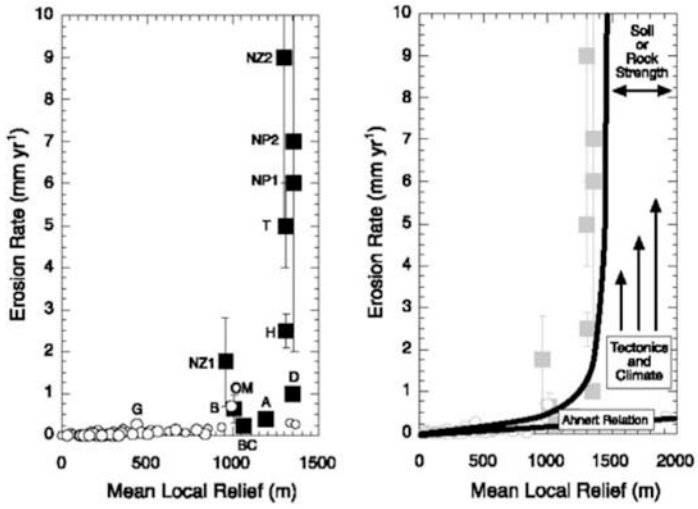

Figure 1.3 : Relation entre taux d'érosion et relief local moyen établie par Montgmery et Brandon (2002). La relation d'Ahnert (1970) est valable pour les reliefs moyens inférieur à ~1000 m mais cesse de l'être dans les reliefs moyens supérieurs à 1000 - 1500 m associés aux chaînes de montagnes actives (B : Bramaputre ; NZ1 & 2 : Alpes du Sud, Nouvelle-Zélande d'après Tippett et Kamp (1999) et Hovius et al. (1997) ; H : central Himalaya d'après Galy et France-Lanord, (2001) ; NP1 & 2 : Indus d'après Burbank et al. (1996) et Shroder et Bishop (2000) ; OM : Olympic Mountains d'après Brandon et al. (1998) ; T : Taiwan d'après Li (1975) ; D : Denali (Alaska) d'après Fitzerald et al. (1993) ; A : Alpes d'après Bernet et al. (2001) BC : Colombie Britannique d'après Farley et al. (2001)).

La tectonique :

La déformation tectonique est un paramètre de premier ordre dans le contrôle de l'érosion et des flux sédimentaire car comme expliqué précédemment, elle produit une topographie disponible à l'érosion (Gunnell, 1998). Dès 1889, Davis associe l'évolution des chaînes de montagnes à une compétition entre processus tectonique de surrection responsable de la croissance de la topographie et processus d'érosion responsable de l'aplanissement consécutif (Fig. 1.4). Hack (1960) introduit la notion d'équilibre du relief, qui correspond un état pour

lequel taux de surrection et taux d'érosion se compensent. Deux phases sont alors décrites pour caractériser l'état du relief des chaîne de montagne soumise à une surrection continue. La première phase correspond à une phase de croissance de la topographie durant laquelle la surrection domine sur l'érosion. Vient ensuite, la deuxième phase pour laquelle la surrection U est compensée par l'érosion ($E = U = K A^m S^n$), ceci après un temps caractéristique dit de mise à l'équilibre du relief (Snyder et al., 2000 ; Lague et al., 2000). Un tel comportement a été conforté par les modélisations analogiques (Lague et al., 2003) mais la durée de ce temps caractéristique apparaît très variable (1 à 100 Ma) suivant le contexte (Pinet et Souriau, 1988 ; Pazzaglia et Brandon, 1996). Un autre aspect des interactions entre surrection et érosion est l'existence d'une rétroaction positive qui implique la réponse de compensation isostatique d'une chaîne à l'érosion et au transport des produits de la sédimentation hors du domaine orogénique (Molnar et England, 1990) (Fig. 1.5). De cette manière, l'érosion influence sensiblement l'évolution structurale des chaînes de montagnes (Pavlis et al., 1997 ; Norris et Cooper, 1997) et également leurs histoires thermiques et métamorphiques (Koons, 1990, 1994 ; Beaumont et al., 1992 ; Willet et al. 1993). Ces observations montrent l'importance de la tectonique dans l'évolution des reliefs et de l'érosion et inversement, que l'érosion est déterminante dans l'évolution des zones orogéniques (Hoffman et Grotzinger, 1993 ; Zeitler et al., 2001 ; Braun et Pauselli, 2004). Les modélisations numériques révèlent que les évènements tectoniques importants, même s'ils sont rapides, sont le plus souvent traduits par une évolution progressive du flux sédimentaire (Allen et Densmore, 2000). Enfin, les zones tectoniquement actives telles que Taiwan et la Nouvelle-Zélande, sont le lieu de glissement de terrains qui trouve une part de leur origine dans la forte séismicité locale (Hovius et al., 1997 ; Dasdon et al., 2003 ; 2004)

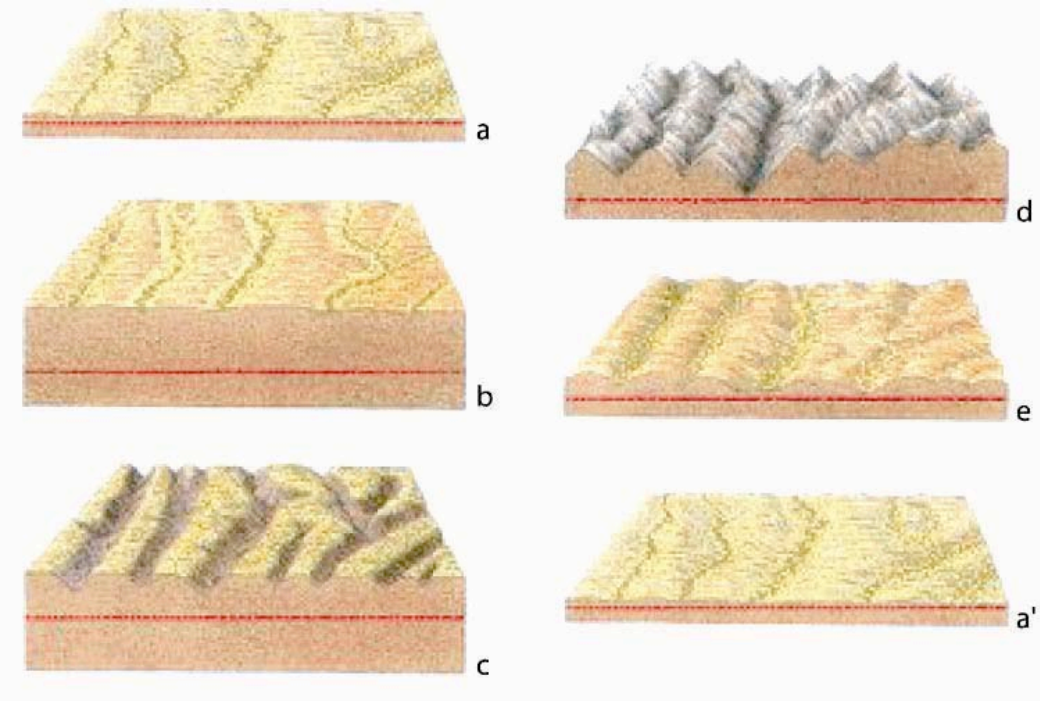

Figure 1.4 : Modèle d'évolution du relief des chaînes de montagne proposé par Davis (1889). A) topographie plane, proche du niveau de base (ligne horizontale). B) le soulèvement rapide intervient. C) l'incision par les rivières commence et des surfaces planes héritées de la topographie initiale sont préservées sur les « crêtes ». D) l'incision se poursuit, et les versants fortement pentés se développent jusqu'aux crêtes. E) l'altitude des crêtes diminue et le relief s'adoucit. D) le stade final est un retour à une topographie de faible relief comparable à celle du stade initial (A). Ce stade est nommé pénéplaine.(d'après Strahler et Strahler, 1992)

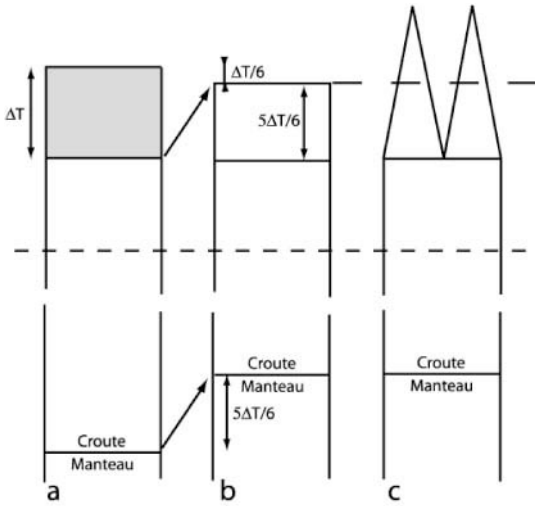

Figure 1.5 : Schéma représentant le rebond isostatique consécutif à l'érosion d'une épaisseur ΔT de croûte (densité ρc. L'érosion est compensée par une remontée de la base de la croûte et du manteau lithosphérique (densité ρm) et entraîne un rebond isostatique de (ρm-ρc)/ρm ~5 ΔT/6, soit, dans le cas b, une diminution de l'altitude de ΔT/6. Dans le cas d'une érosion localisée dans les vallées (cas a), le rebond entraîne une augmentation de l'altitude des crêtes (modifié par S. Bonnet (2005), d'après Molnar et England, 1990).

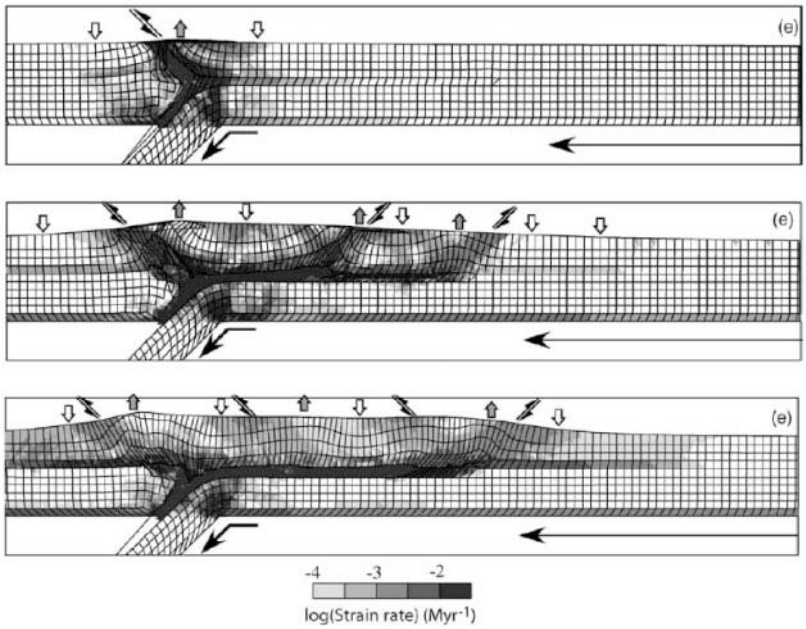

Figure 1.6 : Modélisations numériques thermomécaniques de la déformation crustale dans un contexte de subduction mantellique incluant une érosion de surface par transport fluviatile et diffusif. Les trois expériences montrent la quantité de déformation (niveaux de gris), la localisation des structures et la topographie, suite une convergence identique. Le paramètre variable est le taux d'érosion appliqué (fort en haut, moyen au milieu, faible en bas). Il apparaît que l'érosion et l'exportation du matériel érodé modulent la localisation de la déformation et par conséquent la géométrie de l'orogène (Modifié d'après Braun et Pauselli, 2004).

Le climat et ses variations :

La participation du climat dans le contrôle de l'érosion et des flux sédimentaire est décisive puisque les conditions d'englacement, de précipitation et le couvert végétal sont identifiés comme majeurs dans les processus d'érosion mécanique et chimique (altération) (Summerfield et Hulton, 1994 ; Syvitski et Shaw, 1995). Néanmoins il n'existe pas de relation simple entre les paramètres climatiques locaux (températures, taux de précipitations) et la valeur du flux sédimentaire (Milliman et Syvitsky 1992 ; Summerfield et Hulton, 1994). La relation qui lie érosion et climat est complexe et probablement rendu difficile à identifier à cause de l'influence d'autres facteurs de contrôle (eg. tectonique). Outre la quantité des précipitations, c'est leur mode (fréquence et intensité des évènements) qui apparaît important dans l'intensité de l'érosion et notamment dans le déclenchement de glissements de terrains (Molnar et England, 1990 ; Zhang et al., 2001 ; Molnar 2004 ; Soldati et al., 2004 ; Dymond et al., 2006 ; Lake Tutira Drilling Group, 2007). L'impact des évènements catastrophiques sur les flux est illustré pour la Nouvelle-Zélande (Hovius et al., 1997) ou Taiwan (Dadson et al., 2003 ; 2004). Ainsi, au cours du Cénozoïque, l'influence du climat sur l'érosion est les flux

sédimentaires est mise en évidence par l'augmentation importante de la quantité de sédiments terrigènes déposés au fond des océans et plus particulièrement depuis le Pliocène (Fig. 1.7), coïncidant avec la dégradation climatique globale (Hay et al., 1988 ; Rea, 1993 ; Zhang, 2001 ; Molnar, 2004). Cette augmentation de l'érosion et des flux découlerait du refroidissement et de l'aridification du climat global et d'une augmentation simultanée de la fréquence et de l'ampleur des variations et des évènements climatiques, comme cela est le cas au Pléistocène (Zachos et al., 2001 ; Molnar, 2001). De récentes études sur le dernier cycle glaciaire à 100 ka (Pléistocène supérieur) montrent également qu'une augmentation des flux sédimentaires et des taux de productivité a lieu lors des dégradations climatiques, lorsque les précipitations sont maintenues (Collier et al., 2000 ; Berryman et al., 2000 ; Litchfield et Berryman, 2005 Carter et Manighetti, 2006) (Fig. 1.8). Le ratio entre charge sédimentaire et charge d'eau (capacité de transport) serait alors favorables à l'aggradation (Fig. 1.9) Ces observations illustrent le modèle empirique établi par Penck et Brückner (1909) à partir des terrasses fluviatiles du Danube. Ces phénomènes s'expliquent, au moins en partie, par l'effet du couvert végétal sur l'altération et l'érosion. La présence et le développement d'un couvert végétal ont une action protectrice particulièrement variable suivant la ceinture climatique et l'altitude (précipitation et température). Ainsi, de nombreuses études ont montré, dans la lignée de Huntington (1907), que (1) lorsque le taux précipitations augmente, l'érosion (et le flux sédimentaire) augmente, puis (2) l'apparition d'un couvert végétal consécutive à l'augmentation des précipitations a pour résultat de limiter l'érosion et de la diminuer lorsqu'il est suffisamment dense et protecteur (forêts) et (3) l'érosion augmente ensuite de nouveau (Langbein et Schumm, 1958 ; Summerfield, 1991 : Jiongxin, 2005) (Fig. 1.10).

Molnar et England (1990) discutent aussi du synchronisme et de la relation de causalité possible entre accroissement de la surrection dans les domaines orogéniques, dégradation climatique au Cénozoïque et augmentation des taux d'érosion et des flux sédimentaires. Les auteurs proposent que la formation des chaînes de montagnes au Cénozoïque résulte en une dégradation progressive du climat, qui en augmentant l'érosion et en diminuant les températures, implique une apparente augmentation de la surrection dans ces même chaînes de montagnes. Il y aurait ainsi un entretient et une rétroaction positive entre climat et tectonique. Molnar (2004) montre que l'augmentation du flux sédimentaire au Pliocène (2-4 Ma) implique essentiellement des zones de hautes altitudes et latitudes, où la dégradation climatique est particulièrement bien exprimée par le développement de glaciers notamment. Il apparaît aussi que le relief réagit rapidement aux évènements climatiques important et rapides

(10^{3-4} ans) par des pulses dans les flux sédimentaires (Allen et Densmore, 2000 ; Berryman et al., 2000) et ce, d'autant plus que le réseau hydrographique est petit (Castelltort et Van Den Driessche, 2003) Le climat joue donc un rôle fondamental et complexe dans l'adaptation de l'intensité du taux d'érosion et plus particulièrement au niveau des topographies importantes (chaîne de montagne). Ceci est tout à fait remarquable dans le cas des chaînes de montagne qui développent des systèmes glaciaires importants. Les interactions entre climat et tectonique au niveau des chaînes de montagne apparaît telle qu'il semble difficile de discriminer lequel des deux paramètres revêt le plus d'importance dans le contrôle de l'érosion et des flux. Le corollaire est que l'identification d'une variation de flux sédimentaire au cours des temps géologiques est difficilement strictement imputable à l'un ou l'autre de ces deux paramètres majeurs, du moins sans une connaissance précise des calendriers climatiques et tectoniques.

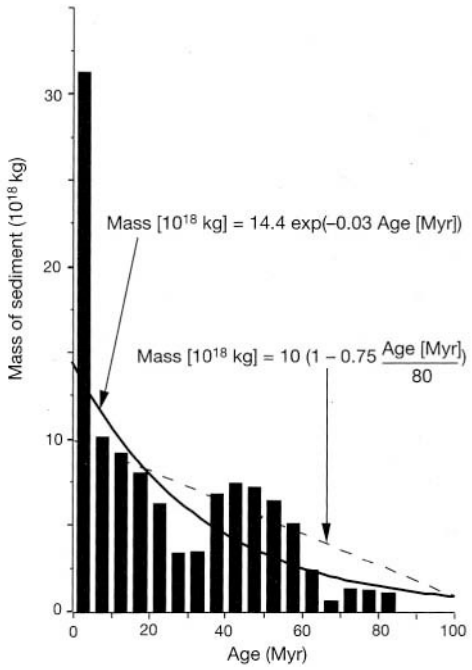

Figure 1.7 : Histogramme montrant la masse totale de sédiments terrigènes déposés au fond des océans de la fin du Mésozoïque à l'actuel (d'après des données de Hay et al., 1989). On peut observer une nette surreprésentation des sédiments déposés au Plio-Pléistocène (5-0 Ma) qui correspond à une augmentation des flux sédimentaires terrigènes (Zhang et al., 2001).

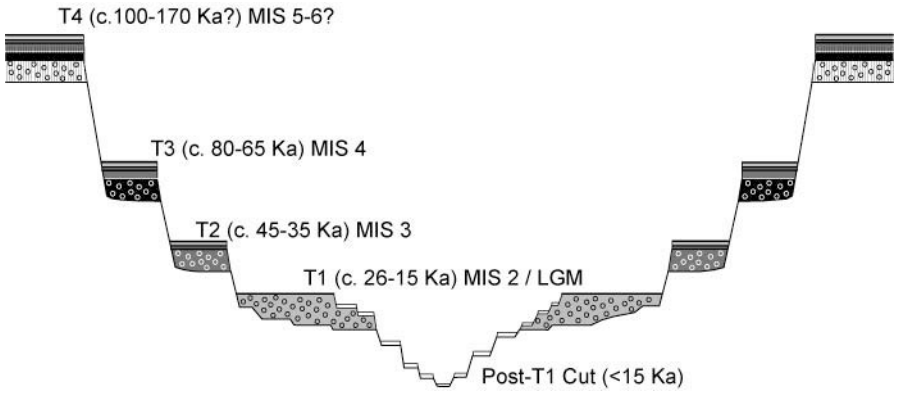

Figure 1.8 : Coupe transversale schématique montrant la succession des terrasses d'aggradation et d'incision dans les vallées de la côte est de l'île Nord de Nouvelle-Zélande (d'après Litchfield, 2003 et Litchfield et Berryman, 2006). Les terrasses sont corrélées régionalement et leurs périodes d'aggradation correspondent aux dégradations climatiques du Pléistocène supérieur des stades isotopiques MIS 4, 3 et 2 (LGM = Last Glacial Maximum).

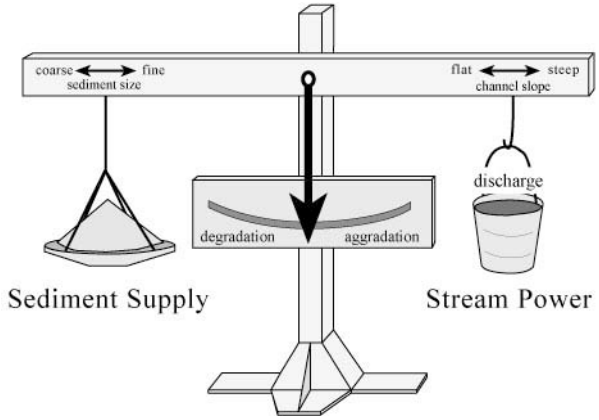

Figure 1.9 : Modèle illustrant le comportement aggradant ou dégradant d'un chenal fluviatile en fonction de la charge sédimentaire et du flux d'eau. L'aggradation a lieu lorsque la charge sédimentaire dépasse les capacités de transport liées aux flux d'eau dans la rivière. D'après un dessin non publié de W. Borland et extrait de Blum et Törnqvist (2001).

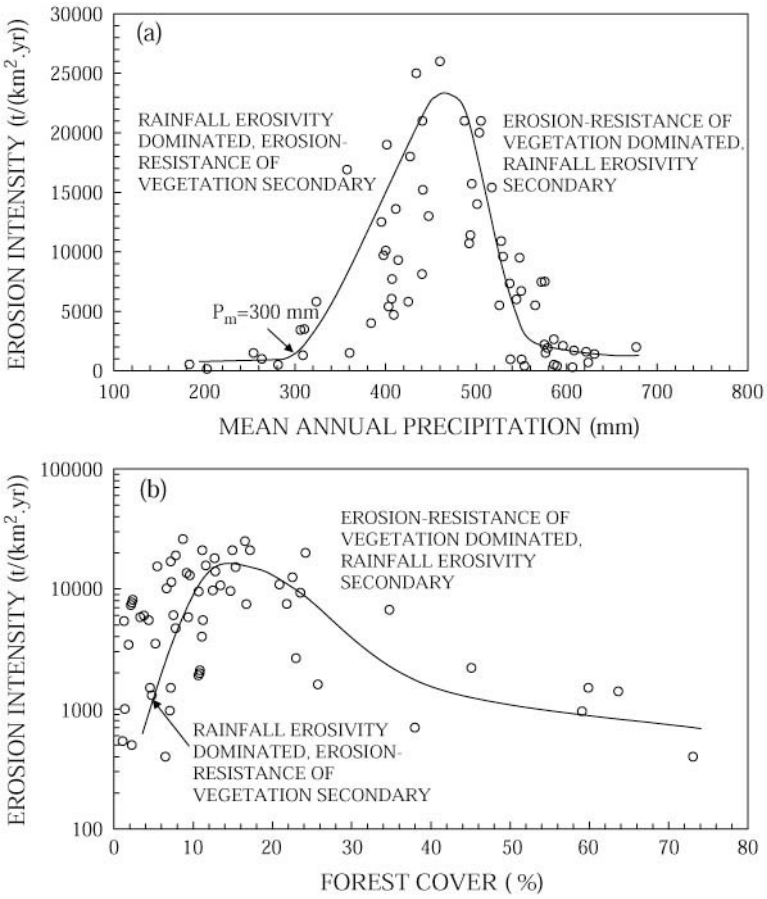

Figure 1.10 : Relation entre taux de productivité (intensité d'érosion) et (a) les précipitations annuelles, et (b) le pourcentage de couvert végétal. L'influence positive des précipitations sur l'érosion opère jusqu'à ce que le pourcentage de couvert végétal, qui croît également avec le taux de précipitation, soit suffisant pour protéger et stabiliser les sols, et ainsi limiter, puis diminuer l'érosion (Jiongxin, 2005).

L'eustatisme :

L'eustatisme correspond aux changements globaux du niveau océans. Ses variations sont dépendent uniquement du temps. Les causes des variations eustatiques sont variées mais peuvent être regroupées en deux catégories. La première regroupe les causes qui ont pour effet de modifier la forme du contenant (bathymétrie du fond des océans et des plateformes continentales) et qui sont essentiellement liées à la géodynamique interne (subsidence thermique, taux de production des dorsales…). La deuxième catégorie regroupe les causes qui ont pour conséquence de modifier le volume du contenu (quantité d'eau liquide en surface). Ces dernières sont variées et sont d'origine interne (dégazage par le volcanisme), cosmique (comètes constituées de glace d'eau) ou climatique (fonte ou formation de la glace dans les calottes polaires et les chaînes de montagnes). L'influence des variations eustatique sur l'évolution des reliefs est principalement relié à la notion de « niveau de base » (Powell,

1875) qui correspond à l'altitude minimale en deçà de laquelle les rivières ne peuvent éroder. Suivant cette définition, Lamothe (1918) et Fisk (1944) propose d'expliquer le calendrier de formation des terrasses (aggradation et incision), respectivement de la Somme et du Mississippi, par l'impact des chutes et des remontées eustatiques Pléistocènes (Fig. 1 .11). Ainsi, une chute du niveau marin provoque une chute du niveau de base et permet l'abandonnement d'une terrasse d'aggradation (plaine d'inondation) et l'incision des rivières. Begin et al. (1981) propose que l'incision initiée au niveau de la côte puisse remonter le long du réseau hydrographique par érosion régressive et migration de points d'inflexion (ie. cascades) le long des profiles longitudinaux. Cette vision est supportée par les modèles stratigraphiques conceptuels (Fig. 1.12) développés dans les années soixante dix et quatre vingt (Vail et al., 1977 ; Jevrey ; 1988 ; Posamentier et Vail, 1988 ; Posamentier et al., 1988) découlant des observations réalisées sur les marges, et par de récentes modélisations, notamment sur la chute eustatique accompagnant la crise Messinière en Méditerranée (Strong et Paola, 2006 ; Loget et al., 2006). En abaissant ainsi l'altitude du lit des rivières, une baisse eustatique favorise l'incision fluviatile, augmente alors le relief, les pentes et donc l'érosion et les flux sédimentaires. Ce modèle entre en compétition avec le modèle de Penck et publié (1909), ce qui met en lumière deux visions confrontant l'influence des zones sources et celle des zones côtières sur le comportement des rivières (voir discussion dans Blum et Törnqvist, 2000). Summerfield (1985) relativise la vision de Fisk (1944) et les modèles stratigraphiques en postulant que l'incision ne peut avoir lieu que si la pente de la plateforme continentale devenant émergeante et plus importante que la pente de la plaine côtière et du profile longitudinal de la rivière (Fig. 1.13). De plus, Dalrymple et al., (1998) propose qu'en s'allongeant sur une plateforme à faible gradient de pente, un espace d'accommodation aérien se créé dans la rivière, interdisant toute initiation et migration régressive d'incision fluviatile. Ce modèle est notamment illustré par Leckie (1994) et publié et Naish (2003) qui mettent en évidence des périodes d'aggradation dans les plaines de Canterbury (Nouvelle-Zélande) lors des périodes de bas niveau glaciaires. L'influence des variations de l'eustatisme, en tant que paramètre de contrôle, sur l'évolution des reliefs, de l'érosion et des flux sédimentaires apparaît complexe est variable suivant les configurations et le contexte géodynamique. De plus, la différenciation de son influence par rapport à celles du climat n'est pas triviale puisque les deux paramètres évoluent conjointement. De la même façon, à cause de l'influence locale de la déformation sur le niveau marin relatif, la discrimination de l'impact de l'eustatisme et de celui de la tectonique est rendue difficile, et plus particulièrement dans

les zones où les vitesses de surrection et de subsidence sont du même ordre de grandeur que les vitesses de chute et de remontée eustatique.

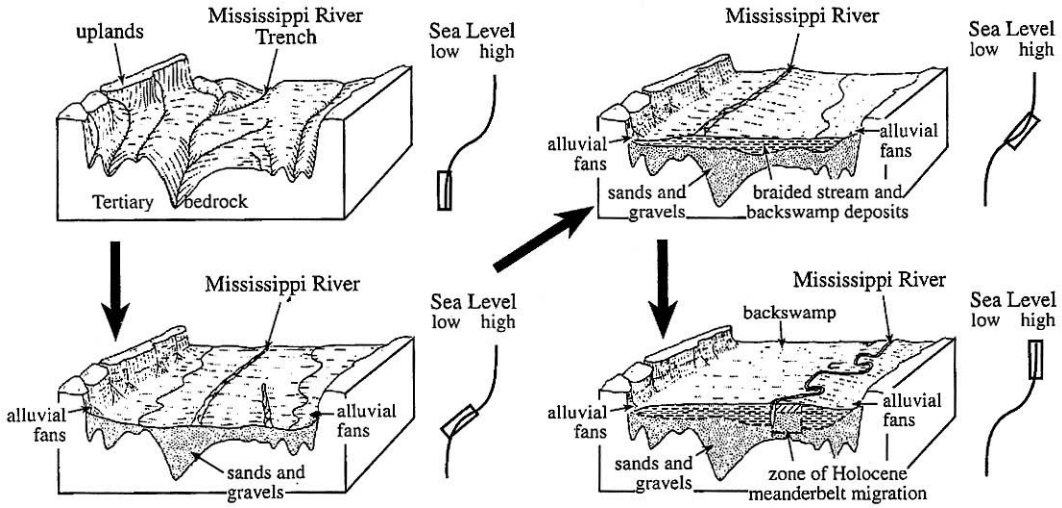

Figure 1.11 : Modèle de développement de la vallée du Mississippi pendant un cycle eustatique, illustrant l'incision durant la chute du niveau de base marin et les différents stades d'aggradation fluviatile durant la remontée et le haut niveau marin (Fisk, 1944).

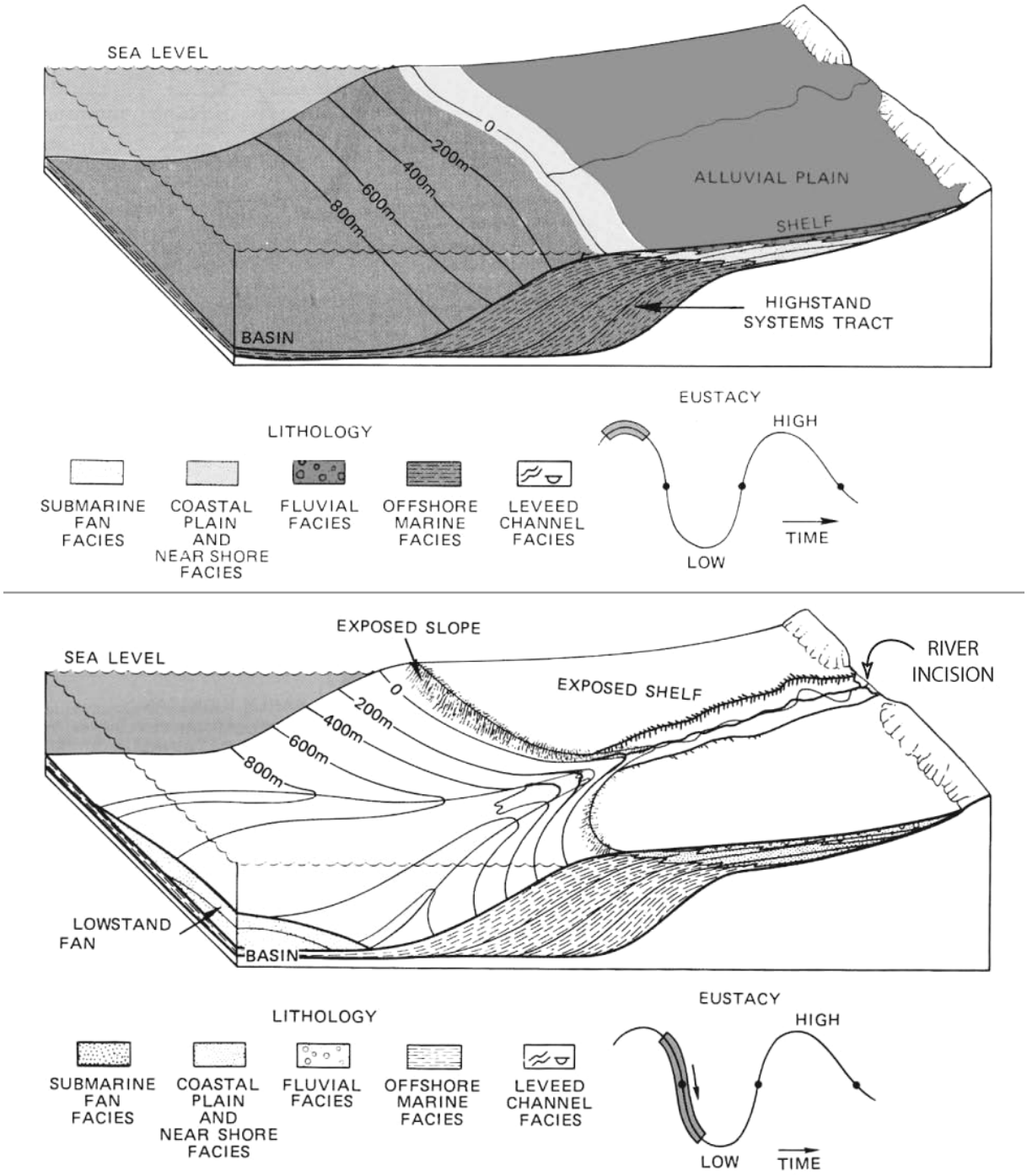

Figure 1.12 : Bloc diagramme illustrant l'effet d'une chute du niveau marin sur la distribution de la sédimentation et sur développement de l'incision dans les vallées (d'après Posamentier et al., 1988).

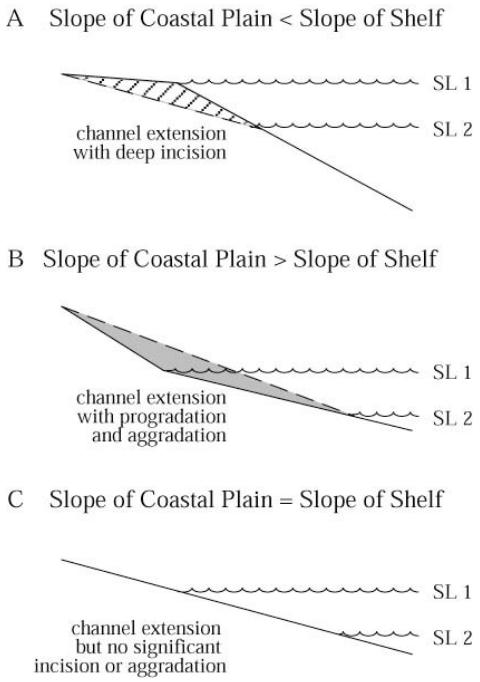

Figure 1.13 : Modèles illustrant la réponse d'une rivière à une baisse du niveau marin, en fonction des gradients de pente de son profil longitudinal et de la plateforme. (A) la pente de la plateforme est supérieure à la pente du profil : il y a incision. (B) la pente de la plateforme est inférieure à la pente du profil : il y a aggradation. (C) les pentes de la plateforme et du profil sont identiques, il y a allongement du profil mais aucune incision ni aggradation (d'après Summerfield, 1985 et extrait de Blum et Törnqvist, 2000).

L'influence de la sédimentation :

La reconnaissance de l'influence rétroactive de la sédimentation sur la dynamique d'érosion n'est intervenue que très récemment, depuis la fin des années quatre vingt dix (Allen et Densmore, 2000 ; publié et Van car Driessche, 2003 ; Carretier et Lucazeau, 2005, Babault et al., 2005a ; Babault et al., 2007). Cette influence repose sur l'effet qu'implique la présence d'un niveau de base érosif aérien (Wheeler, 1964) situé à l'exutoire des zones en érosion (ie. cône alluvial). En effet, si la sédimentation a lieu à une altitude donnée, l'incision des rivières ne peut intervenir sous cette même altitude. Alors, dans le cas d'une aggradation à l'exutoire, l'altitude du niveau de base érosif augmente et induit une diminution et un arrêt de l'incision et favorise le comblement des vallées. Il en résulte une diminution des reliefs, des taux d'érosion (Fig. 1.14), et par conséquent, du flux sédimentaire. Les périodes de forte aggradation de piedmont pourraient ainsi être à l'origine des reliques à reliefs lissés préservées en altitude (Babault et al., 2005b) et considérées auparavant comme des rémanents de pénéplaines soulevés par une surrection postérieure. Il existerait ainsi une boucle de rétroaction négative entre l'érosion dans les chaînes de montagne et la sédimentation dans les zones de piedmont (Fig. 1.15).

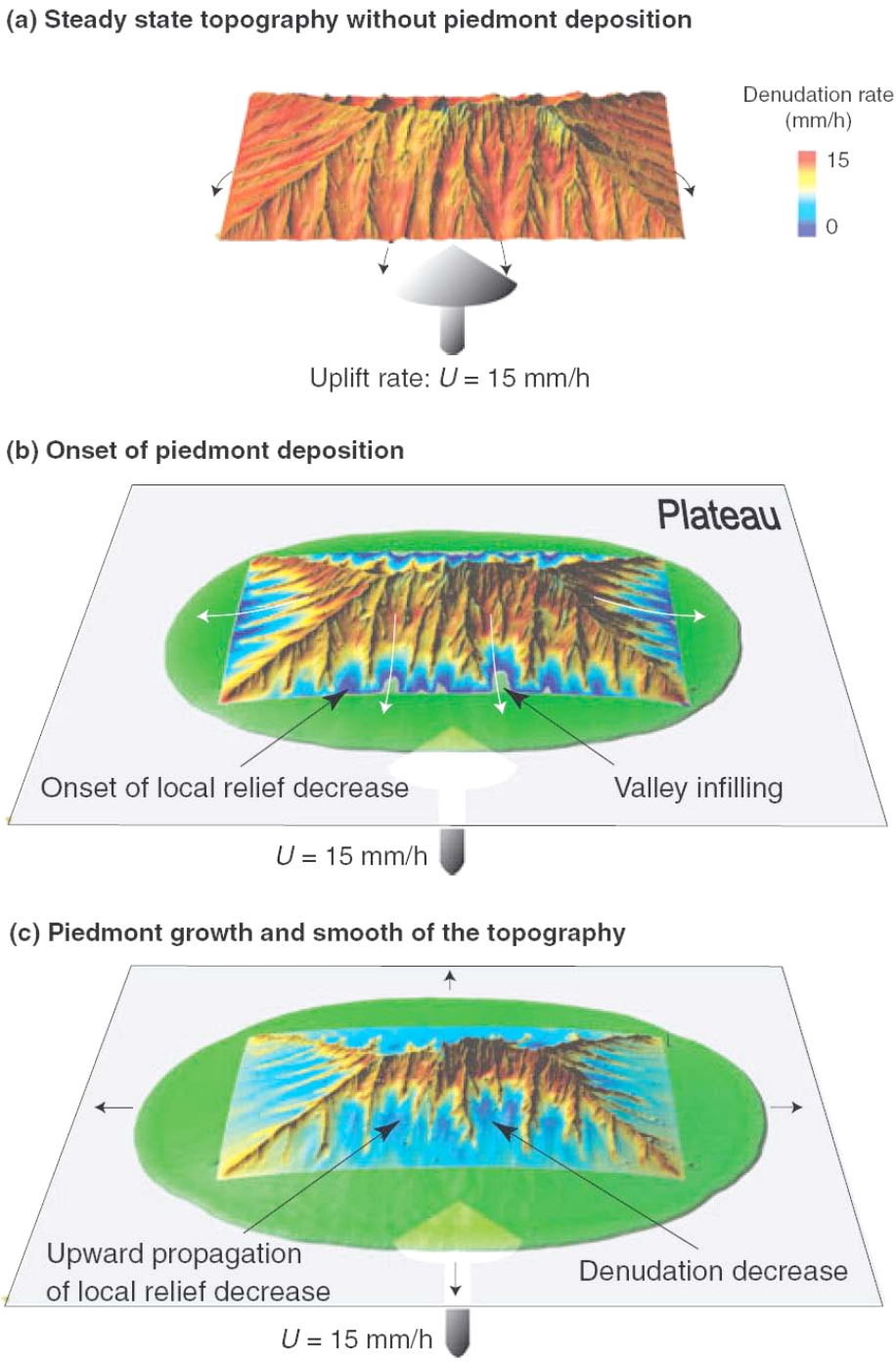

Figure 1.14 : Influence de la sédimentation de piedmont sur l'érosion locale d'une topographie en surrection. (A) topographie à l'équilibre dynamique sans sédimentation de piedmont. (B) mise en place d'un plateau permettant la sédimentation de piedmont. (C) développement de la sédimentation de piedmont entraînant une diminution de l'érosion vers l'amont et le lissage progressif du relief. Noter que les surfaces aplanies au sein de la topographie en surrection ne sont pas des surfaces de dépôts mais des surfaces d'érosion (Babault et al., 2007).

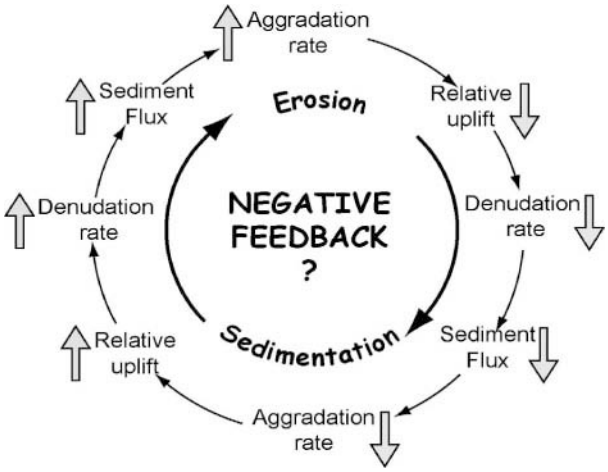

Figure 1.15 : représentation schématique du boucle de rétroaction négative potentielle entre érosion et sédimentation au pied d'un relief (d'après Babault, 2004 ; Bonnet, 2005).

L'impact anthropique :

Un dernier facteur de contrôle majeur de l'érosion et des flux sédimentaires actuels est l'impact anthropique sur l'occupation et la gestion des sols. En effet, en modifiant profondément le couvert végétal dans le cadre du développement de l'agriculture (déforestation), l'homme a bouleversé les « équilibres » climat-végétation-érosion (Kettner et al., 2007 ; Gomez et al., 2007) (Fig. 1.16a). Les constructions sont localement responsables de pertes non négligeables de sols (Syvitski et Milliman, 2007) (Fig. 1.16b). De récentes études montrent qu'au niveau global, l'impact anthropique induit une augmentation des taux d'érosion d'un ordre de grandeur, en passant de quelques dizaines de mètres par million d'années pour le Phanérozoïque à quelques centaines de mètres par million d'années actuellement (Wilkinson, 2005 ; Wilkinson et McElroy, 2007). Cette augmentation est néanmoins limitée aux zones de faible altitude où sont concentrées l'agriculture et les constructions et qui fournissent moins de 20% de la charge globale des rivières (Wilkinson et McElroy, 2007). De plus, une grande partie de « l'excédent » de sédiments érodés est naturellement stockée dans le bassin versant sous la forme de colluvions ou au sein des plaines d'inondation (Métivier et Gaudemer, 1999 ; Phillips, 2003). Enfin, Vörösmarty et al. (2003) et Syvitski et al. (2005) estiment qu'une grande partie (jusqu'à 30 %) du flux sédimentaire actuel est retenue au niveau de lacs de barrages. Ainsi, l'effet anthropique sur l'érosion et les flux sédimentaire est particulièrement complexe et difficile à mesurer depuis les zones sources jusqu'aux débouchés des rivières, car s'il a pour effet d'augmenter l'érosion des sols, les capacités de stockage naturelles (colluvions, plaines d'inondation) et anthropiques (barrages) limitent les apports sédimentaires à l'océan mondial.

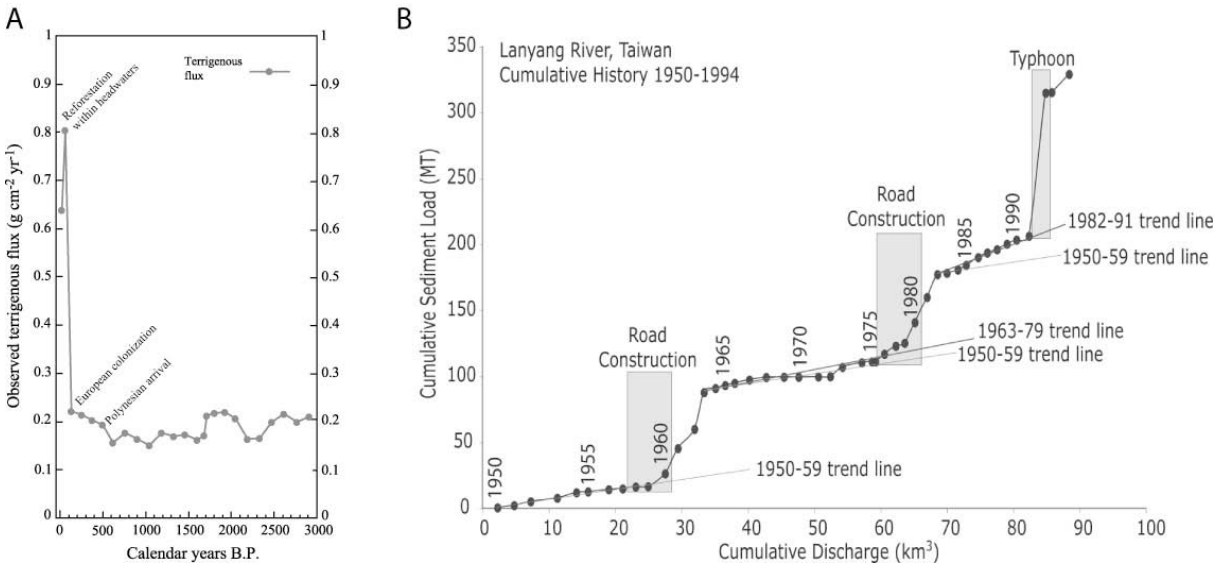

Figure 1.16 : Mise en évidence de l'impact anthropique sur l'évolution des flux terrigènes. (A) évolution du taux de sédimentation terrigène (g.cm^{-2}.yr^{-1}) au cours des derniers 3000 ans, au débouché de la Waipaoa River (Nouvelle-Zélande), établie à partir de données de carotte (MD972122). L'impact anthropique est clairement visible avec le quadruplement du flux terrigène attribué à la déforestation consécutive à la colonisation européenne (données d'après Gomez et al., 2007 ; modifié d'après Kettner et al., 2007). (B) mise en relation de la charge sédimentaire cumulée de la Lanyang River (Taiwan) et du flux d'eau cumulé sur une période de 44 ans. Les deux augmentations brutales de la charge sédimentaire corrélées aux travaux de voirie ont le même ordre de grandeur que l'augmentation liée à un évènement climatique catastrophique de type typhon (données d'après Syvitski et al., 2005c et modifié d'après Syvitski et Milliman, 2007).

Mesure de l'érosion et du flux sédimentaire… :

…à court terme :

Les flux sédimentaires à court terme (instantané à 100 ans) correspondent aux flux dont la valeur est mesurée ou estimée via des mesures in situ. Les valeurs sont essentiellement dérivées des mesures de charge suspendue dans les rivières et intègrent parfois des estimations des charges dissoutes et de fond et sont exprimées en t.yr^{-1} par exemple. Elles correspondent donc à une fraction plus ou moins importante du flux de sédiments transitant par le réseau hydrographique jusqu'au niveau du point de mesure sur le profil longitudinal de la rivière pendant l'intervalle de temps de la prise de mesure. La quantité de sédiment transitant dans le système peut être convertie en quantité de matériel érodé dans le bassin versant amont et ainsi fournir des taux moyens de productivité (t.km^{-2}.yr^{-1}). Cette estimation de la productivité peut être affinée en tenant compte des caractéristiques topographiques

(pente), lithologiques (type de roche et de sol), présentes dans le bassin versant mais aussi les processus d'érosion majeurs et le type de couvert végétal. Des zones de productivité différentes pourront ainsi être identifiées sur l'ensemble du bassin versant (eg. Hicks et Shankar, 2003). Ensuite, par conversion des quantités en volumes par l'utilisation des masses volumiques caractéristiques des roches érodées, il est possible de remonter aux valeurs de flux aux estimations de taux dénudation (mm.yr-1).

…à long terme :

L'estimation de l'érosion et des flux sédimentaires à l'échelle des temps géologiques (10^3 à 10^8 ans) peut être abordée de deux manières différentes. La première se concentre sur l'estimation de l'érosion dans les principales zones sources par l'évaluation de l'exhumation. Il est alors considéré, pour estimer les taux d'érosion, que l'érosion contre balance la surrection et que le relief est à l'équilibre. Cette dernière est obtenue par les méthodes d'analyses géochimiques quantificatives des éléments cosmogéniques et radiogéniques. Les premiers, les isotopes cosmogéniques, apparaissent dans les minéraux lorsque ces derniers approches la surface et qu'ils sont collisionnés par le flux particulaire cosmique secondaire. Ainsi, pour le quartz, ^{28}Si et ^{16}O se transforment progressivement en ^{26}Al et ^{10}Be par spallation. La quantification de ces éléments permet de déterminer l'âge d'une surface (âge d'exposition au rayonnement), les taux d'exhumation passés et donc d'érosion des derniers milliers d'années. Pratiquement, plus l'érosion est rapide dans une zone donnée, moins la quantité d'élément cosmogéniques est importante et inversement pour les zones à faible érosion. Cette méthode peut être appliquée pour déterminer l'âge d'une surface et estimer un taux d'érosion local au niveau d'un site d'échantillonnage, ou un taux moyen de l'ensemble d'un bassin versant, par analyse des sédiments transportés dans les rivières (pondération naturelle effectuée par les rivières) et l'estimation du temps de résidence des quartz (van Blanckenburg, 2005; Granger, 2007). Il est aussi possible de dater, via ces éléments, l'âge de dépôts spécifiques tels que les terrasses ou les moraines, dont la formation documente un état particulier du relief (Anderson et al., 1996 ; Perg et al., 2001). Les éléments radioactifs (U-Th) sont utilisés, de concert avec l'hélium, pour caractériser la thermochronologie des apatites. Ainsi, l'hélium produit par la désintégration des radio-nucléides de la chaîne (U-Th) ne se concentre dans les apatites qu'en deçà de c. 70-75°C. Cette température correspond à un passage au dessus d'une profondeur variant, suivant le contexte tectonique et thermique, entre 1 et 3 km. La quantification de l'hélium permet ainsi de définir le temps passé entre l'isotherme c. 70°C et la surface, et donc la vitesse d'exhumation (Ehlers et Farley, 2003).

Dans les apatites et les zircons, la désintégration de l'Uranium provoque également la création de traces de fission qui peuvent être utilisée en thermochronologie. Celles-ci sont progressivement réparées lorsque la température est supérieure à 90 ± 30°C pour les apatites et 240 ± 50°C pour les zircons (suivant composition chimique). En deçà de ces gammes de températures et par conséquent, au dessus de leurs équivalences en profondeur, les traces de fissions persistent et leur nombre croît avec le temps. Ainsi, il est possible de déterminer les taux d'exhumation et d'érosion des roches, d'après le nombre de traces de fissions préservées (Gallagher, 1995 ; Kamp, 1999).

La deuxième approche pour estimer les flux sédimentaires et les taux d'érosion consiste à établir des bilans sédimentaires volumétriques dans les bassins qui reçoivent les produits de l'érosion. Il est pour cela nécessaire de disposer d'une connaissance détaillée de la stratigraphie, de la géométrie tridimensionnelle du remplissage du bassin, des modalités de dépôt et de distribution et de disposer d'une chronostratigraphie précise. Il est alors possible de déterminer la valeur des volumes déposés et préservés par intervalles de temps dans le bassin. En considérant que la quantité de sédiments déposés par incréments de temps reflète la quantité de matériel érodé et transféré, le flux sédimentaire préservé, le taux de productivité et/ou le taux d'érosion peuvent être déterminés en tenant compte des valeurs de compaction, porosité et/ou densité du matériel érodé et préservé (Hay et al., 1988 ; Pazzaglia et Brandon, 1996 ; Foster et Carter, 1997 ; Métivier et al., 1998 ; Collier et al, 2000 ; Walford et al., 2005 ; Orpin et al., 2006).

1.1.3. La représentativité des valeurs d'érosion et de flux sédimentaire :

Si la variété et l'apparente exhaustivité des paramètres et processus mesurés et estimés par les différentes techniques semblent pouvoir permettre une compréhension approfondie de l'évolution des reliefs, elles révèlent aussi un manque d'homogénéité dans les dimensions mesurées (processus), dans les échelles spatio-temporelles abordées (actuel, temps géologiques), mais aussi le problème de leur représentativité.

Tout d'abord, concernant la quantification des flux actuels, il est important de préciser que l'essentiel des valeurs produites ne correspond qu'à une mesure de la charge suspendue et qu'il ne tient que rarement compte de la charge de fond et de la charge dissoute. Les valeurs de flux actuels sous-estiment donc les flux totaux réels dans des proportions pouvant avoisiner 50 % (Galy et France-Lanord, 2001). De plus, les mesures s'effectuant sur de courtes durées, il se pose le problème de la pertinence des valeurs obtenues. En effet, compte tenu de la forte

variabilité des flux (débit et charge) observables dans les rivières, une mesure unique pourra tour à tour sur- ou sous-estimer les valeurs de flux. De manière générale, il est considéré que les mesures de flux tendent à sous-estimer les flux à plus long termes d'un ordre de grandeur (Kirchner et al., 2001) car l'essentiel du matériel érodable ou stocké à l'intérieur du système est érodés et/ou remobiliser lors d'évènement catastrophiques extrêmes (Kirchner et al., 2001 ; Dadson et al., 2003) (Fig. 1.17). Ces évènements extrêmes, qui sont susceptibles de libérer et transporter de grande quantité de sédiments, comme les cyclones majeurs et les séismes importants, ont des périodes de récurrence qui dépassent souvent l'intervalle de temps couvert par les mesures. Enfin, étant donné la ponctualité spatiale des mesures de flux, celles-ci négligent le possible stockage interne amont (colluvions, plaines d'inondation) et par conséquent, ne rendent pas fidèlement compte de la dynamique des reliefs. Il existe donc un sous échantillonnage systématique des flux sédimentaires actuels, qui ne peut être négligé que dans les cas où la fréquence des évènements extrêmes est suffisamment forte et les caractéristiques géomorphologiques appropriés (reliefs forts, lithologie peu résistante) pour permettre la « vidange » régulière du système. Parallèlement, la signification de valeurs de flux sédimentaires actuels est souvent biaisée par l'influence anthropique, comme décrit précédemment. Déforestation et pratiques agricoles tendent à augmenter artificiellement le flux sédimentaire alors que la présence d'un barrage résulte dans un stockage massif des produits de l'érosion. L'impact anthropique est ainsi particulièrement difficile à quantifier et à soustraire des résultats quand il est question de quantifier l'influence des paramètres naturels.

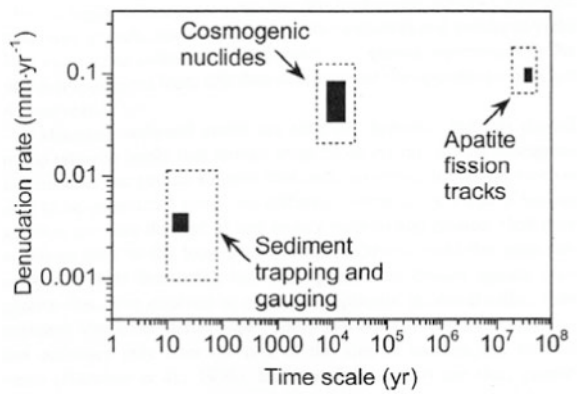

Figure 1.17 : Taux d'érosion estimés dans plusieurs bassins versants à lithologie granitique de l'Idaho à partir de différentes méthodes (mesures de flux et bilans volumétriques, isotopes cosmogéniques et traces de fissions) relatives à des échelles de temps distinctes (10-10^2 ans, 10^4-10^5 ans et 10^7-10^8 ans respectivement). Le cadre en pointillés correspond à l'erreur analytique. Les valeurs estimées sur le court terme (10-10^2 ans) sous-estiment les taux d'érosion établis pour le long terme (Kirchner et al., 2001).

Comme décrit précédemment, l'estimation de l'érosion et des flux, à l'échelle des temps géologiques, est abordée par des méthodes de géochimie quantitative et par les bilans sédimentaires.

Concernant les méthodes géochimiques, faisant intervenir les isotopes stables (cosmogéniques) et radioactifs ((U-Th)/He ; traces de fission), un premier problème est la pertinence d'un échantillon ponctuel lorsque l'on considère la variabilité spatiale des processus de surrection et de taux d'érosion. De plus, en thermochronologie, l'âge du passage d'une isotherme n'a de sens en terme de taux d'exhumation que si le contexte tectonique, le trajet des grains et l'histoire thermique sont contraints. De plus, Braun (2002) a montré que le relief et son évolution ont une incidence sur la géométrie des isothermes jusqu'à une profondeur qui dépend de la longueur d'onde et de l'amplitude du relief. Alors il est délicat d'interpréter un âge de fermeture d'un système comme un âge de passage à une profondeur données, et donc, d'en déduire un taux d'exhumation significatif. L'attribution d'un âge significatif aux dépôts fluviatiles (terrasses) par l'analyse des isotopes cosmogéniques implique que les grains n'aient pas résidés sur des surfaces d'érosion sur de longues périodes, par exemple. On remarque donc que la signification d'un âge cosmogénique ou thermochronologique dépend surtout des modèles établis préalablement pour caractériser le comportement du système étudié.

Les estimations des flux sédimentaires par les bilans volumétriques se heurtent à de nombreuses limites. Ainsi, pour fournir des valeurs compréhensive de flux préservés dans les bassins, qui soient représentatives des flux sédimentaires réels, il est nécessaire de connaître la géométrie tridimensionnelle détaillée du remplissage, la lithologie des dépôts, leur degré de compaction, la chronostratigraphie précise, la proportion de recyclage au cours du temps, la part issue de la production biogénique, le stockage interne et les fuites potentielles liées aux pertes hors du système (circulation océanique, turbidites, charge dissoute…). Tous ces paramètres sont parfois difficiles à déterminer et à contraindre, particulièrement dans les zones de convergence à cause du manque de données disponibles et de la préservation limitée par la déformation (Fig. 1.18).

La présente étude étant basée sur une analyse qualitative et quantitative du remplissage de bassin, dans le but de remonter à la dynamique des flux sédimentaire d'un domaine tectoniquement actif d'avant arc, les paramètres cités précédemment doivent être pris en compte.

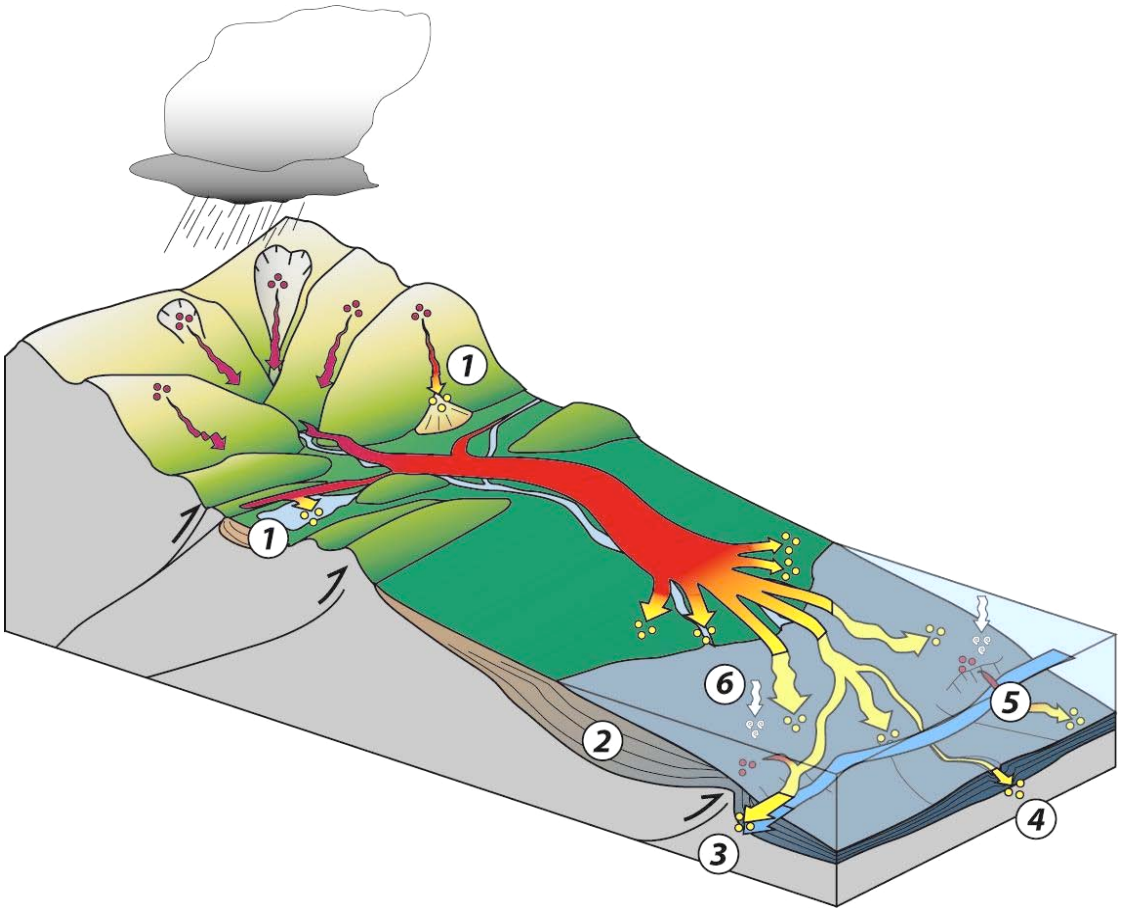

Figure 1.18 : Bloc diagramme schématique rappelant les éléments à prendre en compte lors de l'établissement de bilans volumétriques dans une zone tectoniquement active : 1) stockage interne dans des sous bassins(endoréiques ou connectés), ou sous forme de colluvions et cônes de débris ; 2) géométrie tridimensionnelle (volumes) du remplissage (séquences de dépôt), lithologie, faciès sédimentaire, porosité, chronostratigraphie précise ; 3) pertes par exportation associée à la circulation de courants océaniques ; 4) pertes liées aux courants de turbidité ; 5) Recyclage des sédiments érodés au sein du bassin et qui entraîne une sous estimation des volumes entrants anciens et une sur estimations des flux entrants plus récents ; 6) part de la production biogénique.

1.2. Les subductions océan - continent :

1.2.1. Généralités sur les subductions :

La lithosphère terrestre est constituée de 12 plaques tectoniques principales se déplaçant les unes par rapport aux autres (Fig. 1.19). Ce phénomène de « dérive des continents » énoncé par Wegener (1912) est principalement fonction de la dynamique convective du manteau terrestre. La conséquence de ces mouvements relatifs, sachant que le volume terrestre reste constant, est l'existence de trois types de frontières de plaques (Fig. 1.20):

- Les zones de divergence, qui correspondent aux zones d'accrétion des dorsales océaniques.
- Les zones transcurrentes, qui sont caractérisée par un glissement ou coulissage de deux plaques le long de failles transformantes ou décrochantes.
- Les zones de convergence, qui correspondent aux zones de subduction et de collision. La collision est le stade final de la convergence et marque la fermeture d'un domaine océanique.

Les zones de subduction sont caractérisées par l'enfoncement d'une plaque lithosphérique dans le manteau, sous une autre plaque de densité moindre. Elles font intervenir les deux types de lithosphère (océanique et continentale) et présentent ainsi différentes combinaisons. Les subductions peuvent être regroupées en deux catégories que sont les subductions océaniques (1 et 2) et les subductions continentales (3 et 4). Une subduction peut être du type (1) océan \ océan (15% des cas de subduction), comme c'est le cas pour la subduction des Mariannes (plaque Pacifique sous plaque Philippines) ou l'arc des Antilles (plaque Atlantique sous plaque Caraïbes) ; (2) océan \ continent (67% des cas) , comme la subduction andine (plaque Pacifique sous Amérique du Sud) ou la subduction Hikurangi en Nouvelle-Zélande (plaque Pacifique sous plaque Australienne) ; (3) continent \ continent (17% des cas), lorsque la convergence se prolonge après la collision, comme c'est le cas pour l'Himalaya (plaque Indienne sous plaque Eurasienne) ; et (4) continent \ océan (1% des cas), encore appelé obduction (ex : Oman) (Lallemand et al., 2005).

Une classification des subductions océaniques en deux catégories mêlant l'âge de la plaque plongeante, la nature de la plaque chevauchante, l'importance du couplage entre les deux plaques et d'autres paramètres (Fig. 1.21) est proposée par Uyeda et Kanamori (1979). Deux

types de subductions sont présentés et illustrés par deux cas naturels que sont la subduction des Mariannes (océan – océan ; plaque océanique inférieure vieille et dense ; faible couplage entre les plaques ; panneau plongeant fortement pentu ; faible séismicité ; pas de prisme d'accrétion) et celle du Chili (continent – océan ; plaque océanique jeune et peu dense ; fort couplage entre les plaques ; panneau plongeant faiblement pentu ; forte séismicité ; développement d'un prisme d'accrétion). La première est alors qualifiée de « subduction spontanée » et la deuxième, de « subduction forcée ». Cette classification n'est basée que sur deux cas qui s'opposent selon un grand nombre de critères mais ne rends pas compte de la diversité naturelle observée dans les zones de subduction. Plus récemment, Heuret et al. (2003) et Lallemand et al. (2003) ont noté qu'il existe une corrélation entre pendage de la plaque plongeante et le régime tectonique dominant observable dans la plaque supérieure. Ainsi, à des plaques plongeantes à fort pendage correspondent des plaques supérieures dominées par l'extension et à des plaques plongeantes à faible pendage correspondent des plaques supérieures dominées par la compression. Une autre classification se base sur la différentiation des marges en accrétion tectonique et celles en érosion tectonique. Les marges en accrétion tectonique sont reconnaissables par la présence d'un prisme d'accrétion sédimentaire. Le prisme se forme à partir la dissociation des sédiments présents sur la plaque plongeante lorsque le chevauchement frontal se développe à leur base, dans la fosse de subduction (Fig. 1.22a). Les prismes d'accrétion forment des systèmes plus ou moins développés de chevauchements successifs. Il apparaît que les prismes d'accrétion et par conséquent, l'accrétion tectonique, se forment lorsque des apports sédimentaires suffisants existent (Collot et al., 1996 ; Ranero et al., 2006). L'accrétion tectonique se déroulera donc préférentiellement au pied des subductions océan – continent, le continent servant de source de sédiments. Dans les cas de marges en érosion tectonique, le passage de la plaque plongeante opère un effet de rabot sur la base de la plaque chevauchante et lui arrache du matériel qui est entraîné dans le manteau. Ces marges sont souvent caractérisées par la présence de tectonique extensive et de subsidence au sein de la plaque chevauchante (Fig. 1.22b). La présence de monts sous-marins sur la plaque subduite peut favoriser l'érosion tectonique lors de leur entrée en subduction. Il est important de noter qu'une même zone de subduction peut présenter une transition géographique entre un domaine dominé par l'érosion tectonique et un autre dominé par l'accrétion tectonique (eg. subduction chilienne – Ranero et al., 2006 ; subduction néo-zélandaise – Collot et al., 1996)

Il demeure que l'éventail de configurations des subductions existantes à travers le monde montre une telle diversité qu'il semble difficile de développer des classifications par essence trop simplificatrices.

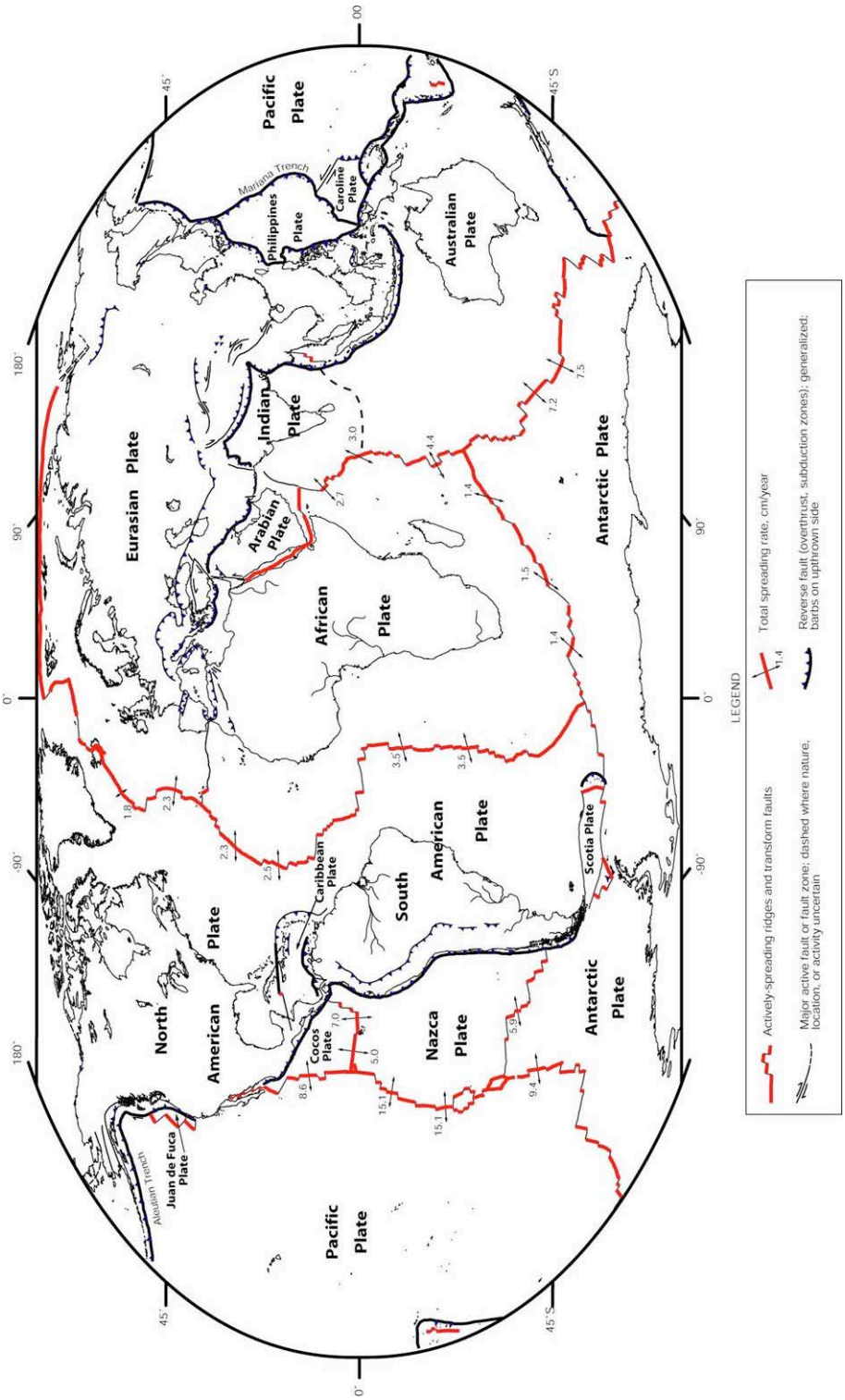

Fig. 1.19 : Carte représentant la répartition des plaques tectoniques principales et précisant la nature de leurs frontières (convergentes, divergentes, décrochantes). Les taux d'expansion au niveau des dorsales sont indiqués en cm/yr. Carte modifiée et simplifiée d'après Digital Tectonic Activity Map of the Earth – Tectonism and Volcanism of the last One Million Years DTAM – 1 (NASA / Goddard Space Flight Centre, 2002). Projection Robinson.

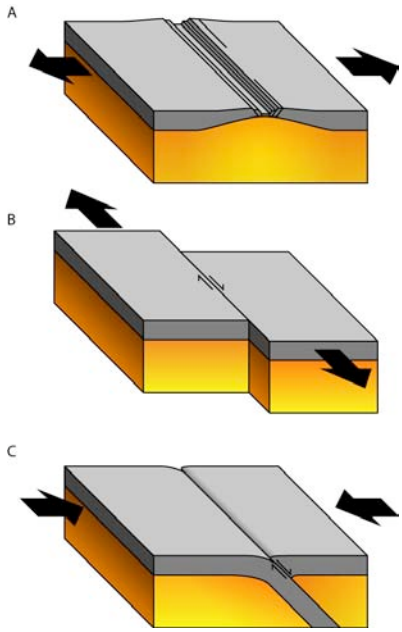

Figure 1.20: Schémas représentant les trois types de frontières de plaques tectonique. La partie supérieure représente la lithosphère (croûte et manteau lithosphérique) et la partie inférieure représente la portion supérieure de l'asthénosphère. (A) frontière divergente caractérisée par de l'extension l'accrétion au niveau d'une dorsale ; (B) frontière transcurrente caractérisée par le glissement entre plaque le long d'un décrochement ou d'une faille transformante ; (C) frontière convergente caractérisé par une zone de subduction.

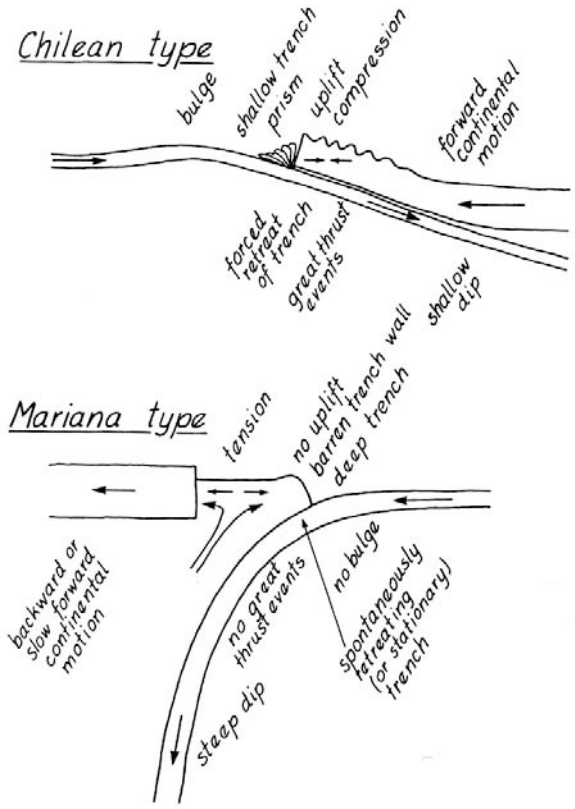

Figure 1.21 : Deux types de zones de subduction à critères opposés et illustrés par deux exemples naturelles : la subduction « forcée » du Chili et la subduction « spontanée » de la fosse des Mariannes (Uyeda et Kanamori, 1979).

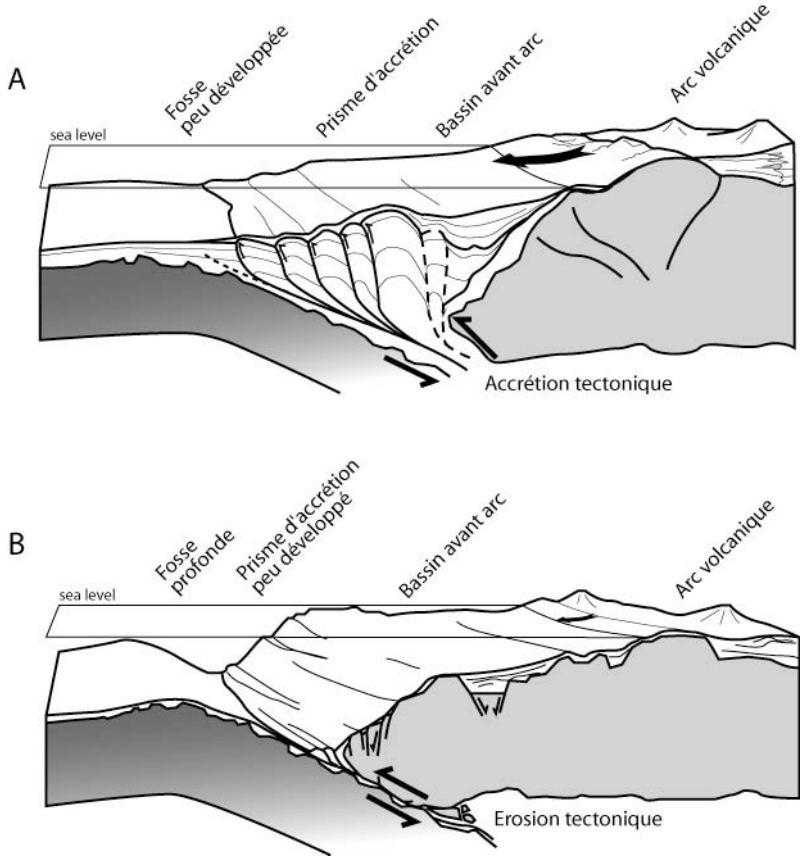

Figure 1.22 : modèles théoriques de subductions océan – continent : (A) subduction avec accrétion tectonique, formation d'un prisme d'accrétion et raccourcissement dans la croûte chevauchante ; (B) subduction avec érosion tectonique et extension dans la croûte chevauchante. La flèche noire sur la topographie représente l'intensité des apports sédimentaires. Modifié d'après Moberly et al. (1982)

1.2.2. Eléments morphostructuraux des subductions océan - continent :

Les subductions océan – continent sont généralement constituées d'éléments structuraux caractéristiques plus ou moins développés suivant le contexte et dont la présence n'est cependant pas systématique. Ces éléments sont, de l'océan vers le continent : la fosse de subduction, le prisme d'accrétion et les bassins de pente, le bassin avant arc, l'arc structural et l'arc volcanique, le bassin d'avant pays (eg. Andes) et le bassin arrière arc extensif (Fig. 1.23).

L'évolution de ces domaines structuraux est complexe et dépend de paramètres internes (géométrie, taux de convergence, couplage des plaques, apports sédimentaires…) et externes (climat, niveau marin, circulation océanique…), et des interactions entre les différents domaines. La présente étude étant focalisée sur le domaine d'avant arc et son bassin, nous ne développerons ici que ce domaine structural.

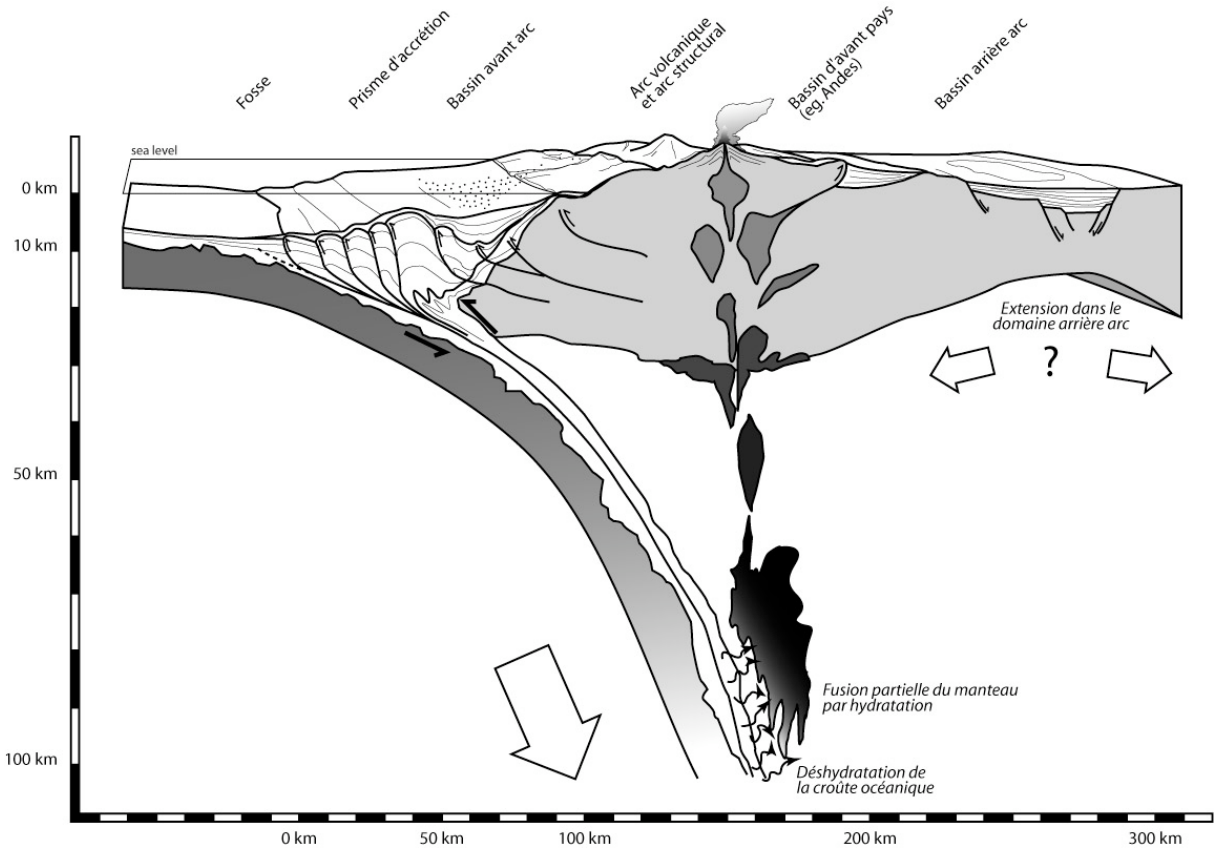

Figure 1.23 : Schéma idéalisé d'une subduction océan – continent, montrant les principaux éléments morphostructuraux pouvant apparaître au sein de la marge active. Exagération verticale ~2x.

Les bassins d'avant arc :

Les domaines d'avant arc sont situés entre le prisme d'accrétion et l'arc structural et / ou volcanique. Ils sont caractérisés par la présence de bassins sédimentaires dont les morphologies sont variées. Dickinson et Seely (1979) proposent une classification de ces morphologies, en fonction du remplissage complet ou non du bassin, de la morphologie de la marge (prisme et arc), et de sa position hypsométrique (Fig. 1.24). Huit types morphologiques sont ainsi différentiés. Cette diversité de configurations induit une grande variété dans la nature du remplissage sédimentaire. On notera que ce dernier peut évoluer d'un pôle à majorité continentale (eg. F et H Fig. 1.24) à un pôle marin profond (eg. C et D Fig. 1.24). Les profiles sismiques acquis sur les marges actives à travers le monde ont montrés que sur une même subduction, plusieurs type de bassins pouvaient coexister, comme le long de la subduction andine (Laursen et al., 2002) (Fig. 1.25). De manière générale, l'évolution spatiale

et/ou temporelle des bassins d'avant arc dépend (1) aux forçages tectoniques relatifs aux paramètres de la subduction (taux de convergence, relief et densité de la plaque subduite, l'accrétion ou l'érosion tectonique), (2) à la charge sédimentaire et le taux de sédimentation (flux sédimentaire) et à la position des exutoires, et (3) aux variations eustatiques (modification du profil de dépôt, partitionnement volumétrique) (eg. Coulbourne et Moberly, 1977 ; Dickinson, 1995 ; Einsele, 1992).

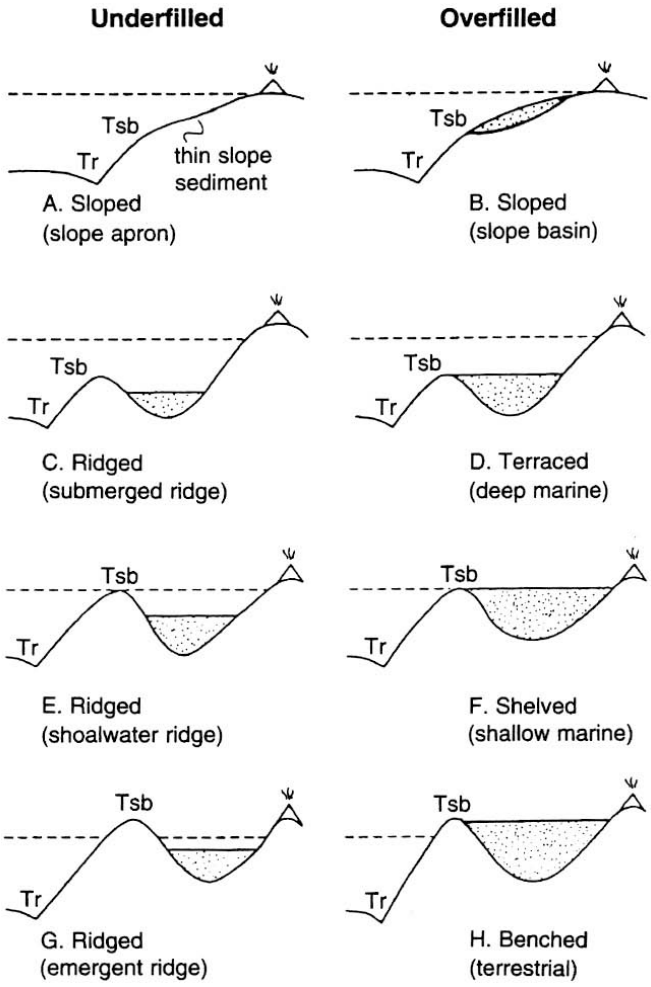

Figure 1 .24 : Différents types de morphologies de bassins d'avant arc. La colonne de gauche regroupe les morphologies caractérisées par un sous remplissage (Underfilled) et la colonne de droite regroupe les bassins caractérisés par un remplissage total de la dépression (Overfilled). La ligne en pointillés représente le niveau marin. Tr = trench (fosse) ; Tsb = Trench-slope break (rupture de pente et/ou bordure de plateforme). Exagération verticale non spécifiée. Modifié d'après Dickinson et Seely (1979) et Dickinson (1995).

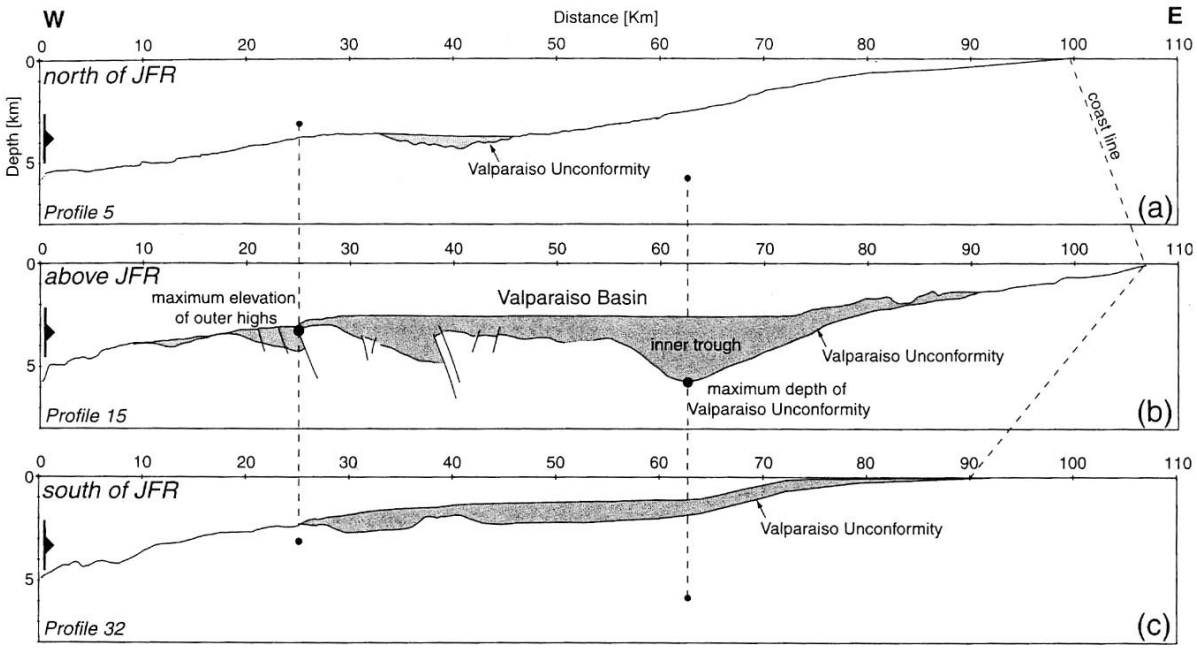

Figure 1.25 : Coupes schématiques réalisées à partir de l'interprétation de lignes sismiques acquises à travers la marge active chilienne et espacées d'environ 100 km . (a) faible remplissage profond (terrasse marine profonde) ; (b) remplissage important en profondeur (morphologie de type terrasse marine profonde totalement remplie) ; (c) remplissage important sur la plateforme et la pente. Exagération verticale ~2x. Modifié d'après Laursen et al.,(2002).

Ces quatre dernières décennies, de nombreuses études se sont attachées à expliquer l'évolution des bassins avant arc (Coulbourne et Moberly, 1997 ; Lewis et Hayes, 1982, 1984 ; Laursen et al., 2002 ; Normack, 2003). La plupart des modèles mettent le paramètre tectonique en avant pour expliquer l'évolution des bassins et plus particulièrement la croissance des prismes d'accrétions en fonction des paramètres de la subduction (reliefs de la plaque océanique, subduction de monts sous-marins). Néanmoins, il apparaît que la plupart de ces modèles sont développés à partir de jeux de données relativement restreints et que les contraintes d'âges (chronostratigraphie) sont souvent très faibles. Ceci limite la quantification des processus dans le temps et l'espace. Quelques études fournissant un bon contrôle de la chronostratigraphie des bassins avant arc colombien (Mountney et Westbrook, 1997) et néo-zélandais (Barnes et al., 2002 ; Barnes et Nicol, 2004) offrent des opportunités de développer des modèles d'évolution mieux contraints.

D'une manière générale, le manque de contraintes sur l'âge et la géométrie du remplissage peuvent être relié au problème d'accessibilité de l'enregistrement sédimentaire des bassins avant arc. En effet, ces derniers sont souvent immergés à forte profondeur (terrasses profondes) ce qui limite les investigations géologiques directes (pas d'affleurement) et indirectes (forages). Les données géophysiques (profils sismiques essentiellement), seules

capables dans ces conditions, de rendre compte des géométries du remplissage, doivent être densément distribuées.

Chapitre 2 :

La subduction Hikurangi

2.1. La subduction Hikurangi :

Cette section est une présentation générale et non exhaustive de la subduction Hikurangi. Les principaux éléments de sa morphostructure y sont présentés, ainsi que l'évolution de la subduction. Une attention particulière est portée sur les évènements Plio-Pleistocènes, qui ont conduit la marge vers sa morphologie actuelle.

2.1.1. Cadre géodynamique:

La subduction Hikurangi fait partie des zones de subductions qui marquent la frontière convergente des plaques Pacifique (PAC) et Australienne (AUS) dans le sud-ouest de l'océan Pacifique (Fig. 2.1). La convergence est marquée au nord, par la subduction PAC sous AUS et au sud par la subduction AUS sous PAC, séparées par une zone de collision intracontinentale oblique développée sur le décrochement dextre majeur de la faille Alpine. La subduction PAC \ AUS montre deux zones différentes avec une subduction océan – océan (Kermadec) au nord et une subduction océan – continent au sud (Hikurangi). C'est cette dernière qui nous intéresse ici. D'environ 1000 km de long, la marge de la subduction Hikurangi se développe le long de la côte est de l'Île Nord de Nouvelle-Zélande. La convergence des deux plaques se fait obliquement à des vitesses qui varient depuis le nord vers le sud, de ~ 47 mm/yr à ~ 42 mm/yr (Beavan et al., 2002) (Fig. 2.2). La subduction s'initie au Miocène inférieur (c. 25 Ma) et se prolonge jusqu'à l'actuel, avec des phases d'extension superficielle et d'inversion des structures, dont les causes sont toujours débattues (Ballance, 1976 ; Pettinga, 1982 ; Field et al., 1997 ; Chanier et al., 1999 ; Barnes et al., 2002 ; Barnes et Nicol, 2004 ; Nicol et al. 2007 ; Nicol et Wallace, 2007). Le taux de raccourcissement a connu une augmentation significative vers ~1.5 Ma et s'est stabilisé depuis (Barnes et Nicol, 2004 ; Nicol et al., 2007 et Nicol et Wallace, 2007).

La plaque Pacifique :

Au droit de la subduction Hikurangi, la plaque pacifique est caractérisée par une zone de croûte océanique épaissie de 10 à 15 km : le Plateau Hikurangi (Fig. 2.1). Ce plateau, d'âge Crétacé, résulte d'une période de magmatisme intense de la dorsale pacifique, ou d'un point chaud (Hoernle et al., 2004 ; Taylor, 2006). Il pourrait constituer une portion d'un ancien plateau géant, regroupant les plateaux de Ontong Java, Manihiki et Hikurangi (Taylor,

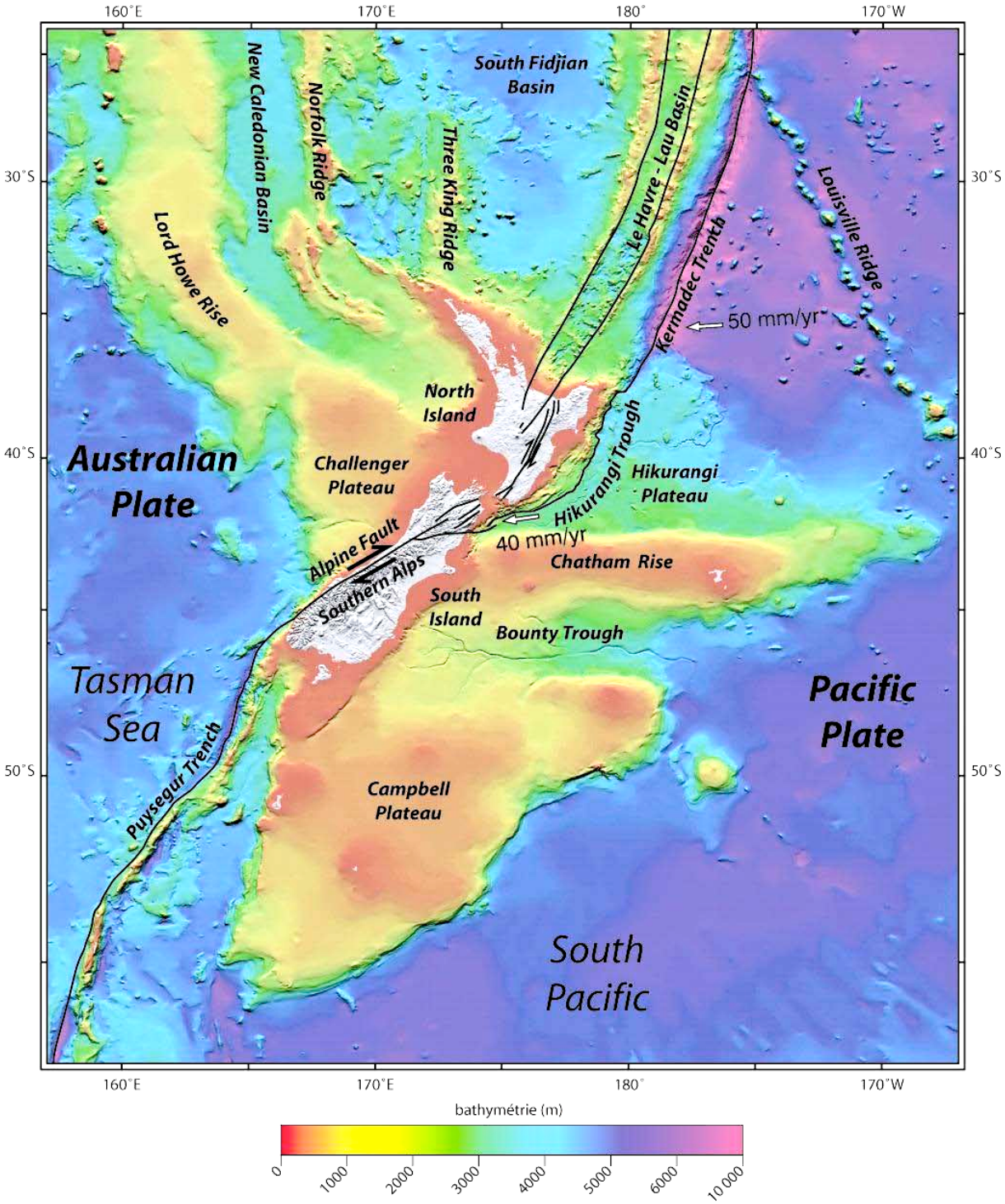

Figure 2.1 : Carte du relief marin autour de la Nouvelle-Zélande, mettant en évidence la trace de la frontière des plaques Australienne et Pacifique et la position de la subduction Hikurangi, le long de la côte est de l'Île Nord. Vecteur et vitesse de convergence relative d'après Beavan et al. (2002). Carte modifiée d'après CANZ (1996).

2006). Il est limité au sud par la ride de Chatham, au nord-est, par une falaise sous-marine d'environ 1000 m. Il entre en subduction à l'ouest sous la marge Hikurangi et sous la partie sud de la fosse de Kermadec. De nombreux monts sous-marins sont présents sur le plateau et certains percent la couverture sédimentaire et deviennent visibles sur les données bathymétriques Wood et Davy (1994). Ces monts sous-marins entrent en subduction sous la marge Hikurangi, qu'ils déforment (Collot et al., 2001 ; Lewis et al., 2004). La fosse de subduction est très peu prononcée et constitue la dépression d'Hikurangi (Fig. 2.1). Elle évolue depuis des bathymétries de 2500 m au sud, à 3500 m au nord. Cette particularité s'explique par le faible angle de plongement de la plaque Pacifique ~ 6° (Ansell et Bannister, 1996) et la forte épaisseur des sédiments accumulés dans la fosse (2 à 3 km – Lewis et Pettinga, 1993). La dépression est parcourue par un chenal sinueux parallèle à la marge par lequel transitent les sédiments majoritairement issus de l'érosion des Alpes du Sud (Lewis et Pantin, 2002) et qui comblent la fosse (Fig. 2.2).

Figure 2.2 : Agencement des éléments morphostructuraux de la marge active de la subduction Hikurangi. (A) Carte de la marge active de la subduction Hikurangi montrant l'affrontement des plaques Pacifique et Australienne. Les différents éléments morphostructuraux sont identifiés et leur juxtaposition en bandes parallèles au chevauchement principal est mise en évidence. Les structures figurant sur la carte affectent les séries du Miocène à l'actuel et sont issues de nombreux travaux antérieurs compilés par Nicol et al., 2007). Les vecteurs représentent les vitesses relatives de convergence des deux plaques (Beavan et al., 2002). (B et C) Coupes lithosphériques montrant le plongement de la plaque Pacifique sous la plaque Australienne et la répartition des éléments morphostructuraux. En noir, la croûte océanique de la plaque Pacifique. En grisé, le socle continental de la plaque Australienne. En blanc, les sédiments du prisme d'accrétion et des bassins des domaines avant arc et arrière arc. Abréviations des coupes : KMFZ : Kapiti-Manawatu Fault Zone ; WF : Wellington Fault ; MF : Mohaka Fault ; Ruahine Fault. Localisation des coupes Fig. 2.2a. Carte et coupes modifiées d'après Beanland, 1995 ; Begg et Mazengarb, 1996 ; Barnes et al., 2002 ; Nicol et al., 2007.

A

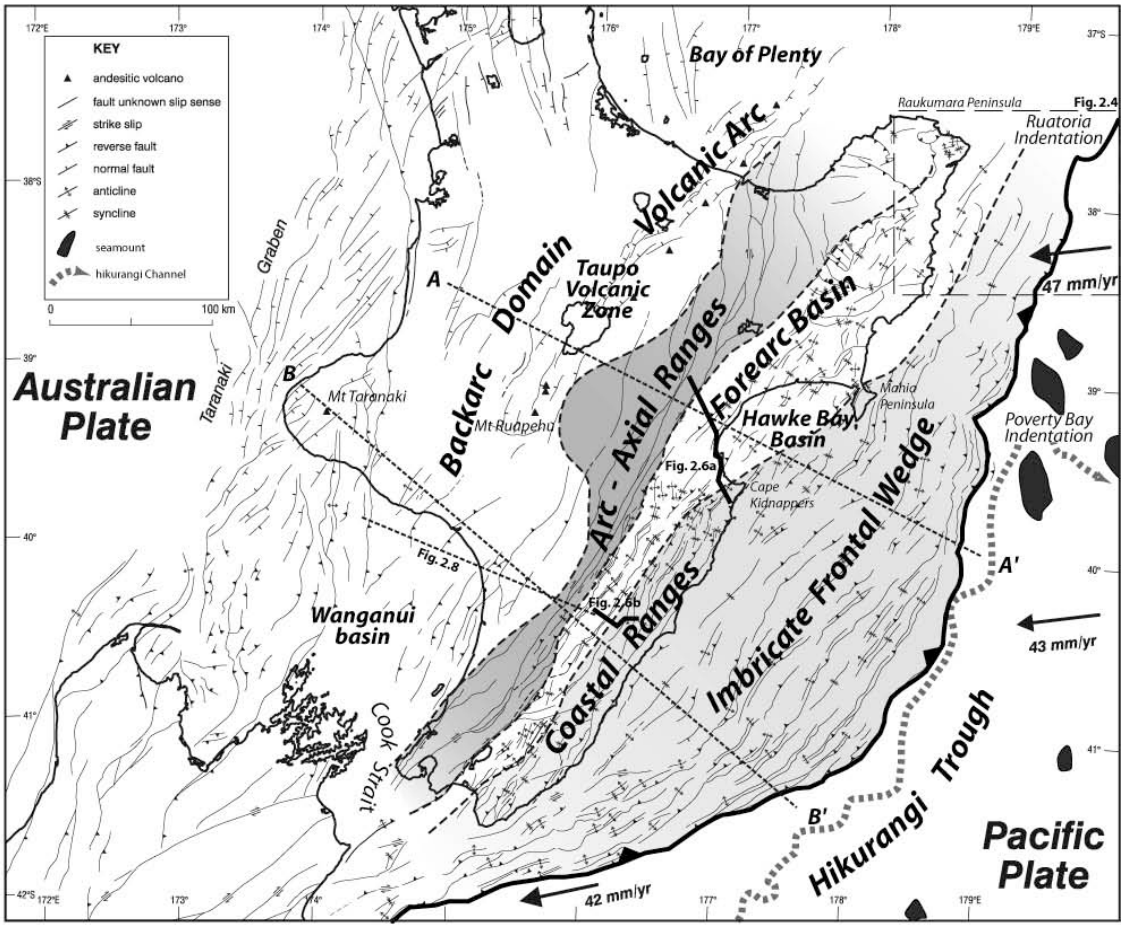
KEY
andesitic volcano
fault unknown slip sense
strike slip
reverse fault
normal fault
anticline
syncline
seamount
hikurangi Channel
0
100 km
Australian Plate
Pacific Plate
Bay of Plenty
Volcanic Arc
Taupo Volcanic Zone
Backarc Domain
Graben
Taranaki
Mt Taranaki
Mt Ruapehu
Arc - Axial Ranges
Forearc Basin
Hawke Bay Basin
Mahia Peninsula
Raukumara Peninsula
Fig. 2.4
Ruatoria Indentation
Poverty Bay Indentation
Fig. 2.6a
Cape Kidnappers
Fig. 2.8
Fig. 2.6b
Wanganui basin
Cook Strait
Coastal Ranges
Imbricate Frontal Wedge
Hikurangi Trough
47 mm/yr
43 mm/yr
42 mm/yr
A
A'
B
B'

B

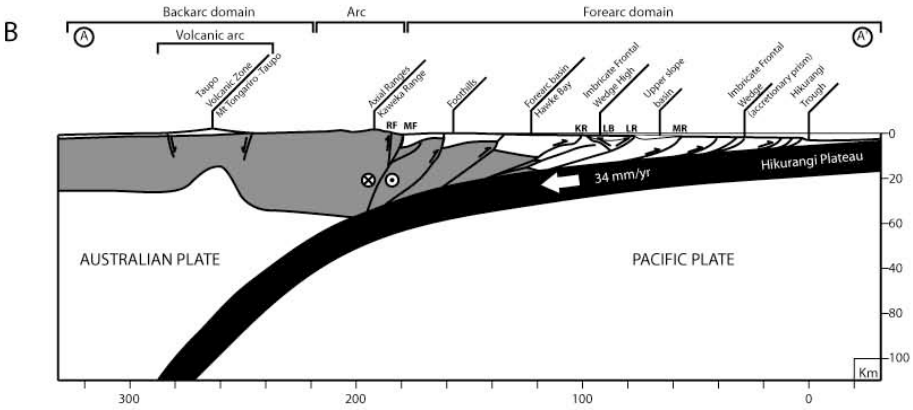
Backarc domain
Arc
Forearc domain
Volcanic arc
Taupo Volcanic Zone
Mt Tongariro
Mt Taupo
Axial Ranges
Kaweka Range
Foothills
Forearc basin
Hawke Bay
Imbricate Frontal Wedge High
Upper slope basin
Imbricate Frontal Wedge (accretionary prism)
Hikurangi Trough
RF
MF
KR
LB
LR
MR
34 mm/yr
Hikurangi Plateau
AUSTRALIAN PLATE
PACIFIC PLATE
Km
300
200
100
0
20
60
40
80
100

C

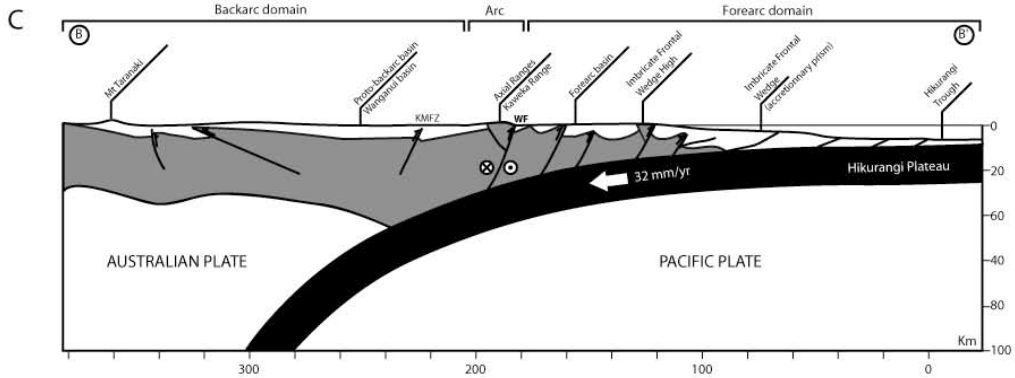
Backarc domain
Arc
Forearc domain
Mt Taranaki
Proto-backarc basin Wanganui basin
KMFZ
Axial Ranges
Kaweka Range
WF
Forearc basin
Imbricate Frontal Wedge High
Imbricate Frontal Wedge (accretionary prism)
Hikurangi Trough
32 mm/yr
Hikurangi Plateau
AUSTRALIAN PLATE
PACIFIC PLATE
Km
300
200
100
0
20
60
40
80
100

La plaque Australienne – La marge active Hikurangi :

Au niveau de la subduction Hikurangi, la plaque Australienne est caractérisée par une croûte continentale émergente, qui forme l'Île Nord de Nouvelle-Zélande. Depuis la fosse, la marge présente les éléments morphostructuraux suivants : (1) un prisme d'accrétion, (2) un bassin avant arc, (3) un arc structural, (4) un bassin arrière au nord, incluant (5) un arc volcanique et un bassin arrière arc juvénile au sud (Fig. 2.2).

- *Le prisme d'accrétion :*

La marge Hikurangi montre un large prisme d'accrétion de forme arquée qui s'étend sur près de 800 km, de la péninsule de Raukumara au nord, au détroit de Cook et au canyon de Kaikoura au sud (Pantin, 1963 ; Lewis, 1980 ; Lewis et Pettinga, 1993). Il se développe au dessus du panneau plongeant de la PAC et atteint une largeur maximale de 80 km au dans sa partie centrale (Lewis et Pettinga, 1993). Le décollement principal limite le front du prisme et le début de la marge, et forme la première ride en base de pente. La majorité des 2 à 3 km de sédiments de la dépression d'Hikurangi sont ici progressivement incorporés au prisme d'accrétion (Lewis et Pettinga, 1993). La morphologie générale du prisme montre une succession de rides d'anticlinaux de chevauchements parallèles au décollement principal séparant des bassins de pente (Lewis, 1980) (Fig. 2.3). Le remplissage sédimentaire de ces bassins est composé de sédiments pélagiques et peut atteindre une épaisseur de 2000 m. La stratification visible sur les profils sismiques montre un basculement des séries vers l'arc liée à la croissance des chevauchements (Lewis et Pettinga, 1993). Deux réentrants ou indentations majeurs (Poverty Bay et Ruatoria) sont visibles sur les données bathymétriques et sur le tracé du chevauchement principal de la subduction (Fig. 2.2). L'origine de ces indentations est attribuée aux perturbations morpho-tectoniques consécutives au passage de deux monts sous marin (Collot et al., 2001 ; Lewis et al., 2004 ; Bodger et al., 2006).

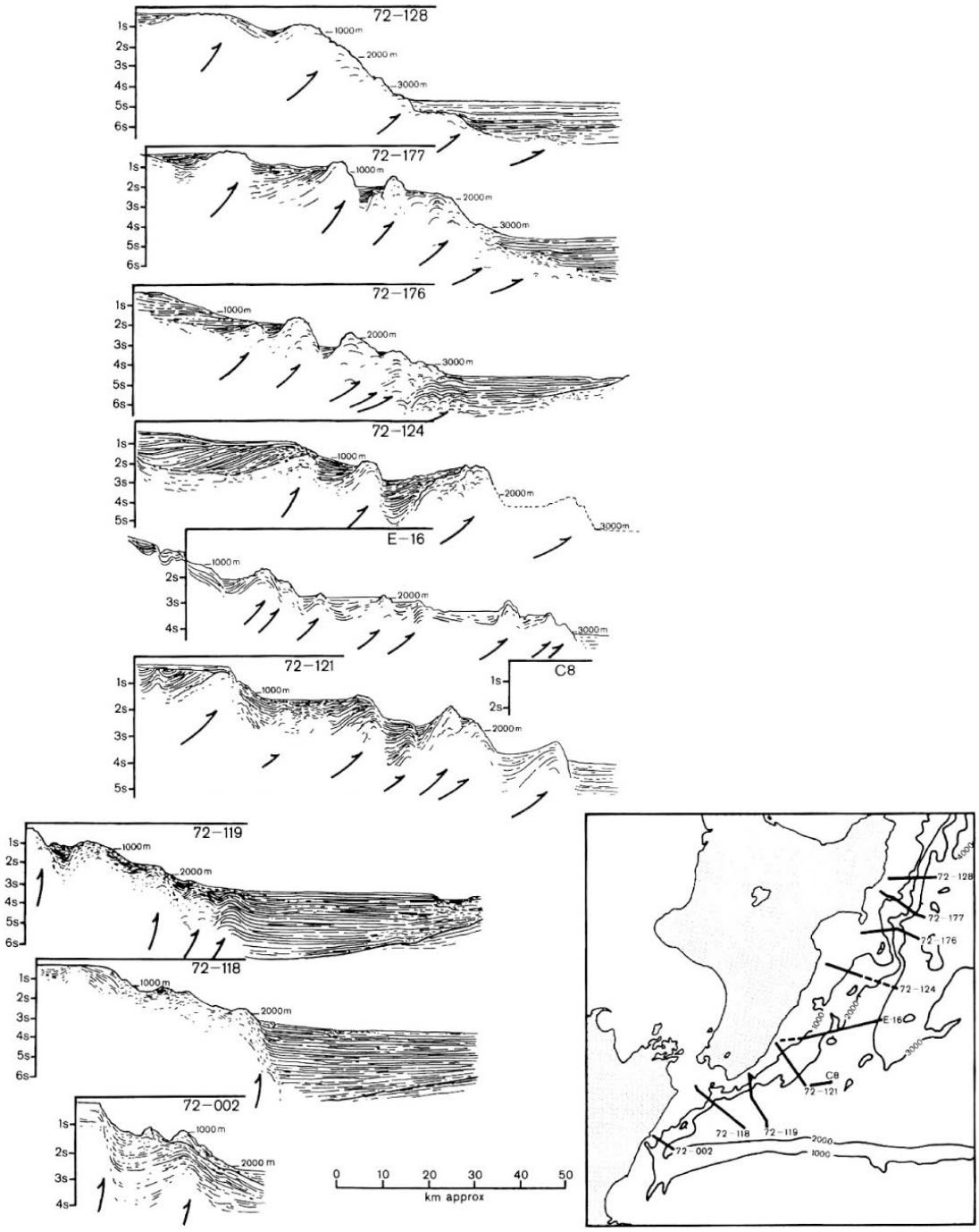

Figure 2.3 : Série de profiles sismiques interprétés du prisme d'accrétion montrant sa morphologie en rides et bassins de pente, depuis la plateforme (gauche) vers la dépression d'Hikurangi (droite) et du nord (haut) au sud (bas). Echelle verticale en seconde temps-double ; échelle horizontale approximative ; indication de profondeur en mètres, le long des profiles. Exagération verticale : 45° sur le dessin correspond à 6° dans la réalité. Modifié d'après Lewis (1980).

La formation du réentrant de Ruatoria s'est accompagnée d'une avalanche sous marine géante dont les débris totalisent une volume non compacté avoisinant les 3000 km^3 (Lewis et al., 2004 ; Lamarche et al., 2002 ; Fig. 2.4). La transition du prisme d'accrétion avec le bassin avant arc est constituée d'une juxtaposition de chevauchements qui émergent partiellement et

forment les chaînes côtières (altitude supérieure à 700 m). Ces dernières se terminent au sud, dans le canyon du détroit de Cook. Vers le nord, les chaînes côtières plongent sous Hawke Bay au niveau de Cape Kidnappers et émergent une dernière fois au niveau de la péninsule de Mahia. Elles plongent de nouveau au large de la côte est se termine à l'est de la péninsule de Raukumara (Fig. 2.2). La croissance du dos du prisme d'accrétion est documentée au Pliocène par la sédimentation de calcaires déposés à faible profondeur sur des crêtes anticlinaux (Caron, 2002). L'émersion des chaînes côtières se produit dans la continuité, au cours du Pléistocène comme en témoigne notamment les séries basculées du Kidnappers Group (< 1.0 Ma). Les taux de surrections estimés pour le dernier million d'années atteignent, voire dépassent 1 mm.yr^{-1} (Pillans, 1986) Le signal gravimétrique montre une nette anomalie positive qui coïncide avec la position du prisme d'accrétion (Fig. 2.5).

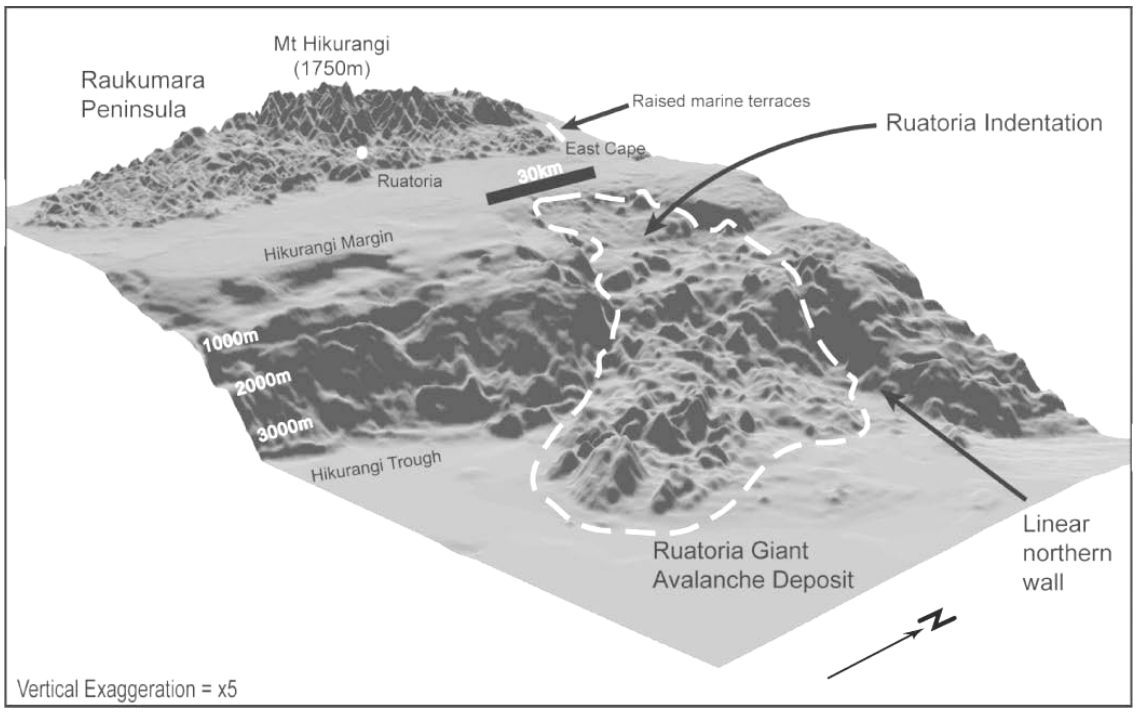

Figure 2.4 : Vue oblique de la bathymétrie et de la topographie au niveau de l'indentation et de l'avalanche géante de Ruatoria (localisation Fig. 2.2). Le mur linéaire nord (Linear northern wall) est interprété comme la trace d'impact créée lors de l'entrée en subduction d'un mont sous marin. L'instabilité consécutive a généré l'avalanche de débris de plus de 3000 km^3 (Modifié d'après Lewis et al., 2004).

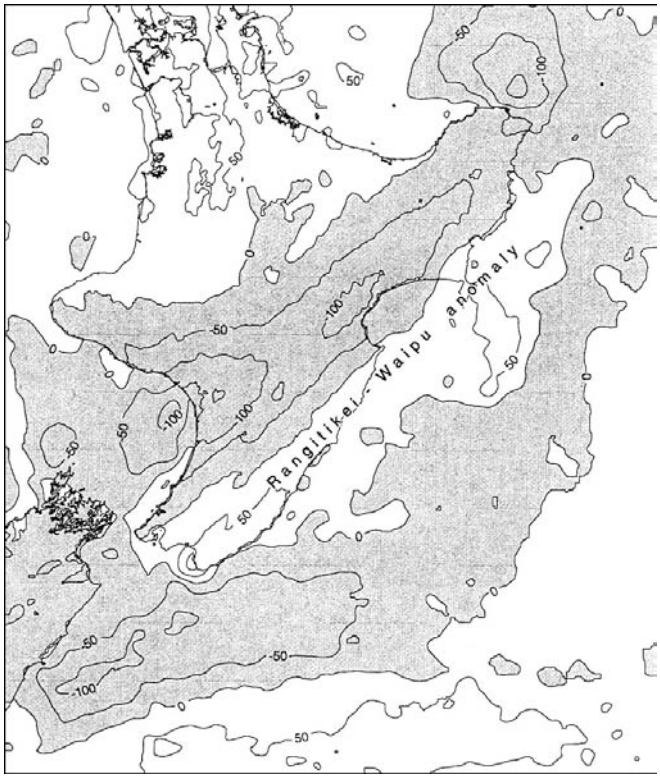

Figure 2.5 : Carte d'anomalie gravimétrique de Bouger (à terre) et à l'air libre (en mer) de la marge active Hikurangi. Notez la coïncidence entre la position de l'anomalie positive « Rangitikei – Waipu » et la positon du prisme d'accrétion. Carte modifiée d'après Field et al. (1997).

- *Le bassin avant arc :*

Le bassin avant arc s'étire entre les chaînes côtières du prisme d'accrétion et l'arc structural. Cette position entre deux domaines en surrection créé une subsidence relative qui permet l'accumulation des sédiments. Très étroit dans sa partie sud (~25 km), il s'élargi au niveau de Hawke Bay (~100 Km) puis s'aminci à son extrémité nord (Fig. 2.2 ; Fig. 2.6). Le bassin est à cheval sur les domaines marin et continental entre c. -100 m et c. + 300 m d'altitude. Le remplissage sédimentaire du bassin avant arc est constitué de 4000 à 6000 m de dépôts Miocène à actuel. La sédimentation évolue du Mio-Pliocène, dominé par des turbidites marines profondes (Pettinga, 1982 ; Harmsen, 1985 ; Francis 1993 ; Field et al., 1997 ; Barnes et al., 2002). Le Maximum d'accumulation de sédiments Mio-Pliocène est localisé dans la partie nord-ouest d'Hawke Bay (Francis et al., 2004). Au cours du Pléistocène, la sédimentation migre progressivement vers l'est et la position actuelle de Hawke Bay. Elle y est caractérisée par les dépôts marins peu profonds du Petane Group au niveau du Tangoio block (Haywick et al., 1991) puis évolue vers une alternance marin peu profond - fluviatile dont la section type est le Kidnappers Group (Kingma, 1971 ; Kamp, 1978 ; Field et al., 1997 ; Proust et Chanier, 2004). L'évolution récente du bassin avant arc est marquée par une

inversion des structures durant le Pléistocène avec des périodes d'intensification au court du dernier million d'années (Barnes et al., 2002 ; Barnes et Nicol, 2004).

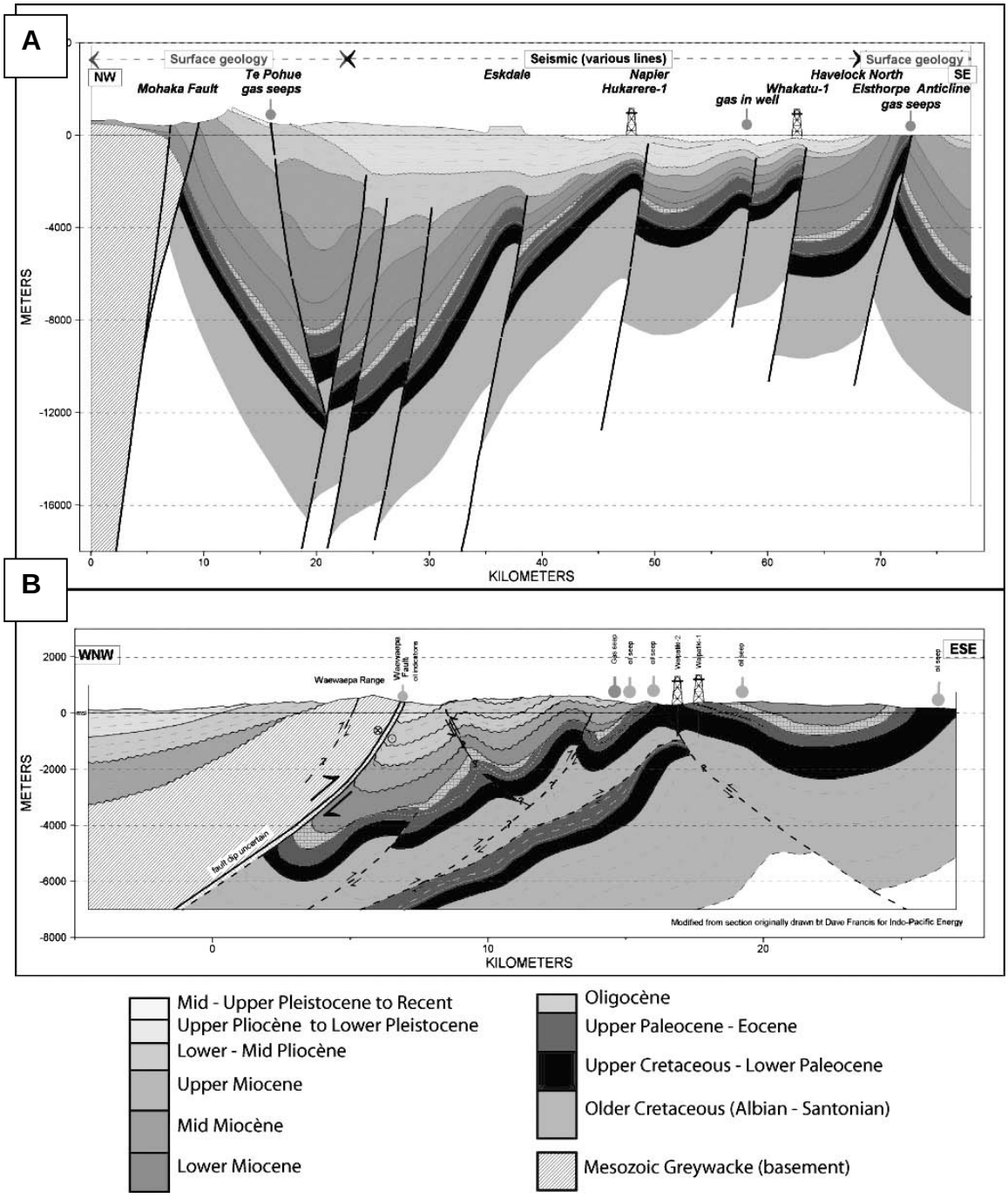

Figure 2.6 : Coupes géologiques régionales du bassin avant arc établies à partir de données géologiques et sismiques (localisation Fig. 2.2). (A) Coupe régionale à travers Hawke Bay, de la limite entre l'arc et l'avant arc à l'ouest (Faille de Mohaka) jusqu'au contreforts du prisme d'accrétion à l'est (Anticlinal d'Elsthorpe). (B) Coupe régionale à travers l'extrême sud de Hawke Bay. Noter la différence d'échelle entre les deux coupes et l'exagération verticale (2x) sur la coupe A. Coupes modifiées d'après Francis (2002) et Francis et al.(2004).

- *L'arc structural – Les chaînes axiales :*

L'arc structural est situé à l'ouest du bassin avant arc (Fig. 2.2) dont il est séparé par une succession de failles décrochantes dextres à composante chevauchantes (eg. failles de Mohaka et de Ruahine), qui forment la ceinture décrochantes dextre de l'Île Nord (North Island Dextral fault belt – NIDFB). La limite cartographique ouest de l'arc et des chaînes axiales avec le domaine arrière arc montre une variabilité du nord au sud. Au nord, la frontière est marquée par la présence de failles normales qui bordent le domaine arrière arc extensif (eg. Whakatane fault – Lamarche et al., 2006). Au sud la limite de l'arc correspond au système de failles de Kapiti-Manawatu et est recouverte par les sédiments du bassin de Wanganui (Lamarche et al., 2005 ; Proust et al., 2005). L'arc structural constitue une barrière orographique faites d'un série de chaînes formant les chaîne axiales et dont l'altitude dépasse 1700 m (eg. Ruahine Range (1715 m), Wakarara Range (1020 m), Kaweka Range (1724 m), Kaimanawa Range (1517 m)). Le socle mésozoïque, correspond à un mélange de grès fins et d'argilites, affleure abondamment dans ces chaînes (Suggate, 1961 ; Kingma, 1962). Les sédiments constitutifs du socle dérivent d'un ancien prisme d'accrétion géant (Spörli et Bell, 1976 ; Barnes et Korsch, 1991). Les chaînes axiales sont caractérisées par la présence de vallées incisées à versant abrupts. Elles sont dominées par les processus d'érosion et la sédimentation y est limitée à quelque dépôts fluviatiles de type terrasses (Smale et al., 1978). Dans la partie centrale des chaînes axiales, à l'exception des plus hauts sommets, le haut des chaînons est caractérisé par la présence de reliques d'une surface d'aplanissement (Fig. 2.7). La présence locale de dépôts marin peu profonds de la fin du Pliocène sous cette surface implique que la majeure partie de l'émersion et la croissance des chaînes axiales s'est faite au Pléistocène (Beu et al., 1980 ; Erdman et Kelsey, 1992). Ce calendrier est compatible avec la présence de discontinuités majeures dans le bassin de Wanganui qui datent le début de l'activité de l'arc entre 1.7 et 1.0 Ma (Proust et al., 2005 ; Lamarche et al., 2005). Il est fort possible que le domaine de l'arc structural ait connu des phases antérieures de surrection et d'émersion, comme l'indique, par exemple, la présence de faciès conglomératique à galets de Greywacke datés du Mangapanien (~ 3,0 à ~2,5 Ma) dans le bassin adjacent de la dépression Ohara (Erdman et Kelsey, 1992 ; voir aussi : Kamp, 2002 ; Browne, 2004). La surrection de l'arc sur le dernier million d'années est estimée à ~ 1 $mm.yr^{-1}$ (Pillans, 1986). Une conséquence de la surrection des chaînes axiales et de leur émersion est la déconnexion progressive des bassins avant et arrière arc pendant le Pliocène et le Pléistocène. Seuls deux « détroits » peu profonds (Manawatu et Kuripapango) ont subsisté entre les bassins jusqu'à la fin du Pliocène (Lillie, 1953 ; Browne, 2004)

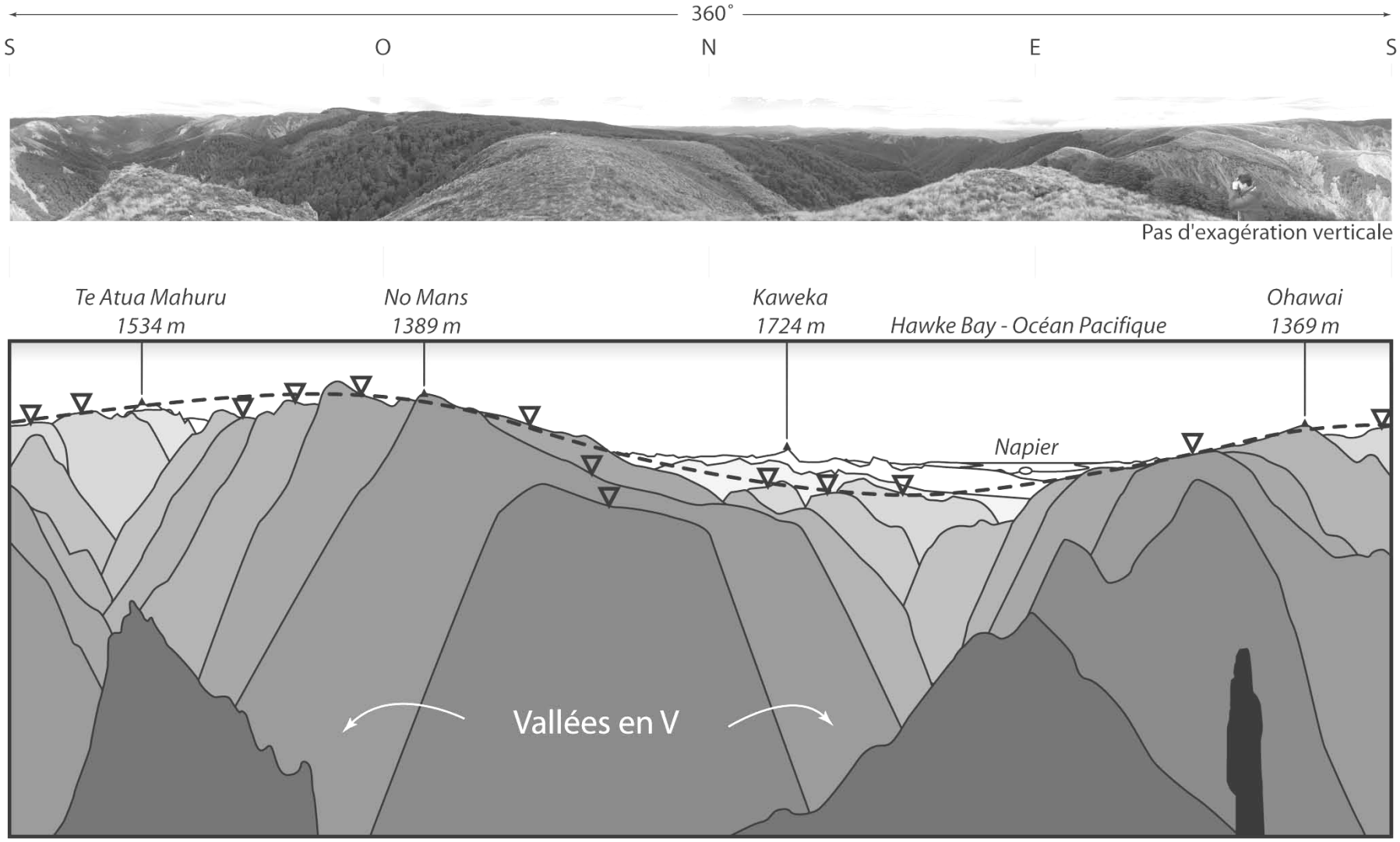
360°
S
O
N
E
S
Pas d'exagération verticale
Te Atua Mahuru
1534 m
No Mans
1389 m
Kaweka
1724 m
Hawke Bay - Océan Pacifique
Ohawai
1369 m
Napier
Vallées en V
Exagération verticale : x 4

Figure 2.7 : Panorama photographique complet (360°) pris depuis la zone sommitale du nord de la Ruahine Range (Memorial Cairn – No Mans Road, 1320 m) et dessin interprétatif (exagération verticale : 4x). La surface plane de faible relief est clairement visible sur la photo et sur le dessin. La ligne tirets correspond approximativement à l'enveloppe de la surface. Les flèches indiquent les rémanants de la surface dont l'enveloppe est représentée par la ligne. Les vallées issues de l'incision fluviatiles (profil en « V »), sont bien visibles.

- *Le domaine arrière arc et l'arc volcanique :*

Le domaine d'arrière arc s'étend à l'ouest des chaînes axiales de l'arc structural. Il est constitué de deux sous domaines distincts. Dans sa partie nord, il correspond au prolongement, sur la croûte continentale, de l'arrière arc extensif Le Havre – Lau de la subduction océan – océan des Kermadec (Fig. 2.1 & 2.2). Ce rift actif est caractérisé par une série de grabens (Whakatane, Motiti, Taupo) qui se développent de la Bay of Plenty (en mer) à la Taupo Volcanic Zone (TVZ – à terre). Les taux d'extensions varient du nord au sud depuis 12 - 15 mm.yr-1 dans la Bay of Plenty (Walcott, 1987 ; Wallace et al., 2004 ; Lamarche et al., 2006) jusqu'à 2,3 ± 1.2 mm.yr-1 au Ruapehu Graben, à la limite sud de l'arrière arc extensif (Villamor et Berryman, 2001 ; 2006). Le rift abrite un volcanisme calco-alcalin (eg. Mont Ruapehu) et une activité géothermale importante. Les éruptions fréquentes sont à l'origine de la mise en place de nombreux tephras ou ignimbrites (eg. Potaka Tephra vers 1.0 Ma) qui s'interstratifient dans les séries sédimentaires des bassins de la marge active et permettent de dater avec précision les séquences sédimentaires (eg. Shane et al., 1996). Pendant le développement de la subduction, la position d'arcs volcaniques successifs montre une rotation de la région du Northland-Coromandel au Miocène, vers la position actuelle. Cette rotation de l'arc suit la rotation générale de toute la marge, qui se poursuit de nos jours (eg. Lamb, 1988 ; Wallace et al., 2004 ; Nicol et al., 2007). La transition entre la partie nord extensive, et la partie sud compressive est marquée par un phénomène de bombement centré sur la région du Mt Ruapehu (Kamp et al., 2004 ; Pullford et Stern, 2004). Au sud, le domaine arrière arc correspond au bassin partiellement émergé de Wanganui. Soumis au raccourcissement et exempt de volcanisme, il ne peut être considéré comme un bassin arrière arc classique (Fig. 2.2 & 2.8). La subsidence du bassin est attribuée (1) au couplage entre les deux plaques qui entraîne une traction exercée vers le bas par le panneau plongeant et (2) à la charge sédimentaire (Stern et Davey, 1989 ; Stern et al., 1992). Le remplissage marin Mio-Pliocène localisé dans le nord du bassin est basculé et érodé, consécutivement au bombement, sur plus de 2,5 km d'épaisseur (Kamp et al., 2004). Le bombement a aussi provoqué la migration de la zone de subsidence vers le sud (Fig. 2.9a). Le remplissage marin peu profond Plio-Pléistocène est ainsi localisé au sud, dans la partie immergée du bassin et atteint 4 km

d'épaisseur (Anderton, 1981). L'affleurement des séquences Plio-Pléistocène sur la côte offre une coupe unique du Quaternaire (Carter et al., 1999 ; Saul et al., 1999 ; Abbott et al., 2005 ; Naish et al., 2005). L'interprétation des lignes sismiques acquises ces dernières décennies a permis de mettre en évidence l'existence de deux mega-séquences (Proust et al., 2005). La seconde se développe au Pléistocène partir de c. 1.35 Ma et présente des évidences de déformation syn-sédimentaire importante avec une migration des dépocentres vers l'est et l'arc structural (Fig. 2.9b - Proust et al., 2005).

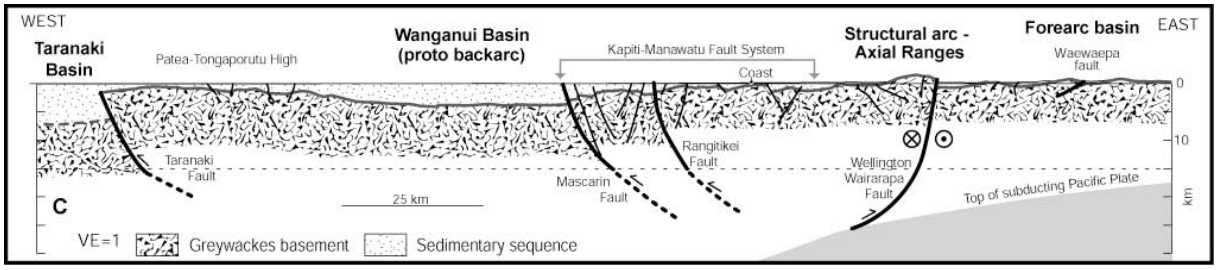

Figure 2.8 : Coupe régionale synthétique compilée à partir des coupes de Anderton (1981) et Katz et Leask (1990). Le basin de Wanganui est soumis à une déformation compressive et n'est pas affecté par un volcanisme arrière arc. Modifié d'après Lamarche et al. (2005) et Proust et al. (2005).

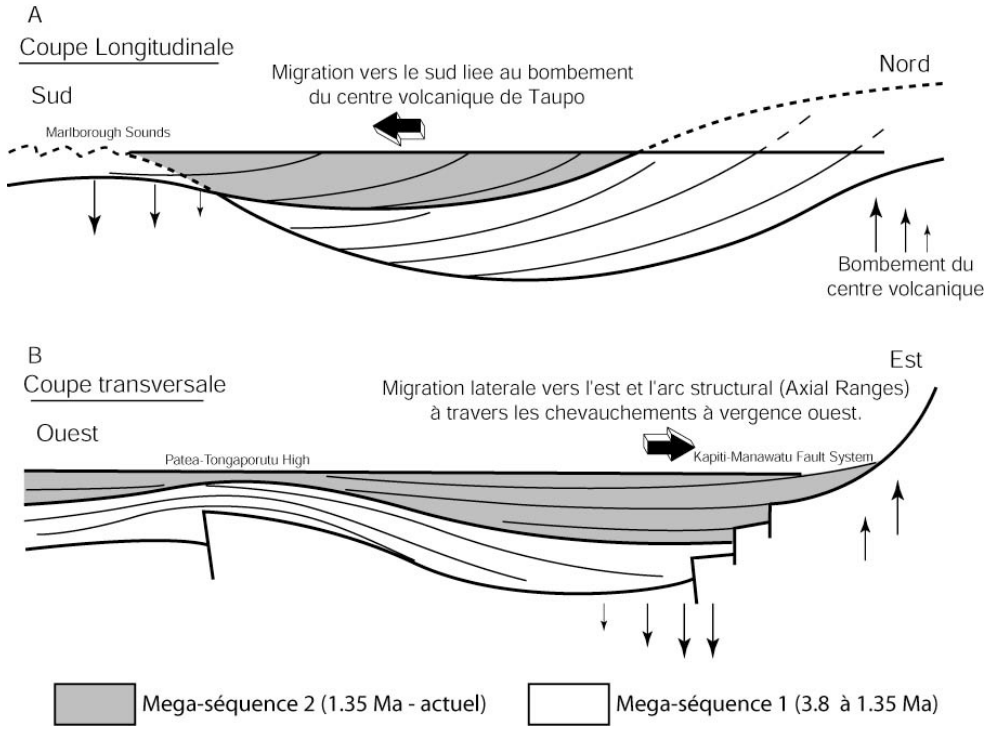

Figure 2.9 : Coupes schématiques du remplissage Plio-Pléistocène du bassin de Wanganui figurant les deux mega-séquences de dépôt et la déformation. (A) Coupe N-S montrant le contrôle effectué par le bombement sur la migration nord-sud des dépôts. (B) Coupe E-0 montrant le contrôle effectué par le jeu des failles du système de failles de Kapiti-Manawatu sur la migration vers l'est des dépôts. Proust et al. (2005).

2.1.2. Conclusion :

Les éléments morphostructuraux de la marge active de la subduction Hikurangi sont clairement identifiés. Leur évolution depuis l'initiation de la subduction est globalement connue. Les reconstitutions paléogéographiques et tectoniques (Lamb, 1988 ; King, 2000 ; Nicol et al., 2007) offrent une image de plus en plus fine de l'évolution générale de la marge (Fig. 2.10) et de la frontière de plaques autour de la Nouvelle-Zélande (Fig. 2.11). Les études récentes, focalisées sur le prisme d'accrétion, les bassins marginaux et l'arc structural montrent une intensification généralisée de l'activité structurale de la marge à partir de 1.5 – 1.0 Ma, jusqu'à l'actuelle (eg. Beu et al., 1981 ; Erdman et Kelsey, 1992 ; Barnes et Nicol, 2004 ; Proust et Chanier, 2004 ; Proust et al., 2005). L'explication de cette (ré) activation de la marge n'est pas encore clairement établie et fait sûrement intervenir et interagir de nombreux paramètres internes, tels le taux de convergence des plaques, le couplage entre plaques, les variations de l'accrétion au niveau du prisme, et/ou externes, comme la transition climatique du Pléistocène moyen (Head and Gibbard, 2005; Murray-Wallace, 2007), qui voit s'installer une cyclicité à 100 Ka caractérisée par des changements de forte amplitude des conditions climatiques (température, pluviométrie, fréquence des évènements catastrophiques, variations climato-eustatiques…).

L'activité tectonique et le climat particulier du Pléistocène concourent donc à la génération et l'évolution des topographies et des reliefs caractéristiques de marge active en subduction.

Les bassins sédimentaires de la marge et leur remplissage sont particulièrement importants car ils enregistrent les variations tectoniques locales, les changements climatiques et eustatiques globaux, ainsi que la croissance des reliefs, sous la forme de variations du flux sédimentaire (voir Chapitre 1). Deux bassins principaux, Wanganui et Hawke Bay, permettent grâce à leur position de part et d'autre de l'arc, d'étudier les modifications morphostructurales de la marge Hikurangi.

Le bassin de Wanganui, en position arrière arc est à l'heure actuelle le bassin Plio-Pleistocène dont le remplissage marin à continental, ainsi que le calendrier et le type de déformation sont les mieux décrits (Naish et al., 1998 ; Saul et al., 1999 ; Naish et al., 2005 ; Proust et al., 2005 ; Pillans, 2007 ; Kamp et al., 2004 ; Lamarche et al., 2005). Les études stratigraphiques ont montré l'existence de séquences de dépôt dont le développement est parfaitement corrélé aux variations eustatiques Plio-Pléistocène (cyclicité de 41 ka à 100 ka). La quantification des volumes et flux sédimentaires pléistocènes est actuellement en cours et permettra de remonter

aux valeurs du flux entrant et approcher ainsi la dynamique des reliefs dans la partie arrière arc de la marge Hikurangi (Letetrel, 2006).

Le bassin avant arc d'Hawke Bay, de par la configuration du bassin et bien que moins densément documenté, offre un accès à un enregistrement sédimentaire unique, dans un domaine où la déformation est particulièrement importante. La stratigraphie complète du Pléistocène, la géométrie du remplissage et les flux sédimentaires restent à déterminer. Cette étude vise à combler ces lacunes dans l'objectif de remonter à l'évolution morphostructurale.

Il sera ensuite possible d'envisager une intégration des résultats obtenus sur les domaines avant et arrière arc pour fournir des estimations des flux sédimentaire globaux sur la marge active et de comprendre comment celle-ci acquiert sa morphostructure.

Le chapitre suivant est consacré plus spécifiquement à Hawke Bay. Après l'exposition de la démarche scientifique nécessaire pour répondre aux questions, un état des connaissances acquises et restant à acquérir sera dressé. Enfin un aperçu des données utilisées lors de ce travail sera présenté.

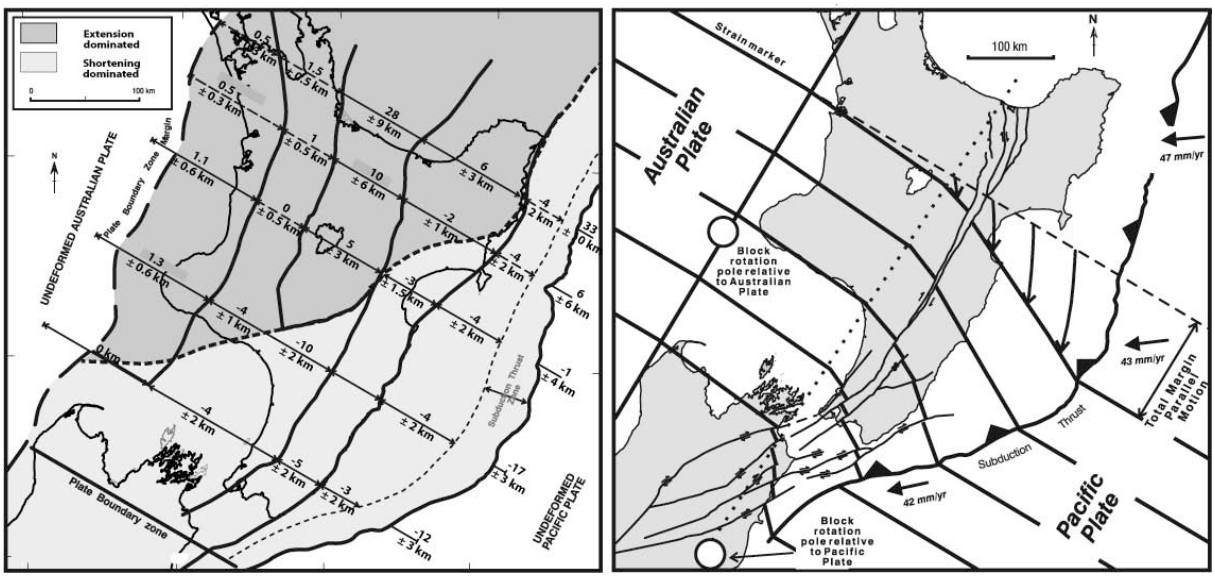

Figure 2.10 : Cartes schématique de la marge active de la subduction Hikurangi montrant, à gauche : les taux de raccourcissement et d'extension le long de cinq profiles perpendiculaires à la marge, pour les derniers 5 Ma (Noter la valeur totale de déformation à l'extrême droite des profiles) ; et à droite : les failles décrochantes (dextres), la rotation horaire de la marge et la position des pôles de rotation. Au cours des derniers 10 Ma. Modifié d'après Nicol et al. (2007). Position des pôles d'après Wallace et al. (2004).

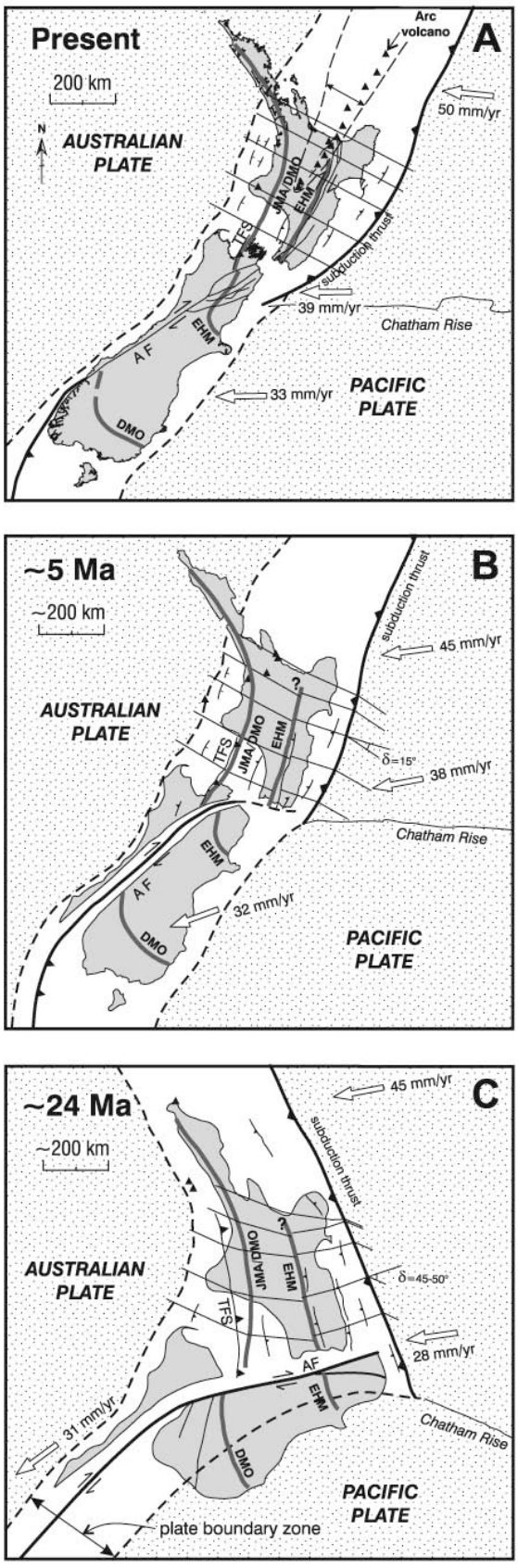
Present
A
200 km
N
AUSTRALIAN PLATE
Arc volcano
50 mm/yr
JMA/DMO
EHM
TFS
subduction thrust
39 mm/yr
Chatham Rise
EHM
AF
33 mm/yr
PACIFIC PLATE
DMO
~5 Ma
B
~200 km
subduction thrust
45 mm/yr
AUSTRALIAN PLATE
TFS
JMA/DMO
EHM
δ=15°
38 mm/yr
Chatham Rise
EHM
AF
32 mm/yr
PACIFIC PLATE
DMO
~24 Ma
C
45 mm/yr
~200 km
subduction thrust
AUSTRALIAN PLATE
JMA/DMO
EHM
δ=45-50°
TFS
28 mm/yr
AF
EHM
31 mm/yr
Chatham Rise
DMO
PACIFIC PLATE
plate boundary zone

Figure 2.11 : Reconstitutions de la frontière des plaques Pacifique et Australienne, autour de la Nouvelle-Zélande, et de la marge active d'Hikurangi (A) au présent, (B) à ~5 Ma et (C) à ~24 Ma. La position des cinq profiles perpendiculaires à la marge de la figure 2.10 (gauche) sont reportés et font office de marqueurs de la déformation. TFS : Taranaki Fault System ; AF : Alpine Fault ; DMO : Dun Mountain Ophiolite ; EHM : Esk Head Melange. Les flèches blanches indiques la direction et les taux de convergence relative entre les deux plaques à l'actuel (Beavan et al, 2002) et pour les temps géologiques (négligeables et Stock, 2004).Note : le trait de côte est reporté de façon indicative sur les reconstitutions à ~5 et ~24 Ma, mais ne reflète aucunement la paléogéographie. Modifié d'après Nicol et al. (2007).

Chapitre 3 :

Méthodologie, état des connaissances et données

3.1. Méthodologie & démarche scientifique :

Les sections suivantes visent à détailler la démarche scientifique suivie pour répondre aux questions posées (choix du bassin, méthodologie). Un aperçu des connaissances et des lacunes est donné. Enfin, la dernière section du chapitre correspond à un catalogue des principales données utilisées durant cette étude.

3.3.1. Les avantages du bassin avant arc de Hawke Bay :

Le bassin de Hawke Bay occupe une place prépondérante dans le bassin avant arc Pléistocène de la subduction Hikurangi. Malgré la surrection modérée mais généralisée du domaine avant arc et son émersion progressive entre les chaînes axiales et côtières, le bassin de Hawke Bay est demeuré la zone de sédimentation continue la plus importante de tout l'avant arc. Ainsi, le Hawke Bay, à l'instar du bassin de Wanganui, renferme dans ses archives sédimentaires, l'histoire de l'avant arc Pléistocène et de son évolution. Outre l'intérêt de sa localisation au sein de l'avant arc, le bassin Pléistocène de Hawke Bay s'étend à cheval sur les domaines marin et continental. Cette particularité permet un accès direct au remplissage sédimentaire à terre ce qui est souvent limité par les fortes bathymétries des bassins avant arc mondiaux (voir chapitre 1). De plus, cette position hypsométrique du bassin permet l'expression optimale des variations eustatiques du Pléistocène et des changements d'environnement de dépôts associées dans l'enregistrement stratigraphique. Enfin, au cours des cinquante dernières années, le bassin d'Hawke Bay a fait l'objet de nombreuses études géologiques (études structurales, sédimentologiques et stratigraphiques, géomorphologiques, géochronologiques) et de campagnes d'acquisition de données géologiques et géophysiques (données sismiques, forages, carottages), qui fournissent autant d'éléments permettant de reconstituer et de discuter l'évolution du bassin avant arc. Enfin, les résultats déjà obtenus dans le bassin « arrière arc » de Wanganui permettent de comparer ceux à venir sur le bassin de Hawke Bay et de mettre l'ensemble en perspective en terme d'évolution morphostructurale de l'ensemble de la marge Hikurangi.

La figure 3.1 présente la géographie du domaine avant arc de Hawke Bay avec la localisation des sites ou objet majeurs.

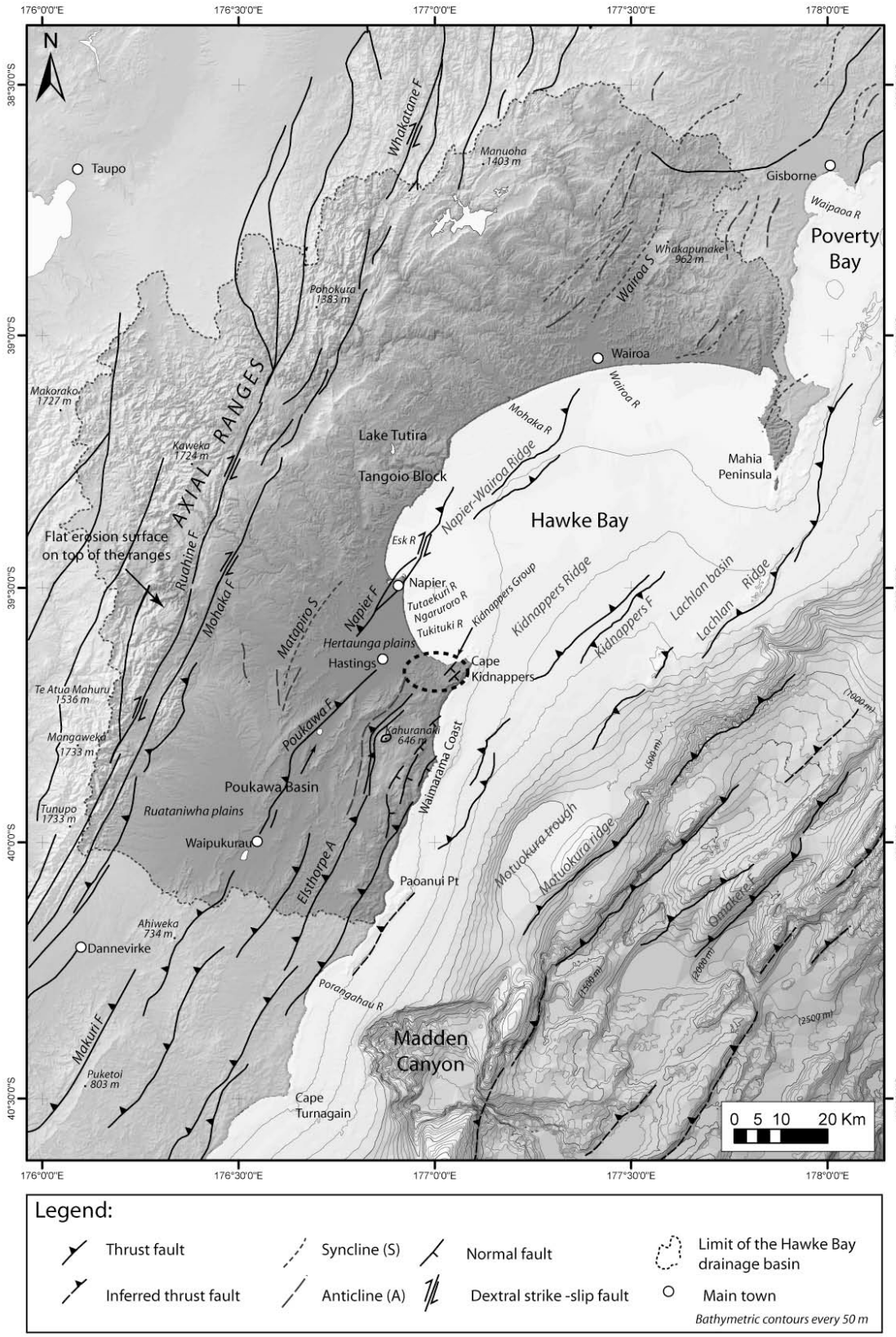

Figure 3.1 : Carte de la géographie de Hawke Bay avec la localisation des principaux sites (chaînes, plaines, bassins, failles majeures). Topographie extraite du NIDEM (North Island Digital Elevation Model) d'après LINZ (2000) et bathymétrie d'après NIWA.

3.3.2. La démarche scientifique :

La démarche scientifique adoptée pour cette étude se présente en une succession de points qui permettent d'aboutir aux objectifs de description et de quantification de l'évolution morphostructurale du domaine avant arc :

- Le premier point est la détermination de la **stratigraphie** détaillée du remplissage du bassin, incluant la connaissance des faciès sédimentaires, de la paléogéographie , des séquences de dépôt et de leur emboîtement.
- L'établissement de la **chronostratigraphie** (échantillons datés et corrélations de la stratigraphie séquentielle à la courbe climatique et eustatique $\delta^{18}O$) permet ensuite d'offrir un cadre temporel nécessaire pour établir un calendrier des évènements et pondérer les quantifications.
- La détermination de la **géométrie tridimensionnelle** du remplissage et plus particulièrement, des séquences de dépôt, grâce à un maillage serré des données et à la cartographie des séries à terre.
- L'**analyse structurale** (cartographie, style et taux) autorisée par la connaissance des géométries et de la chronostratigraphie.
- Calcul des **volumes** déposés et préservés dans le bassin à partir de l'établissement de cartes d'isopaques de chacune des séquences, puis conversion des volumes en **masses**.
- L'association des masses de sédiments préservés et de la chronostratigraphie permet l'estimation des **flux sédimentaires préservés** dans le bassin.

Dans l'objectif d'établir un modèle détaillé et bien contraint de séquence de dépôt type du bassin de Hawke Bay, les efforts ont d'abord été concentrés sur la partie supérieure du remplissage. En effet, celle-ci est imagée par des données hautes – résolutions (Boomer, 3.5 KHz), qui permettent de mieux caractériser les surfaces de discontinuités, les terminaisons stratigraphiques et environnements de dépôt (via les faciès sismiques). La méthodologie décrite ci-dessus, les résultats et les implications qui en découlent sont abordés et détaillés dans le chapitre suivant (Chapitre 4 - Article 1).

L'ensemble du bassin de Hawke Bay et l'emboîtement des séquences antérieures sont ensuite étudiés en se basant sur les résultats obtenus sur la première séquences. La période considérée ici correspond au dernier c. 1.1 Ma (Castelcliffian et Haweran) Cette partie de l'étude fait l'objet du Chapitre 5 (Article 2). Les résultats y sont discutés de manière déterminer

l'influence des paramètres internes et externes sur la stratigraphie, l'évolution des flux sédimentaires et celle de la morphostructures de la marge.
Les résultats de ces deux parties de l'étude sont enfin repris et développés en guise de conclusion, régionale et générale sur l'évolution morphostructurale des marges.

Avant cela, il est important (1) de présenter un état des connaissances sur le bassin de Hawke Bay pour faire le bilan des points à préciser ou compléter, puis (2) de présenter le jeu de données géophysiques et géologiques utilisé et interprété dans cette étude.

3.2. Etat des connaissances :

Cette section est consacrée à l'état des lieux des connaissances dans les domaines abordés par la démarche scientifique. Pour chacun de ces domaines, un bilan est dressé et les lacunes à combler sont présentées.

3.2.1. Les frontières du bassin :

Dès lors que des quantifications sont envisagées, il est nécessaire de délimiter les frontières physiques du bassin, c'est-à-dire la zone ou la majeure partie ou la totalité des sédiments issus du bassin versant sont déposé et préservés. A l'heure actuelle, aucune étude n'a traité le problème de l'étendue totale du bassin « actif » de Hawke Bay (Lewis, 1973 a et b ; Barnes et al., 2002 ; Barnes et Nicol ; 2004). Ce point est donc à résoudre via l'interprétation des données à terre et en mer.

3.2.2. La stratigraphie séquentielle et la chronostratigraphie :

Le remplissage sédimentaire Pléistocène du bassin de Hawke Bay est l'objet de nombreuses études depuis cinq décennies. Ces études ont permis de préciser la nature du remplissage (faciès sédimentaires continentaux à marin) et le découpage séquentiel avec des contraintes plus ou moins fortes (eg. Barnes et al., 2002 ; Barnes et Nicol, 2004 ; Proust et Chanier, 2004) (Fig. 3.2 et 3.3). Les objets traités sont d'extension temporelle et/ou spatiale trop réduite pour disposer d'une vision globale de la stratigraphie de la marge. Ils peuvent néanmoins être utilisés comme bases pour une interprétation plus complète de l'ensemble du bassin et, dans le cas d'échantillon datés (téphrochronologie, paléontologie), servir à l'établissement de la

chronostratigraphie (eg. Shane, 1994 ; Shane et al., 1996 ; Beu et Pillans, 1987). A ce titre, la coupe du Kidnappers Group offre un contrôle fort sur la sédimentologie, stratigraphie séquentielle et la chronostratigraphie de l'intervalle c. 1.1 Ma – 0.5 Ma (Kingma, 1971 ; Proust et Chanier, 2004 et références internes). Cette coupe est utilisée dans cette étude comme un moyen de valider une partie des interprétations sédimentologiques et séquentielles, ainsi que la chronologie (Fig. 3.1). La stratigraphie proposée pour les parties émergées de Hawke Bay par Barnes et al. (2002) est également à prendre en référence (Fig. 3.2)

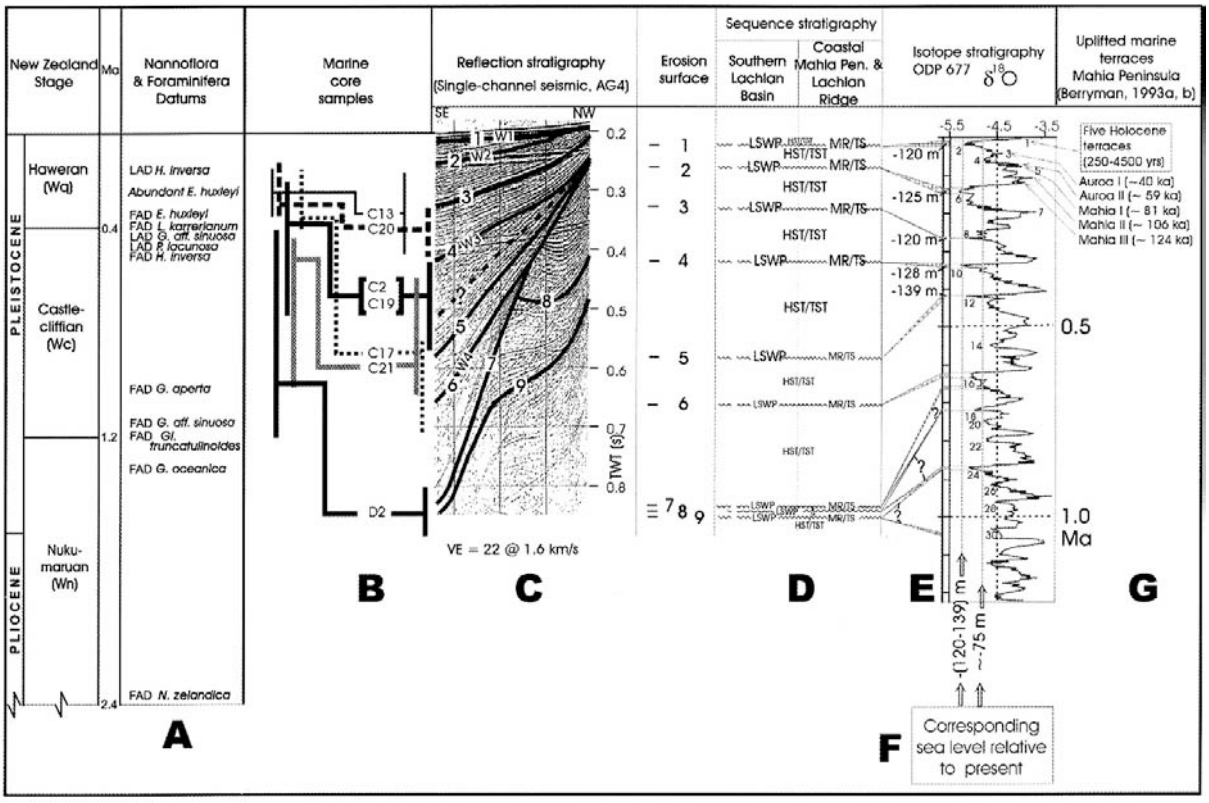

Figure 3.2 : Stratigraphie sismique et séquentielle proposée par Barnes et al. (2002). (A) Charte stratigraphique néo-zélandaise et microfossiles clés (abréviations : FAD, première apparition ; LAD, dernière apparition ; H, Helicoshaera ; E, Emiliania, L, Loxostomum ; G, Gephyrocapsa ; P, Pseudoemiliania, Gl, Globorotalia, N, Notorotalia). (B) Echantillons de carottages marins. (C) Extrait de ligne sismique monotrace (AG-4) dans le basin de Hawke Bay montrant neuf discontinuités érosives régionales. (D) Stratigraphie sismique interprétée (abréviations : LSWP, surface marine d'aplanissement de bas niveau ; HST, cortège de haut niveau marin ; TST, cortège transgressif ; MR/TS, surface de ravinement marin ou surface de transgression. (E) Corrélations déduites des discontinuités avec la courbe $\delta^{18}O$ établie à partir de l'enregistrement des foraminifères benthiques du site ODP 677 (Shackleton et al., 1990 ; Tiedmann et al., 1994). (F) Lignes verticales indiquant les correspondances des niveaux marins à la courbe $\delta^{18}O$ (stratigraphie isotopique) d'après les calibrations de Pillans et al. (1998) et Rohling et al. (1998). (G) Corrélation à la courbe $\delta^{18}O$ des terrasses marines identifiées sur la côte de la Péninsule de Mahia (Berryman, 1993 a et b).

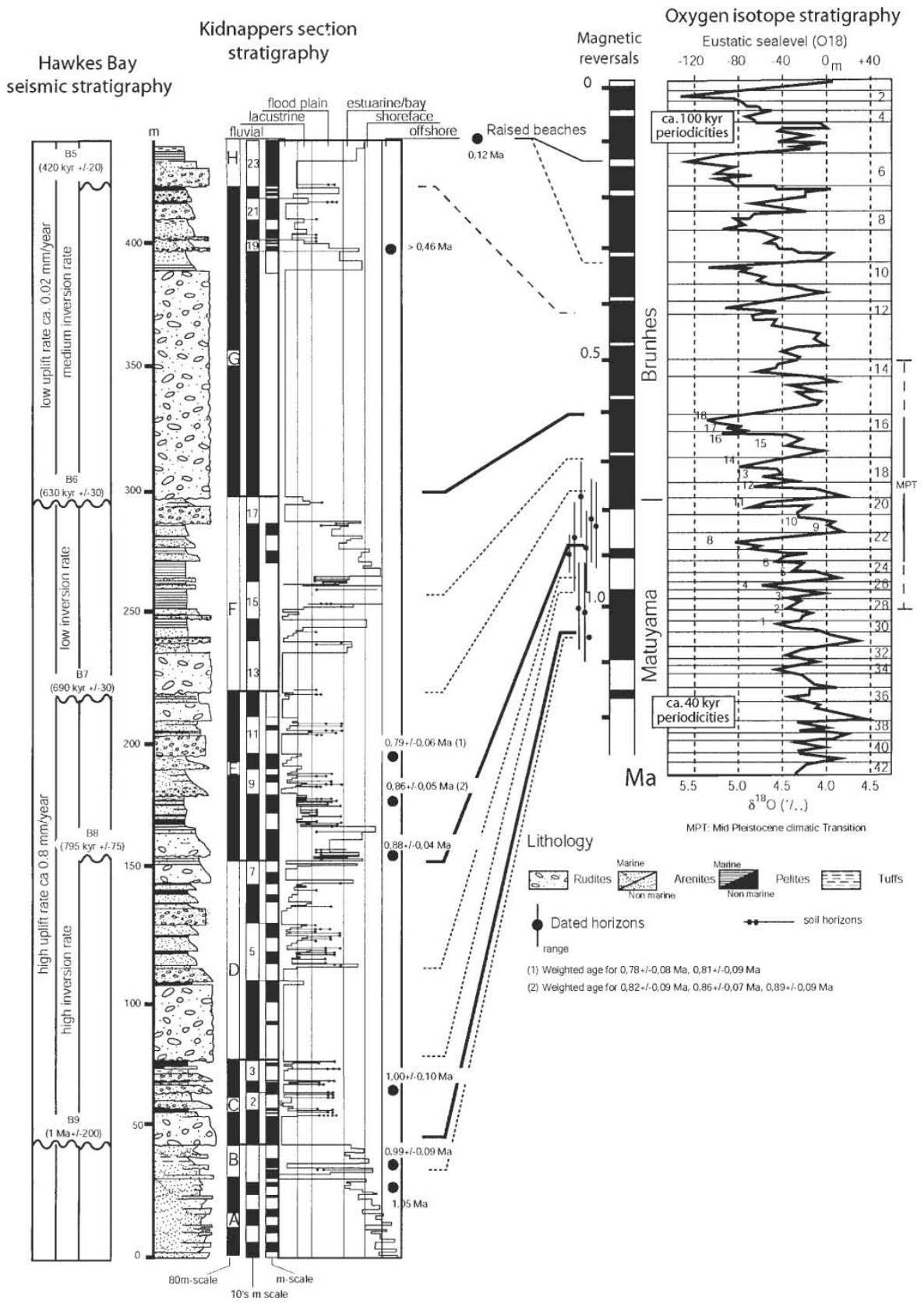

Figure 3.3 : Proposition de corrélation de stratigraphie de la coupe du Kidnappers Group avec la courbe $\delta^{18}O$ (stratigraphie isotopique) établie à partir de l'enregistrement des foraminifères benthiques du site ODP 677 (Shackleton et al., 1990) et avec la stratigraphie sismique haute résolution établie au large par Barnes et al. (2002) ; Proust et Chanier (2004)

3.2.3. La séquence de dépôt type :

La description d'une séquence de dépôt type bien imagée est un préalable essentiel pour permettre des interprétations sismiques contraintes. A ce jour, les interprétations existantes (Lewis, 1973 a et b ; Barnes et al., 2002 ; Barnes et Nicol, 2004) ne sont pas suffisamment détaillées sur l'ensemble du domaine de Hawke Bay et semble montrer quelques inadéquations. Il est donc nécessaire de fournir une image la plus complète et exhaustive possible de la dernière séquence depuis les zones sources jusqu'aux pieds des cortèges de bas niveau en utilisant l'ensemble des données disponibles.

3.2.4. La paléogéographie :

La connaissance des variations de paléogéographie lors d'une séquence de dépôt type est essentielle pour comprendre les influences interactions de la tectonique, du climat et de l'eustatisme sur l'évolution des paysages. Très peu de travaux renseignent sur la paléogéographie de Hawke Bay lors des différents extrêmes environnementaux. La plupart ne proposent que des reconstitutions limitées à la position de la ligne de côte (eg. Lewis, 1971 ; Lewis 1973a ; Dravid et Brown, 1997). Il est intéressant de signaler, d'un point de vue anecdotique, les reconstitutions de Hill (1908), qui offrent, malgré des contraintes faibles et des interprétations erronées, deux visions intéressantes par leur aspect global et leur potentielle vraisemblance (Fig. 3.4).

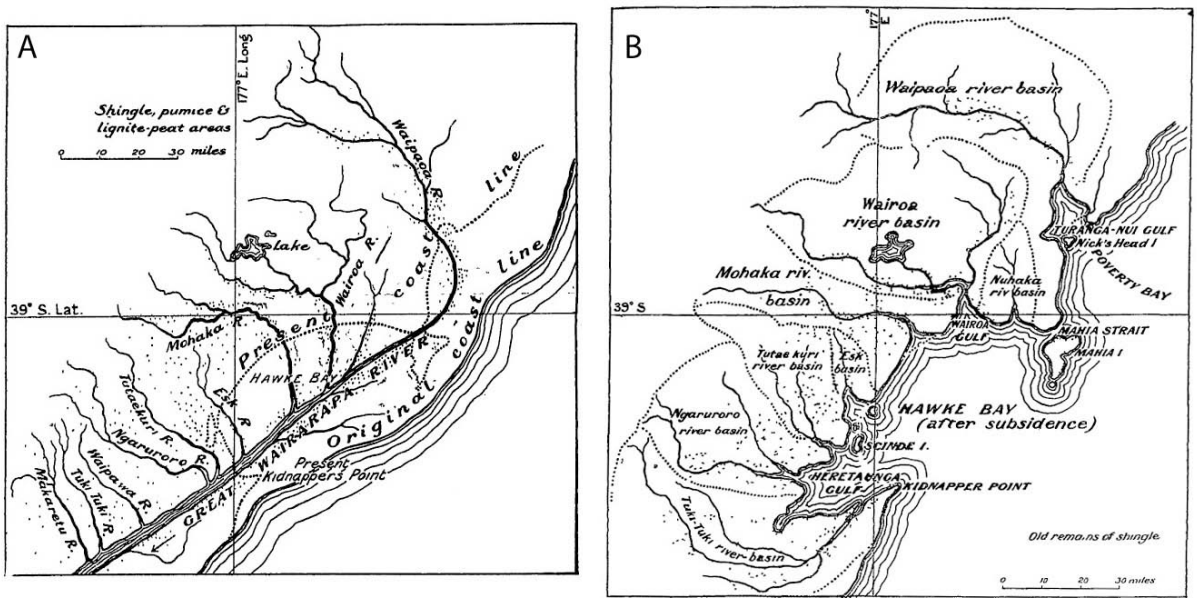

Figure 3.4 : Reconstitutions paléogéographiques de la région de Hawke Bay. (A) Paléogéographie antérieure à la « subsidence ». Noter la représentation de la rivière « Great Wairarapa », longeant la côte est, vers le sud et responsable de l'accumulation de conglomérats dans les plaine d'Heretaunga. (B) Paléogéographie après la « subsidence ». Noter la reconfiguration du réseau fluviatile. Modifié d'après Hill (1908).

3.2.5. La géométrie des séquences :

La connaissance de la géométrie des séquences de dépôts identifiées à partir des interprétations sismiques est limitée et parcellaire (Lewis, 1973a ; Barnes et al., 2002 ; Barnes et al., 2004). De plus, elle est limitée aux parties externes de Hawke Bay à cause du manque de qualité des données disponibles à l'époque des travaux. La géométrie des séquences de dépôt est donc à revoir entièrement par l'interprétation des données géophysiques, mais aussi par la cartographie des formations Pléistocènes du Kidnappers Group, qui affleurent dans l'extrême nord des chaînes côtières, sur la côte sud de Hawke Bay. L'extension cartographique du Kidnappers Group est connue (Kingma, 1962 ; Kamp, 1978 ; Francis, 1993) mais la géométrie des formations n'a pas encore été déterminée convenablement (Fig. 3.5).

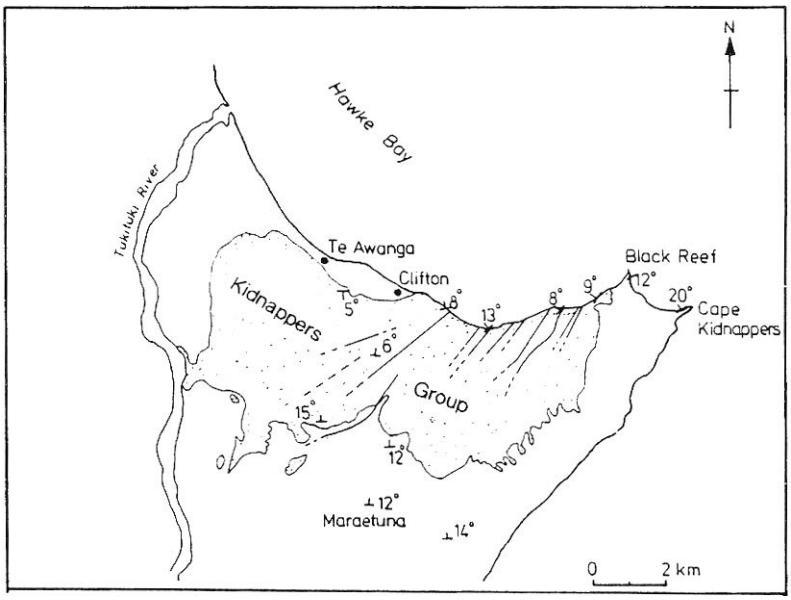

Figure 3.5 : Carte montrant l'extension géographique du Kidnappers Group et des données structurales (Kamp, 1978).

3.2.6. La déformation tectonique :

Les études de la déformation tectonique et des taux de surrection Pléistocènes au sein du domaine avant arc de Hawke Bay, à terre comme en mer, sont nombreuses et détaillées (eg. Lewis, 1971a ; Pillans, 1986 ; Hull, 1987 ; négligeables et Kelsey, 1990 ; Erdman et Kelsey, 1992 ; Beanland et al., 1998 ; Barnes et al., 2002 ; Barnes et Nicol, 2004 ; Pettinga, 2004 ; Litchfiel et Berryman, 2006, Nicol et al, 2007). L'objectif est de compléter la cartographie structurale en mer (Barnes et al., 2002 ; Barnes et Nicol, 2004) et d'établir le calendrier d'activité des failles et quantifier les déplacements verticaux, en tenant compte de la nouvelle

stratigraphie. Ce calendrier sera utile pour détecter les périodes de réactivation tectonique régionale et leur influence potentielle sur la stratigraphy et la morphostructure de l'avant arc.

3.2.7. Les volumes, masses et flux sédimentaires :

Peu de données existent quant aux volumes déposés et préserver dans le bassin avant arc. Deux études sont à signaler car elles fournissent des cartes d'isopaques et/ou des valeurs de volumes pour les parties superficielles du remplissage dans Hawke Bay (Wright et Lewis, 1991) et au large de la côte est (Lewis, 1973a). La quantification des volumes, des masses et des flux sédimentaire de l'ensemble du remplissage des derniers 1.1 Ma reste à faire.

3.2.8. Les volumes érodés :

L'estimation des volumes érodés dans le bassin versant de Hawke Bay est cruciale. Elle permet notamment de fournir un point de comparaison et de validation des volumes préservés estimés dans le bassin sédimentaire. Cet aspect n'est pas encore documenté dans Hawke Bay. Seules existent des études du taux d'incision verticale des rivières depuis la fin de l'aggradation glaciaire (c. 18 à l'actuel) rendu possible par les séries de terrasses fluviatiles (Litchfield et Berryman, 2006).

3.2.9. Le climat et l'eustatisme :

Le climat et l'eustatisme Pléistocènes sont particulièrement bien connus grâce aux études entreprises à travers le monde sur la stratigraphie isotopique de l'oxygène (Imbrie et al., 1984 ; Shackleton et al., 1990 ; Waelbroeck et al., 2002 ; Lisiecki et Raymo, 2005). Les courbes climatiques et eustatiques issues de ces études sont tout à fait comparables entre elles sur la période qui nous intéresse (1.1 Ma à l'actuel). Si une courbe devait être choisie pour cette étude, le choix se porterait sur la courbe composite de Lisiecki et Raymo (2005), qui présente l'intérêt d'être le résultat de la combinaison de 57 courbes originales du signal isotopique, réparties à travers le globe.

D'un point de vue régional, les variations climatiques sont particulièrement bien documentées pour le Pléistocène supérieur, par un grand nombre d'études stratigraphiques et palynologiques effectuées à terre (tourbières d'altitude : Kaipo bog, lacs : Poukawa, Tutira), sur des carottages en mer, ou à partir de synthèses globales (Lowe et al., 1999 ; McGlone, 2001 Shulmeister et al., 2001; Carter, 2002 ; Okuda, et al., 2002 ; Newnham et al., 2003 ; Shane et Sandiford, 2003 ; Alloway, 2007).

3.3. Les données :

Cette section présente les principales sources de données utilisées dans cette étude pour établir la (1) stratigraphie séquentielle détaillée, (2) la géométrie tridimensionnelle des séquence de dépôt, (3) leur âge, (4) la distribution des faciès sédimentaire et (5) la cartographie structurale du bassin avant arc de Hawke Bay.

L'essentiel des données est constitué par un réseau dense de sismique marine ou terrestre, complété par des données de puits et de carottages. Il est issu de différentes missions scientifiques et d'exploration pétrolière ayant eu lieu ces cinq dernières décennies. Des données géologiques (cartes, coupes, échantillons) provenant de la bibliographie ou acquises spécifiquement pour ce travail s'ajoutent au jeu de données. Des modèles numériques de terrain (MNT) de la topographie et de la bathymétrie ont également été utilisés.

Les données seront donc présentées comme suit :

- Les missions de sismique marine :
- Les missions de sismique terrestre :
- Les carottages :
- Les puits :

3.3.1 Les missions de sismique marine :

- CR 8024 (AG & S):

Année / year : ……...*1988*
Opérateur / operator : ……...*Conquest Exploration Ltd NZ*
Navire / Vessel : ……...*GRV Rapuhia*
Type de données : ……*3.5 KHz (profiles AG & S)*
Sismique monotrace (AG)
Longueur totale interprétée : ……*1200 km*
Rapports ou publications significatives :……..*Conquest Exploration – PR2059 (1988)*

Les profiles 3.5 KHz sont de relativement bonne qualité. La résolution diminue dans les zones de faible tranche d'eau de Hawke Bay. La densité des lignes est variable avec un maximum d'échantillonnage entre les Kidnappers Ridge et Lachlan Ridge (Fig. 3.6).

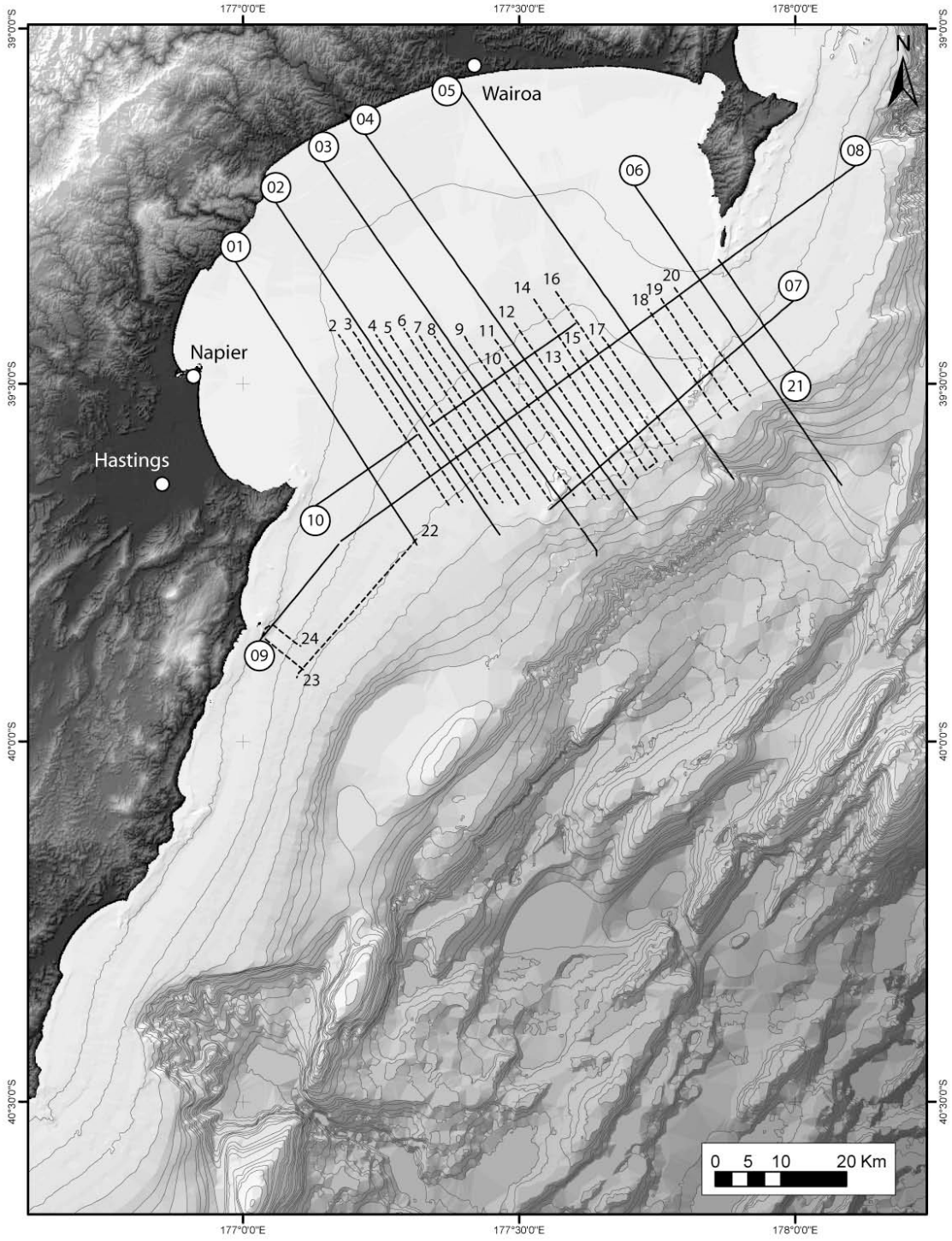

Figure 3.6 : Plan de positionnement des lignes sismiques de la campagne AG & S (Conquest Exploration, 1988). Les lignes continues représentent la sismique monotrace et le 3.5 KHz. Les lignes en pointillés représentent le 3.5 KHz uniquement.

- CQX – H90 :

Année / year : ……...*1990*
Opérateur / operator : ……...*NZ CQX Ltd.*
Navire / Vessel : ……...*M/V Western Pacific*
Type de données : …… *Sismique multitrace (60 folds)*
Longueur totale interprétée : ……*1000 km*
Rapports ou publications significatives :……..*Sullivan – PR1666 (1990) ;*
Barnes et al. (2002) ; Barnes et Nicol (2004)

Les profiles sont de relativement bonne qualité. La résolution diminue dans les zones de faible tranche d'eau de Hawke Bay. Les lignes 1 à 17 couvrent l'ensemble de Hawke Bay, au-delà de la Lachlan Ridge, avec une densité d'échantillonnage correcte (Fig. 3.7). La ligne B1 longe la Waimarama Coast vers la tête du Madden Canyon.

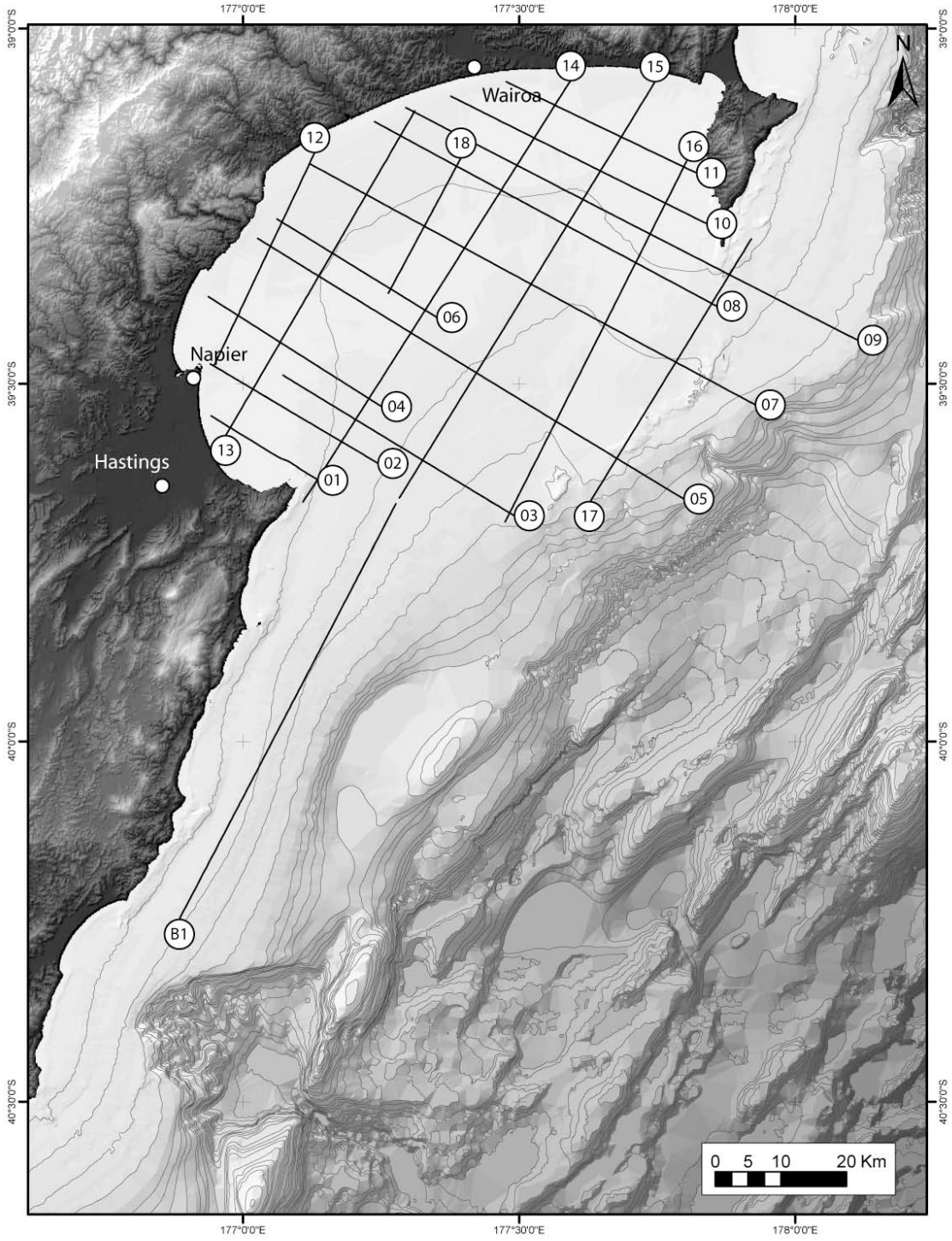

Figure 3.7 : Plan de positionnement des lignes sismiques de la campagne CQX – H90 (Sullivan, 1990).

- WE00 :

Année / year : ……...*2000*
Opérateur / operator : ……...*Westech Energy NZ Ltd.*
Navire / Vessel : ……...*M/V GECO MY*
Type de données : …… *Sismique multitrace (240 canaux)*
Longueur totale interprétée : ……*305 km*
Rapports ou publications significatives :……..*Geo-Prakla – PR2483 (2000) ;*

Les profiles sont de relativement bonne qualité. La résolution diminue dans les zones de faible tranche d'eau de Hawke Bay. Les lignes 101 à 108 couvrent le sud du Lachlan basin. Les lignes 109 à 115 couvrent le sud de Hawke Bay entre Napier et Cape Kidnappers. Les lignes 117 à 120 couvrent le nord de Hawke Bay ensemble de Hawke Bay, au large de Wairoa (Fig 3.8).

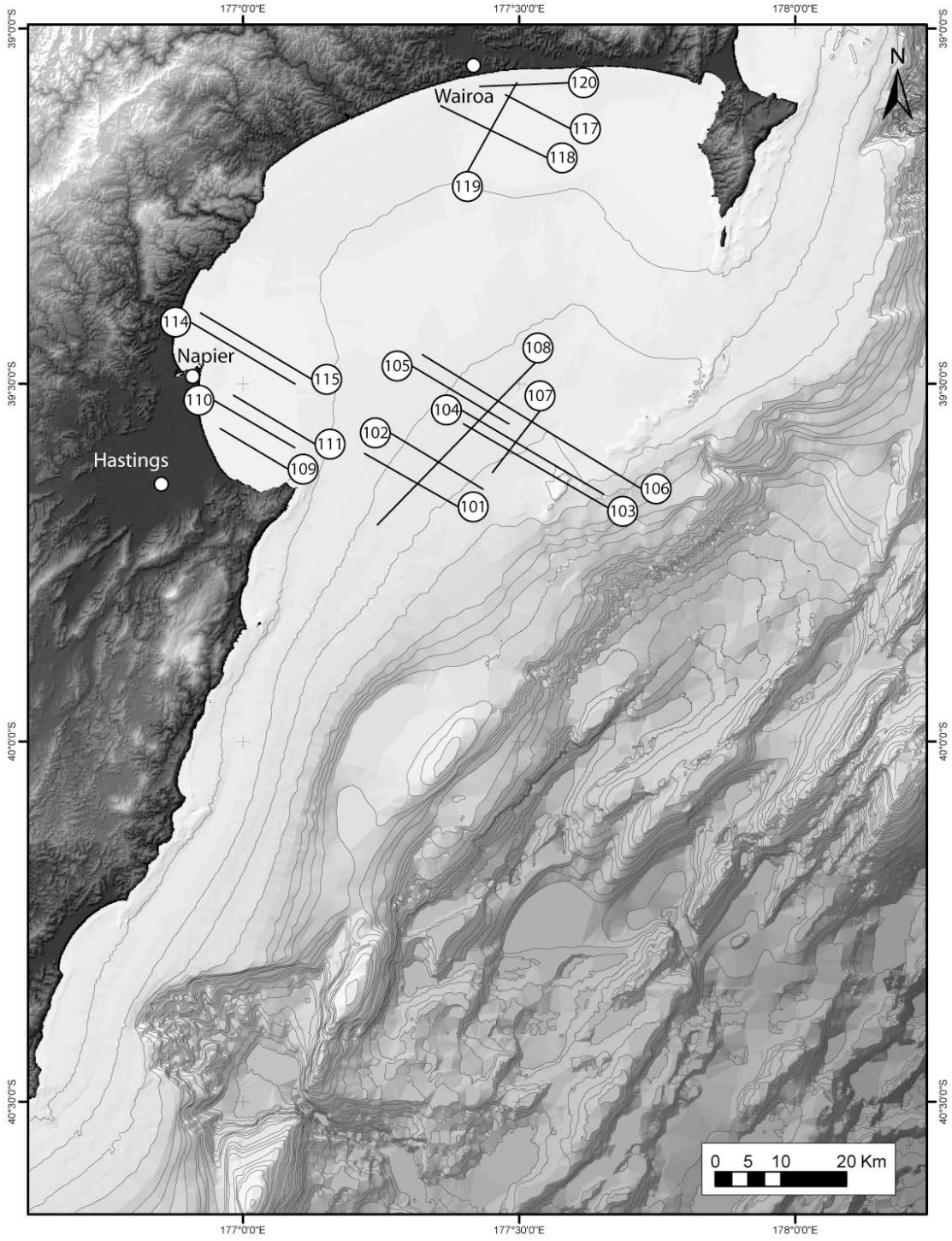

Figure 3.8 : Plan de positionnement des lignes sismiques de la campagne WE00 (Geo-Prakla, 2000).

- TAN 0313 :

Année / year : ……...*2003*
Opérateur / operator : ……...*NIWA*
Navire / Vessel : ……...*RV Tangaroa*
Type de données : ……*3.5 KHz*
Sismique multitrace (48 canaux)
Longueur totale interprétée : ……*830 km*
Rapports ou publications significatives :……..*Aucune publication antérieure.*

La campagne TAN 0313 a été acquise en août 2003 pour répondre notamment aux objectifs de cette étude.
Les profiles 3.5 KHz et multitrace sont de bonne qualité. La résolution est excellente entre le fond marin et le premier multiple mais diminue significativement dans les zones de faible tranche d'eau de Hawke Bay. Les lignes couvrent la partie sud de Hawke Bay et s'étendent au large de la Waimarama Coast (Fig. 3.9). Leur positionnement spécifique a pour objectif de compléter le jeu de données existant et de l'étendre (au Sud).

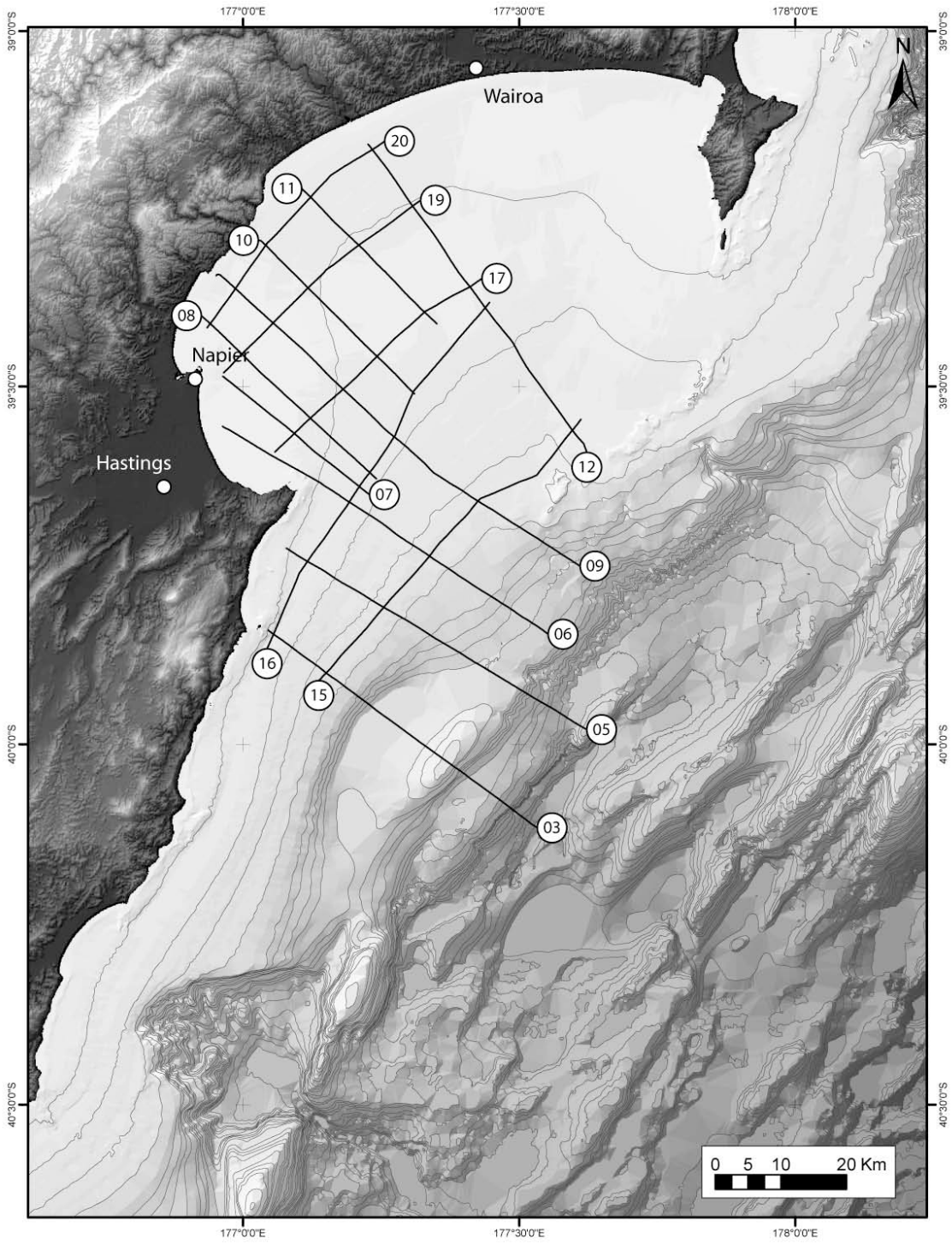

Figure 3.9 : Plan de positionnement des lignes sismiques de la campagne TAN 0313.

- TAN 0412 :

Année / year : ……...*2004*
Opérateur / operator : ……...*NIWA*
Navire / Vessel : ……...*RV Tangaroa*
Type de données : ……*3.5 KHz (enregistrement numérique)*
Sismique multitrace (48 canaux)
Longueur totale interprétée : ……*298 km*
Rapports ou publications significatives :……..*Aucune publication antérieure.*

La campagne TAN 0412 a été acquise en novembre 2004 pour répondre aux objectifs de cette étude.
Les profiles 3.5 KHz et multitrace sont de bonne qualité, comparables à ceux de la campagne TAN 0313. La résolution est excellente entre le fond marin et le premier multiple mais diminue significativement dans les zones de faible tranche d'eau de Hawke Bay. Le positionnement spécifique des profiles a pour objectif de compléter le jeu de données apporté par la campagne TAN 0313 (Fig. 3.10). Les lignes couvrent l'extrême sud de Hawke Bay, en s'intercalant entre les profils TAN 0313, et s'étendent davantage vers le sud et au large de la Waimarama Coast.

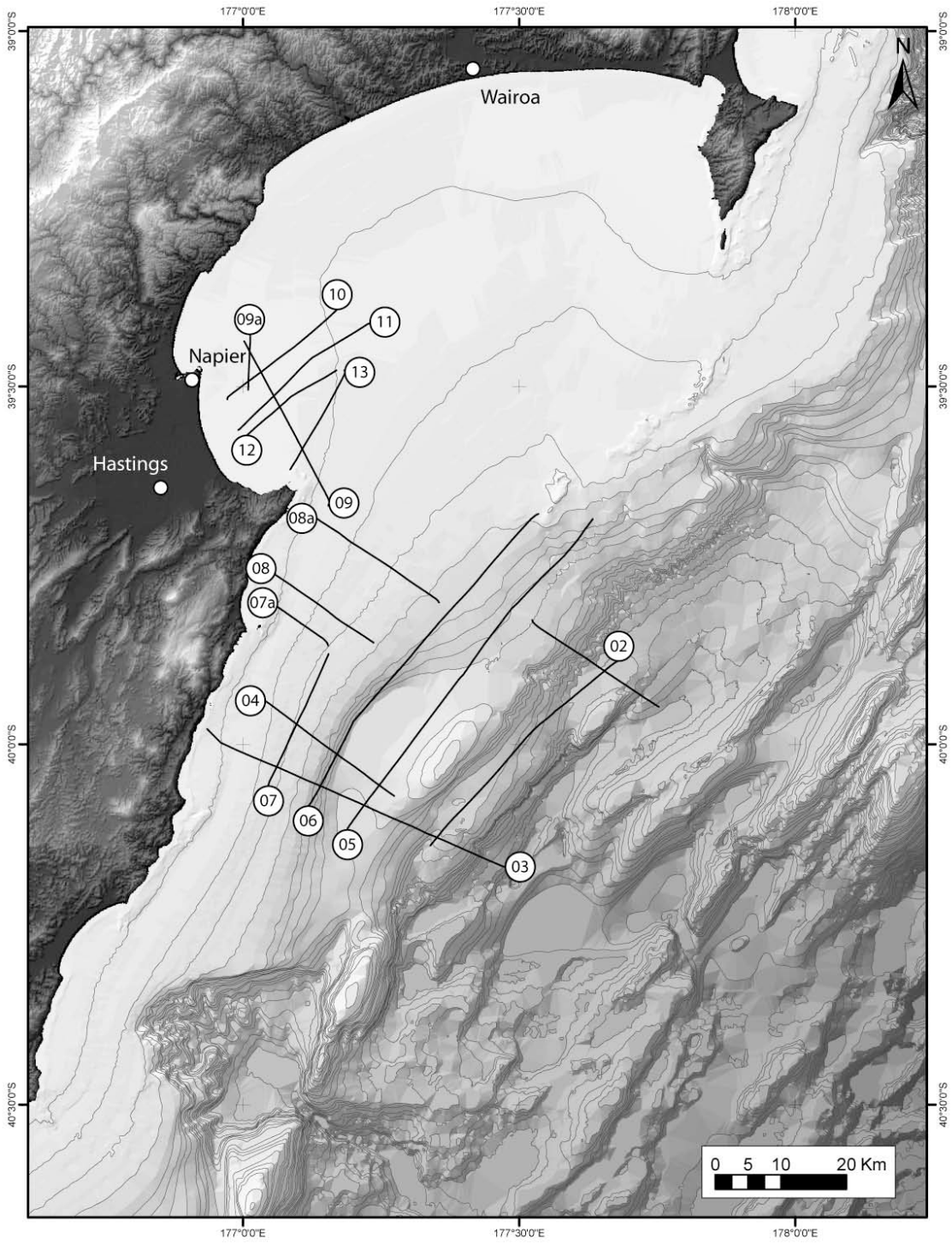

Figure 3.10 : Plan de positionnement des lignes sismiques de la campagne TAN 0412.

- 05CM :

Année / year : ……...*2005*
Opérateur / operator : ……...*Ministry of Economic Development NZ*
Navire / Vessel : ……...*M/V Pacific Titan*
Type de données : …… *Sismique multitrace (640 / 960 canaux)*
Longueur totale interprétée : ……*720 km*
Rapports ou publications significatives :……..*Multiwave (2005).*

La campagne 05CM a été acquise en novembre 2005 par le ministère de l'économie néo-zélandais pour réévaluer le potentiel économique de la côte est de l'île Nord.
Les profiles multitrace sont d'excellente qualité. La résolution est très bonne pour aux profondeurs de pénétration permettant d'imager le remplissage cénozoïque et les multiples sont bien corrigés. La qualité globale du jeu de données permet des corrélations fiables entre profiles et avec les profiles des campagnes antérieures. Les profiles sont positionnés sur les parties externes de Hawke Bay et au large de la Waimarama Coast (Fig. 3.11).

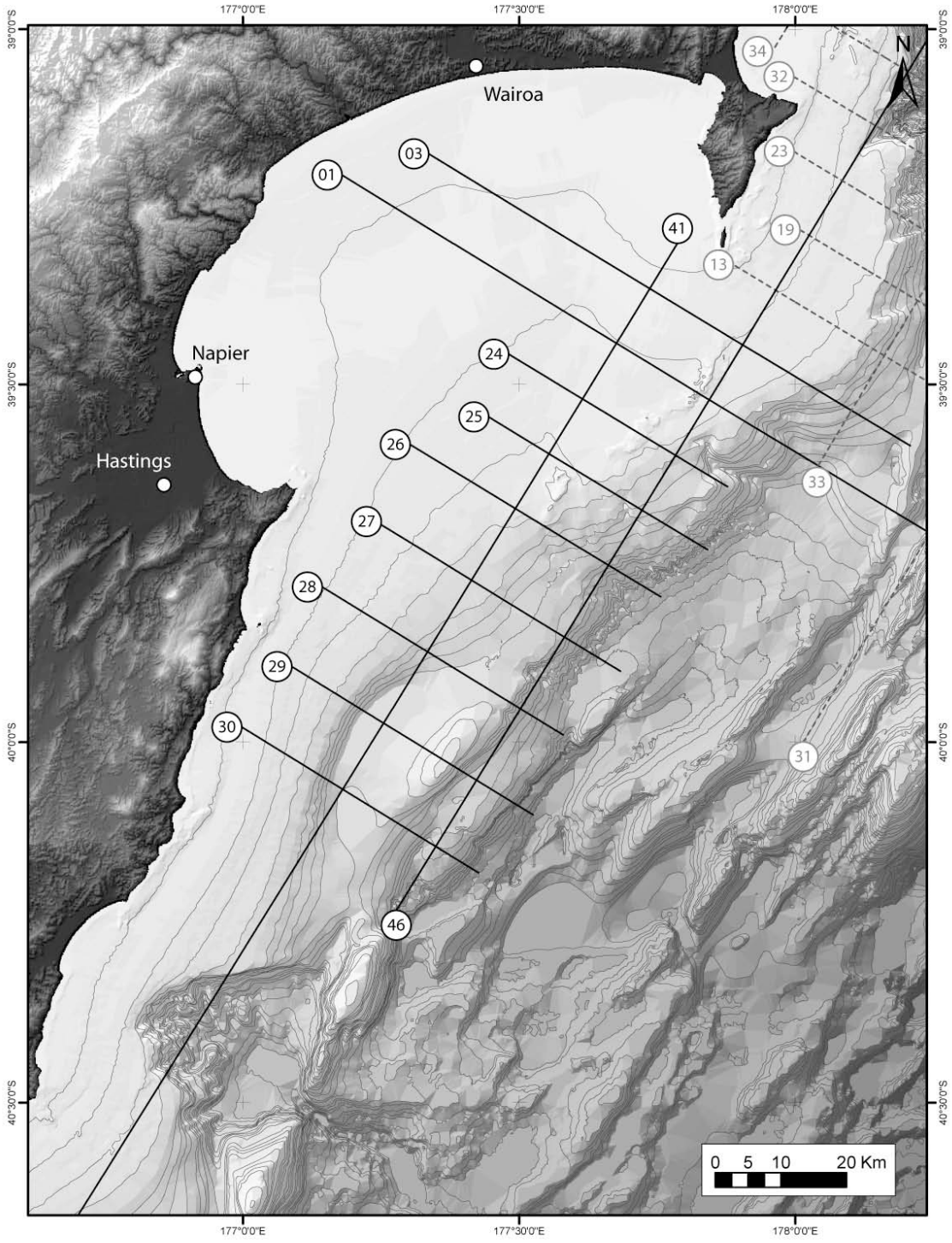

Figure 3.11 : Plan de positionnement des lignes sismiques de la campagne 05CM.

- GSR05301 :

Année / year : ……...*2005*
Opérateur / operator : ……...*NIWA - CNRS*
Navire / Vessel : ……...*Big Kahuna*
Type de données : …… *Boomer*
Longueur totale interprétée : ……*175 km*
Rapports ou publications significatives :……..*Aucune publication antérieure.*

Les données de la campagne GSR05201 ont été acquises en février et mars 2003 pour permettre de corréler les interprétations des jeux de données en mer et à terre (sismique et cartographie géologique).
Les profiles Boomer sont de bonne qualité et pénètre jusqu'à 100 ms (TWTT). Les lignes couvrent l'extrême sud de Hawke Bay au large des plaines d'Heretaunga (Fig. 3.12).

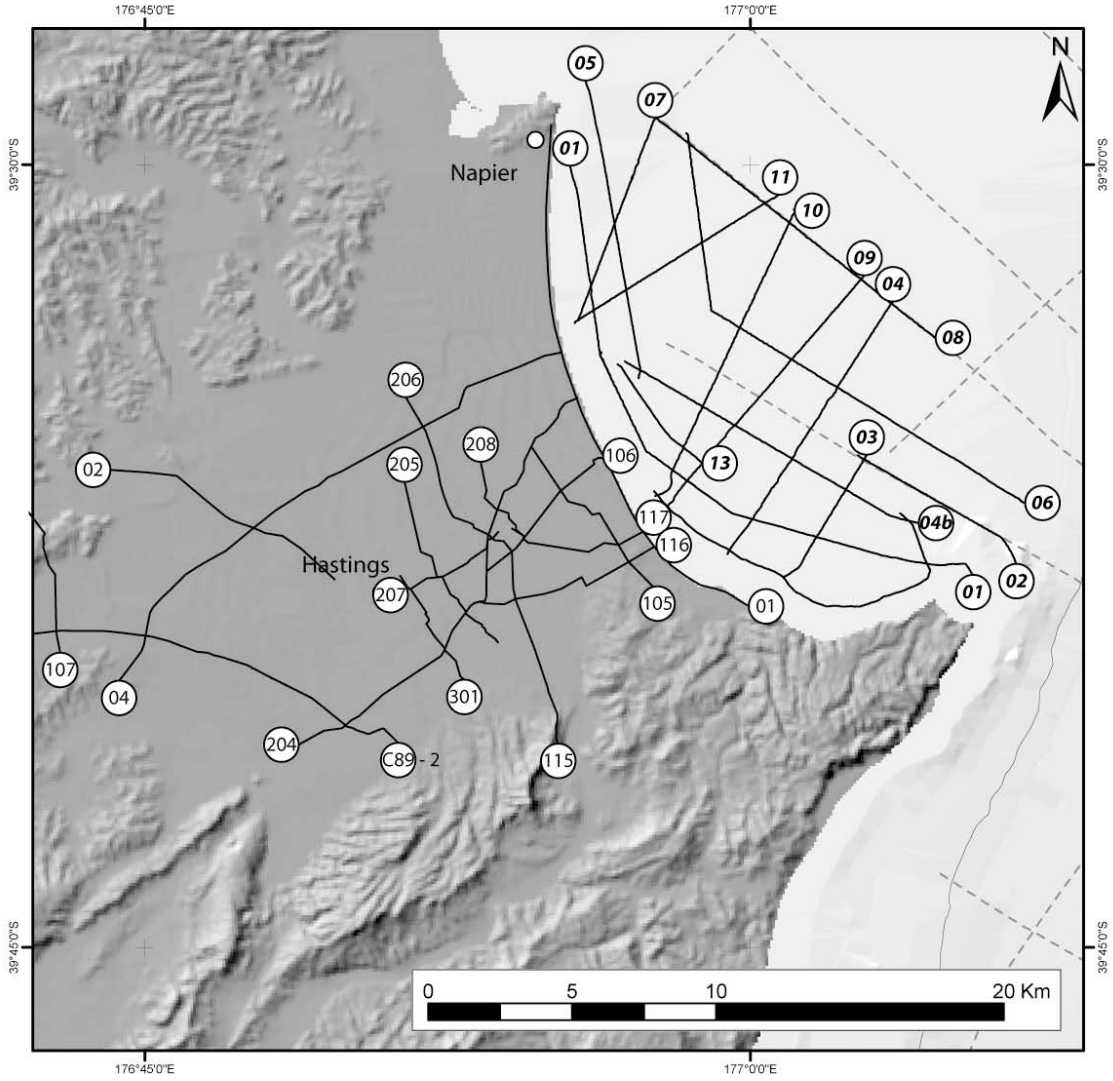

Figure 3.12 : Plan de positionnement des lignes sismiques de la campagne GSR05301 (italique) et des campagnes C89 et « 328 ».

3.3.2. Les missions de sismique à terre :

- C89 :

Année / year : ……...*1989*
Opérateur / operator : ……...*Croft Exploration Ltd.*
Survey equipment : ...……*Vibrator VVCA*
Type de données : …… *Sismique terrestre.*
Longueur totale interprétée : ……*1 profile C89-2 partiellement interprété*
Rapports ou publications significatives :……..*B.C.M. Geophysics Ltd – PR 1522 (1989)*

- IP 328-97/98/99 :

Année / year : ……...*1997, 98 et 99*
Opérateur / operator : ……...*Indo Pacific Energy NZ Ltd.*
Survey equipment : ...……*Vibrator VVCA*
Type de données : …… *Sismique terrestre.*
Longueur totale interprétée : ……*15 profiles partiellement interprétés*
Rapports ou publications significatives :……..*Small, Michael & others – PR 2299 (1997)*
Schlumberger Geco Prakla – PR 2392, PR 2393 (1998, 1999)

Les profiles sismiques sont de qualité variable et couvrent la majeure partie des plaines d'Heretaunga (Fig. 3.12).

3.3.3. Carottes et dragages en mer :

- MD152 / Matacore :

Année / year : ……...*2006.*
Opérateur / operator : ……...*IPEV / CNRS / NIWA / AWI / VIMS / SIO.*
Navire / Vessel : ……...*Marion-Dufresne II.*
Survey equipment : ...……*Carottier géant "Calypso" & 3.5 KHz.*
Type de données : …… *Carotte sédimentaire en domaine marin.*
Longueur totale interprétée : ……*6 carottes de 1 à 30 m (longueur totale de 81,5 m).*
Rapports ou publications significatives :……..*Proust et al. (2006).*

La mission de carottage MATACORE s'est déroulée en janvier et février 2006. Les objectifs de cette mission étaient (1) la caractérisation et la quantification des sédiments issus de l'érosion des chaînes en surrections au sein de la marge active Hikurangi, et déposés dans les bassins avant et arrière arc (Hawke Bay, Wanganui, Poverty Bay) depuis ~1.5 Ma ; (2) reconstituer le calendrier des phénomènes gravitaires des méga-avalanches de Ruatoria et Matakoa et déterminer leurs caractéristiques ; (3) reconstituer les circulations océaniques passées et leurs relation avec les changements climatiques globaux. Six carottes ont été récoltées, découpées, passées au banc MST (multi-sensor tarck) et décrites (Fig. 3.13).
Le positionnement des six carottes récoltées au large de Hawke Bay a été défini pour pouvoir caractériser les sédiments et les milieux de dépôt associés visibles sur les données sismiques, ainsi que leur âge, en vue d'un calage de la chronostratigraphie (Fig. 3.14 – Table 3.1).
Les trois premières carottes sont situées au-delà de la rupture de pente, dans le bassin de pente de Motuokura. Les carottes MD06-2995 (19 m) et MD06-2996 (27 m) sont localisées sur la ride de Motuokura (vers -500 m), au pied du dernier cortège sédimentaire de bas niveau, où une partie du remplissage du bassin de Motuokura est condensé. Elles devaient notamment fournir des âges des séquences de dépôt, permettant de confirmer les estimations produites à partir des interprétations sismiques (0.5 Ma à l'actuel). La carotte MD06-2997 (30 m) est située sous la rupture de pente de la plateforme et traverse le dernier cortège de bas niveau (vers -400 m). Elle est localisée dans une zone où la déformation des bancs observée en sismique est attribuée à un glissement sous marin : le « Kidnappers Slide » (Lewis, 1971b ;

Barnes et Lewis, 1991). L'objectif était de déterminer la nature et l'âge des sédiments du cortège de bas niveau, supposés appartenir au dernier maximum glacière (~30 à 15 ka).

Les trois dernières carottes sont situées sur la plateforme, dans la partie interne de Hawke Bay, au sein du bassin avant arc *sensu stricto*. Les carottes MD06-2998 (3 m), MD06-2999 (1 m) et MD06-3000 (1 ,6 m) sont situées sur la ride structurale de Kidnappers à des profondeurs respectives de 90, 80 et 70 mètres. Elles pénètrent des séquences identifiées en sismique, basculées par la croissance de la ride et amenées à l'affleurement sous le fond marin. Leur âge est estimé entre 0.3 et 0.5 Ma.

Quelques résultats préliminaires sur les âges sont déjà disponibles et les analyses sont toujours en cours.

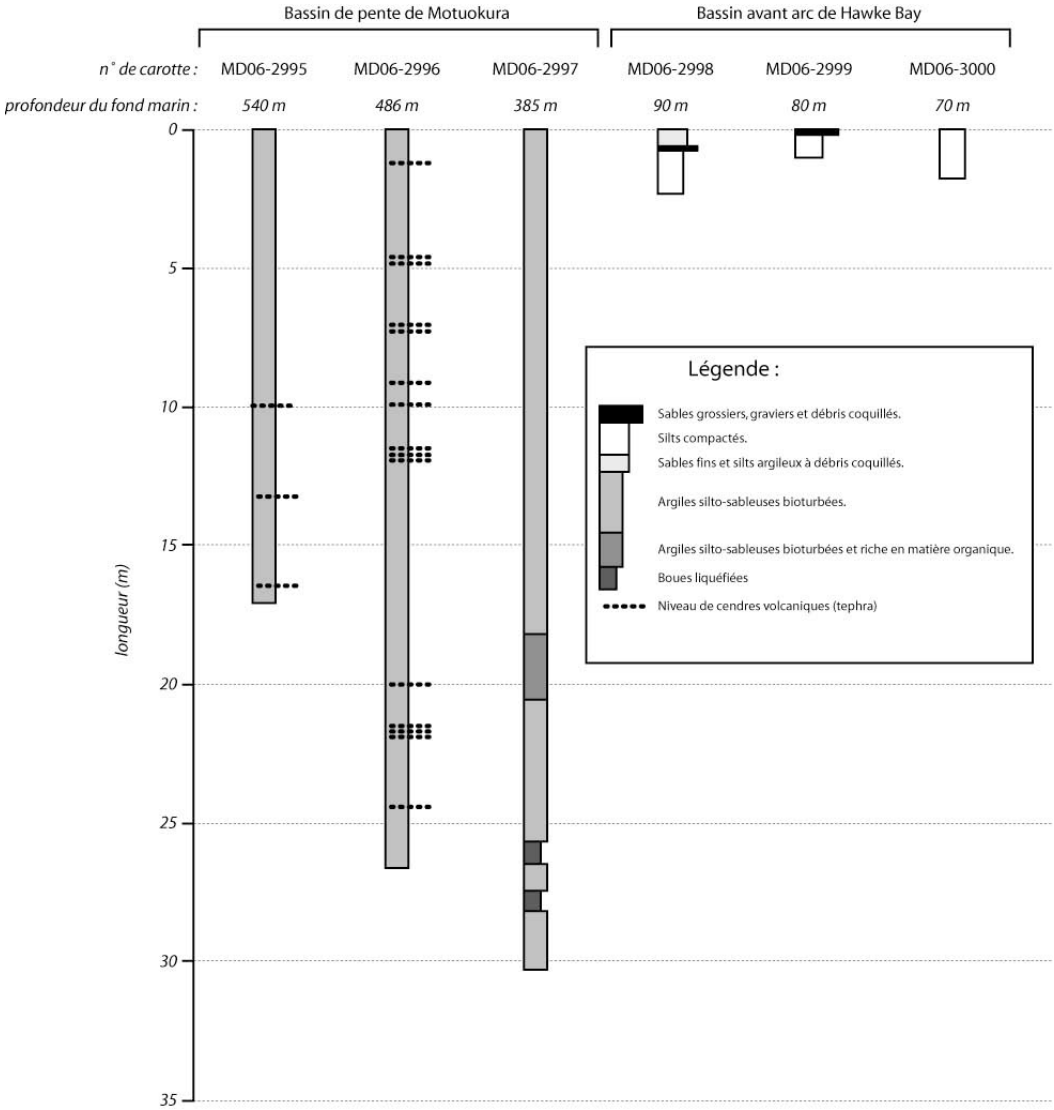

Figure 3.13 :Descriptions rapides du contenu sédimentaire des six carottes collectées dans le domaine avant arc d'Hawke Bay lors de la mission MD152 – MATACORE, à bord du Marion-Dufresne II..

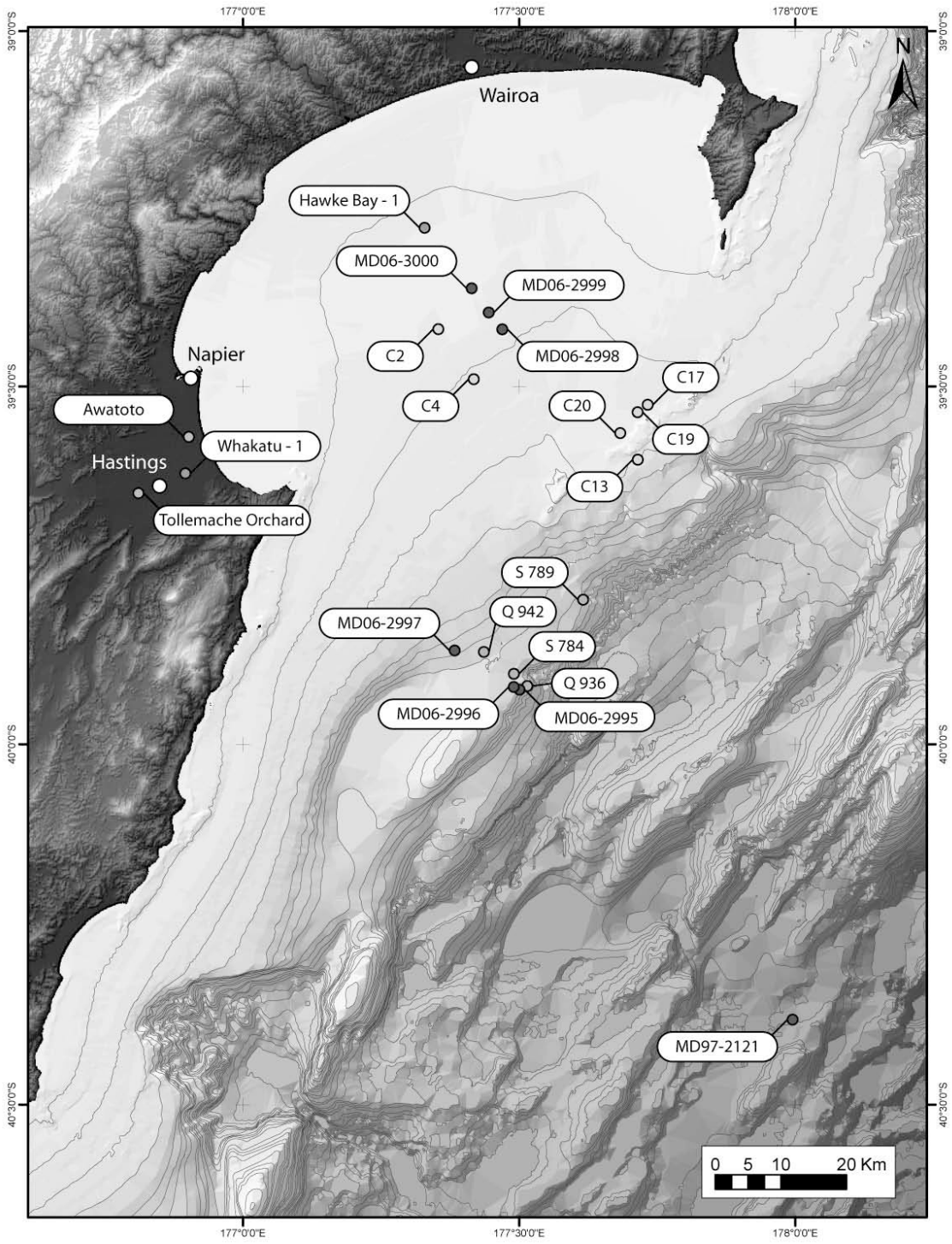

Figure 3.14 : Plan de positionnement des carottes, puits, forages pétroliers et dragages utilisés dans cette étude pour calibrer les faciès sismiques et déterminer les âges des séquences identifiées à partir des interprétations sismiques. Les carottes de la mission MATACORE sont identifiées par le préfixe « MD06 ».

N° de carotte	Latitude	Longitude	Profondeur (m)	Longueur d'échantillonnage (m)
MD06-2995	39°55,53'	177°30,24'	540	19,04
MD06-2996	39° 55,11'	177° 29,41'	486	26,80
MD06-2997	39° 52,07'	177° 22,91'	385	30,30
MD06-2998	39° 25,16'	177° 28,16'	90	2,95
MD06-2999	39° 23,80'	39° 21,83'	80	0,98
MD06-3000	39° 21,83'	177° 24,88'	70	1,61

Tableau 3.1 : Tableau rappelant la position géographique, la bathymétrie du site de carottage et la longueur d'échantillonnage de chacune des carottes de la mission MATACORE.

Les données 3.5 KHz enregistrées au cours de la campagne MATACORE sont de très bonne qualité (résolution et pénétration) et facilitent les corrélations entre les données sismiques conventionnelles et les carottes. L'acquisition s'effectuait en continu sur l'ensemble de la mission. Trois profiles peuvent être reconstitués et utilisés pour les interprétations. Le premier, suit l'alignement MD06-2995 / 96 / 97 et remonte jusqu'à la rupture de pente (recouvre une partie du profile TAN 0313-05 – voir Fig. 3.9). Le second profile continu le premier en direction du site de carottage de MD06-2998 (recouvre une partie du profile TAN 0313-15 – voir Fig. 3.9). Le troisième suit l'alignement MD06-2998 / 99 /3000 (recouvre une partie du profile TAN 0313-12 – voir Fig. 3.9).

- Carottes obtenues par NZ Oceanographic Institue :

Année / year : ……...*1987 & 1988.*
Opérateur / operator : ……...*NZ Oceanographic Institue.*
Navire / Vessel : ……...*GRV Rapuhia & RV S.P. Lee*
Survey equipment : ...……*Carottier.*
Type de données : …… *Carottes sédimentaires.*
Longueur totale interprétée : ……*4 carottes.*
Rapports ou publications significatives :……..*Kvenvolden (1988) ; Barnes et al. (1991).*

Les données issues de cette mission fournissent des âges intéressant pour la chronostratigraphie du Pléistocène supérieur et de l'Holocène. Quatre carottes collectées permettent de mieux contraindre la chronostratigraphie. Les carottes sont localisées sous la rupture de pente, au dessus du Motu-o-Kura trough (Fig. 3.14).

- Petroleum industry Hawke Bay sea floor samples :

Année / year : ……...*1989.*
Opérateur / operator : ……...*NZ CQX Ltd.*
Navire / Vessel : ……...*GRV Rapuhia.*
Survey equipment : ...……*Carottier et dragage.*
Type de données : …… *Carottes sédimentaires et dragage en domaine marin.*
Longueur totale interprétée : ……*6 carottes et 1 dragage.*
Rapports ou publications significatives :……..*Strong et al. – PR 1470 (1989) ; Barnes et al. (2002).*

Les données issues de cette mission fournissent des âges intéressant pour la chronostratigraphie du Néogène. Sept échantillons collectés dans le remplissage Pléistocène permettent de mieux contraindre la chronostratigraphie. Les carottes (C) et le dragage (D) sont localisés sur les rides de Kidnappers et Lachlan (Fig. 3.14).

3.3.4. Puits d'exploration pétrolière et hydrologique:

- Hawke Bay - 1 :

Année / year : ……...*1976.*
Opérateur / operator : ……...*BP Shell Aquitaine Todd Petroleum Developments.*
Navire / Vessel : ……...*Navire de forage Glomar Tasman.*
Type de données : ……*Forage en mer.*
Longueur totale interprétée : ……*288 m sur 2305 m.*
Rapports ou publications significatives :……..*Heffer et al. – PR 667 (1976).*

Hawke Bay – 1 est localisé dans Hawke Bay pénètre les dépôt Néogènes de Hawke Bay (Fig. 3.14). Bien que traversés, les niveaux Pléistocènes n'ont pas fait l'objet d'attention particulière en terme de description. Les 288 premiers mètres du forage sont attribués à l'Haweran (c. 340 ka – actuel).

- Whakatu - 1 :

Année / year : ……...*2000.*
Opérateur / operator : ……...*Indo-Pacific Energy (NZ) Ltd.*
Navire / Vessel : ……...*Navire de forage Glomar Tasman.*
Type de données : ……*Forage à terre.*
Longueur totale interprétée : ……*307 m sur 1455 m.*
Rapports ou publications significatives :……..*Ozolins et Francis PR 2476 (2000).*

Whakatu – 1 est localisé dans les plaines de Heretaunga, au sud de Hawke Bay et pénètre les dépôt Néogènes (Fig. 3.14). Les 307 premiers mètres traversent les dépôts Holocène et le Kidnappers group.

- Tollemache Orchard :

Année / year : ……...*1993.*
Opérateur / operator : ……...*Hawke's Bay Regional Council / IGNS.*
Type de données : …… *Forage.*
Longueur totale interprétée : ……*257 m.*
Rapports ou publications significatives :……..*Brown (1993); Dravid and Brown (1997).*

Tollemache Orchard est un forage hydrologique de 257 m de profondeur, situé au sein des plaines de Heretaunga (Fig. 3.14). Des descriptions géologiques ainsi que des âges issus des sont disponibles sur tout ou partie du puit.

- Awatoto :

Année / year : ……...*1995.*
Opérateur / operator : ……...*Hawke's Bay Regional Council / IGNS.*
Type de données : …… *Forage.*
Longueur totale interprétée : ……*254 m.*
Rapports ou publications significatives :……..*Brown and Gibbs (1996);Dravid and Brown (1997)*

Awatoto est un forage hydrologique de 254 m de profondeur, situé au sein des plaines de Heretaunga (Fig. 3.14). Des descriptions géologiques ainsi que des âges issus des sont disponibles sur tout ou partie du puit.

Chapitre 4 :

La sédimentation dans Hawke Bay au Pléistocène supérieure : nouveaux apports pour la compréhension de l'évolution morphostructurale des bassins avant arc.

LATE PLEISTOCENE SEDIMENTATION IN HAWKE BAY, NEW ZEALAND:
New insights into forearc basin morphostructural evolution

Fabien PAQUET (1), Jean-Noël PROUST (1), Phil BARNES (2), Jarg PETTINGA (3)

(1) UMR Géosciences, CNRS Université de Rennes 1, Campus de Beaulieu, 35042 Rennes cedex
(2) National Institute of Water and Atmospheric Research (NIWA) Ltd, Private Bag 14-901, 301 Evans Bay Parade, Greta Point, Wellington, New Zealand
(3) Department of Geological Sciences, University of Canterbury, Private Bag 4800, Christchurch, New Zealand

Corresponding author:
Fabien Paquet
email fabien.paquet@univ-rennes1.fr;
Ph. 00 33 2 23 23 57 26;
Fax 00 33 2 23 23 61 00

ABSTRACT :

The influence of eustasy, tectonic deformation pattern and sediment fluxes as control parameters on basin stratigraphy and depositional sequence development are largely accepted. Eustasy is usually considered as the dominant mechanism of sequence generation especially for Pleistocene time (promptness and amplitude of changes). In active subduction margin settings, the role of high rate tectonic deformation is expected to have stronger influences on basin fill architecture. Effects of the sediment flux are generally less constrained, and therefore less considered. The Hawke Bay forearc basin of the Hikurangi active subduction margin in New Zealand offers the opportunity to study the impact of these parameters. The present work is a quantitative source-to-sink study of the Late Pleistocene forearc domain (c. 140 Ka to Present). The use of an extensive seismic data set as well as cores and well data, sedimentological sections and geomorphological analyses allow the identification of a complete climatically-driven 100 kyr-type depositional sequence. It also reveals the interactions and the influences of (i) the structural pattern; (ii) the activity of structures; and (iii) the amount of sediment fluxes on the sediment distribution and the landscape evolution over the area. Two paleogeographic reconstructions illustrate the face of the Hawke Bay forearc domain as a result of eustasy changes, tectonic settings and sediment fluxes at the two climatic extremes of the Last Glacial Maximum and the Holocene Optimum.

1- INTRODUCTION

Eustasy, climate and deformation are key parameters that control erosion, sediment supply and transport, deposition and preservation and thus stratigraphic patterns in sedimentary basins (Jervey, 1988; Posamentier et al., 1988; Blum and Törnqvist, 2000). To date, most descriptions and related stratigraphic models are based on studies from passive continental margins characterized by simple shelf ramp and upper slope morphology resulting from only moderate subsidence-dominated deformation (Payton, 1977), and eustatic sea-level changes control the distribution and preservation of sediments (eg. Vail et al., 1977). This is particularly emphasized during the Pleistocene as high amplitude climate-driven eustatic changes are controlling the development of well-expressed depositional sequences (eg. Proust and Chanier, 2004). In active margin basins, tectonic deformation is characterized by local uplift and subsidence creating complex topography that may in turn influence the distribution of sediments and the architecture of depositional sequences. Globally, there is a scarcity of well-exposed active margin basin fills. As a consequence, the combined influence of tectonic deformation, sediment fluxes and climate change on topography, and thus on sediment architecture, has not been properly illustrated or understood (Okamura and Blum, 1993; Christie-Blick and Driscoll, 1995; Catuneanu, 2006). We describe here the upper Pleistocene sedimentary fill of the Hawke Bay forearc domain of the Hikurangi active subduction margin of New Zealand. Temporally, this sequence corresponds to the well exposed and investigated sediments deposited during a complete high amplitude climato-eustatic cycle (Lewis, 1971a, Proust et Chanier, 2004) and a well-documented tectonically active period (eg. Pillans, 1986; Cashman and Kelsey, 1990; Barnes et al., 2002; Barnes and Nicol, 2004; Pettinga, 2004; Proust and Chanier, 2004; Litchfield and Berryman, 2006).

After a brief review of the geodynamic development of the Hikurangi margin and of the Late Pleistocene climate evolution and morphostructural setting of the present day Hawke Bay forearc basin domain, we describe: (1) the Upper Pleistocene marine sediment record of the forearc and trench slope basins (seismic facies and units, stratigraphic architecture, age controls); (2) the Upper Pleistocene terrestrial sediment record of the foothills; and (3) the correlation of these two components of the forearc basin domain integrated into a “source to sink” reconstruction of the Upper Pleistocene sediment record. These results provide the opportunity to illustrate two end-member models in the paleogegraphic evolution of the forearc domain of this active margin, characteristic of glacial and interglacial conditions.

Based on this we evaluate the late Pleistocene sediment budget of the margin and explore relationships between the marine and non-marine parts of the late Pleistocene morphostructural evolution.

2- REGIONAL SETTING OF THE HAWKE'S BAY FOREARC DOMAIN

The Late Pleistocene evolution of the Hawke Bay forearc domain results from the interaction of both long and short term climatic and tectonic forcing factors. In the Following section we broadly review the geodynamic and paleo-climatic evolutions and the resulting morphostructure of the forearc part of the margin.

2.1- Geodynamic evolution

The active Hikurangi margin of New Zealand is forming in response to the oblique subduction of a thickened wedge of the oceanic Pacific plate beneath the continental crust of the North Island of New Zealand (Australian Plate) (Fig.1). The active margin comprises from west to east: Mio-Pliocene, calc-alkaline volcanic arcs (Northland and Coromandel peninsulas); a Plio-Pleistocene, rapidly subsiding basin in a backarc position (Wanganui Basin); a Pleistocene–Recent calc-alkaline volcanic (Central Zone); a still uplifting axial range composed of Triassic to Cretaceous turbidites affected by poly-hased deformation and recent dextral shears (frontal ridge); a forearc basin filled by up to 6000m of Mio-Pliocene turbidites and Plio-Pleistocene shallow marine to fluvial sediments; and an accretionary prism or imbricate frontal wedge, made up of deformed sediments of the forearc shelf and slope, partly exposed in the coastal ranges and of slivers accreted from the trench fill during the Quaternary in its outer part (from Proust and Chanier, 2004; see also: e.g. Ballance et al., 1982; Walcott, 1987; Lewis and Pettinga, 1993; Barnes and Mercier de Lépinay, 1997). To the east, the surface of the accretionary wedge (forming the slope) dips gently towards the Hikurangi Trough. The present day structure of the margin is the result of multiple changes in its tectonic regimes. Subduction started during Miocene ca. 25 Ma and tectonic deformation was dominated by thrusting with a Late Miocene-Pliocene phase of shallow extension (Balance, 1976; Pettinga, 1982; Spörli and Balance, 1989; Field and Uruski, 1997; Barnes et al., 2002). The margin is now broadly characterized by shortening and inversion (Chanier, 1991; Chanier et al., 1992; Buret et al., 1997, Barnes et al., 2002).

2.2- Climatic evolution

Late Pleistocene climate changes over the East Coast of North Island are mainly documented by palynology and depositional environment studies in lakes, peat bogs and offshore cores (Lowe et al., 1999; McGlone, 2001; Okuda et al., 2002; Newnham et al., 2003; Shane & Sandiford, 2003). Glacial ice conditions in North Island were limited to the highest crests fo the Tararua Range (southern axial ranges) and to highest volcanoes of the Central Volcanic Zone at the last glacial maximum (McArthur and Shepherd, 1990; Pillans et al., 1993; Brook and Brock, 2005). No evidence of glaciation has been reported in the major segments of the axial ranges, west of the Hawke Bay, during The Late Pleistocene. In southern Hawke's Bay, a nearly 200 m deep core drilled in the Poukawa basin (Fig. 2), provides a complete and detailed record of late Pleistocene vegetation changes for the area (Shulmeister et al., 2001; Carter, 2002; Okuda et al., 2002). Results show that climatic conditions changed from warm and moist (podocarp/hardwood forest) at the Last interglacial (Oxygen Isotopic Stage 5) to colder and drier (grass & shrub lands) at the Last Glacial Maximum and finally warm and moist through to the present day (Okuda et al., 2002). The drier conditions of the last glacial maximum probably resulted from lower precipitation and enhanced wind speeds (McGlone, 2001; Shulmeister et al., 2001). Nevertheless, rainfall was sufficient over North Island as small lakes (eg. Maratoto Lake) persisted in the Waikato region (McGlone, 2001). Shulmeister et al. (2001) propose a mean annual temperature decline of c. 7°C at the LGM based on the development of tussock grassland environment. These results are in accordance with conclusions reached in other palynological studies the climate reconstitutions for the Late Pleistocene (Newnham et al., 1999 & 2003; Shane & Sandiford, 2003; Barrell et al., 2005; Alloway et al., 2007).

2.3- Morphostructure

The Hawke's Bay comprises five approximately parallel NNE trending morphostructural domains including : the axial ranges (Frontal Ridge), the western foothills, the forearc basin, the eastern imbricate frontal wedge, including the emergent sector forming the coastal ranges.

The Frontal Ridge axial ranges

Deformation in the western axial ranges is dominated by oblique dextral shear. Several major strike-slip faults with reverse slip-component (e.g. Mohaka and Ruahine faults) dissect the highly deformed Mesozoic Torlesse basement terrane (Suggate, 1961; Kingma, 1962). In the Hawke Bay region, the emergence of the modern ranges occurred close to the Plio-Pleistocene boundary (Beu et al., 1981; Erdman and Kelsey, 1992). Except for the highest

peaks and the sharpest crests, the tops of the axial ranges are characterized by flat and relatively smooth remnant topographic surface (Fig.2). A modern fluvial network that drains much of the Hawke Bay sector of the forearc region dissects this surface. Rivers are deeply incised into the basement and form V-shaped valleys. Erosional incision is the dominant process controlling slope morphology in the axial ranges. Constructional landforms such as aggradational terraces are very limited in extent and confined to the major valleys (Smale et al., 1978). Estimated Pleistocene uplift rates range from 1-1.3 $mm.yr^{-1}$ (Nicol in Litchfield and Berryman, 2006; Beu et al., 1981).

The western forearc foothill domain

The foothills domain is located immediately east of the axial ranges (Fig.2). The foothills landscape corresponds to a series of well-rounded hills formed on Neogene sediments affected by thrust faults and gentle folds (Cashman et al., 1992; Beanland et al., 1998). It comprises recently uplifted marine to terrestrial Miocene to Pleistocene formations (Kingma, 1958; Grant-Taylor 1978). During the upper Pleistocene, down-cutting rivers formed wide U-shaped valleys with sets of cut and fill terraces (Litchfield, 2003; Litchfield and Berryman, 2005). In the last 125 Ka, uplift rates have been calculated from fluvial terrace elevations by Litchfield and Berryman (2006), and range from 3 $mm.yr^{-1}$ along the Ruahine range-front to <1 $mm.yr^{-1}$ further to the east.

The forearc basin

The Hawke's Bay forearc basin corresponds to a subsiding area bounded by major structures (eg. Napier fault, Fig.2) that accommodate shortening and dextral shearing (Cashman et al., 1992; Beanland et al., 1998; Barnes et al., 2002). Except for the marginal coastal plains (Heretaunga plains), the major part of the basin is currently submerged beneath Hawke Bay. The sedimentation rate is estimated to have reached 3.6 $mm.yr^{-1}$ during the last 18 Ka (Litchfield and Berryman, 2006) below the Heretaunga plains. Recent subsidence rate estimates for the coastal area of northern Hawke's Bay, from Cochran *et al.* (2006), indicate values of ~1 $mm.yr^{-1}$. The average subsidence rates for the entire Pleistocene (last 1.8 Myrs) range from ~1-1.5 $mm.yr^{-1}$ (Pillans, 1986; Proust and Chanier, 2004).

The ridges and basins of the accretionary wedge

The imbricate frontal wedge (Lewis and Pettinga, 1993) is composed of Cretaceous and Cenozoic sedimentary rocks that are highly deformed by N to NE trending thrust and backthrust faulting and associated folds (Pettinga, 1980, 1982; Lewis, 1982; Van der Lingen

and Pettinga, 1982; Cashman et al. 1992; Lewis and Pettinga, 1993, Beanland et al., 1998). Offshore, narrow liner thrust ridges separate numerous trench-slope basins. The western inbound margin of the wedge is emergent, corresponding to the coastal hills in southern Hawke Bay (Pettinga, 1980, 1982) and continue to the north into Hawke Bay as the en-échelon Kidnappers and Lachlan submarine ridges separated by the Lachlan basin (Barnes et al., 2002). In addition to the regional shortening across the margin, onshore structural studies have revealed several normal faults and gravitational collapses that accommodate superficial extension (Pettinga, 1980; Pettinga 1985, Cashman and Kelsey, 1990; Pettinga, 2004). Estimates of recent uplift of the Coastal Ranges, based on elevation of Last Interglacial and Holocene marine terraces, range from 1.0 $mm.yr^{-1}$ to 2 $mm.yr^{-1}$ (Hull, 1985; Hull, 1987; Pillans, 1986). The vertical displacement rates along fault segments of both the Kidnappers and Lachlan ridges vary between 0.5 $mm.yr^{-1}$ and 5.0 $mm.yr^{-1}$ during the last ca.1Ma (Berryman, 1993; Barnes et al., 2002). To the south-east of this highest ridge complex lies the highest relatively subsiding trench-slope or upper slope basins (Lewis, 1980). The shelf edge and both Highstand and Lowstand System Tracts here develop in this basin in the vicinity of Hawke Bay. The western boundary to this basin is the uplifting Motuokura ridge. Further offshore deep-seated west verging thrusts of the imbricate frontal wedge form a series of almost parallel narrow liner submarine ridges uplifting at about 0.3 $mm.yr^{-1}$ (Lewis, 1974; Lewis and Bennett, 1985; Lewis and Pettinga, 1993), separating subsiding trench-slope basins. The size of these trench-slope basins usually ranges from 5-30 km wide and 10-60 km long and relative subsidence rates reaching up to 3 $mm.yr^{-1}$. (Lewis, 1980). The infilling of the trench slope basins is made up of hemipelagic sediments accumulated at a rates of 0.1 to 0.3 $mm.yr^{-1}$ (Lewis 1980; Carter and Manighetti, 2006).

3- DATA AND METHODOLOGY

This study presents the interpretation and integration of a large dataset acquired both in the onshore continental and in the marine parts of the forearc basin in the Hawke's Bay region. The onshore data were provided by fieldwork as part of this study, as well as previous geological mapping tied to studies of fluvial terraces and interpretations from groundwater wells draws. This study represents a comprehensive effort of integration of an extensive grid of marine data of diverse origin including bathymetry, 3.5 KHz, Multichannel (MCS) and boomer seismic data and piston core data (Table 1; Fig. 3).

Preliminary results from cores (MD06-2995 to MD06-3000) collected in the Hawke Bay and SE of Cape Kidnappers during the MD152 /Matacore survey (Table 1; Fig. 3)are also

presented in this paper as they help in stratigraphic and paleoenvironmental interpretation (Proust et al., 2006).

Seismic interpretations of Boomer and 3.5 KHz data sets that covers different areas with different resolution, were run independently. Both datasets were then compared in overlapping areas to develop the late Pleistocene seismic stratigraphy over the whole Hawke Bay domain.

Isopach maps were compiled by estimating sediment thicknesses. The conversion of TWT time intervals into sediment thickness values was achieved by using an average velocity of 1600 $m.s^{-1}$ in sediment. We then calculate the volume of sediment preserved and the rates of mass accumulation (sediment budget) using bulk density values provided in the literature (Barnes et al., 1991; Foster and Carter, 1997; Carter et al., 1999).

4- RESULTS

4.1- The Late Pleistocene sedimentary record in the Hawke's Bay forearc and trench slope basins

The morphostructural evolution of the Hikurangi Margin forearc domain is recorded in sediments preserved within the different sectors of a "source to sink" depositional profile extending from the axial ranges to the trench slope basins. The Late Pleistocene sediments in the Hawke's Bay region are only preserved in two sections of the depositional profile: (i) the onshore foothills of the axial ranges and (ii) the forearc basin (mostly offshore) and the proximal upper basins of the frontal accretionary wedge. The latter includes the coastal plains, the shelf and the upper slope to water depth of 500 m at the toe of the late Pleistocene, lowstand wedge offshore and east of Hawke Bay.

Hawke Bay is characterized by an overall flat shelf to water depth of c.150m of water depth. Below that depth, the slope increases sharply to 1°-3°. This break in slope at 150m of water depth is interpreted as the modern shelf edge (Fig. 2). In detail however, the Hawke Bay shelf and slope is characterized by an approximate flat-and-ramp morphologic geometry. Flats are located between the tectonically active structural ridges (Kidnappers, Lachlan and Motuokura ridges) (Fig. 2) and exhibit gentle slopes from 0.1° to 0.2° and from smooth depressions while ramps are characterized by steeper slopes ranging from 0.3° to 25°. Ramps usually face eastward towards the subduction front with a marked scarp along the east side of the

Motuokara ridge forming the base of the steepest slopes on the imbricate frontal wedge (Fig. 2).

On the inner shelf, both the boomer and 3.5 KHz profiles reveal flat lying horizons that gradually dip westward as they approach the Kidnappers ridge (Fig. 4). On the outer shelf to upper slope, the profiles exhibit prograding reflectors organized in an overall sigmoidal geometry, wedging out c. 350 m below the shelf edge (Fig. 4). The seismic reflections are truncated by five major unconformities (S1 to S5) that separate six seismic units (U1 to U6) (Fig. 4) that comprise 11 seismic facies (Fs1 to Fs11) (Tables 1 and 2).

Results are presented here along three key boomer profiles (Lines 6, 8 and 11) located in the inner part of Hawke Bay (Fig. 3; Fig. 5) and two 3.5 KHz profiles (AG1 and MD152) in the mid-shelf to upper slope (Fig. 3; Fig. 6).

Seismic unit 1: U1 forms the acoustic basement to the late Pleistocene seismic units and the core of the tectonically active Kidnappers, Lachlan and Motuokura ridges (Fig. 2, and Fig. 4). In the latter case, internal reflections are highly deformed with an overall 5-10° tilt to the northwest. The lower boundary to U1 can rarely be identified throughout the area. U1 is truncated above by a sharp erosional surface S1 (Fig. 5). The TWT thickness of U1 ranges from 150 ms to over 1.3s TWT. In the inner part of Hawke Bay, U1 is comprised of two sub-units (U1a, U1b) separated by a sharp truncation surface dipping 10° to the NW (Fig. 4, Fig. 5). The lower sub-unit U1a is made up of homogenous, high frequency, parallel reflectors (seismic facies Fs1, Tables 1 and 2) interpreted as a well-bedded sandstone and siltstone succession. The upper sub-unit U1b has a sheet- to wedge-shaped reflector configuration, with low continuity, wavy to chaotic, high amplitude reflections with superimposed channel-shape diffractions that alternate with medium continuity, sub parallel, high amplitude reflections (well-bedded) in Fs2-Fs6 (Tables 1 and 2; Fig. 5). In the outer part of Hawke Bay, the U1 deformed acoustic basement is overlain by a complex suite of wedge shape seismic units that remain largely unexplored.

The internal unconformity between U1a and U1b, observed over the inner shelf, physically correlates to the major regional unconformity that separates the Pleistocene Kidnappers Group and the Pliocene Black Reef Sandstones Formation onshore at Cape Kidnappers (Proust and Chanier, 2004) (for location refer Fig. 2). The underlying U1a is therefore directly correlated to the shallow marine, regressive, sandstones and siltstones of the Waipipian /Opoitian (early to mid-Pliocene) Flat Rock and Black Reef Formations (Harmsen, 1985). In the middle part of U1b, a thick package of chaotic reflections correlates to the 90m- thick

Clifton conglomerate exposed in the coastal cliffs, equivalent to the upper part of the Kidnappers Group (Fig. 5c) Thus, the lower half of U1b correlates to the Pleistocene Kidnappers Group deposits, that are made up of over c. 400 m-thick conglomerates, sandstones and siltstones strata deposited in shallow marine (inner bay to upper slope offshore) and terrestrial (fluvial, braid-fan) environments (Kingma, 1971; Kamp, 1978, 1990; Proust and Chanier, 2004). The upper half of U1b corresponds to thick packages of fluvial conglomerates and sands encountered in the lower part of the Awatoto and Tollemache onshore wells (line11 collected close to Awatoto well, see Fig.3, Fig. 6). These correlations in the inner bay are further corroborated by core sampling from the mid-shelf to upper slope strata by the Marion-Dufresne in 2006. Two long piston cores MD06-2995 and MD06-2996, of respectively 19 m and 26.8 m, penetrated U1 over the Motuokura ridge, at approximately 500 m of water depth (Fig. 2). These sediments are made up of gas-rich, highly compacted, silty mud (Proust et al., 2006). The absence of *Bolivinita pliozea* and the presence of more than 25% of sinistral form of *Gr. Truncatulinoides* in the basal part of MD06-2995 are consistent with an age younger than 0.5 Ma (B. Hayward pers. comm., in Proust et al., 2006). The absence of *Bolivinita pliozea* and the presence of dextral *T. Truncatulinoides* in the basal part of MD06-2996 (B. Hayward pers. comm., in Proust et al., 2006) are cosistent with an age ranging from 0.5 Ma to 0.6 Ma. Three 1 to 2 m-long piston cores MD06-2998, MD06-2999 and MD06-3000, penetrated U1 over the Kidnappers ridge at 70-90m of water depth (Fig. 2). These sediments correlate to the mid-Pleistocene Series (630-400 kyr) noted in Barnes et al., 2004). These preliminary results confirm the interpretation of U1 as Plio-Pleistocene in age, but also imply that the whole mid-Pleistocene to Present section is condensed below the shelf break, at circa 500 m of water depth (Fig. 4, Fig. 7).

Seismic unit 2: Beneath the inner shelf, U2 is a 160 ms TWT thick wedge-shape unit thinning out eastward against the Kidnappers ridge (Fig. 4, Fig. 5) and where it is tilted 1-2°NW with a progressive northwestward decreasing dip. Beneath the outer-shelf and upper slope region, U2 is more than 300 ms TWT thick, lens shape (Fig. 4, Fig. 9a), and locally deformed by active ridge uplift. U2 lies conformably on surface S1 with evidences of rare evidences of onlapping reflections beneath the upper slope (Fig. 9a). It is truncated above by an irregular surface with channels S2 dipping 1° NW in the SE and flattening to the NW (Fig. 5, Fig. 9b).

On the shelf, U2 is made up of facies Fs2 with sub-parallel, low continuity reflections above S1 passing upward to chaotic reflections with diffractions below S2 (Fig. 5). On the outer

shelf and upper slope, U2 is comprised of three seismic facies (Fs7, Fs8, Fs9) organized in 10ms-thick lens-shaped seismic reflection packages bounded by conformable high amplitude surfaces that can be correlated only with difficulty around the seismic grid (Fig. 9a). In an individual seismic package, Fs9 exhibits reflections with a regular sub-parallel configuration and good continuity that pass progressively to a sub-parallel, wavy (seismic facies Fs8) configuration in a basinward direction, while to landward reflection free configuration (seismic facies Fs7) is evident (Fig. 9a). Towards the top of the unit, the seismic facies becomes progressively more chaotic (Fig. 9a). The stacked arrangement of seismic reflection packages exhibit an overall retrogradational and then progradation pattern (Fig. 9a). This progradational stacking pattern appears in both the Lachlan and Motuokura basins, where lens shape packages are separated by clear downward shifts (Fig. 9a and 9b). In the Lachlan basin, the downward shift trend reveals a south-west progradation of packages, along the axis of the basin (Fig. 9b).

On the inner shelf, S1 can be geometrically traced to the 120ky old marine terrace at the top of the Kidnappers cliffs (Hull, 1985), and to the first marine incursion observed in coastal wells (Fig. 6). It correlates offshore to the wave ravinement surface (WR) of the last interglacial (OIS 5) wedging out against the Kidnappers ridge (Lewis, 1971a; Barnes et al., 2002). Seismic facies Fs2 with sub-parallel, low continuity reflections passing upward to chaotic reflections with diffractions is interpreted as an alternation of shallow marine siltstones and sandstones passing upward to stacked lenses of channelized terrestrial conglomerates interbedded with sandstone strata. This interpretation is supported by the overall coarsening upward succession of shallow marine silty sands and fluvial gravel conglomerates observed in the coastal wells (Fig. 6). This succession is organized into a set of parasequences that can fit to the MIS5-MIS3 sea level changes (Fig. 6). In outer part of the Hawke Bay seismic facies Fs7, Fs8 and Fs9 are comprised of reflection free to sub-parallel and then wavy reflection configurations that may correspond to a series of massive to well-bedded and sandstones and siltstones succession that pass basinward to a set of large scale bedforms interpreted as sediment waves. This last facies becomes more chaotic up section. Fs7, Fs8 and Fs9 are arranged into a progradational facies tracts that are organized into a broad retrogradational and then progradational stack made up of two landward stepping packages overlain by three seaward stepping packages respectively (Fig. 9a and b). The shallowing upward succession of shallow marine sandstone and siltstone to fluvial conglomerates, gives rise to a laterally deepening and vertically shallowing stack of

sequences comprised of shore-connected, massive sandstones with channels (Fs7), well bedded deep marine siltstones (Fs8) passing basinward to sediment bedforms (Fs9).

Seismic unit 3: U3 is a thin, 10 to 20 ms thick (TWT), slightly concave up, discontinuous, sheet drape unit. Reflections onlap at the base onto S2 and, are either concordant, or truncated above, along S3 (Fig. 4, Fig. 5, Tables 1 and 2). S2 is an irregular truncation surface with channels that give rise to a concordant surface in a seaward direction from the northern part of the Lachlan basin (Fig. 7, Fig. 8, Fig. 9b) to the offshore. S2 truncates U2 as it approaches the structurally active ridges. Nevertheless S2 is not preserved on top of the active ridges (Fig. 5, Fig. 8).

Beneath the shelf, U3 is made up of random alternations of stacked, channel shaped, and minor sub-parallel reflections assigned to seismic facies Fs3. On the outer shelf to upper slope, U3 is made up of facies Fs9, Fs10, Fs11. Fs9 exhibits sub-parallel, high continuity, medium amplitude reflections that pass upwards to chaotic, high amplitude reflector configurations in Fs10, or in a seaward direction, to wavy, parallel and highly continuous reflections in Fs11 (Fig. 7). The latter are characterized by long thin and faint lee-side reflections and usually short, thick and high amplitude stoss-side reflections. The stacked wavy undulations exhibit an apparent progressive landward/upslope migration (S-type sediment wave) (Fig. 7) together with a convex-upward geometry and a decreasing height and wavelength. Reflection-free configuration patches occur randomly into Fs11 on the seaward dipping side of the undulations. The seaward end of Fs11 coincides with the progressive wedging-out and condensation of its internal reflections as they approach the first slope scarp of the imbricate frontal wedge at a water depth of c.500m.

The S2 surface is an irregular truncation surface with channels incised into lenses of inferred terrestrial gravels interbedded with sands. It correlates to the maximum downward shift of baselevel at base of the thickest gravel bed in the coastal wells (Fig. 6). It is interpreted as the last sequence boundary (SB) of the last glacial maximum (OIS 2, c. 20 kyr). The overlying facies Fs3, on the shelf, is interpreted as fluvial, channel belt conglomerates and overbank sandstones deposits. It passes basinward to well bedded marine sandstones and siltstones (Fs9, Fig.7) that give rise at the shelf edge to massive sands and channels of high amplitude chaotic configurations (Fs10, Fig.7). Below the shelf edge Fs10 passes to wavy reflections Fs11. Fs11 geometries, e.g. continuous reflections, upward convexity, and no headwall scarp, are consistent with a large field of upslope migrating sediment waves (Lee et al., 2002). This interpretation differs from those of Lewis (1971b) and Barnes and Lewis (1991), that

proposed to interpret these undulations as the result of a large submarine landslide, the 'Kidnappers slide'. A 30 m-long piston core (MD06-2997) penetrated through the whole Fs11 sediment wave package, and revealed that bioturbated silty to sandy clays with organic rich layers resting over gas-rich liquefied mud. The presence of gas at the base of the core is compatible with the base of a reflection free patch seen on the 3.5 KHz profile (Fig. 7). Radiocarbon measurements on shell samples taken from cores penetrating the top of U3, provide ages ranging from c. 19,240±310 yrs to c.18,060±200 yr (Barnes et al., 1991). This confirms that the upper part of U3 was deposited during the last glacial maximum (20 to 18 Ka).

Seismic unit 4: U4 is 30 ms thick (TWT), wedge shaped unit that is only represented in the inner Hawke Bay region (Fig. 4, Fig. 5) as it thins out south-eastward, against the western flank of the Kidnappers ridge. It is slightly tilted seaward (c.1°) except for local deformation along the Kidnappers Ridge (Fig. 5B). U4 reflections clearly onlap S3 and are truncated above by a sharp and planar erosion surface S4 (Fig. 5). U4 is made up of seismic facies Fs3 with sub-parallel, highly discontinuous, wavy and channel-shape reflectors.
S3 is interpreted as a transgressive surface (TS) onlapped by U4 fluvial sediments that may have developed during the post-glacial sea level rise. It is tentatively correlated to the change in lithology from fluvial gravels to fluvial gravelly sands at 35m depth in the Awatoto well (Fig. 7). The gravelly sands are bracketed by two dated samples, 10247±99yrs BP at base and 7889±114 yrs BP at top, that point to the early stage of post-glacial sea level rise in the inner part of Hawke Bay.

Seismic unit 5: U5 is a 25-40 ms thick (TWT), bank to lens shape, slightly concave up unit that thins out towards the coastline and drapes over the active ridges (Fig. 4). It reaches a maximum thickness across the inner shelf over Hawke Bay and immediately landward of the shelf edge, offshore Waimarama coast (Fig. 4, Fig. 7, Fig. 8). U5 internal reflections onlap onto a sharp and planar erosion surface of regional extend S4 (Fig. 5, Fig. 8). S4 extends all over the inner part of the bay and truncates all units as they are tilted against the Kidnappers ridge (Fig. 5). U5 is bounded above by a concordant surface S5 that slightly dips seaward and is overlain by downlapping reflections (Fig. 7). In the inner bay, U5 is comprised of low amplitude, average continuity and frequency, sub-parallel reflections of seismic facies Fs4 (Fig. 5). In the outer bay, U5 is made up of sub-parallel, continuous reflections of seismic facies Fs7 which drape the undulations of Fs11 below the shelf edge (Fig. 8).

The basal S4 planar erosion surface is interpreted as the wave ravinement surface (WR) that developed as the sea flooded the area during the postglacial sea level rise (c.18 to c. 7.2 Kyrs; Gibb, 1986). Numerous authors have previously recognized this prominent surface along the East Coast margin (Lewis, 1973a; Barnes et al., 2002). The topmost S5 surface, slightly dipping seaward, is interpreted as the maximum flooding surface (MFS) and formed as the sea reached its highest elevation at the Holocene optimum c.7.2 Ka B.P.

In the inner shelf, U5 is interpreted as a horizontal, poorly bedded silts and sands succession, probably deposited in a low energy, marine shelf environment (seismic facies Fs4). These deposits are time equivalent to the coastal and floodplain carbonaceous silty clays (Fig. 6) preserved at the back of a prominent retrogradational gravel beach on land (U4; see also Dravid and Brown, 1997). In the outer parts of Hawke Bay, U5 is comprised of Fs7 sub-parallel, continuous reflections that represent marine silts and sands. Piston cores MD06-2998 and MD06-3000 probably penetrated U5 where it thins out over the Kidnappers Ridge. It is made up of poorly-sorted pebbly-muddy sands that may correspond to retrogradational shore deposits.

Seismic unit 6: U6 is a 10-35 ms thick (TWT), sheet drape to lens shaped unit slightly dipping seaward (Fig. 4, Fig. 5). U6 drapes most of the shelf and upper slope and, as for U5, thickens markedly, offshore Waimarama coast (Fig. 7). Below the shelf edge, U6 thins out rapidly and can hardly be distinguished from U5, as they show almost no internal reflections. Internal reflections downlap onto a concordant surface S5 and are either truncated, or gently top-lapped, by the seafloor above (Fig. 7).

In the inner parts of Hawke Bay, U6 is made up of low amplitude, oblique parallel to sigmoidal reflections in dip direction, and parallel reflections in an along strike direction (facies Fs5) (Fig.5). Further offshore, U6 is comprised of sub-parallel, low continuity to reflection free (seismic facies Fs8). Below the shelf edge, this facies drapes the undulations observed in U5 and U3 forming a wavy seabed.

Onto the shelf, facies Fs5 is interpreted as poorly bedded, marine silts deposit prograding towards the shelf break. These deposits are capped inland by coastal and floodplain deposits (Fig. 6). On the upper slope, sediment collected in the down-lapping seismic facies Fs8, in the top of cores MD06-2997 and MD06-2998 (Fig. 7) are made up of marine bioturbated silty to sandy clays and clayey silts and sands with shell debris. Tephra and shell samples from shallow cores in the same unit provide age ranging from c. 6,644 yr+-98 to c.1,215+-78 yr

(Barnes et al., 1991). U11 is interpreted as a prograding marine highstand system tract HST developed along the MFS since the Holocene optimum (7.2 kyr).

4.2- Sequence stratigraphic architecture of the Late Pleistocene forearc and trench slope basin successions in the offshore Hawke Bay

The late Pleistocene sedimentary record in the offshore Hawke Bay sector of the forearc is comprised of two major seismic sequences. The lower sequence (Late Pleistocene 1 - LPS1) is preserved in small structural basins bounded by tectonic ridges (Kidnappers, Lachlan and Motuokura basins, Fig. 4). The upper sequence (Late Pleistocene 2 - LPS2) is draping over both the subsiding basins and the ridges (Fig. 4).

LPS1 lies unconformably on a Plio-Pleistocene substratum (seismic unit U1). The substratum comprises early- to mid-Pliocene, shallow marine siltstones and sandstones that gives rise up section to Plio-Pleistocene fluvial and braided fan gravels. The substratum crops out at the seafloor along the uplifting Kidnappers, Lachlan and Motuokura Ridges by where it provides evidence of tilting and folding (Fig. 5C). On the shelf, the polygenic unconformity at the top of U1 is reworked by wave action along most of its surface to form the widespread, well recognized, sharp and planar, wave ravinement surface of the last interglacial c. 130 Ka (S1). On the outer shelf and upper slope, S1 is an onlap surface that becomes progressively concordant in a basinward direction. LPS1 is truncated and incised above by a surface of large extent on the inner shelf (S2) underlain by channel incisions. This surface becomes concordant beyond the shelf edge. This surface is interpreted as the sequence boundary of the last glacial maximum c.20-18 Kyrs (S2).

Over the inner shelf, within the Kidnappers basin (Fig. 5), **LPS1** is made up of thin basal, deepening up, transgressive marine sands overlain by a shallowing upward succession of shallow marine silts and sands to floodplain and fluvial sands and gravels (seismic unit U2) (Fig. 4, Fig. 6). From mid-shelf to upper slope, within the Lachlan and the Motuokura basins, **LPS1** exhibits deeper water paleoenvironments, with massive to well-bedded marine sands and silts passing basinward to a set of large scale bedforms interpreted as sediment waves, but with a retrogradational and progradation patterns that are inferred to relate the deepening and shallowing up trends observed on the shelf. These trends may correspond respectively to lowstand, transgressive, highstand and regresive systems tracts of an individual depositional sequence (Fig. 4, Fig. 9a and 9b). Towards the top and in the offshore, LPS1 exhibits chaotic facies interpreted as channelized and downdip remobilization of massive volume of sediment.

This massive sediment transport, due to a relative sea level fall, predates immediately the formation of S2 unconformity.

LPS2 lies on the LGM S2 unconformity on the shelf and on a concordant surface on the slope (Fig. 4). On the inner shelf, in the Kidnappers basin, it comprises four seismic units U3, U4, U5, U6 respectively bounded above by the S3, S4, S5 surfaces and the sea floor (Fig. 4). On the mid shelf and upper slope, in the Lachlan and Motuokura basins, it comprises only two seismic units, U5 and U6 (Fig. 4) bounded above by the S5 surface and the sea floor respectively (Fig. 4). The S4 surface merges, locally on the ridges, with the SB (S2) and the TR (S3) surfaces. The age of S4 can be interpreted to encompass a period from the LGM at c. 20 kyr (S2) to the time when the wave base razor passed above the shelf at c.10 kyr (S4 in the inner shelf).

On the shelf, LPS2 is comprised of entrenched lenses of lowstand fluvial channel gravels and overbank silts and sands (U3). On the outer shelf, LPS2 grades upward from well-bedded, transgressive marine silts and sands to prograding, shore-connected massive sands with scattered channels. Further offshore, beyond the shelf edge, on the upper slope, LPS1 is comprised of a field of upslope migrating sediment waves made up of gas-rich, bioturbated marine siltstones (Fig. 4, Fig. 7). LPS2 wedges out in the Motuokura basin at c. 500 m water depth.

These lowstand systems tract deposits are overlain by extensive transgressive fluvial sediments (U4) deposited during the early stage of the postglacial sea level rise above the transgressive TR (S3) surface (Fig. 4). These sediments are truncated above by a widespread, flat, strongly diachronous wave ravinement surface WR (S4) covered by a thin veneer of coquina sands. The WR surface is onlapped by low energy, marine silts (U5) passing in a landward direction, through a prominent gravel beach, to coastal plain silts. The transgressive fluvial sediments together with the onlapping marine silts are interpreted as part of an overall transgressive systems tract. The uppermost sediment package is composed of prograding shelf to upper slope siltstones (U6) downlapping onto a flat maximum flooding surface dated at 7.2 kyr (S5). These silts give rise on land to coastal and flood plain silts, sands with few encased gravels in channels (Fig. 6). U6 is interpreted as the first part of a highstand systems tract.

4.3- Age calibration of the sedimentary sequences and correlation to the climato-eustatic sea-level curve

The age of LPS1 can be bracketed by considering : (1) the age of the condensed section at the base of the sediment waves (U1) dated at ca. 500 Ka to 600 Ka (Proust et al., 2006); (2) the age of the uplifted marine terrace on top of the Cape Kidnappers (Hull, 1985) geometrically tied to S1 and dated at c. 120 Ka; and (3), the age of a tephra located in the upper part of U3 sampled by shallow coring and dated at c.25 Kyrs (Te Rere tephra, Barnes et al., 1991). We therefore correlate the basal ravinement surface S1 to the last interglacial sea level rise that occurred from c. 135 Ka to c. 125 Ka (MIS6 to MIS5) and the topmost unconformity S2 to the LGM c.20 Kyr erosion. Accordingly, the LPS1 sediments record the last interglacial MIS6 to MIS5 period of time, and the overall glacial sea-level fall that occurred from MIS5 to MIS2 times. These correlations are corroborated by the observation in the offshore (Fig.9a and 9b) of two landward stepping units that represent the transgressive and early highstand systems tracts of LPS1 overlain by three seaward stepping units that are related to the three main stages of the late highstand and regressive systems tracts in LPS1 (MIS5d, MIS5b and MIS4) (Fig. 6, 9a, 9b, and 12).

The age of LPS2 can be approached through a set of dated horizons that include from base to top: (1) the radiocarbon ages of gastropod shells collected next to the merged LPS2 basal unconformity (S2) and transgressive surface (S3) dated from 18,060±200 yr to 19,240±310 yr (Barnes et al., 1991); (2) the ages of tephra overlying the unconformity, dated from c. 6,644±98 yr to 1,215±78 yr (Barnes et al., 1991); (3) the radiocarbon age of the oldest sample collected in the uppermost part of the fluvial TST of LPS2, in the coastal plain areas that surround the Kidnappers basin, dated at 10,247±99 yr B.P. (Dravid and Brown, 1997); (4) the ages of sediments located immediately below and above the maximum flooding surface S5 ranging from c. 95,00 yr B.P. to c. 5,300 yr B.P. (Cochran et al., 2006; Dravid and Brown, 1997); and (5) the ages of the Waimihia and Taupo tephras preserved in the terrestrial deposits that cover the marine highstand deposits in the coastal plains dated at c. 3,450 yr and c. 1,750 yr (Cochran et al., 2006; Dravid and Brown, 1997). We therefore correlate the merged sequence boundary at the base of LPS2 to the last glacial maximum incision (c. 25 Ka – MIS2) and the transgressive/wave ravinement surfaces to the postglacial sea level rise that occurred from c. 18 Ka to c. 7.2 Ka (MIS1 to MIS2) as proposed by Gibb (1986). The maximum flooding surface, within LPS2, may correlate to the end of the last sea level rise at c. 7.2 Ka (and later). The highstand systems tract, which terminates LPS2, correlates to the current sea level high (MIS1) (see Fig. 12).

4.3- The Late Pleistocene sediment record in the foothills of the axial ranges

Sets of uplifted aggradational fluvial terraces are well preserved along major river valleys (Tukituki, Ngaruroro, Mohaka, Wairoa) within the foothill domain, east of the axial ranges in Hawke's Bay (Litchfield, 2003; Litchfield and Berryman, 2005). Aggradational terrace fill is usually made up of fluvial, poorly sorted and bedded greywacke gravels derived from axial ranges basement, with an unsorted sandy matrix. Aggradational gravels are occasionally overlain by silts (overbank) or topped by loess covers. Few tephras from the Taupo Volcanic Zone (Fig.1) are intercalated and visibly preserved in the fluvial deposits or loess covers. The fluvial aggradational terrace deposits are usually ~6 m-thick but can locally reach up to 30 m (Litchfield, 2003). Litchfield (2003) and Litchfield and Berryman (2005) correlate four major terrace fill units (T1 to T4) between catchment along Eastern North Island, using different age calibration methods, including 14C, optical simulated luminence (OSL) and tephrostratigraphy (Litchfield, 2003; Litchfield and Berryman, 2005). The most extensive and best dated fill terraces are T1, T2 and T3 (Fig. 10a and 10b). In addition to OSL ages of T1 fill that range from 16.3±1.5 Ka to 23.9±1.8 Ka, Litchfield and Berryman (2003) also have identified the Kawakawa tephra (c. 26.5 Ka - Frogatt & Lowe (1990)) within aggradational deposits. T1 is topped by thin loess (Loess 1) dated from 11.2±0.8 Ka to 13.2±0.9 Ka using OSL and including Rerewhakaaitu tephra (c.17.7 Ka). Thus, aggradation of T1 started at the end of MIS3 (c. 30 Ka) and finishes at the end of MIS 2 (c.15 Ka) (Fig. 11a and 11b). The age of T2 aggradation is constrained by tephra cover including the Kawakawa (c. 26.5 Ka) and the Omataroa (c. 30.5 Ka). T2 formed during the MIS3 cooling stage that occurred at c. 40 Ka (Fig. 11a and 11b). T3 fill deposits are dated from 67.6±6.8 Ka to 75.3±5.5 Ka using OSL including the Rotoehu tephra (c.43 Ka to 50 Ka) in terrace cover. Two distinctive loess formations top the T3 fluvial deposits. They are identified as Loess 1 (also T1 loess cover) that overlies Loess 2 (39.7±2.5 Ka OSL) (Litchfield and Berryman, 2005). The aggradation of T3 terrace occurred during MIS4, probably from c. 80 Ka to c. 60 Ka (Fig. 11a and 11b). Older uplifted terrace remnants, including the Salisbury terrace (Kingma, 1958; Raub, 1985), are also locally present in the foothill domain between Ngaruroro and Tukituki catchments. A topographic section across the foothills from the Tukituki to the Ngaruroro reveals the presence of two elevated and dissected flat surface remnants (Fig. 10a and 10b). The topmost is the widespread Salisbury terrace at c.550 m of elevation (Fig.10a). Another one, here called "T4", is located immediately below the Salisbury terrace at c.400 m of elevation, and is observed south of Ngaruroro River (Fig. 10b). Except for rare examples in other catchments (Litchfield and Rieser, 2005), age control on these terraces is lacking but an estimate of their stratigraphic position of these older terraces is possible. By combining old terrace elevations

with younger age-dated terraces from Litchfield and Berryman (2006), it is possible to infer an age ranging from c. 120 Ka to c. 100 Ka (MIS5) for the T4 terrace and an age ranging from c. 150 Ka to c. 130 Ka (MIS6), for the Salisbury terrace (Fig. 11a and 11b). This latter estimation is compatible with the youngest ages of the underlying sedimentary succession of mid-Pleistocene age (Raub, 1985; Shane et al., 1996; Paquet et al., in prep) (Fig.10a). These data are also consistent with the average local uplift rates of the foothills domain (c.1.5 to 2.5mm/year, Fig.10C) (Litchfield and Berryman, 2006). The Salisbury terrace is a time-equivalent to the Marton terrace of the Rangitikei River flowing along the western side of the axial ranges in the Wanganui basin (Milne, 1973a, 1973b; Pillans, 1994).

Phases of aggradation separate periods of river incision. This incision accommodates contemporaneous regional uplift and both the regional uplift that occurred during the period of aggradation and the thickness of the aggradational terrace itself. The formation of fill-terraces broadly correlates with late Pleistocene cool/cold periods while incision corresponds to warm stages (Fig. 11b, Fig. 12b). Aggradation during T2, T3 and T4 times are time equivalent to the deposition of the seaward stepping units of LPS1 observed in the offshore Hawke's Bay (Fig.9). T1 aggradation started by the end of LPS1, during maximum rate of sea level fall, and stopped at the beginning of LPS2, during the early stage of sea level rise. T1 aggradation is then probably equivalent to the interpreted deposition of the lowstand and early transgressive systems tracts in the offshore. The incision, that follows the deposition of T1, occurred during the last sea level rise and may continue today during the highstand. The old Salisbury terrace is considered as the Penultimate Glacial Maximum equivalent of T1. Its offshore equivalent is therefore inferred to be the LPS1 basal lowstand (Fig.9a and 9b, Fig 12b). This scenario implies that the base of aggradational terraces correlates to the sequence boundary-type unconformities that delineate both 100 Ka sequences and their internal packages described offshore.

4.4- The sediment distribution within the forearc in Hawke's Bay

We have compiled isopach maps based on our seismic interpretations of sequences LPS1 and LPS2 (Fig. 13 and 14). The isopach maps highlight the distribution of sediments over the Hawke's Bay forearc domain from the foothills, as a set of fluvial terraces, to the toe of the late Pleistocene lowstand systems tracts at c. 500 m of water depth. The deposition of LPS1 occurred during one complete 100 Ka climato-eustatic cycle. The effect of sea level variation on the distribution is therefore attenuated, compared to the influence of persitent tectonic deformation. Lowstand and Transgressive/highstand depocenters of LPS2 are differenciated

on LPS2 isopach map in order to reveal the potential effect of the rapid and high amplitude effect of the last sea level rise.

LPS1 deposits are mainly preserved in the Kidnappers, Lachlan and Motuokura basins (Fig. 13). LPS1 deposits are not preserved over the uplifting active Kidnappers and Lachlan tectonic ridges and wedge out dramatically as they approach the Motuokura ridge at c. 500 m of water depth (Fig. 13). The volume of sediment preserved in LPS1 is about c. 340 ± 50 km^3. This volume is distributed into four main, depocenters that are roughly arranged "en-echelon" and separated by tectonically active ridges: (1) the Kidnappers basin cropping out both offshore in Hawke Bay and onshore in the Heretaunga Plains; (2) the Mahia basin (proposed name for the basin located west of the Mahia Peninsula), in the inner shelf, offshore from Wairoa; (3) the Lachlan Basin located on the outer shelf and (4) the Motuokura basin along the shelf edge (Fig. 13).

The Kidnappers depocenter is arranged into a broad asymmetric NE trending syncline with a steep western flank along the Napier fault, and a lower-angle eastern flank along the Kidnappers ridge. The sediment thickness reaches 160 m beneath the Heretaunga plains, decreasing rapidly southward and more progressively in a northward direction (Fig. 13). The northern part connects to the circular-shape Mahia depocenter where sediment thickness reaches c. 150 m. The Mahia depocenter connects to the Lachlan depocenter by a c. 100 m-thick channel that follows the Lachlan basin syncline. The Lachlan depocenter is located in the southern part of the Lachlan basin. The sediment thickness reaches c. 150 m, directly west of the Lachlan Bank. The Lachlan depocenter connects along the shelf edge to the lens-shaped Motuokura depocenter where sediment bodies drape the outer shelf and upper slope offshore Hawke's Bay (Fig. 13). The maximum sediment thickness reaches c. 300 m between the shelf edge and the Waimarama coast. The active Waimarama thrust fault complex disturbs this large depocenter. LPS1 deposits are also present in the foothill domain as fluvial aggradational terraces (T2, T3, T4 and Salisbury) that can reach thickness up to c. 10 m.

LPS2 is widely preserved over the forearc domain. It thins out over the ridges where the Plio-Pleistocene basement locally crops out directly at the seabed. These exposures are particularly apparent in central Hawke's Bay (Fig. 14) along the Kidnappers and Lachlan ridges. Overall LPS2 wedges out progressively with depth below the shelf edge. The volume of deposits preserved into LPS2 reaches c. 140 ± 20 km^3. LPS2 can be subdivided in two distinctive sediment packages that correspond to (1) the Lowstand System Tract (LST) deposits; and (2)

the Transgressive and Highstand System Tract (TST/HST) deposits. The potential differences between LST and TST/HST depocenter location may reflect the influence of the eustatic sea level variations on sediment distribution and partitioning. Thick black dashed lines and white dashed lines respectively surround LST and TST/HST depocenters on LPS2 isopach map within the Motuokura basin (Fig. 14). The LST part of LPS2 corresponds approximately to one third of the LPS2 total volume (c. 55 ± 8 km^3). This volume is distributed into three depocenters that partially overlap the LPS1 depositional areas: (1) the Kidnappers basin and Heretaunga Plains; (2) the southern part of the Lachlan basin; and (3) the Motuokura basin (see below). In the Kidnappers basin LST sediment thickness reaches up to c. 30 m and is deposited in a broad syncline of similar shape as LPS1. The LST sediments thin out to the North and are little or not preserved in the Mahia basin. LST deposits reappear seaward in the northern part of the Lachlan basin, in the continuation of the channelized incision surface recognized as the Sequence Boundary and that can be traced within the Mahia basin. In the NE trending Lachlan depocenter the sediment thickness reaches a maximum of c. 30 m below the shelf edge. In the Motuokura basin, the LST depocenter trends to the NE, in the continuation of the Lachlan depocenter. It reaches its maximum thickness (c. 30 m) below the shelf edge, as for the Lachlan depocenter. The LST part also includes extended fluvial aggradational terraces (T1) up to 10 metre-thick in the foothill domain. It is not preserved over the active ridges (e.g. Kidnappers, Lachlan and Motuokura ridges).

The TST/HST part of LPS2 drapes most of both the submerged parts of Hawke Bay and the coastal plain areas and its volume corresponds to two thirds of the total LPS2 volume (c. 85 ± 12 km^3). This volume is distributed in three main basins that partially overlap both LPS1 and the LST part of LPS2 deposits: (1) the Kidnappers basin, (2) the Mahia basin and (3) the Motuokura basin. Nevertheless, the full extent of the TST/HST shows less influences of the local active structures and its preservation is more widespread than for LPS1 or the LST part of LPS2. In the Kidnappers basin, within the Heretaunga plains, the depocenter is arranged into a NE trending syncline. The sediment thickness reaches c. 60 m. This TST/HST depocenter widens and thins rapidly offshore. The Mahia depocenter is located above its LPS1 equivalent and reaches sediment thickness of c. 30 m. The northern depocenter extends and links into the Lachlan basin. The Motuokura TST/HST depocenter is located between the Waimarama coast and the shelf edge, on the hanging wall of the active Waimarama thrust faults complex. The thickness decreases dramatically against the Waimarama thrust zone, forming the seaward structural ridge. The TST/HST is not present in the foothill domain, as

river incision was predominant at that time. It is only preserved as thin aggradational terraces that form inside meanders, during the river incision.

In the Kidnappers basin, more than half of the LPS2 sediment section is made up of fluvial transgressive deposits, overlain by shallow marine TST and HST. The sediment section of the Motuokura basin depocenter is comprised of marine HST and TST that form a thick wedge.

5- DISCUSSION

Two late Pleistocene sedimentary sequences (LPS1 and LPS2) in the Hawke's Bay forearc domain correlate to climato-eustatically driven cycles (Fig. 12). Geometry of these sequences provide an opportunity to document and discuss aspects of the Late Pleistocene paleogeography of the forearc domain, the controls on its morphostructural evolution with a special emphasis on sediment budgets and relationships between continental and marine landscapes development.

5.1 The facies partitioning in the forearc domain: from source to sink

The interpretation of the seismic data and their correlation to wells, piston cores and inland formations lead to the reconstruction of a "source to sink" stratigraphic model for the Upper Pleistocene Hawke's Bay forearc domain (Fig.15). This model extends from the eastern range front of the axial ranges to the toe of the Lowstand wedge for the late Pleistocene sequences. The model comprises: (1) fluvial channel and overbank (flood plain) gravels, sands and silts; (2) coastal plain and lagoonal sands and silts; (3) shoreface gravels and sands; (4) shallow marine sands and silts; and (5) upper slope silts and muds (Fig. 15), organized into two tens to hundreds of metres thick sequences (LPS1, LPS2). LPS1 deposits are mainly preserved in the sub-basins, whereas LPS2 drapes most of the shelf and upper slope. LPS1 and LPS2 are dated respectively from c.140 Ka to c. 30 Ka (MIS 6 to 2) and from c. 30 Ka to Present day (MIS 2 to 1). LPS1 corresponds to a complete climato-eustatically driven 100Ka-type depositional sequence. The knowledge of both facies distribution and stratigraphic stacking patterns, within LPS1, results in the establishment of a detailed model for a 100 Ka-type sequence in the active the Hawke's Bay sector of the forearc domain (Fig.15). LPS2 is an incomplete sea-level cycle sequence as the upper part of the modern highstand system tract is lacking, as well as the potentially following regressive system tracts. Nevertheless, LPS2 provides the most accessible and best resolved record of both glacial and interglacial environments for Hawke's Bay. The general facies distribution also highlights a sediment distribution characterized by:

(1) a long depositional profile with fluvial deposition from the range front (c. 300 m) to the lower shelf and marine deposition until the Lowstand wedge (c. -500 m) during sea level; and (2) a shorter depositional profile with the beginning of long-term fluvial deposition restricted to the lower continental realm (< 20 m) and the essential marine deposition concentrated on the shelf (above -150 m). The sediment partitioning in the Hawke's Bay sector of the forearc basin differs from passive margin related models. Such behaviour suggests the existence of complex relationships between eustasy, tectonic deformation, climate and sediment fluxes.

5.2 Reconstruction of the late Pleistocene forearc landscape

The rates of vertical tectonic deformation on active structures (ridges and basins) in the Hawke's Bay region range from - 2 to +4 mm/yr (Berryman, 1993; Barnes et al., 2002; Cochran et al., 2006), while rates of climato-eustatic sea level fall and rise reach respectively -4 mm/yr and +11 mm/yr (Imbrie et al., 1984; Waelbroeck et al., 2002). These rates drastically impacted the sedimentation pattern and led to one of our findings that the preservation of sediment in the two observed depositional sequences is certainly primarily driven by climate changes and glacial-interglacial fluctuations. We present in the following two different paleogeographical reconstructions representative of the past condition of the forearc domain: a cold and dry period during a low eustatic sea level (-120 m) at the Last Glacial Maximum (LGM c.20 Ka) corresponding to the LPS2 lowstand systems tracts (Fig. 16A) and a warm and moist period at a high eustatic sea level comparable to the present mean sea level (c. 0 m) at the Holocene optimum (7.2 Kyrs) corresponding to the LPS2, late transgressive to early highstand systems tracts (Fig. 16B). These reconstructions result from documenting the distribution of sediments and facies presented in this study, and also from the compilation of data available in the literature (See figure 16 caption for details).

The reconstruction of the depositional environments at the LGM (Fig. 16A) illustrates that fluvial gravels and overbank sands and silts were widespread in Hawke's Bay just (Fig. 16A). The major rivers in southern Hawke's Bay (e.g. Ngaruroro, Tukituki) flowed through the Kidnappers basin before joining the northern Hawke's Bay rivers (e.g. Mohaka, Wairoa) in the Mahia basin, and turning SE into the Lachlan basin. The gravels occupied most of the main valleys on land and tapered in the narrow connection between the uplifted Kidnappers and Lachlan Ridges (Fig. 16A). This coarse-grained alluvial domain gave rise through a contracted coastal plain, characterized by a high gradient shoreface. This shoreface is comprised of a shore-connected, massive sandwedge with scattered channels that may correspond either to a delta front sediment wedge or an estuarine subtidal mouth-bar complex.

The seismic interpretation cannot confirm this latter hypothesis. However it fits better with the tidal amplification that may have induced the narrow between the two ridges. With essentially no submerged continental shelf, the shoreface sands and silts give rise, after a short break in slope (Fig. 7, Fig 16A.), to a field of fine-grained upslope migrating sediment waves on the upper slope.

The reconstruction of the depositional environments at the Holocene Optimum shows an overall generalization of marine sedimentation in Hawke's Bay (Fig. 16B). Low energy, shallow marine silts and muds cover most of the Hawke Bay. On land, sedimentation is reduced except in small lacustrine structural basins (Poukawa basin; e.g. Shulmeister et al., 2001). Sheltered embayments preserve some coarse-grained alluvial gravels at the outlet of the major rivers (eg. Tukituki, Ngaruroro, Wairoa) and fine grained silts and clays associated with lagoonal environments (eg. Heretaunga plains). Deposition of marine sediments is locally condensed or absent within Hawke Bay and over structural ridges, including the Kidnappers ridge in the central part of the bay and the west of the Kidnappers ridge (Fig. 16B).

5.3- Landscape evolution from interglacial to glacial conditions

The shift from interglacial to glacial conditions between MIS 5 and MIS 2 is characterized by 120m of eustatic sea level fall. Sea level fell at a long term rate of -1 mm/yr, but occurred in reality as a succession of rapid drops at c.-5.5 mm/yr during MIS 5e, MIS 4 and MIS 2, that correlate to cooling climate pulses. When rivers started to flow on the progressively emerging shelf, the subsiding Kidnappers basin (-1.5 mm/yr) and the uplifting Kidnappers ridges (+2 mm/yr) and Napier fault formed an asymmetric "gutter-shaped" valley in which southern Hawke's Bay rivers (Ngaruroro, Tukituki) were confined. At the same time, northern Hawke's Bay rivers (Mohaka, Wairoa) passed through the Mahia basin. As the sea level continued to fall, southern Hawke's Bay rivers finally connected to the northern Hawke's Bay rivers in the Mahia basin, around the northern end of the Kidnappers ridge. During the last stages of sea level fall, the outer shelf emerged and rivers passed to the SSW in a second valley coinciding with the subsiding Lachlan basin. Rivers reached the LGM shoreline (c.-120 m) in the center of the Lachlan basin providing sediments directly to the Motuokura basin which received sediments also from the eroded Waimarama coast. Sediments accumulated below the shelf edge (c.-150 m) as a thick package of upslope migrating sediment waves. These sediment waves formed beneath an overcharged current (hyperpycnal flows) flowing at the seabed (detached flow conditions) (Wynn and Stow, 2002). Together with the high

discharge rate at the outlet of Hawke's Bay, the formation of the sediment wave field could have been enhanced by the increasing velocity of the Wairarapa Coastal Current (Lewis, 1973; Carter and Heath, 1975; Chiswell, 2000) due to the cooling temperature at the approach of the LGM and the re-organization of the ocean circulation patterns (Carter et al., 1998; Carter, 2001).

5.4- Landscape evolution from glacial to interglacial conditions

Shifts from glacial to interglacial conditions occurred during MIS 6 to 5e and MIS 2 to 1 transitions. Rapid, eustatically-driven transgression led to major flooding of the shelf at a vertical rate of c.11 mm/yr (Fig. 12C). The transgressive gravel beaches developed a widespread wave abrasion/ravinement surface that erased/plained the ridge and swale topographies formed by active structures and partly filled during the regression. The sea level rise resulted in a rapid creation of significant accommodation space, on the shelf, and base level rise, on land. This is illustrated in the marine domain by the onlap of a transgressive marine unit onto the wave ravinment surface and on land, in the Kidnappers basin, by the onlap of a thick fluvial unit on a transgressive surface during last glacial-interglacial transition (MIS 2 to 1) as suggested in several models (eg. Zaitlin et al., 1994). In the Motuokura basin, the narrowness of the shelf (compared to Hawke Bay), due to a higher slope gradient, resulted in the deposition of a remarkably thick (c. 50 m) transgressive wedge of postglacial mud.

At the maximum flooding of the Holocene Optimum (c. 7.2kyr), the four subsiding basins were flooded. Lagoons developed in the coastal areas of both the Kidnappers and Mahia basins behind protective gravel-bar beaches. Shallow marine deposition was widespread on the shelf but reduced or absent over the re-submerged structurally active Kidnappers and Lachlan ridges, where the Plio-Pleistocene substratum may are exposed. This depositional hiatus may result from: (1) the joint effects of basement uplift and low sediment supply to the outer shelf (eg. Lachlan ridge on Fig. 16B); (2) wave abrasion (eg. shallow tidal flat offshore Cape Kidnappers); and/or (3) Hawke Bay current circulation pattern and substantial bottom current turbulence over rough seafloor. According to Ridgway,1960 : "The main inflow takes place approximately along the mid-line of the bay… bifurcates and the two currents thus formed follow the coastline and leave the bay at the northern and southern extremities." Both northward and southward along-shore currents decreased in velocity and encounter overcharged freshwater currents from the major Hawke's Bay rivers. This description, has been confirmed later by alternative models of water circulation (Ridgway, 1962; Ridgway and Stanton, 1969; Francis, 1985), is compatible with: (1) marine erosion or the lack of marine

deposition in the central part of Hawke Bay (Fig. 14, Fig. 16b); and (2) deposition in sheltered areas with depocenters not systematically associated with subsiding basins (Fig. 14). The same kinds of features remain today as revealed by seismic interpretations and seafloor mapping (Pantin, 1966; Wright and Lewis, 1991, this study). Further offshore, the upslope migration of sediment waves decreases, and attested by the postglacial draping of units this evolution confirms the hypothesis of a postglacial weakening of the Wairarapa Coastal Current (Carter, 2001).

5.5- Late Pleistocene sediment budget of the forearc domain

The mass accumulation rates of late Pleistocene sediments deposited in the inner forearc was evaluated by using volume estimations from the isopach maps (Figs. 14, 15) and mean porosity values estimated from various porosity curves and varying from 45% to 60%. Error estimates have been determined by evaluating the maximum and minimum values of each parameter that are used in the sediment budget calculation (*i.e*. Velocity, surface, volume, porosity, sequence duration). Errors on mass accumulation rates vary from 26% to 39% so values have to be understood with care. Nevertheless we believe that general trends are consistent.

The mass accumulation rates over the Hawke's Bay inner forearc domain range from 3.95±1.15 Mt/yr (Error: 29%) in LPS1 to 5.67±1.97 Mt/yr (34%) in LPS2. In the latter, LST and the combined TST-early HST accumulation rates reach 5.56±2.18 MT/yr (39%) and 5.75±1.80 MT/yr (31%) respectively. The late highstand sediments are interpreted to record a lower accumulation rate than the LST and TST -early HST. High mass accumulation rates on the shelf during the LGM (LPS2 - LST) are attributed to an increase in erosion onland. This increase was also noted by McGlone et al., (1984), Newnham et al. (2003), and Harper and Collen (2002) and attributed to the replacement of protective vegetation cover (Notofagus – Podocarp forests) by unprotective shrubland and grassland over the ranges (McLea, 1990; Newnham and Lowe, 2000; McGlone, 2001, 2002). The higher accumulation rate for TST-early HST may be the result of the postglacial commencement of river incision in the foothills (Litchfield and Berryman, 2005) and the recycling of LST shelf deposits. Despite the higher LPS2 mass accumulation rates, and considering the potential errors, it appears that the mass accumulation rates are broadly constant over the late Pleistocene with an average value of 4.23±1.09 Mt/yr (26%). This value is one third of the current Hawke's Bay rivers suspended sediment yield estimations of 12 Mt/yr (Hicks and Shankar, 2003). This difference can be

explained by (1) the occurrence of shelf sedimentation outside of our study area, and possible escape or loss of mud from the shelf to the deeper slope basins (also not investigated as part of this study) during either storm related and/or seismically induced submarine mass wasting, and/or (2) the increase of recent sediment supply due to the anthropogenic influence, with post-settlement (century-scale) deforestation and related erosion described by Marutani et al. (1999) and Gomez et al. (2001). This latter hypothesis has been proposed for the Poverty Bay shelf north of our study area, where mass accumulation on the shelf during Holocene represents only ~10% of the current river sediment supply (Foster and Carter, 1997; Orpin et al., 2006).

5.6- Relationships between continental and marine landscape development

Aggradation periods observed in terms of terraces deposits in the eastern foothills of the North Island axial ranges appear synchronous with cooling period associated to sea level falls on the shelf and upper slope of (see section 4.2 above). Incision of rivers occurs during warm periods and sea level rises and/or stillstand/highstand. This timing is different from models currently proposed in the literature that describe maximum river incision during maximum rate of sea level fall and river aggradation during sea level rise (Van Wagoner et al., 1988; Posamentier et al., 1988; Posamentier and Vail, 1988; Strong and Paola, 2006). However, alternative models may explain the differences of timing observed in our study area. These models involve either: (1) climate; or (2) both shelf morphology and sea level change as the predominant control parameters.

The first model, developed by Litchfield and Berryman (2005) for the eastern North Island rivers of New Zealand, proposes that climate controls sediment supply and stream power (water flux) through time and therefore aggradation and incision in rivers. Thus, aggradation occurred during cool to cold stages as a result of: (1) increasing sediment supply to the rivers, due to enhanced erosion and slope instability within the cold and unprotected axial ranges (Froggatt and Rogers, 1990; McGlone, 2001, 2002; Newnham et al., 2003; Shulmeister et al., 2004); and (2) a decrease of stream power due to dryer conditions (Shulmeister et al., 2001; Newnham et al., 2003). Incision occurs during warm and moist periods (e.g. MIS1), to compensate the effects of both aggradation and permanent tectonic uplift, as: (1) forests regenerate in the axial ranges and prevent dramatic erosion; and (2) stream power increases along with increasing rainfall rates.

The second model is based on the impact of the shelf morphology on the stream equilibrium profile during a sea level fall (Dalrymple et al., 1998). It proposes that the lengthening of river

profiles on a broad and low-gradient shelf during sea level fall and lowstand conditions implies an elevation of the stream equilibrium profile above the river profile. Such a change corresponds to the creation of accommodation space along the river and favors the regressive alluvial aggradation. Several examples and variations of this model are presented in the literature (Posamentier et al., 1992; Miall, 1991; Shumm, 1993; Dalrymple et al.,1998; Woolfe et al., 1998; Browne and Naish, 2003).

The paleogeographic reconstruction of the LGM environment (Fig. 16A) including, rivers and sediment pathways at the end of the late Pleistocene regression, shows that rivers flowed within the Kidnappers basins on a low-gradient emerging shelf, before turning SE to the northern Lachlan basin where they finally reached the LGM shoreline (-120 m). The initiation of erosional retreat was limited because the LGM shoreline did not pass beyond the shelf edge (c. -150 m) and preexisting canyons are absent on the shelf (Talling, 1998). These conditions, with rivers flowing around the Kidnappers ridge, prevailed for most of the late Pleistocene eustatic sea level fall. This particular river course implies a significant lengthening of the river profiles. At the LGM, the courses of rivers were c. 110 km longer than today in southern Hawke's Bay, and c. 80 km longer in northern Hawke's Bay. The Tukituki, Ngaruroro, Mohaka and Wairoa rivers were respectively 250 km, 280 km, 250 km and 220 km long at LGM whereas present day profiles are respectively 140 km, 170 km, 170 km, and 140 km. Such lengthening of river profiles is consistent with the creation of sub-aerial accommodation space, as proposed by Dalrymple et al. (1998) and illustrated by Browne and Naish (2003) for the Canterbury plains and shelf. Thus, fluvial aggradation could have occurred during the lengthening river valleys, as a response to the creation of aerial accommodation space during eustatic sea level fall. River incision occurred when sea level stopped falling and local uplift in the foothills again become the prevalent factor influencing river behavior. Tectonic deformation and sea level changes acted together as control parameters on fluvial aggradation and incision and the timing of their shifts. Nevertheless, the role of climate as a control parameter on sediment and water fluxes provided to the system cannot be ruled out. We believe that interplay of both models is required to explain correctly the evolution of the fluvial network during late Pleistocene.

6- CONCLUSION

The interpretation of a dense grid of high-resolution marine seismic data, coupled with both onland and offshore core and well descriptions, and the integration of geomorphic studies lead

to the determination of the detailed source to sink sedimentary architecture of the late Pleistocene Hawke's Bay forearc domain. This sedimentary architecture comprises sediment packages, interpreted as system tracts and constitutive of two climato-eustatically driven depositional sequences (LPS1 & 2), including one complete 100 Ka sequence (LPS1). Isopach mapping of both sequences reveals changes in sediment distribution and preservation that provide input parameters to tectonic deformation and eustasy. Four long-lasting depocenters are identified over the forearc domain and located into four subsiding basins (Kidnappers, Mahia, Lachlan and Motuokura basins). Significant shifts of the depocenter location in the basins are correlated with eustatic sea level changes. An study of the distribution of terrestrial sedimentation through time reveals that, in the foothills, fluvial aggradation occurred during phases of rapid sea level fall (fill terraces T1, T2, T3, T4, Salisbury) and climate cooling whereas river incision occurred during sea level rise and climate warming (cut terraces). Such sediment partitioning differs from classical models that predict incision during falling stages and aggradation during rising stages. We propose that (1) lengthening and shortening of river profiles during rapid sea level changes, that modify the accommodation space, and that together with (2) climatically induced erosion rate changes, which tune the sediment supply, are responsible for the observed and documented behaviour of Hawke's Bay rivers. Estimations of sediment volumes and masses from isopach maps tend to show higher mass accumulation rates during climato-eustatic extremes and abrupt transitions of LST and TST-early HST (LPS2). We correlate this with the onland response to climato-eustatic extremes and the abrupt changes between LGM and Holocene optimum. Estimated late Pleistocene mass accumulation rates are half of the present day estimations of the Hawke's Bay sediment yield. This can be attributed to sediment exportation out of the studied area and/or from the recent increase of sediment supply due to post-settlement deforestation. Facies distribution within LPS1 & 2 along two key sections and hypothetical reconstructions of two late Pleistocene environmental extremes, corresponding to glacial and interglacial conditions, provide: (1) a detailed model of a 100 Ka-type depositional sequence for the Hawke's Bay forearc domain; and (2) good insights to understand the impact of tectonic deformation, eustasy and climate changes on sediment distribution and preservation. Postglacial rising sea level tends to restrict sedimentation on the shelf (from c. 0 m to c. -150 m) whereas glacial falling sea level tends to lengthen the depositional profile from the range (c. 300 m) front to the toe of the low stand wedge (c. -500 m). The location of structures and their deformation style and intensity control both the long-term preservation and the sediment distribution. The latter control is particularly effective during regression (sea

level fall). Climate and its variations tune the onland erosion (slope stability) and the sediment supply and fluxes by modifying the vegetation cover and the rainfall style and rate. Water circulation is also considered as a parameter of control of sediment distribution on the shelf during highstand stages and of the development of specific sediment facies (eg. upper slope sediment waves during the LGM).

Acknowledgements :

This study was funded by the CNRS-INSU, CNRS Research Department n°6118 – 'Géosciences Rennes', the University of Rennes 1, the 'Active Tectonics and Earthquake Hazards Research Program' at the University of Canterbury. French Ministry of Foreign Affairs.

NIWA for access to the extensive seismic data set and acquisition of new data, ship time..

The IPEV and Marion-Dufresne II crew for Calypso long piston-cores acquisition…

This research project was undertaken under a co-tutelle agreement between Université de Rennes 1 and University of Canterbury.

REFERENCES

Alloway BV, Lowe DJ, Barrell DJA, Newnham RM, Almond PC, Augustinus PC, Bertler NAN, Carter L, Litchfield NJ, McGlone MS, Shulmeister J, Vandergoes MJ, Williams PW, NZ-INTIMATE members. 2007. Towards a climate event stratigraphy for New Zealand over the past 30 000 years (NZ-INTIMATE project). *Journal of Quaternary Science* **22**: 9-35.

Ballance PF. 1976. Evolution of the upper Cenozoic magmatic arc and plate boundary in northern *New Zealand. Earth and planetary science letters* **28**: 356-370.

Ballance PF, Pettinga JR, Webb C. 1982. A model of the Cenozoic evolution of the northern New Zealand and adjacent areas of the southwest Pacific. *Tectonophysics* **87**: 37–48.

Barnes PM, Lewis KB. 1991. Sheet and rotational failures on a convergent margin: the Kidnappers Slide, New Zealand. *Sedimentology* **38**: 205-22 1.

Barnes PM, Cheung KC, Smits AP, Almagor G, Read SAL, Barker PR, Froggatt P. 1991: Geotechnical analysis of the Kidnappers Slide, upper continental slope, New Zealand. *Marine geotechnology* **10**: 159-188.

Barnes PM, Mercier de Lépinay B. 1997. Rates and mechanics of rapid frontal accretion along the very obliquely convergent southern Hikurangi margin, New Zealand. *Journal Geophysical Research* **102**: 24 931–24 952.

Barnes PM, Nicol A. 2004. Formation of an active thrust triangle zone associated with structural inversion in subducting setting, eastern New Zealand. *Tectonics* **23**(1): TC1015.

Barnes PM, Nicol A, Harrison T. 2002. Late Cenozoic evolution and earthquake potential of an active listric thrust complex above the Hikurangi subduction zone, New Zealand. *Geological Society of America Bulletin* **114**: 1379–1405.

Barrell DJA, Alloway BV, Shulmeister J, Newnham RM (eds). 2005. Towards a climate event stratigraphy for New Zealand over the past 30,000 years. *GNS Science Report* SR **2005/07**: 12 pp.

Beanland S, Melhuish A, Nicol A, Ravens J. 1998. Structure and deformation history of the inner forearc region, Hikurangi subduction margin, New Zealand. *New Zealand Journal of Geology and Geophysics* **41**: 325–342.

Berryman K. 1993. Distribution, age, and deformation of Late Pleistocene marine terraces at Mahia Peninsula, Hikurangi Subduction Margin, New Zealand, *Tectonics* **12**: 1365– 1379.

Beu AG, Browne GH, Grant-Taylor TL. 1981: New *Chlamys delicatula* localities in the central North Island and uplift of the Ruahine Range. *New Zealand Journal of Geology and Geophysics* **24**: 127-132.

Blum MD, Törnquist TE. 2000. Fluvial responses to climate and sea-level change: a review and look forward. *Sedimentology* **47**: 2–48.

Brook MS, Brock BW. 2005. Valley morphology and glaciation in the Tararua Range, southern North Island, New Zealand. *New Zealand Journal of Geology and Geophysics* **48**: 717-724.

Browne GH, Naish TR, 2003. Facies development and sequence architecture of a late Quaternary fluvial-marine transition, Canterbury Plains and shelf, New Zealand: implications for forced regressive deposits. *Sedimentary Geology* **158**: 57–86.

Buret Ch, Chanier F, Ferrière J, Proust JN. 1997. Individualization of a forearc basin during the active margin evolution: Hikurangi subduction margin, New Zealand. *Comptes Rendus Académie Sciences Paris* **325**: 615–621.

Carter JA. 2002. Phytolith analysis and paleoenvironmental reconstruction from Lake Poukawa core, Hawkes Bay, New Zealand. *Global and Planetary Change* **33**: 257– 267.

Carter L. 1974. Sedimentation in Hawke Bay off Hastings. *NZOI Oceanographic Summary* **3**: 8 pp.

Carter L, 2001. Currents of change: the ocean flow in a changing world. *Water and Atmosphere* **9**: 15-17 http://www.niwa.co.nz/pubs/wa/09-4/

Carter L, Heath RA. 1975. Role of mean circulation, tides and waves in the transport of bottom sediment on the New Zealand continental shelf. *New Zealand Journal of Marine and Freshwater Research* **9**: 423-428.

Carter L, Lewis KB. 1976. Subsurface structure and its influence on nearshore sedimentation off southern Hawkes Bay. *NZOI Records* **3**(5): 33-40.

Carter L, Garlick RD, Sutton P, Chiswell S, Oien NA, Stanton BR. 1998. Ocean Circulation New Zealand. *NIWA Chart Miscellaneous Series* **76**.

Carter RM, McCave IN, Richter C, Carter L, et al. 1999. Southwest Pacific Gateways, Sites 1119-1125. *Proceedings of Ocean Drilling Program, Initial Reports* **181**: 1-112.

Cashman SM, Kelsey HM. 1990. Forearc uplift and extension, southern Hawke's Bay, New Zealand: Mid-Pleistocene to present. *Tectonics* **9**: 23-44.

Cashman SM, Kelsey HM, Erdman CF, Cutten HNC, Berryman KB. 1992. A structural transect and analysis of strain partitioning across the forearc of the Hikurangi subduction zone, southern Hawke's Bay, North Island, New Zealand. *Tectonics* **11**: 242-257.

Catuneanu O. 2006. *Principles of sequence stratigraphy*. Elsevier Science: Amsterdam; 386.

Chanier F. 1991. *Le Prisme d'accrétion Hikurangi: un témoin de l'évolution géodynamique d'une marge active péripacifique (Nouvelle-Zélande)*. Thèse de Doctorat de l'Université des Sciences et Techniques de Lille – Flandres-Artois.

Chanier F, Ferrière J, Angelier J. 1992. Extension et érosion tectonique dans un prisme d'accrétion: l'exemple du prisme Hikurangi (Nouvelle Zélande). *Compte Rendus de l'Académie des Sciences Paris* **315**: série II, 741–747.

Chiswell SM. 2000. The Wairarapa Coastal Current. *New Zealand Journal of Marine and Freshwater Research* **34**: 303-315.

Christie-Blick N, Driscoll NW. 1995. Sequence stratigraphy. *Annual Review of Earth and Planetary Sciences* **23**: 451-478.

Cochran U, Zachariasen J, Mildenhall D, Hayward B, Southall K, Hollis C, Barker P, Wallace L, Alloway B, Wilson K. 2006. Paleoecological insights into subduction zone earthquake occurrence, eastern North Island, New Zealand. *GSA Bulletin*, **118**: 1051-1074.

Collot J-Y, Delteil J, Lewis KB, Davy B, Lamarche G, Audru J-C, Barnes P, Chanier F, Chaumillon E, Lallemand S, de Lépinay BMD, Orpin AR, Pelletier B, Sosson M, Toussaint B, Uruski C. 1996. From oblique subduction to intra-continental transpression: structures of the southern Kermadec-Hikurangi margin from multibeam bathymetry, side-scan sonar and seismic reflection. *Marine Geophysical Researches* **18**: 357–381.

Cooke PJ., Campbell NS. 1988. Micropalaeontology and climatic implications of the latest Quaternary section at DSDP Site 594, Southeast New Zealand. *Geological Society of New Zealand Miscellaneous Publication*
41a: 55 pp.
Conquest Exploration Co. 1989. Hawkes Bay shallow seismic and bottom sampling 38322 New Zealand. *New Zealand unpublished openfile petroleum report* **1471**. Ministry of Economic Development, Wellington.

Dalrymple M, Prosser J Williams B. 1998. A dynamic systems approach to the regional controls on deposition and architecture of alluvial sequences, illustrated in the statfjord formation (United Kingdom, northern North Sea). In Shanley KW, McCabe PJ, Relative Role of Eustasy, Climate, and Tectonism in Continental Rocks. *Special Publication* **59**, Society Economic Paleontologists Mineralogists: Tulsa, OK; 65-81.

Dravid PN, Brown LJ. 1997. *Heretaunga Plains—Groundwater study, Vol. I & II*. Napier, New Zealand. Hawke's Bay Regional Council: 254 pp.

Erdman CF, Kelsey HM. 1992. Pliocene and Pleistocene stratigraphy and tectonics, Ohara Depression and Wakarara Range, North Island, New Zealand. *New Zealand Journal of Geology and Geophysics* **35**: 177-192.

Field BD, Uruski CI and others. 1997. Cretaceous-Cenozoic geology and petroleum systems of the East Coast region, New Zealand. *Institute of Geological & Nuclear Sciences Monograph* **19**. Institute of Geological & Nuclear SciencesLimited, Lower Hutt, New Zealand: 301pp.

Foster G, Carter L. 1997. Mud sedimentation on the continental shelf at an accretionary margin—Poverty Bay, New Zealand. *New Zealand Journal of Geology and Geophysics* **40**, 157–173.

Francis RICC. 1985. An alternative water circulation pattern for Hawke Bay, New Zealand. *New Zealand Journal of Marine and Freshwater Research* **19**: 399-404.

Froggatt PC, Rogers GM. 1990. Tephrostratigraphy of high altitude peat bogs along the axial ranges, North Island, New Zealand. *New Zealand Journal of Geology and Geophysics* **33**: 111–125.

Gibb JG. 1986. A New Zealand regional Holocene eustatic sea-level curve and its application for determination of vertical tectonic movements. In Reilly, W.I., and Harford, B.E., eds., Recent crustal movements of the Pacific region: Wellington, *Bulletin of Royal Society of New Zealand* **24**: 377–395.

Gomez B, Filipelli G, Carter L, Trustrum N. 2001. *Recent sedimentation on an actively subsiding shelf: Hikurangi subduction margin, North Island, New Zealand*. In: MARGINS Chapman Conference, Puerto Rico, June 2001.

Grant-Taylor TL. 1978. The geology and structure of the Ruataniwha Plains. *In:* Speden, I. *ed*. Geology and erosion in the Ruahine Range. *New Zealand Geological Survey report* **G20**: 31-51.

Harmsen FJ. 1985. Lithostratigraphy of Pliocene strata, central and southern Hawke's Bay, New Zealand. *New Zealand journal of geology and geophysics* **28**: 413 -433.

Harper MA, Collen J. 2002. Glaciations, interglaciations and reworked microfossils in Poukawa Basin, New Zealand. *Global and Planetary Change* **33**: 43–256.

Hayward B, Grenfell HR, Sabaa AT, Carter R, Cochran U, Lipps JH, Shane PR, Morley M. 2006. Micropaleontological evidence of large earthquakes in the past 7200 years in southern Hawke's Bay, New Zealand. *Quaternary Science Reviews* **25**: 1186-1207.

Hicks DM, Shankar U. 2003. Sediment yield from New Zealand rivers. *NIWA Chart, Miscellaneous Series* **79**.

Hull AG. 1985. *Late Quaternary geology of the Cape Kidnappers area, Hawkes Bay, New Zealand*. MSc thesis, Victoria University, Wellington, New Zealand.

Hull AG. 1986. Pre-A.D. 1931 tectonic subsidence of Ahuriri Lagoon, Napier, Hawkes Bay, New Zealand. *New Zealand Journal of Geology and Geophysics* **29**: 75-82.

Hull AG. 1987. A late Holocene uplifted shore platform on the Kidnappers coast, North Island, New Zealand. some implications for shore platform development processes and uplift mechanism. *Quaternary Research* **28**: 183-195.

Imbrie J, Hays JD, Martinson DG, McIntyre A, Mix AC, Morley JJ, Pisias NG, Prell WL, Shackleton NJ, 1984. The orbital theory of Pleistocene climate: support from a revised chronology of the marine $\delta^{18}O$ record. In: Berger A, Imbrie J, Hays J, Kukla G, Saltzman B. (Eds.), Milankovitch and climate. Reidel Publishing Company, Dordrecht, pp. 269-305.

Jervey MT. 1988. Quantitative geological modeling of siliciclastic rock sequences and their seismic expression. In Sea-level Changes—An Integrated Approach, Wilgus CK, Hastings BS, Kendall

ChStCG, Posamentier HW, Ross CA, Van Wagoner JC (eds). Special Publication 42, Society Economic Paleontologists Mineralogists: Tulsa, OK: 47-69.

Kamp PJJ. 1978. *Stratigraphy and sedimentology of conglomerates in the Pleistocene Kidnappers Group, Hawkes Bay*. Unpublished MSc thesis, University of Waikato, Hamilton, New Zealand

Kamp PJJ. 1990. Kidnappers Group (middle Pleistocene), Hawke Bay.*Geological Society of New Zealand miscellaneous publication* **50B**: 105-118.

Kamp PJJ, Vonk AJ, Bland KJ, Griffin AG, Hayton S, Hendy AJW, McIntyre AP. 2002. Megasequence architecture of Taranaki, Wanganui, and King Country basins and Neogene progradation of two continental margin wedges across western New Zealand. *Proceedings NZ Petroleum Exploration Conference*, Auckland, February: 464-481.

Kingma JT, 1958. Geology of the Wakarara Range, central Hawke's Bay. *New Zealand Journal of Geology and Geophysics* **1**, 76-91.

Kingma JT. 1962. Sheet 11—Dannevirke. Geological map of New Zealand 1:250 000. Wellington, New Zealand Department of Scientific and Industrial Research.

Kingma JT. 1971. Geology of the Te Aute subdivision. *New Zealand Geological Survey bulletin* **70**: 173 pp.

Lee HJ, Syvitski JPM, Parker G, Orange D, Locat J, Hutton EWH, Imram J. 2002. Distinguishing sediment waves from slope failure deposits: field examples, including the 'Humboldt Slide', and modelling results. *Marine Geology* **192**: 79-104.

Lewis KB. 1971a. Growth rate of folds using tilted wave planed surfaces: coast and continental shelf, Hawke's Bay, New Zealand. *In*: Collins, B. W.; Fraser, R. *ed*. Recent crustal movements. *The Royal Society of New Zealand Bulletin* **9**: 225-231.

Lewis KB. 1971b. Slumping on a continental slope inclined at *l°-4°*. *Sedimentology* **16**: 97-110.

Lewis KB. 1973a. Erosion and deposition on a tilting continental shelf during Quaternary oscillations of sea level. *New Zealand journal of geology and geophysics* **16**: 281-301.

Lewis KB. 1973b. Sediments on the continental shelf and slope between Napier and Castelpoint, New Zealand. *New Zealand journal of marine and freshwater research* **7**: 183-208.

Lewis KB. 1974. Upper Tertiary rocks from the continental shelf and slope of Southern Hawke's Bay. *New Zealand journal of marine and freshwater research* **8**: 663-670.

Lewis KB. 1980. Quaternary sedimentation on the Hikurangi oblique-subduction and transform margin, New Zealand. In *Sedimentation in obliqueslip mobile zone*, Ballance, P.F., Reading, H.G. (eds). Special publication International Association of Sedimentologists **4**: 171-189.

Lewis KB, Bennett DJ. 1985. Structural pattern on the Hikurangi Margin: an interpretation of new seismic data. in *New seismic profiles, cores, and dated rocks from the Hikurangi margin, New Zealand*, Lewis, K.B. (comp). New Zealand Oceanographic Institute field report **22**. Division of Marine and Freshwater Science, Department of Scientific and Industrial Research, Wellington.

Lewis KB, Pettinga JR. 1993. The emerging, imbricate frontal wedge of the Hikurangi margin. *In*: South Pacific sedimentary basins. *Sedimentary Basins of the World 2, Basins of the Southwest Pacific*, Ballance PF (ed.). Elsevier, Amsterdam: 225–250.

Lewis KB, Collot J-Y, Davy BW, Delteil L, Lallemand SE, Uruski CI & GeodyNZ team. 1997. North Hikurangi GeodyNZ swath maps: depth, texture and geological interpretation. *NIWA chart miscellaneous series* **72**. National Institute of Water and Atmospheric Research, Wellington.

Lisiecki LE, Raymo ME. 2005. A Pliocene-Pleistocene stack of 57 globally distributed benthic $\delta^{18}O$ records. *Paleoceanography* **20**: PA1003, doi:10.1029/2004PA001071.

Litchfield N. 2003. Maps, stratigraphic logs and age control data for river terraces in the eastern North Island. *Institute of Geological and Nuclear Sciences Science Report* **31**: 102 pp.

Litchfield NJ, Berryman KR. 2005. Correlation of fluvial terraces within the Hikurangi Margin, New Zealand: Implications for climate and base level controls. *Geomorphology* **68**: 291-313.

Litchfield NJ, Berryman KR. 2006. Relations between postglacial fluvial incision rates and uplift rates in North Island, New Zealand. *Journal of Geophysical Research* **111**: doi:10.1029/2005JF000374.

Litchfield N, Rieser U. 2005. OSL age constraints for fluvial aggradation terraces and loess in the eastern North Island, New Zealand, *New Zealand Journal of Geology and Geophysics* **48**: 581-589.

Lowe DJ, Newnham RM, Ward CM. 1999. Stratigraphy and chronology of a 15 ka sequence of multi-sourced silicic tephras in a montane peat bog in eastern North Island, New Zealand. *New Zealand Journal of Geology and Geophysics* **42**: 565-579.

Marutani T, Kasai M, Reid LM, Trustrum NA. 1999. Influence of storm-related sediment storage on the sediment delivery from tributary catchments in the upper Waipaoa River, New Zealand. *Earth Surface Processes and Landforms* **24**: 881–896.

McArthur JL, Shepherd MJ. 1990. Late Quaternary glaciation of Mt Ruapehu, North Island, New Zealand. *Journal of The Royal Society of New Zealand* **20**: 287-296.

McGlone MS. 2001. A late Quaternary pollen record from marine core P69, southeastern North Island, New Zealand. *New Zealand Journal of Geology and Geophysics* **44**: 69-77.

McGlone MS. 2002. The late Quaternary peat, vegetation and climate history of the Southern Oceanic Islands of New Zealand. *Quaternary Science Reviews* **21**: 683-707.

McGlone MS, Howorth R, Pullar WA. 1984. Late Pleistocene stratigraphy, vegetation and climate of the Bay of Plenty and Gisborne regions, New Zealand. *New Zealand Journal of Geology and Geophysics* **27**: 327-350.

McLea WL. 1990. Palynology of the Pohehe Swamp, northwest Wairarapa, New Zealand: a study of climatic and vegetation changes during the last 41 000 years. *Journal of the Royal Society of New Zealand* **20**: 205-220.

Miall AD. 1991. Stratigraphic sequences and their chronostratigraphic correlation. *Journal of Sedimentary Petrology* **61**: 497-505.

Milne JDG. 1973a. *Upper Quaternary geology of the Rangitikei Drainage Basin, North Island, New Zealand*. Unpublished PhD thesis, Massey University, Palmerston North.

Milne JDG. 1973b. Map and sections of river terraces in the Rangitikei Basin, North Island, New Zealand. *New Zealand Soil Survey Report* **4**, Department of Scientific and Industrial Research, Wellington, New Zealand.

Mitchum JR, Vail PR, Thompson S. 1977. Seismic Stratigraphy and Global Changes of Sea level, Part 2: The Depositional Sequence as a Basic Unit Stratigraphic Analysis. In *Seismic Stratigraphy – applications to hydrocarbon exploration*, Payton E (Ed). American Association of Petroleum Geologist Memoir **26**: 53-62.

Mitchum JR, Vail PR, Sangree JB. 1977. Seismic Stratigraphy and Global Changes of Sea Level, Part 6: Stratigraphic Interpretation of Seismic Reflection Patterns. In Depositional Sequences. In *Seismic Stratigraphy – applications to hydrocarbon exploration*, Payton E (Ed). American Association of Petroleum Geologist Memoir **26**: 117-133.

Multiwave. 2005. 05CM 2D Seismic Survey, Offshore East Coast - North Island. New Zealand unpublished openfile petroleum report 3136. Ministry of Economic Development, Wellington.

Nelson CS, Hendy CH, Jarrett GR, Cuthbertson AM. 1985. Near-synchroneity of New Zealand alpine glaciations and Northern Hemisphere continental glaciations during the past 750 kyr. *Nature* **318**: 361-363.

Newnham RM, Lowe DJ, Williams PW. 1999. Quaternary environmental change in New Zealand: a review. *Progress in Physical Geography* **23**: 567-610.

Newnham RM, Lowe DJ. 2000. Fine–resolution pollen record oflate-glacia l climate reversal from New Zealand. *Geology* **28**: 759-762.

Newnham RM, Eden DN, Lowe DJ, Hendy CH. 2003. Rerewhakaaitu Tephra, a land-sea marker for the last termination in New Zealand with implications for global climatic change. *Quaternary Science Reviews* **22**: 289–308.

Okamura Y, Blum P. 1993. Seismic stratigraphy of Quaternary stacked progradational sequences in the southwest Japan forearc: an example of fourth-order sequences in an active margin, Sequence Stratigraphy and Facies Associations. *International Association of Sedimentologists, Special Publication* **18**: 213-232.

Okuda M, Shulmeister J, Flenley JR. 2002. Vegetation changes and their climatic implications for the late Pleistocene at Lake Poukawa, Hawkes Bay. *Global and Planetary Change* **33**: 269-282.

Orpin AR, Alexander C, Carter L, Kuehl S, Walsh JP. 2006. Temporal and spatial complexity in post-glacial sedimentation on the tectonically active, Poverty Bay continental margin of New Zealand. *Continental Shelf Research* **26**: 2205-2224.

Pantin AM. 1966. Sedimentation in Hawke Bay. *New Zealand Department of Scientific and Industrial Research bulletin* **171**: 70 pp.

Payton CE. 1977. *Seismic Stratigraphy – applications to hydrocarbon exploration*. American Association of Petroleum Geologist Memoir **26**: 516 pp.

Pettinga JR. 1980. *Geology and landslides of the eastern Te Aute District, southern Hawke's Bay*. Unpublished PhD thesis, Geology Department, University of Auckland Library, Auckland, New Zealand. 602 pp.

Pettinga JR. 1982. Upper Cenozoic structural history, coastal southern Hawke's Bay, New Zealand. *New Zealand journal of geology and geophysics* **25**: 149-19 1.

Pettinga JR. 1985. Seismic evidence of the offshore extension of the Kairakau-Waimarama regional slump, Hikurangi Margin. In *New seismic profiles, cores, and dated rocks from the Hikurangi margin,*

New Zealand, Lewis, K.B. (comp) New Zealand Oceanographic Institute field report **22**. Division of Marine and Freshwater Science, Department of Scientific and Industrial Research, Wellington.

Pettinga JR, 2004. Three-stage massive gravitational collapse of the emerging imbricate frontal wedge, Hikurangi Subduction Zone, New Zealand. *New Zealand Journal of Geology & Geophysics* **47**: 399-414.

Pillans B. 1986. A late Quaternary uplift map for North Island, New Zealand. In *Recent crustal movements of the Pacific region*, Reilly, W.l., Harford, B.E. (eds). Royal Society of New Zealand bulletin **24**: 409-417.

Pillans B, McGlone M, Palmer A, Mildenhall D, Alloway B, Berger G. 1993. The Last Glacial Maximum in central and southern North Island, New Zealand: a paleoenvironmental reconstruction using Kawakawa Tephra Formation as a chronostratigraphic marker. *Palaeogeography Palaeoclimatology Palaeoecology* **101**: 283-304.

Pillans B. 1994. Direct marine–terrestrial correlations, Wanganui Basin, New Zealand: the last 1 million years. *Quaternary Science Reviews* **13**: 189-200.

Posamentier HW, Jervey MT, Vail PR. 1988. Eustatic controls on clastic deposition I-Conceptual framework. In *Sea-level Changes—an Integrated Approach*, Special Publication 42, Wilgus CK, Hastings BS, Kendall ChStCG, Posamentier HW, Ross CA, Van Wagoner JC
(eds). Society Economic Paleontologists Mineralogists: Tulsa, OK; 109-124.

Posamentier HW, Vail PR. 1988. Eustatic controls on clastic deposition II-Sequence and systems tract models. In *Sea-level Changes—an Integrated Approach*, Wilgus CK, Hastings BS, Kendall ChStCG, Posamentier HW, Ross CA, Van Wagoner JC (eds). Special Publication 42, Society Economic Paleontologists Mineralogists: Tulsa, OK; 125-154.

Posamentier HW, Allen GP, James DP, Tesson M. 1992. Forced regressions in a sequence stratigraphic framework: concepts, examples and exploration significance. *American Association of Petroleum Geologists Bulletin* **76**: 1687-1709.

Proust J-N, Chanier F. 2004. The Pleistocene Cape Kidnappers section in New Zealand : orbitally forced controls on active margin sedimentation? *Journal of Quaternary Science* **19**: 591-603.

Proust J-N, Lamarche G, Migeon S, Neil H, and Shipboard party. 2006. MD152 / MATACORE "Tectonic and climate controls on sediment budget". *Les rapports de campagnes à la mer* : pp. 107.

Raub ML. 1985. *The neotectonic evolution of the Wakarara area*, M.Sc. thesis, Auckland Univ., Auckland, New Zealand: pp. 122.

Ridgway NM. 1960. Surface water movements in Hawke Bay, New Zealand. *New Zealand journal of Geology and Geophysics* **3** (2): 253-261.

Ridgway NM. 1962. Nearshore surface currents in southern Hawke Bay, New Zealand. *New Zealand journal of Geology and Geophysics* **5**: 545-66.

Ridgway NM, Stanton BR. 1969. Some hydrological features of Hawke Bay and nearby shelf waters. *New Zealand journal of marine and freshwater research* **3**: 545-559.

Roksandi'c M M. 1978. Seismic Facies Analysis Concepts. *Geophysical Prospecting* **26**: 383-398.

Sangree JB, Widmier JM. 1977. Seismic Stratigraphy and Global Changes of Sea Level, Part 9: Seismic Interpretation of Clastic Depositional Facies. In *Seismic Stratigraphy – applications to*

hydrocarbon exploration, Payton E (Ed). American Association of Petroleum Geologist Memoir **26**: 117-133.

Shane PAR. 1994. A widespread, early Pleistocene tephra (Potaka tephra, 1 Ma) in New Zealand: Character, distribution, and implications. *New Zealand Journal of Geology and Geophysics* **37**: 25-35.

Shane PAR, Black TM, Alloway BV, Westgate JA 1996. Early to middle Pleistocene tephrochronology of North Island, New Zealand: implications for volcanism, tectonism, and paleoenvironments. *Geological Society of America Bulletin* **108**: 915–925.

Shane P, Sandiford A. 2003. Paleovegetation of marine isotope stages 4 and 3 in Northern New Zealand and the age of the widespreade Rotoehu tephra. *Quaternary Research* **59**: 420-429.

Sheriff RB. 1980: *Seismic Stratigraphy*. IHRDC, Boston: 227pp.

Shulmeister J, Shane P, Lian OB, Okuda M, Carter JA, Harper M, Dickinson WW, Augustinus P, Heijnis H. 2001. A long late-Quaternary record from Lake Poukawa, Hawkes Bay, New Zealand. *Palaeogeography Palaeoclimatology Palaeoecology* **176**: 81– 107.

Shulmeister J, Goodwin I, Renwick J, Harle K, Armand L, McGlone MS, Cook E, Dodson J, Hesse PP, Mayewski P, Curran M. 2004. The Southern Hemispher westerlies in the Australasian sector over the last glacial cycle: a synthesis. *Quaternary International* **118-119**: 23-53.

Shumm SA. 1993. River Response to Baselevel Change: Implications for Sequence Stratigraphy. *The journal of Geology* **101**: 279-294.

Smale D, Houghton BF, McKellar IC, Mansergh GD, Moore PR. 1978. Geology and erosion in the Ruahine Range: a reconnaissance study. In *Geology and erosion in the Ruahine Range*, Speden, I. (ed.). *New Zealand Geologicalsurvey report* **G20**: 7-30.

Spörli KB, Ballance PF. 1989. Mesozoic-Cenozoic ocean floor-continent interaction and terrane configuration, southwest Pacific area around New Zealand. In. *Mesozoic and Cenozoic evolution of the Pacific Ocean margins*, Ben Avraham Z. (ed.). Oxford University Monograph, geology and geophysics **8**: 176-190.

Strong CP, Scott GH, Edwards AR. 1989. Foraminifera and calcareous nannoplankton from Hawke's Bay sea floor samples PPL 38321 PPL 38322 PPL 38323. New Zealand unpublished openfile *Petroleum Report* **1470**. Ministry of Economic Development, Wellington.

Strong N, Paola C. 2006. Fluvial Landscapes and Stratigraphy in a Flume. *The Sedimentary Record* **4**: 4-8.

Suggate RP. 1961. Rock-strati graphic names for the South Island schists and undifferentiated sediments of the New Zealand geosyncline. *New Zealand Journal of Geology and Geophysics* **4**: 392-399.

Suggate RP. 1990. Late Pliocene and Quaternary glaciations of New Zealand. *Quaternary Science Review* **9**: 175–197.

Sullivan D. 1990. 2D Marine Seismic Survey Acquisition Report PPL 38322, PPL 38321. New Zealand unpublished openfile *Petroleum Report* **1666**. Ministry of Economic Development, Wellington.

Talling PJ. 1998. How and where do incised valleys form if sea level remains above the shelf edge? *Geology* **26**: 87-90.

Vail PR, Mitchum JR, Todd RG, Widmier JM, Thompson S, Sangree JB, Bubb JN, Hatlelid WG. 1977. Seismic Stratigraphy and Global Changes of Sea Level. In Depositional Sequences. In *Seismic Stratigraphy – applications to hydrocarbon exploration*, Payton E (Ed). American Association of Petroleum Geologist Memoir **26**: 49-212.

van der Lingen GJ, Pettinga JR. 1980. The Makara Basin: a Miocene slope-basin along the New Zealand sector of the Australian-Pacific obliquely convergent plate boundary. In *Sedimentation in oblique strike-slip mobile zones*, Ballance, P.F., Reading, H.G. (eds). Special publication of the International Association of Sedimentologists: 191-215.

Van Wagoner JC, Posamentier HW, Mitchum RM, Vail PR, Sarg JF, Loutit TS, Hardenbol J, 1988. An overview of fundamentals of sequence stratigraphy and Key definitions. *In Sea-level Changes—an Integrated Approach*, Wilgus CK, Hastings BS, Kendall ChStCG, Posamentier HW, Ross CA, Van Wagoner JC (eds). Special Publication **42**, Society Economic Paleontologists Mineralogists: Tulsa, OK; 39-45.

Van Wagoner JC, Mitchum RM, Campion KM, Rahmanian VD, 1990: Siliciclastic Sequence Stratigraphy in Well Logs, Cores and Outcrops: Concepts for high resolution Correlation of Time and Facies. American Association of Petroleum Geologists Methods in Exploration Series **7**, Tulsa: 55 pp.

Waelbroeck C, Labeyrie L, Michel E, Duplessy JC, McManus JF, Lambeck K, Balbon E, Labracherie M. 2002. Sea-level and deep water temperature changes derived from benhic foraminifera isotopic records. *Quaternary Science Reviews* **21**: 295-305.

Walcott RI. 1987. Geodetic strain and the deformation history of the North Island of New Zealand during the late Cenozoic. *Philosophical Transaction Royal Society London* **A321**: 163–181.

Woolfe KJ, Larcombe P, Naish T, Purdon RG. 1998. Lowstand rivers need not incise the shelf: an example from the Great Barrier Reef, Australia, with implications for sequence stratigraphic models. *Geology* **26**: 75–78.

Wright IC, Lewis KB. 1991. Seafloor sampling as a window to deeper structure along offshore accretionary systems: an example from offshore East Coast, North Island, New Zealand. *Proceedings of 1991 New Zealand Oil Exploration Conference* **1**: 101-109.

Wynn RB, Stow DAV, 2002. Classification and characterisation of deep-water sediment waves. *Marine Geology* **192** 7–22.

Zaitlin BA, Dalrymple RW, Boyd R. 1994. The stratigraphic organisation of incised valley systems associated with relative sea-level change. Soc. Econ. Paleont. Miner., Spec. Publ. **51**, 391p.

FIGURE CAPTIONS :

Table 1:

Description of the data set interpreted or used in this study.

Table 2:

Characteristics of the seismic facies recognised on seismic data covering the offshore Hawke's Bay forearc domain.

Table 3:

Characteristics of the 11 seismic facies recognised on seismic data covering the offshore Hawke's Bay forearc domain with description, interpretation in sedimentary facies and examples in MCS, Boomer and/or 3.5 KHz data.

Figure 1:

Tectonic setting of the active Hikurangi subduction margin. (A) Australian-Pacific plate boundary and their relative movements in the New Zealand region. Light gray shading corresponds to submerged continental crust and dark gray shading represents the emergent continental crust of the New Zealand micro-continent. (B) Arrangement of the major morphostructural elements of the Hikurangi subduction margin in the North Island including the Hikurangi Trough, the imbricate frontal wedge emergent in the coastal ranges, the Neogene forearc basin, the axial ranges and the backarc basins (See descriptions in the text). The location of both Mio-Pliocene and Pleistocene volcanic arcs reflects the progressive rotation of the margin. The dashed line A-A' correspond to the trace of the crustal cross section. (C) Crustal cross section A-A' modified from Beanland (1995), Begg et al. (1996) and Barnes et al. (2002) showing the structure of the central part of the subduction margin. RF: Ruahine Fault; MF: Mohaka Fault; KR: Kidnappers Ridge; LB: Lachlan Basin; LR: Lachlan Ridge; MR: Motuokura Ridge. (D) Map showing the arrangement of the characteristic morphostructural elements in the Hawke's Bay region.

Figure 2:

Map showing the current Hawke's Bay onshore and offshore morphology and the main tectonic structures. The bathymetry contours and illuminated digital elevation model are from Collot et al. (1994, 1995, 1996), Lewis et al. (1997) and unpublished data acquired by NIWA. The topographic contours and illuminated digital elevation model are from the NZTopo digital elevation model (Land Information New Zealand). Contours are in meters.

Figure 3:

Location map of seismic surveys, long piston cores and wells used for this study. Seismic profiles and topographic sections that appear in figures (sections) are respectively in bold solid and dashed black lines with reference to the figure.

Figure 4:

Schematic sections across the submerged Hawke's Bay sector of the forearc domain showing the general geometry of the seismic units and unconformities described in this study. (A) Location map for cross sections A and B. KB: Kidnappers Basin ; MaB: Mahia Basin ; LB: Lachlan Basin ; MoB: Motuokura Basin. (B) cross section parallel to the slope and passing over the active uplifting Kidnappers ridge. U6 and U5 are the only seismic units that can be traced over the ridge in the southern part of Hawke Bay. (C) cross section turning around the active Kidnappers ridge and passing through the major subsiding basins identified in the Hawke's Bay forearc domain. All seismic units, excepted U4, can be traced from the onshore area to the upper slope area (c. 500 m water-depth).

Figure 5:

Interpretation of the inner shelf Boomer profiles from GSR 05301 survey, showing raw data with unconformities (S1 to S5) and seismic units (U1 to U6), and the corresponding interpretation for (A) line 11, (B) line 8 and (C) line 6 (see location map on Fig.3). The vertical exaggeration is approximately x45. The legend shows the interpretation of seismic units as system tracts and their correlation to the stratigraphic chart. Refer text for full discussion

Figure 6:

Lithological logs of Tollemache Orchard and Awatoto wells (see location map on Fig. 3), modified from Dravid and Brown (1997). The figure depicts the evolution of the interpreted depositional environments, the position of dated samples, and the proposed correlation to both the seismic stratigraphy from Boomer interpretations and the oxygen isotope stratigraphy and curve (Lisiecki & Raymo, 2005; Waelbroeck et al., 2002; Imbrie et al., 1984). The correlation to the oxygen isotope stratigraphy is based on: (1) on the available dated samples: (2) on the succession of depositional environments that fits to the tendency observed on the oxygen isotope curve; and (3) on the occurrence of marine deposits at the base of the section that we assume to be last interglacial in age.

Figure 7:

Interpretation of the outer shelf / upper slope 3.5 KHz profile from MD 152 survey (Proust et al., 2006; see location map on Fig. 3), showing raw data profile and the corresponding interpretation with seismic facies (Fs9 to Fs 11) unconformities (S1, S2, S4, and S5), seismic

units (U1b, U2, U3, U5 and U6). The caption shows the interpretation of seismic units as system tracts and their correlation to the stratigraphic chart. On the northwestern part, unconformity S1 is projected from Multichannel seismic profiles #05 from TAN 0313 survey and #28 from 05CM survey (Multiwave, 2005; see S1 on Fig.9). The vertical exaggeration is approximately x35 with depth conversion assuming 1500 $m.s^{-1}$.

Figure 8:

Interpretation of the inner shelf to outer shelf 3.5 KHz profile AG#1 from AG&S survey (Conquest Exploration, 1988; see location map on Fig.3), showing raw data profile and the corresponding interpretation with unconformities (S1 to S5) and seismic units (U1 to U6). Insert shows the interpreted boomer line 8 that allows correlation between inner and outer shelf. The vertical exaggeration is approximately x100.

Figure 9:

Interpretation of the outer shelf / upper slope Multichannel Channel Seismic profile #29 (A) and #41 (B) from 05CM survey (Multiwave, 2005; see location map on Fig.3), showing the migrated profile and the corresponding interpretation with unconformities (S1, S2, S4, and S5) and seismic units (U1, U2, U3, U5 and U6). Dashed and solid bold lines correspond respectively to maximum flooding surfaces and sequence boundaries. Landward and seaward stepping trends within LPS1 are indicated. The vertical exaggeration is approximately x10.

Figure 10:

Topographic sections across the foothill domain that summarize the location of major fluvial terraces. (A) transverse profile across major southern Hawke's Bay river valleys (Tukituki, Waipawa, Makaroro and Ngaruroro) showing: the location of age calibrated fluvial terraces T1, T2 and T3 (Litchfield and Berryman, 2005), the location of undated older terraces (T4 and Salisbury terrace), the uplift rate estimations U (from Litchfield and Berryman, 2006) and the lithological log of the Pleistocene substratum (Makaroro section) with age calibrated tephras (Shane, 1994). (B) Longitudinal profiles of the river bed (RB) terraces, T1, T3 and T4 along the Ngaruroro valley and corresponding uplift rate estimations using method from Litchfield and Berryman (2006).

Figure 11:

(A) age estimation of undated older terraces T4 and Salisbury, using their elevation at the same point of the stream profile, assuming a constant uplift rates (U) and similar conditions of formation. (B) Correlation of fluvial aggradation periods within valleys to the oxygen isotope stratigraphy and mean sea level curve (Lisiecki & Raymo, 2005; Waelbroeck et al., 2002; Imbrie et al., 1984) using age calibrated samples (Litchfield and Berryman, 2005; Litchfield and Rieser, 2006) and age estimation of T4 and Salisbury terrace.

Figure 12:

Schematic sections across the Hawke's Bay forearc domain depicting the "source to sink" interpretation of seismic units (U2 to U6) and fluvial terraces (T1 to Salisbury, on section A) as system tracts and the correlation to the oxygen isotope stratigraphy and mean sea level curve (Lisiecki & Raymo, 2005; Waelbroeck et al., 2002; Imbrie et al., 1984). (A) cross section parallel to the slope and passing over the active uplifting Kidnappers ridge. (B) cross section turning around the northern en of the active Kidnappers ridge and passing through the major subsiding basins identified in the Hawke's Bay forearc domain, from the axial range front to the upper slope area (c. 500 m water-depth). Location of section on Figure 4.

Figure 13:

Isopach map of the late Pleistocene sequence LPS1 as identified from seismic interpretation. Two-way travel times were converted to depth, then thickness, using an average velocity of 1600 $m.s^{-1}$. Isopach contours have been digitized and the map has been generated in GIS software. The four main depocenters are located and designated by the following abbreviations: KB, Kidnappers Basin; MB, Mahia Basin; LB, Lachlan basin; MB, Motuokura Basin. Aggradational terraces of LPS1 (T2, T3, T4 and Salisbury) are mapped but not differentiated. Active and inferred tectonic structures are superimposed in order to reveal the impact of tectonic deformation on the distribution of sediments. The volume of LPS1 sediments deposited and preserved reaches c.340 km^3.

Figure 14:

Isopach map of the late Pleistocene sequence LPS2 as identified from seismic interpretation. Two-way travel times were converted to depth, then thickness, using an average velocity of 1600 $m.s^{-1}$. Isopach contours have been traced from our seismic interpretation and completed from previous studies for the northern Hawke's Bay area (Wright and Lewis, 1991) and the Poverty shelf (Foster and Carter, 1997; Orpin et al, 2006). Contours have been digitized and

the map has been generated in GIS software. The four main depocenters are located and designated by the following abbreviations: SKB, Southern Kidnappers Basin; NKB, Northern Kidnappers Basin; LB, Lachlan basin; MB, Motuokura Basin. Aggradational terraces T1 are mapped. Active and inferred tectonic structures are superimposed in order to reveal the strong impact of tectonic deformation on the distribution of sediments. The volume of LPS2 sediments deposited and preserved reaches c.140 km^3.

Figure 15: Schematic sections across the Hawke's Bay forearc domain depicting the "source to sink" interpretation of seismic units (U2 to U6) and fluvial terraces (T1 to Salisbury, on section A) as sedimentary facies and depositional environments (See text for details). (A) cross section parallel to the slope and passing over the active uplifting Kidnappers ridge. (B) cross section turning around the northern end of the active Kidnappers ridge and passing through the major subsiding basins identified in the Hawke's Bay forearc domain, from the axial range front to the upper slope area (c. 500 m water-depth). Location of section on Figure 4.

Figure 16:

Paleogeographic reconstructions for the late Pleistocene environmental extremes that integrate results from seismic interpretation, piston-cores, onshore and offshore wells and mapping as well as results from previous studies (Ridgway, 1960; Pantin, 1966; Ridgway and Stanton, 1969; Lewis, 1973a,b; Carter, 1974; Smale et al., 1978; Grant-Taylor, 1978; Francis, 1985; Hull, 1985, 1986; Lewis and Barnes, 1991; Barnes et al., 1991; Dravid and Brown, 1997; Carter et al., 1998; Carter, 2001; Shulmeister et al., 2001; Harper and Collen, 2002; Okuda et al., 2002; Litchfield, 2003; Litchfield and Berryman, 2006; Hayward et al., 2006; Cochran et al., 2006; Proust et al., 2006; this study): (A) reconstruction of the depositional environment distribution within the Hawke's Bay forearc domain during the Last Glacial Maximum (c. 20 Ka). Position of braided channels are schematic as we haven't been able to map them. (B) Reconstruction of the depositional environment distribution within the Hawke's Bay forearc domain during the Holocene optimum (c. 7.2 Ka).

Table 1

Survey Name	Data type	Length (interpreted)	Operator / Country	Vessel	Year	Avaliable report (PR) or publications :
GeodyNZ	Bathymetry EM12		Ifremer / France	R/V Atalante	1993	Collot et al. (1996) Lewis et al. (1998)
Various	Bathymetry EM300		NIWA / NZ	R/V Tangaroa	1993 to 2005	
GSR 05301	Boomer	175 km	NIWA / CNRS	Big Kahuna	2005	
CQX H90	MCS (60 folds)	1000 km	NZ CQX Ltd.	M/V Western Pacific	1990	Sullivan – PR 1666 (1990)
05CM	MCS (640/960 channels)	720 km	Ministry of Economic Development / NZ	M/V Pacific Titan	2005	Multiwave – PR 3186 (2005)
CR3044	3.5 KHz & MCS (48 channels)		NIWA / NZ	R/V Tangaroa	1998	Barnes et al. (2002) ; Barnes and Nicol (2004)
TAN 0313	3.5 KHz & MCS (48 channels)	830 km	NIWA / NZ	R/V Tangaroa	2003	
TAN 0412	3.5 KHz & MCS (48 channels)	298 km	NIWA / NZ	R/V Tangaroa	2004	
AG & S	3.5 KHz	1200 km	Conquest Exploration Ltd / NZ	GRV Rapuhia	1988	Conquest Exploration - PR2059 (1988)
MD152 / Matacore	3.5 KHz & 6 giant calypso piston cores (MD06-2995/96/97 on the upper slope and MD06-2998/99 /3000 on the shelf)	c. 100 km (core length up to c. 30 m)	IPEV / CNRS-INSU / NIWA / AWI / VIMS SIO	R/V Marion-Dufresne	2006	Proust et al. (2006)

Table 2

Seismic units	Lower boundary surface	Upper boundary surface	Seismic facies
U1	-	S1, truncation	Fs1, Fs2, Fs3, Fs4, Fs5, Fs6
U2	S1, concordant	S2, truncation	Fs2, Fs7, Fs8, Fs9
U3	S2, concordant	S3, truncation	Fs3, Fs9, FS10, FS11
U4	S3, onlap	S4, concordant	Fs3
U5	S4, onlap	S5, truncation	Fs4, Fs7
U6	S5, onlap	seafloor	Fs5, Fs8

Table 3A:

Seismic facies	Description	Interpretation	Examples	
			MCS	Boomer
Fs1	Good continuity, average amplitude, high frequency, parallel configuration	Well-bedded marine sandstones and siltstones	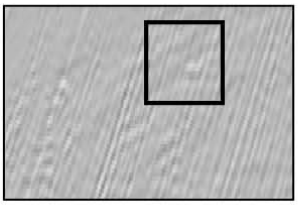	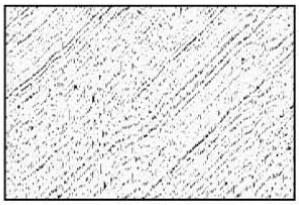
Fs2	Low to good continuity, low to high amplitude, average frequency, sub-parallel to chaotic configuration with channels	Shallow marine and terrestrial siltstones, sandstones, and congl-merates	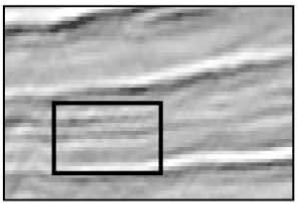	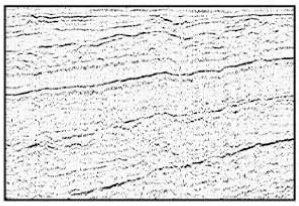
Fs3	Average to good conti-nuity, low to high amplitude, average frequency, sub-parallel to chaotic configuration with incision channels	Fluvial gravels and overbank sand deposits	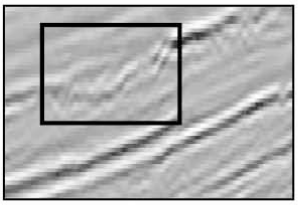	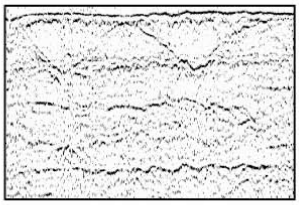
Fs4	Low to average conti-nuity, low amplitude, average frequency, sub-parallel to chaotic configuration with small channels	Poorly-bedded shallow marine sand and silt succession deposited in a high energy shelf environment		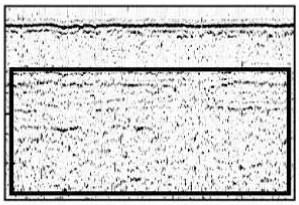
Fs5	Average continuity, transparent to low amplitude, low frequency, parallel to oblique parallel configu-ration	Poorly-bedded shallow marine sands and silts prograding towards the shelf break		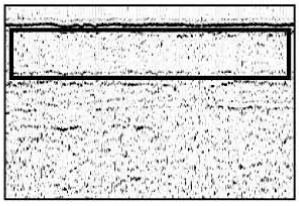
Fs6	Average to good conti-nuity, low amplitude, high frequency, parallel configuration	Well-bedded shallow marine sandstones		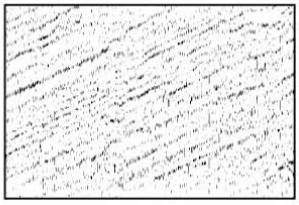

Table 3B:

Seismic facies	Description	Interpretation	Examples	
			MCS	3.5 KHz
Fs7	Average to good continuity, low to average amplitude, low to average frequency, parallel to reflection free configuration	Shallow to deep marine sands and silts	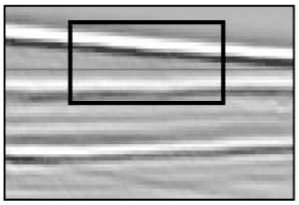	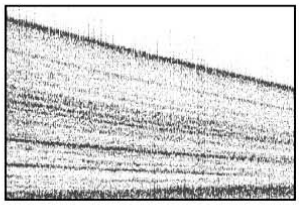
Fs8	Average to good continuity, average to high amplitude and frequency, parallel and slightly wavy configuration	Well-bedded deep marine silstones	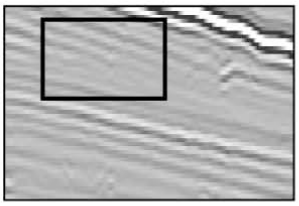	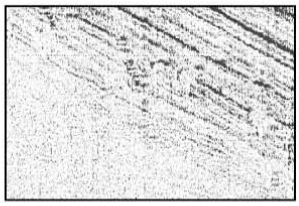
Fs9	Average to good continity, average to high amplitude and frequency, parallel and wavy configuration	Well-bedded and wavy deep marine siltstones	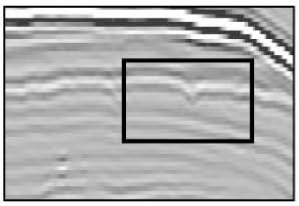	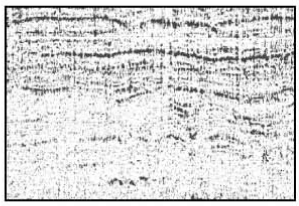
Fs10	Average continuity, high amplitude, average frequency, sub-parallel to chaotic configuration	Terrestrial to shallow marine sands with possible channels and gas	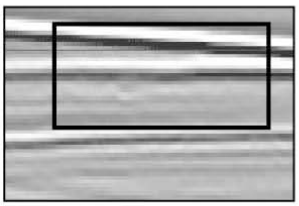	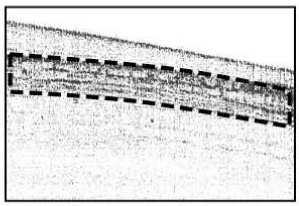
Fs11	Average to good continuity, high amplitude and frequency, undulating and parallel configuration	Well-bedded marine silty to sandy clays forming an extensive field of sediment waves	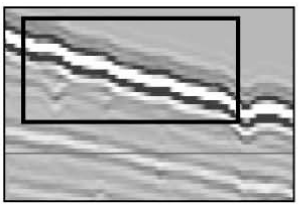	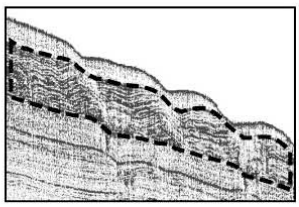

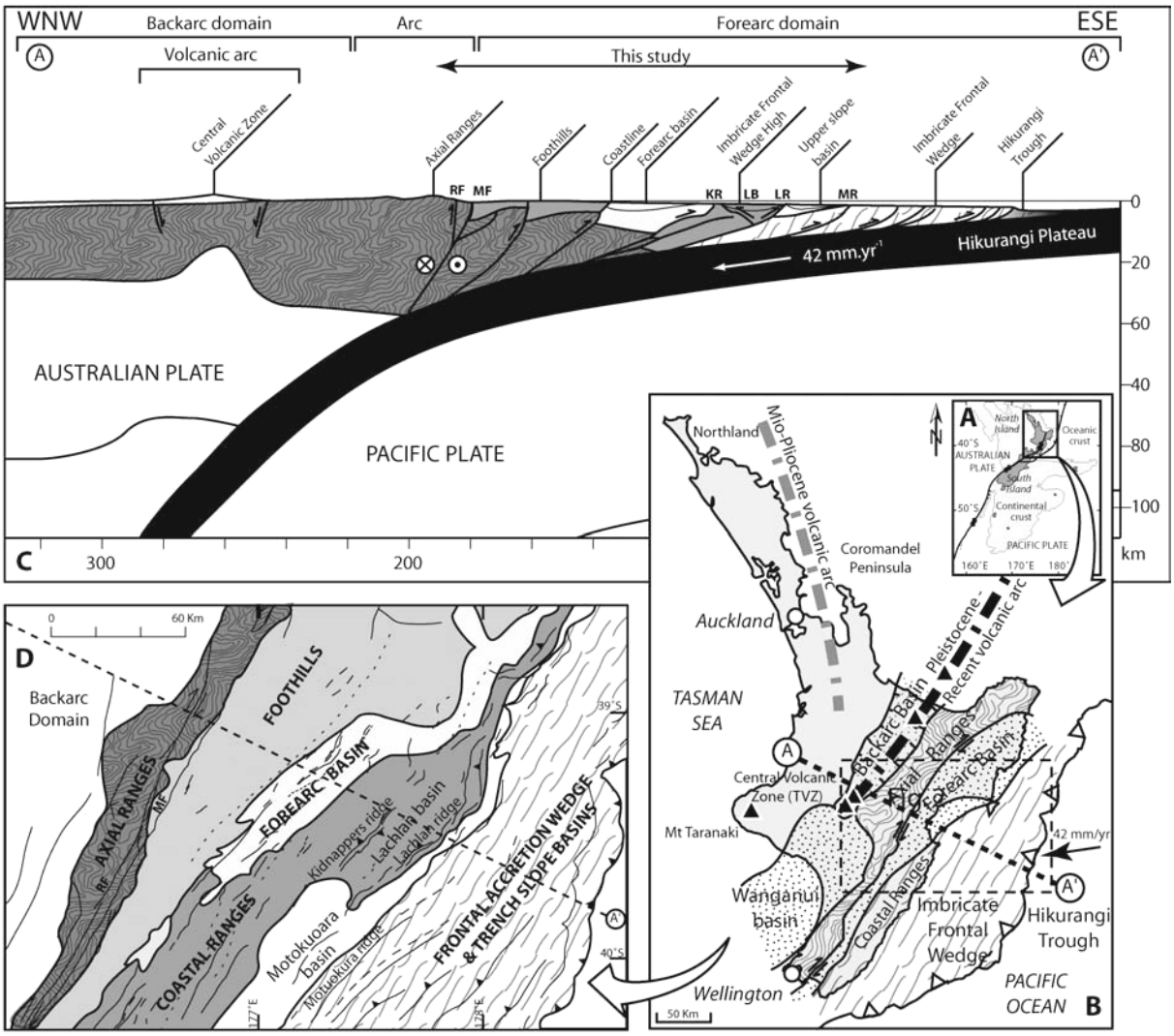
WNW
Backarc domain
Arc
Forearc domain
ESE
Volcanic arc
This study
Central Volcanic Zone
Axial Ranges
Foothills
Coastline
Forearc basin
Imbricate Frontal Wedge High
Upper slope basin
Imbricate Frontal Wedge
Hikurangi Trough
RF MF
KR LB LR MR
42 mm.yr-1
Hikurangi Plateau
AUSTRALIAN PLATE
PACIFIC PLATE
C
300
200
km
0
20
60
40
80
100
Northland
Mio-Pliocene volcanic arc
Coromandel Peninsula
Auckland
Pleistocene-Recent volcanic arc
TASMAN SEA
Backarc Basin
Axial Ranges
Forearc basin
Central Volcanic Zone (TVZ)
Mt Taranaki
42 mm/yr
Wanganui basin
Coastal Ranges
Imbricate Frontal Wedge
Hikurangi Trough
Wellington
PACIFIC OCEAN
B
50 Km
A
North Island
Oceanic crust
40°S
AUSTRALIAN PLATE
South Island
Continental crust
50°S
PACIFIC PLATE
160°E
170°E
180°
D
0
60 Km
Backarc Domain
FOOTHILLS
AXIAL RANGES
RF
MF
EOBEARC BASIN
Kidnappers ridge
Lachlan basin
Lachlan ridge
FRONTAL ACCRETION WEDGE & TRENCH SLOPE BASINS
COASTAL RANGES
Motokuoara basin
Motuokura ridge
39°S
40°S
175°E
176°E

Figure 1.

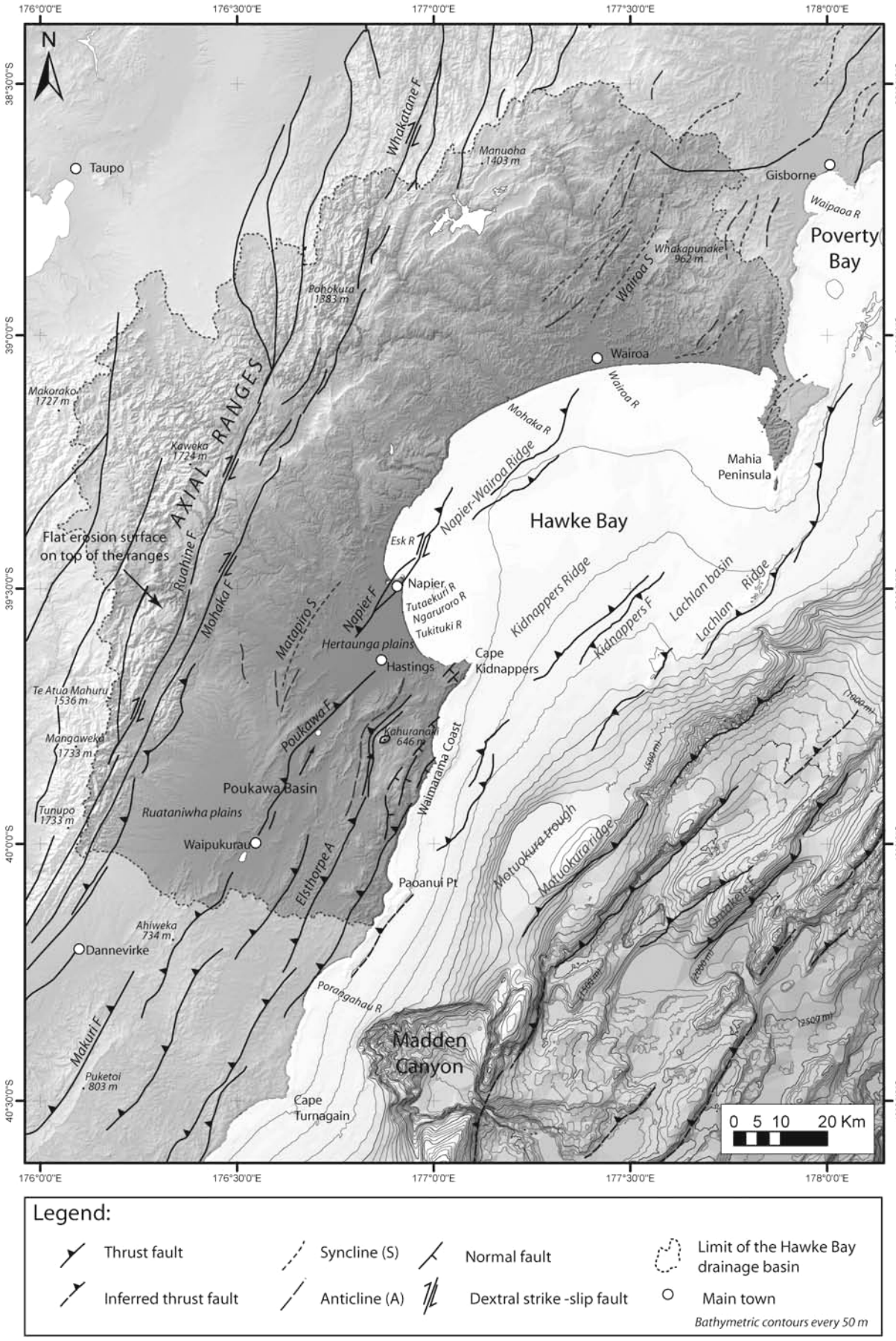
176°0'0"E
176°30'0"E
177°0'0"E
177°30'0"E
178°0'0"E
38°30'0"S
39°0'0"S
39°30'0"S
40°0'0"S
40°30'0"S
N
Taupo
Gisborne
Poverty Bay
Waipaoa R
Whakapunake 962 m
Manuoha 1403 m
Whakatane F
Waioa S
Pohokura 1883 m
Wairoa
Wairoa R
Makorako 1727 m
Kaweka 1724 m
AXIAL RANGES
Flat erosion surface on top of the ranges
Ruahine F
Mohaka F
Mohaka R
Napier-Wairoa Ridge
Mahia Peninsula
Hawke Bay
Esk R
Napier
Tutaekuri R
Ngaruroro R
Tukituki R
Napier F
Matapiro S
Hertaunga plains
Hastings
Kidnappers Ridge
Kidnappers F
Lachlan basin
Lachlan Ridge
Cape Kidnappers
Te Atua Mahuru 1536 m
Mangaweka 1733 m
Tunupo 1733 m
Poukawa F
Kahuranaki 646 m
Waimarama Coast
Poukawa Basin
Ruataniwha plains
Waipukurau
Elsthorpe A
Paoanui Pt
Motuokura trough
Motuokura ridge
Ahiweka 734 m
Dannevirke
Porangahau R
Makuri F
Puketoi 803 m
Madden Canyon
Cape Turnagain
0 5 10 20 Km
Legend:
Thrust fault
Inferred thrust fault
Syncline (S)
Anticline (A)
Normal fault
Dextral strike -slip fault
Limit of the Hawke Bay drainage basin
Main town
Bathymetric contours every 50 m

Figure 2.

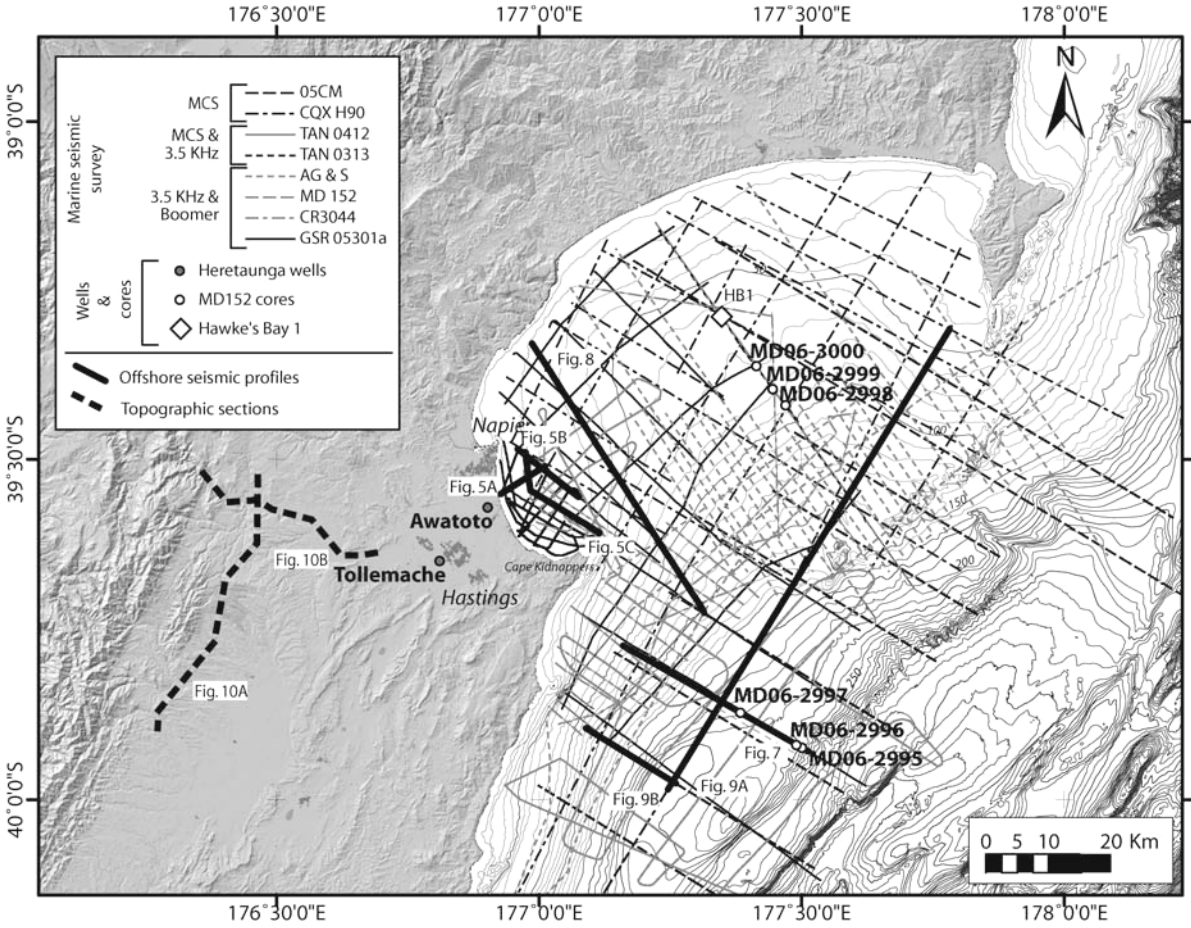
176°30'0"E
177°0'0"E
177°30'0"E
178°0'0"E
39°0'0"S
39°30'0"S
40°0'0"S
N
Marine seismic survey
MCS
05CM
CQX H90
MCS & 3.5 KHz
TAN 0412
TAN 0313
3.5 KHz & Boomer
AG & S
MD 152
CR3044
GSR 05301a
Wells & cores
Heretaunga wells
MD152 cores
Hawke's Bay 1
Offshore seismic profiles
Topographic sections
HB1
Fig. 8
MD06-3000
MD06-2999
MD06-2998
Napier
Fig. 5B
Fig. 5A
Awatoto
Fig. 5C
Cape Kidnappers
Fig. 10B
Tollemache
Hastings
Fig. 10A
MD06-2997
MD06-2996
MD06-2995
Fig. 7
Fig. 9A
Fig. 9B
100
150
200
250
0 5 10 20 Km

Figure 3.

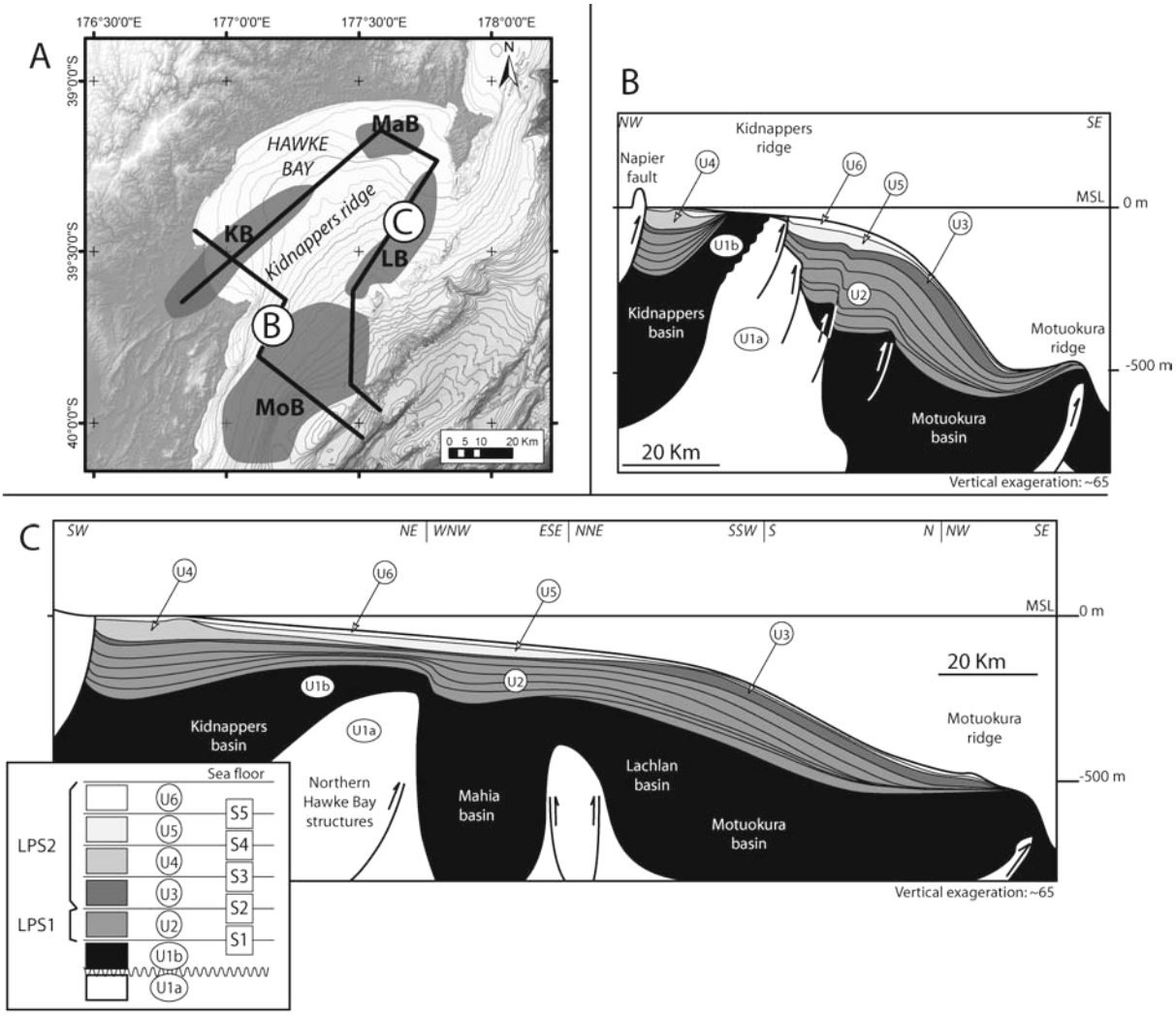
A
176°30'0"E
177°0'0"E
177°30'0"E
178°0'0"E
39°0'0"S
39°30'0"S
40°0'0"S
N
HAWKE BAY
MaB
KB
Kidnappers ridge
C
LB
B
MoB
0 5 10 20 Km
B
NW
SE
Kidnappers ridge
Napier fault
U4
U6
U5
MSL
0 m
U3
U1b
U2
Kidnappers basin
U1a
Motuokura ridge
-500 m
Motuokura basin
20 Km
Vertical exageration: ~65
C
SW
NE
WNW
ESE
NNE
SSW
S
N
NW
SE
U4
U6
U5
MSL
0 m
U3
20 Km
U1b
U2
Kidnappers basin
U1a
Motuokura ridge
Lachlan basin
-500 m
Northern Hawke Bay structures
Mahia basin
Motuokura basin
Vertical exageration: ~65
Sea floor
U6
U5
U4
U3
U2
U1b
U1a
S5
S4
S3
S2
S1
LPS2
LPS1

Figure 4.

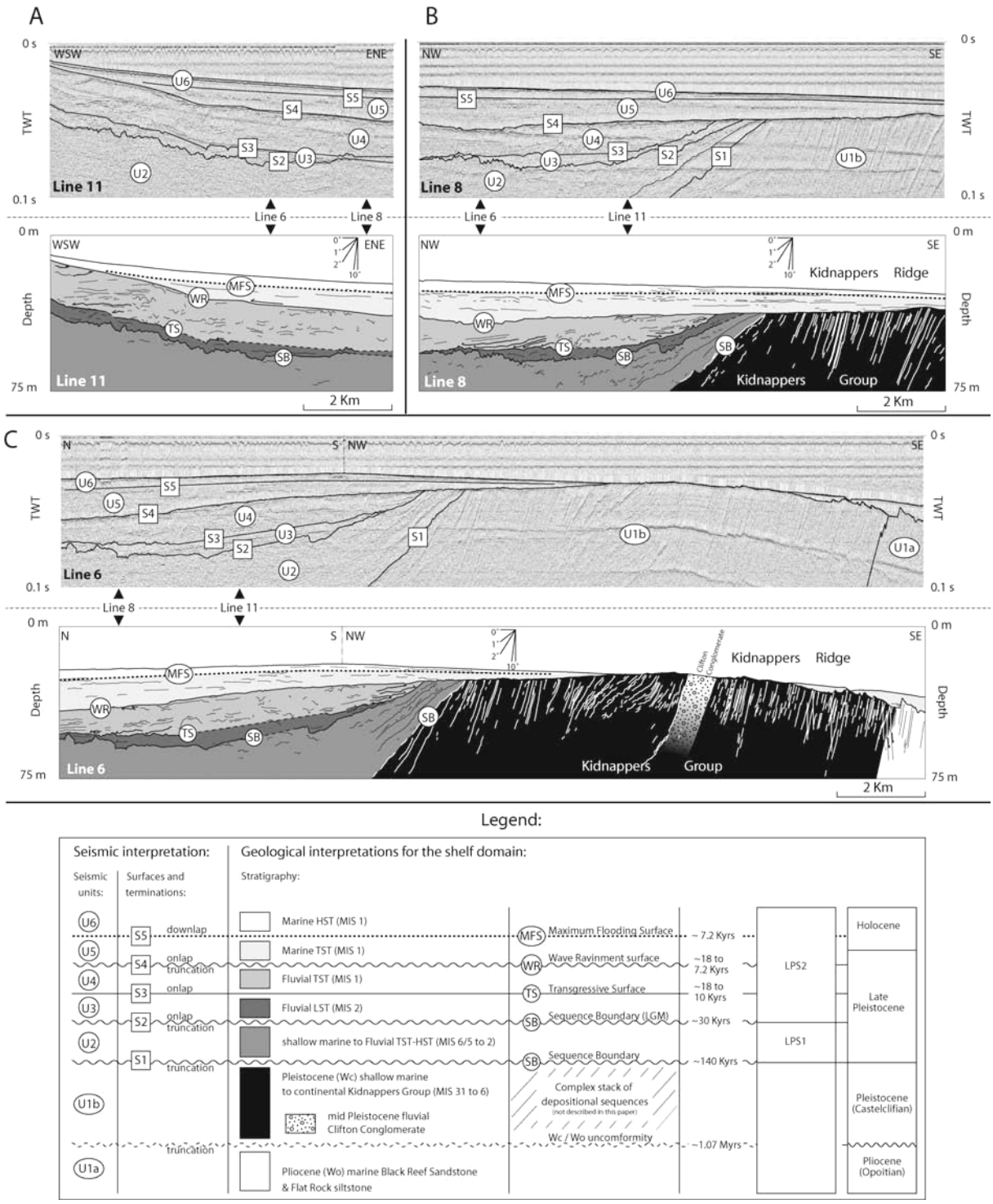
A
B
C
Line 11
Line 8
Line 6
WSW
ENE
NW
SE
N
S
TWT
Depth
0 s
0.1 s
0 m
75 m
2 Km
U1a
U1b
U2
U3
U4
U5
U6
S1
S2
S3
S4
S5
MFS
WR
TS
SB
Kidnappers
Ridge
Group
Clifton Conglomerate
Legend:
Seismic interpretation:
Geological interpretations for the shelf domain:
Seismic units:
Surfaces and terminations:
Stratigraphy:
downlap
onlap
truncation
Marine HST (MIS 1)
Marine TST (MIS 1)
Fluvial TST (MIS 1)
Fluvial LST (MIS 2)
shallow marine to Fluvial TST-HST (MIS 6/5 to 2)
Pleistocene (Wc) shallow marine to continental Kidnappers Group (MIS 31 to 6)
mid Pleistocene fluvial Clifton Conglomerate
Pliocene (Wo) marine Black Reef Sandstone & Flat Rock siltstone
Maximum Flooding Surface
Wave Ravinment surface
Transgressive Surface
Sequence Boundary (LGM)
Sequence Boundary
Complex stack of depositional sequences
(not described in this paper)
Wc / Wo uncomformity
~ 7.2 Kyrs
~18 to 7.2 Kyrs
~18 to 10 Kyrs
~30 Kyrs
~140 Kyrs
~1.07 Myrs
LPS2
LPS1
Holocene
Late Pleistocene
Pleistocene (Castelclifian)
Pliocene (Opoitian)

Figure 5.

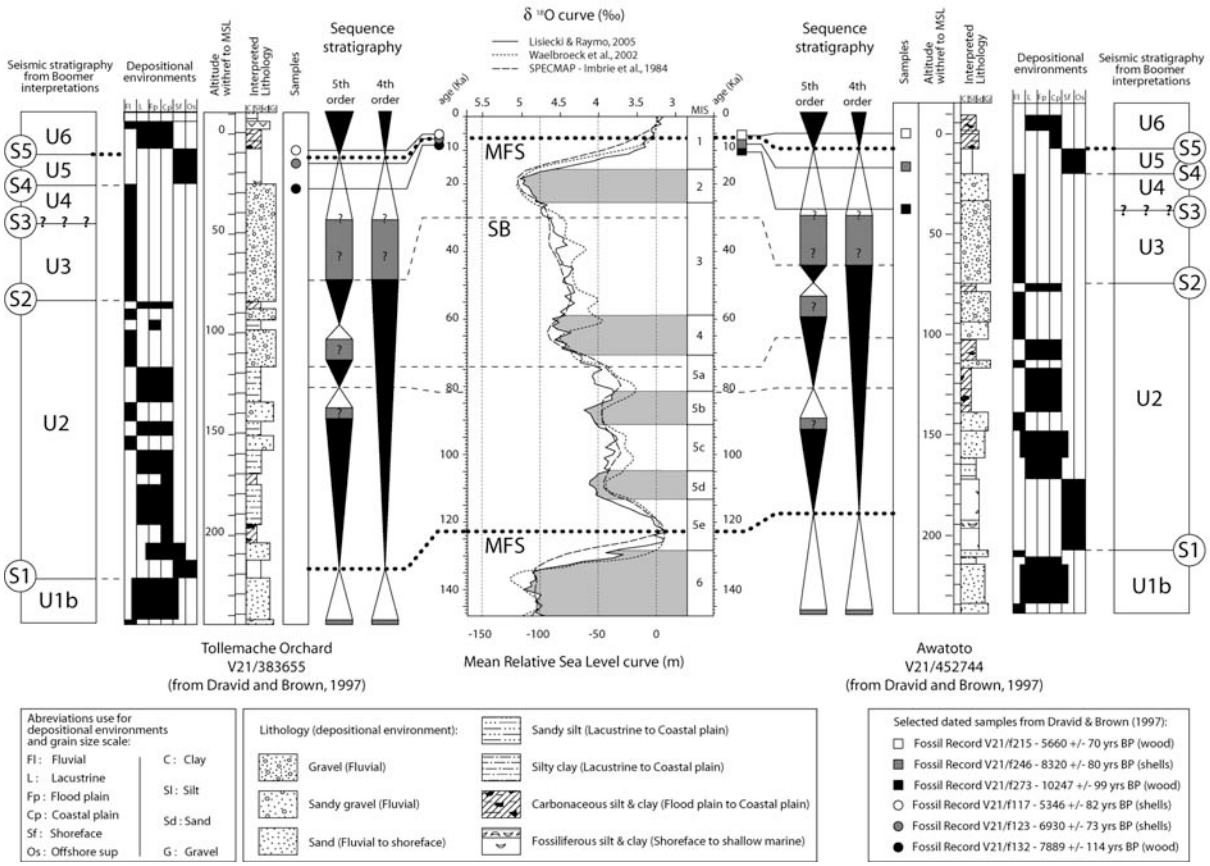
Seismic stratigraphy from Boomer interpretations
Depositional environments
Altitude withref to MSL
Interpreted Lithology
Samples
Sequence stratigraphy
5th order
4th order
δ 18O curve (‰)
Lisiecki & Raymo, 2005
Waelbroeck et al., 2002
SPECMAP - Imbrie et al., 1984
age (Ka)
MIS
MFS
SB
MFS
U6
U5
U4
U3
U2
U1b
S5
S4
S3
S2
S1
Tollemache Orchard
V21/383655
(from Dravid and Brown, 1997)
Mean Relative Sea Level curve (m)
Awatoto
V21/452744
(from Dravid and Brown, 1997)
Abreviations use for depositional environments and grain size scale:
Fl : Fluvial
L : Lacustrine
Fp : Flood plain
Cp : Coastal plain
Sf : Shoreface
Os : Offshore sup
C : Clay
Sl : Silt
Sd : Sand
G : Gravel
Lithology (depositional environment):
Gravel (Fluvial)
Sandy gravel (Fluvial)
Sand (Fluvial to shoreface)
Sandy silt (Lacustrine to Coastal plain)
Silty clay (Lacustrine to Coastal plain)
Carbonaceous silt & clay (Flood plain to Coastal plain)
Fossiliferous silt & clay (Shoreface to shallow marine)
Selected dated samples from Dravid & Brown (1997):
Fossil Record V21/f215 - 5660 +/- 70 yrs BP (wood)
Fossil Record V21/f246 - 8320 +/- 80 yrs BP (shells)
Fossil Record V21/f273 - 10247 +/- 99 yrs BP (wood)
Fossil Record V21/f117 - 5346 +/- 82 yrs BP (shells)
Fossil Record V21/f123 - 6930 +/- 73 yrs BP (shells)
Fossil Record V21/f132 - 7889 +/- 114 yrs BP (wood)

Figure 6.

MD152 - 3.5 KHz profile
NW
SE
5 Km
0°
1°
2°
10°
100 m
200 m
300 m
400 m
500 m
Fs10
Fs11
Fs 9
gaz
S1 projected from 05CM#29
MD06-2997
MD06-2996
0.5 to 0.6 Ma
S1
S2
S4
S5
U1ab
U2
U3
U5
U6
Caption
Seismic interpretation:
Seismic units:
Surfaces and terminations:
Geological interpretation:
Stratigraphy:
Marine HST (MIS 1)
Marine TST (MIS 1)
Marine LST (MIS2)
Marine TST/HST (MIS6 to 3)
Plio-Pleistocene substratum
Maximum Flooding Surface
Wave Ravinement / Transgressive surface
Sequence Boundary (LGM)
Sequence Boundary (LGM)
~ 7.2 Kyrs
~18 Kyrs
~30 Kyrs
~140 Kyrs
onlap
concordant
truncation/ concordant
onlap
truncation/ concordant
onlap
truncation/ concordant
Holocene
Late Pleistocene
Plio-Pleistocene
LPS2
LPS1

Figure 7.

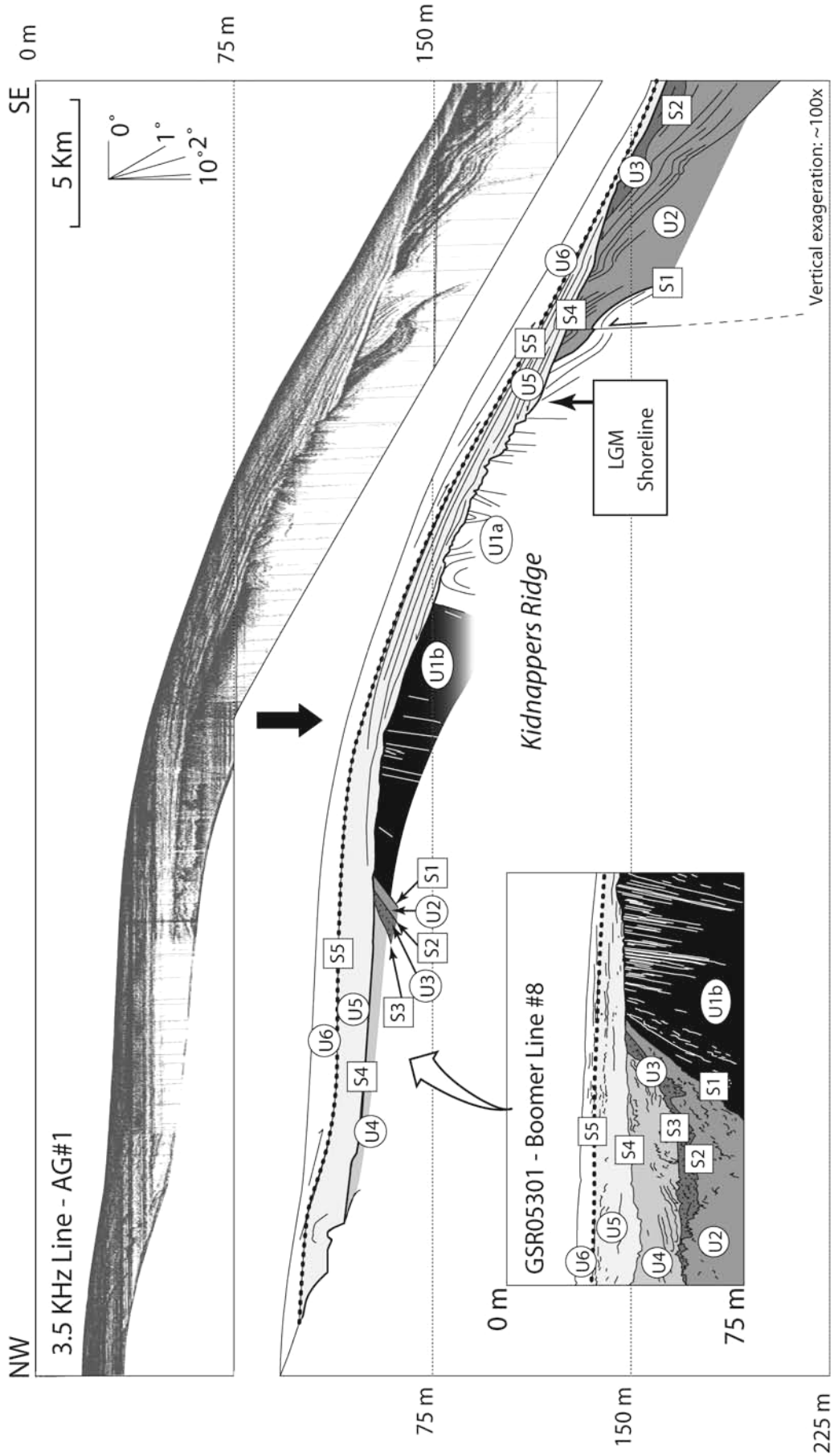
SE
NW
0 m
75 m
150 m
225 m
5 Km
0°
1°
2°
10°
3.5 KHz Line - AG#1
Vertical exageration: ~100x
LGM
Shoreline
Kidnappers Ridge
GSR05301 - Boomer Line #8
U1a
U1b
U2
U3
U4
U5
U6
S1
S2
S3
S4
S5

Figure 8.

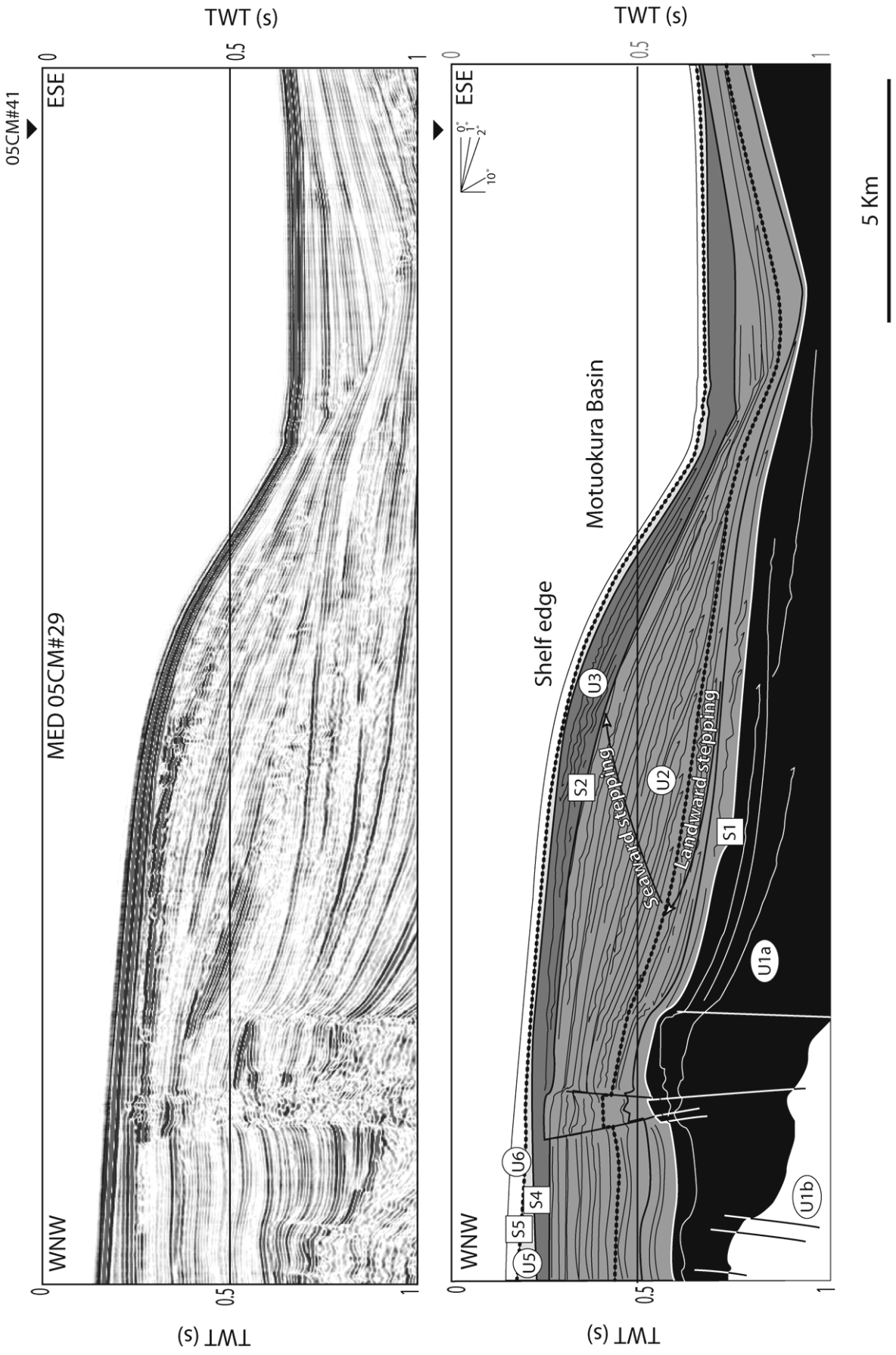
TWT (s)
0
0.5
1
05CM#41
ESE
MED 05CM#29
WNW
TWT (s)
0
0.5
1
ESE
0°
1°
2°
10°
Shelf edge
Motuokura Basin
U3
S2
U2
S1
U1a
U1b
U6
S4
S5
U5
Seaward stepping
Landward stepping
WNW
TWT (s)
0
0.5
1
5 Km

Figure 9a.

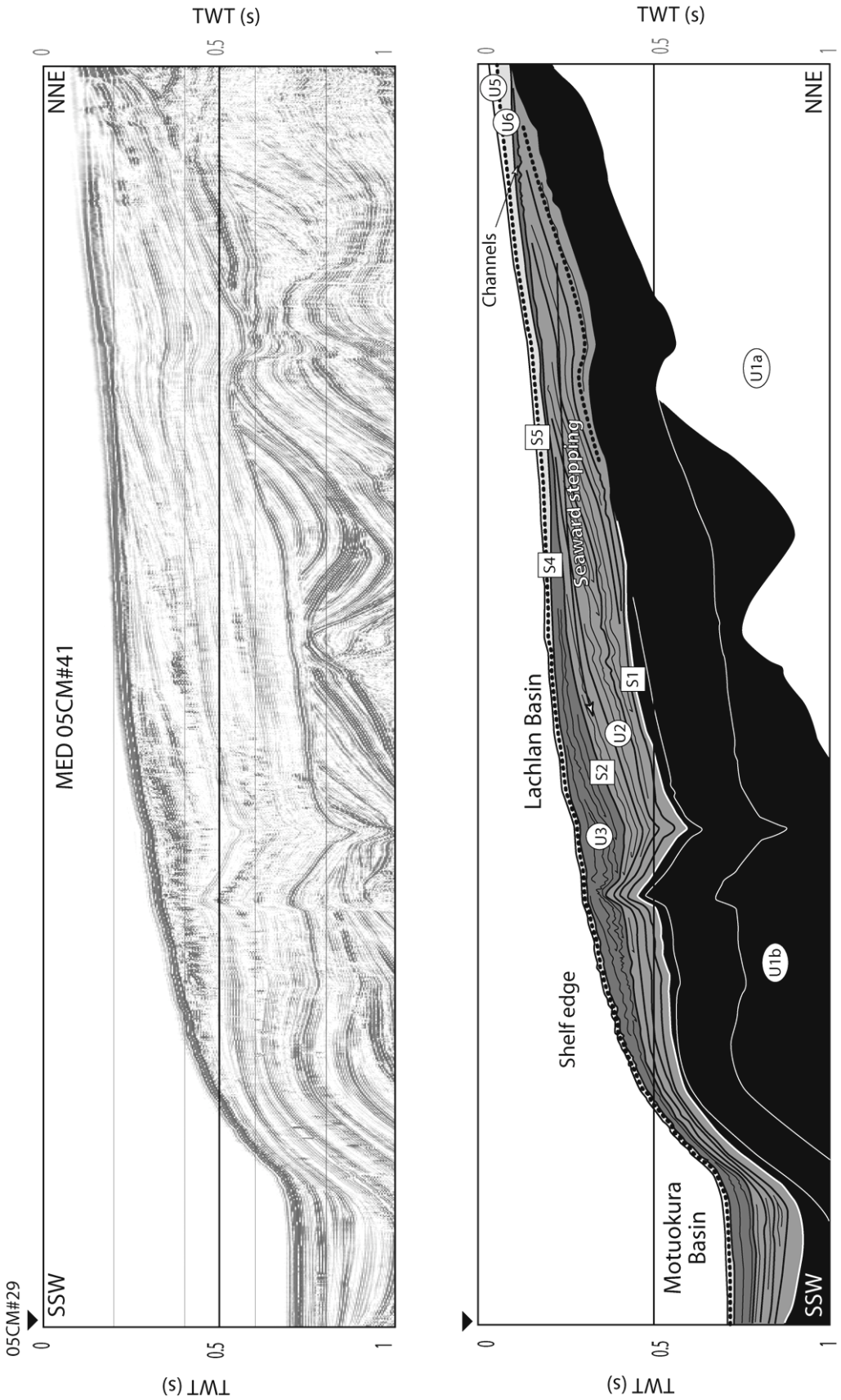
TWT (s)
0
0.5
1
NNE
SSW
MED 05CM#41
05CM#29
TWT (s)
0
0.5
1
NNE
SSW
Channels
U5
U6
S5
S4
S1
S2
U2
U3
U1a
U1b
Seaward stepping
Lachlan Basin
Shelf edge
Motuokura Basin
TWT (s)
0
0.5
1

Figure 9b.

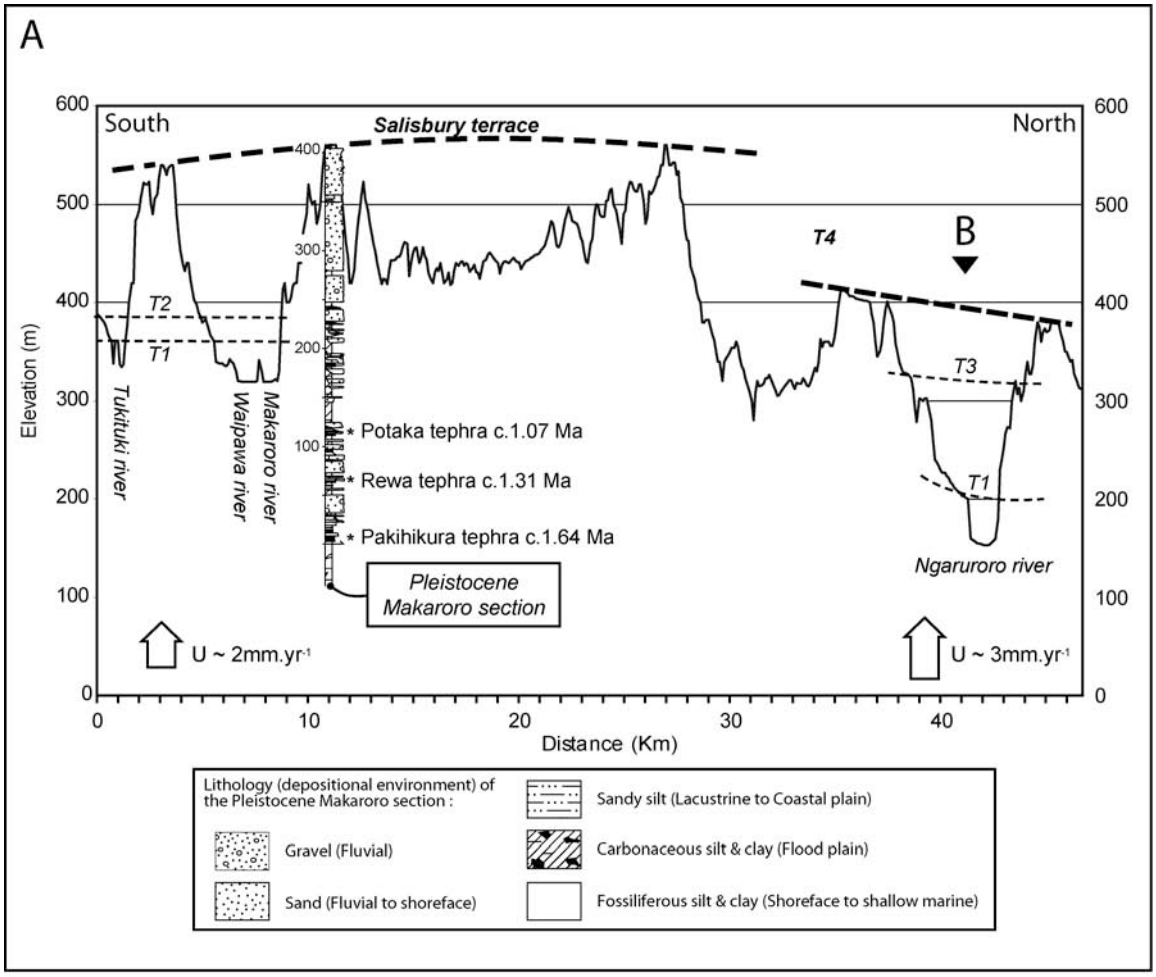
A
South
Salisbury terrace
North
T4
B
T2
T1
T3
T1
Tukituki river
Waipawa river
Makaroro river
Ngaruroro river
* Potaka tephra c.1.07 Ma
* Rewa tephra c.1.31 Ma
* Pakihikura tephra c.1.64 Ma
Pleistocene
Makaroro section
U ~ 2mm.yr-1
U ~ 3mm.yr-1
Elevation (m)
Distance (Km)
Lithology (depositional environment) of the Pleistocene Makaroro section :
Gravel (Fluvial)
Sand (Fluvial to shoreface)
Sandy silt (Lacustrine to Coastal plain)
Carbonaceous silt & clay (Flood plain)
Fossiliferous silt & clay (Shoreface to shallow marine)

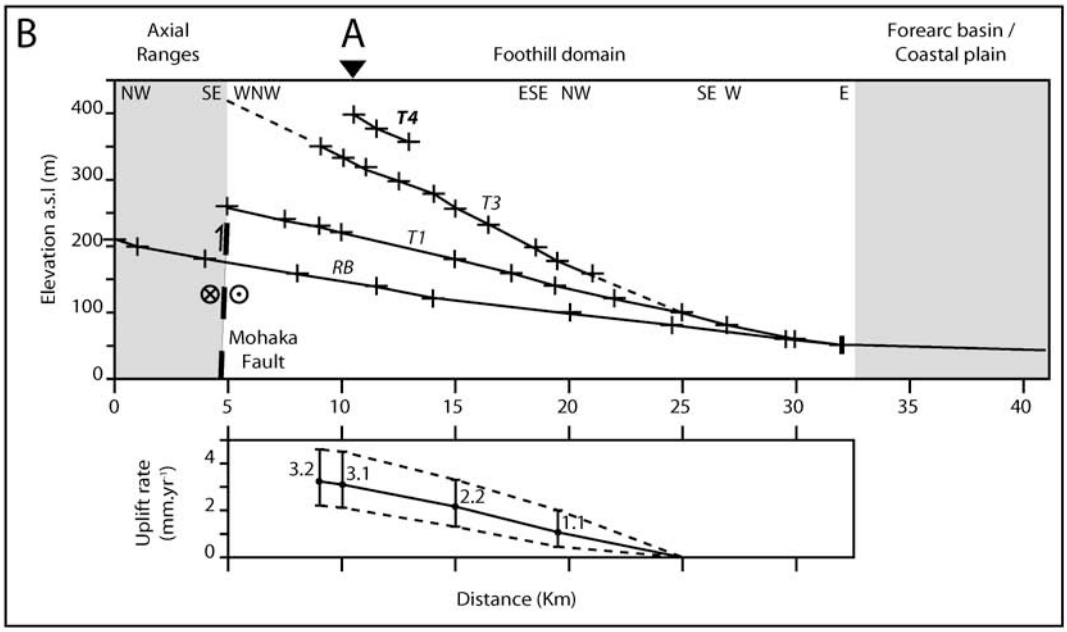
B
Axial
Ranges
A
Foothill domain
Forearc basin /
Coastal plain
NW
SE
WNW
ESE
NW
SE
W
E
T4
T3
T1
RB
Mohaka
Fault
Elevation a.s.l (m)
Uplift rate
(mm.yr-1)
3.2
3.1
2.2
1.1
Distance (Km)

Figure 10.

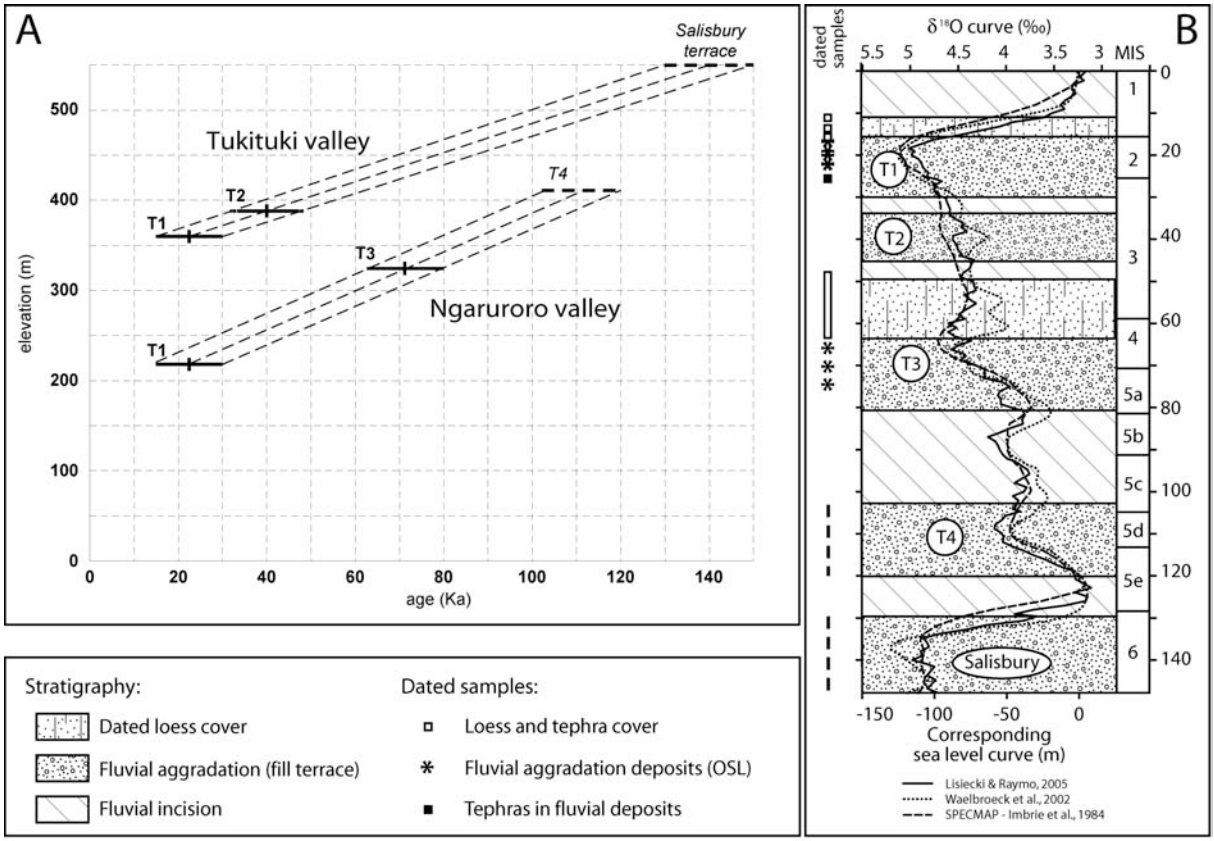
A
Salisbury terrace
Tukituki valley
T1
T2
T3
T4
Ngaruroro valley
elevation (m)
age (Ka)
B
dated samples
δ18O curve (‰)
MIS
Corresponding sea level curve (m)
Lisiecki & Raymo, 2005
Waelbroeck et al., 2002
SPECMAP - Imbrie et al., 1984
Salisbury
Stratigraphy:
Dated loess cover
Fluvial aggradation (fill terrace)
Fluvial incision
Dated samples:
Loess and tephra cover
Fluvial aggradation deposits (OSL)
Tephras in fluvial deposits

Figure 11.

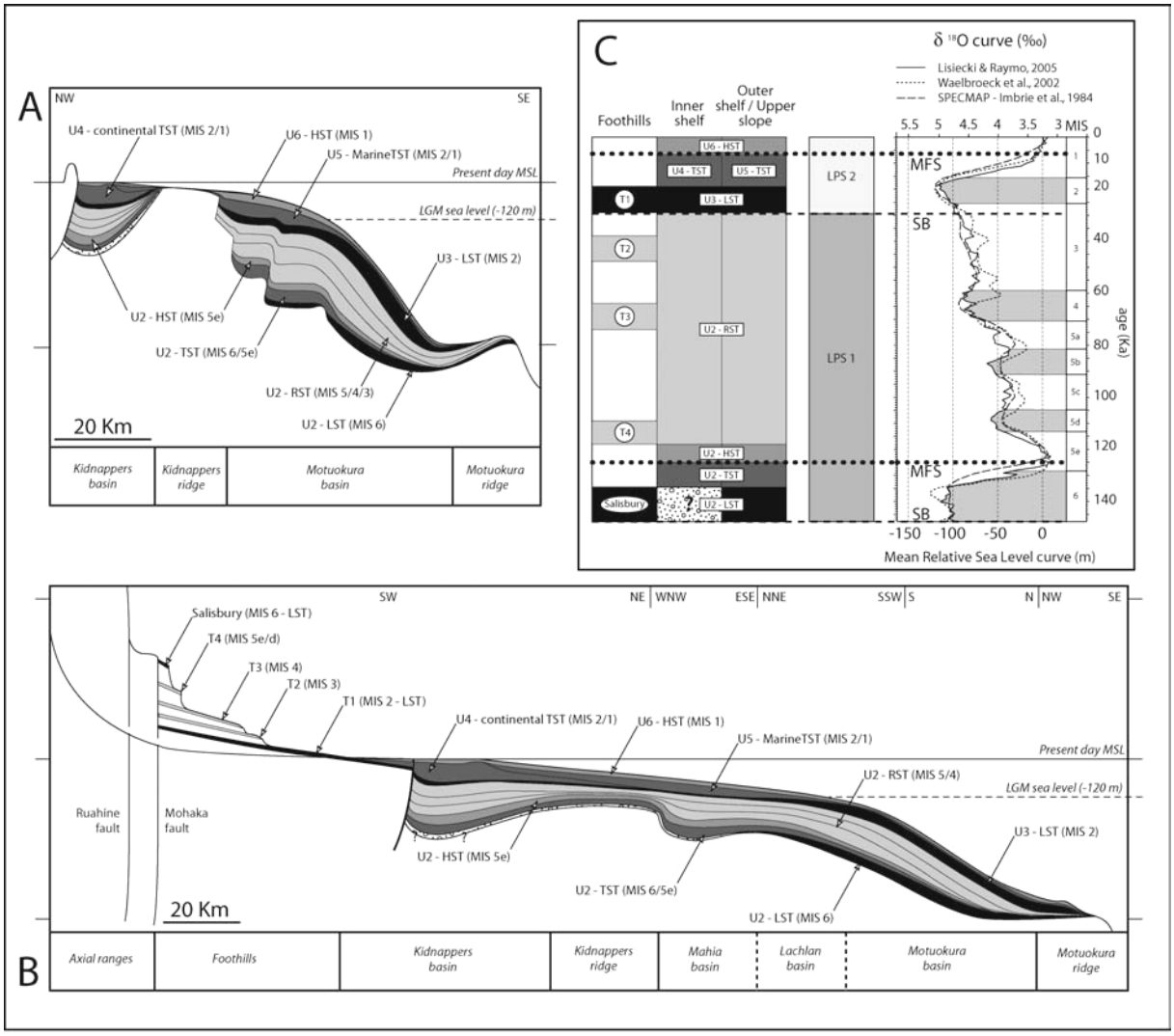
A
NW
SE
U4 - continental TST (MIS 2/1)
U6 - HST (MIS 1)
U5 - MarineTST (MIS 2/1)
Present day MSL
LGM sea level (-120 m)
U3 - LST (MIS 2)
U2 - HST (MIS 5e)
U2 - TST (MIS 6/5e)
U2 - RST (MIS 5/4/3)
U2 - LST (MIS 6)
20 Km
Kidnappers basin
Kidnappers ridge
Motuokura basin
Motuokura ridge
C
δ 18O curve (‰)
Lisiecki & Raymo, 2005
Waelbroeck et al., 2002
SPECMAP - Imbrie et al., 1984
Foothills
Inner shelf
Outer shelf / Upper slope
U6 - HST
U4 - TST
U5 - TST
U3 - LST
U2 - RST
U2 - HST
U2 - TST
U2 - LST
T1
T2
T3
T4
Salisbury
LPS 2
LPS 1
MFS
SB
MFS
SB
5.5 5 4.5 4 3.5 3 MIS
0 10 20 40 60 80 100 120 140
age (Ka)
-150 -100 -50 0
Mean Relative Sea Level curve (m)
B
SW
NE
WNW
ESE
NNE
SSW
S
N
NW
SE
Salisbury (MIS 6 - LST)
T4 (MIS 5e/d)
T3 (MIS 4)
T2 (MIS 3)
T1 (MIS 2 - LST)
U4 - continental TST (MIS 2/1)
U6 - HST (MIS 1)
U5 - MarineTST (MIS 2/1)
Present day MSL
U2 - RST (MIS 5/4)
LGM sea level (-120 m)
Ruahine fault
Mohaka fault
U3 - LST (MIS 2)
U2 - HST (MIS 5e)
U2 - TST (MIS 6/5e)
U2 - LST (MIS 6)
20 Km
Axial ranges
Foothills
Kidnappers basin
Kidnappers ridge
Mahia basin
Lachlan basin
Motuokura basin
Motuokura ridge

Figure 12.

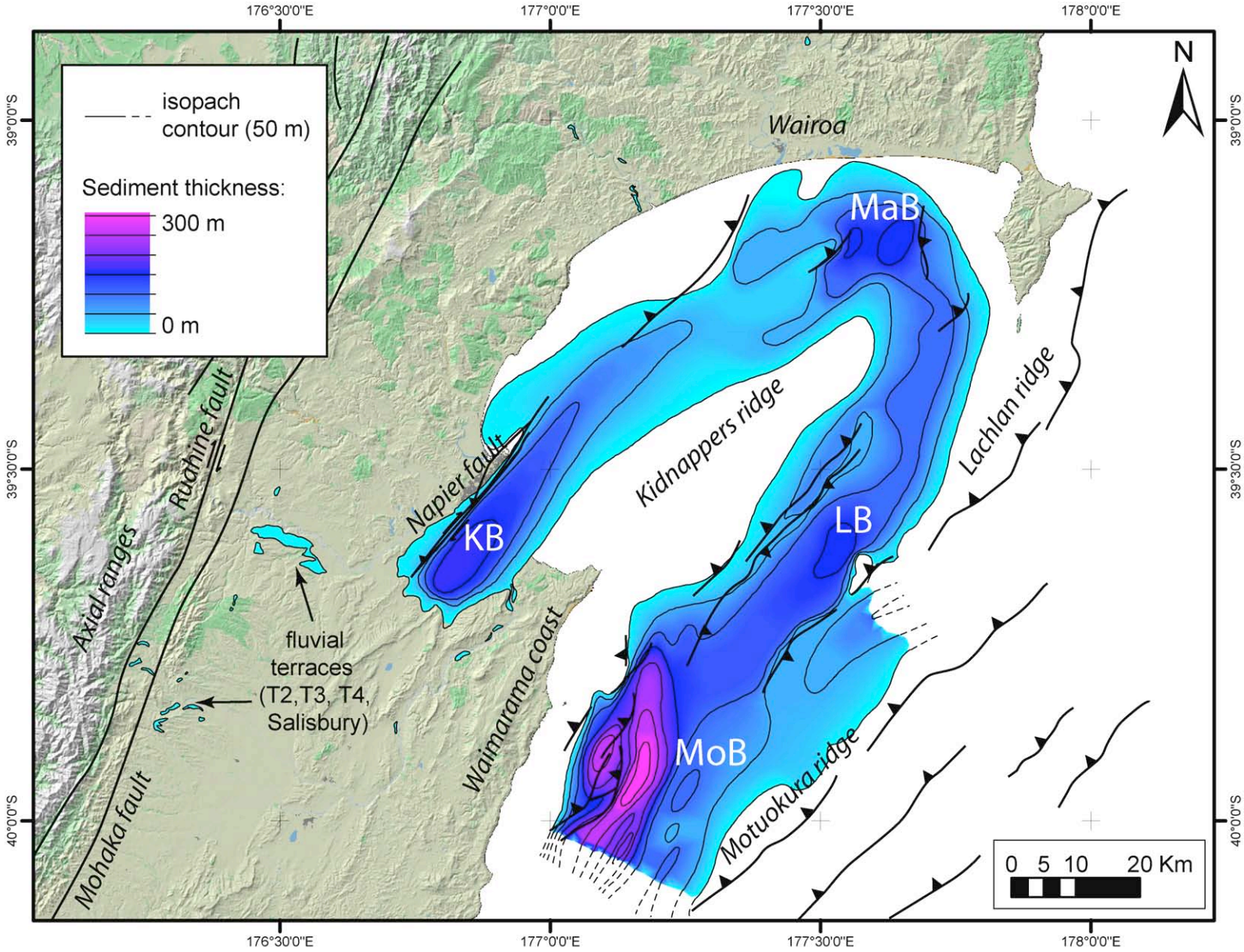
176°30'0"E
177°0'0"E
177°30'0"E
178°0'0"E
39°0'0"S
39°30'0"S
40°0'0"S
N
isopach
contour (50 m)
Sediment thickness:
300 m
0 m
Wairoa
MaB
LB
KB
MoB
Kidnappers ridge
Lachlan ridge
Napier fault
Ruahine fault
Axial ranges
Mohaka fault
Waimarama coast
fluvial
terraces
(T2,T3, T4,
Salisbury)
Motuoku ridge
0 5 10 20 Km

Figure 13.

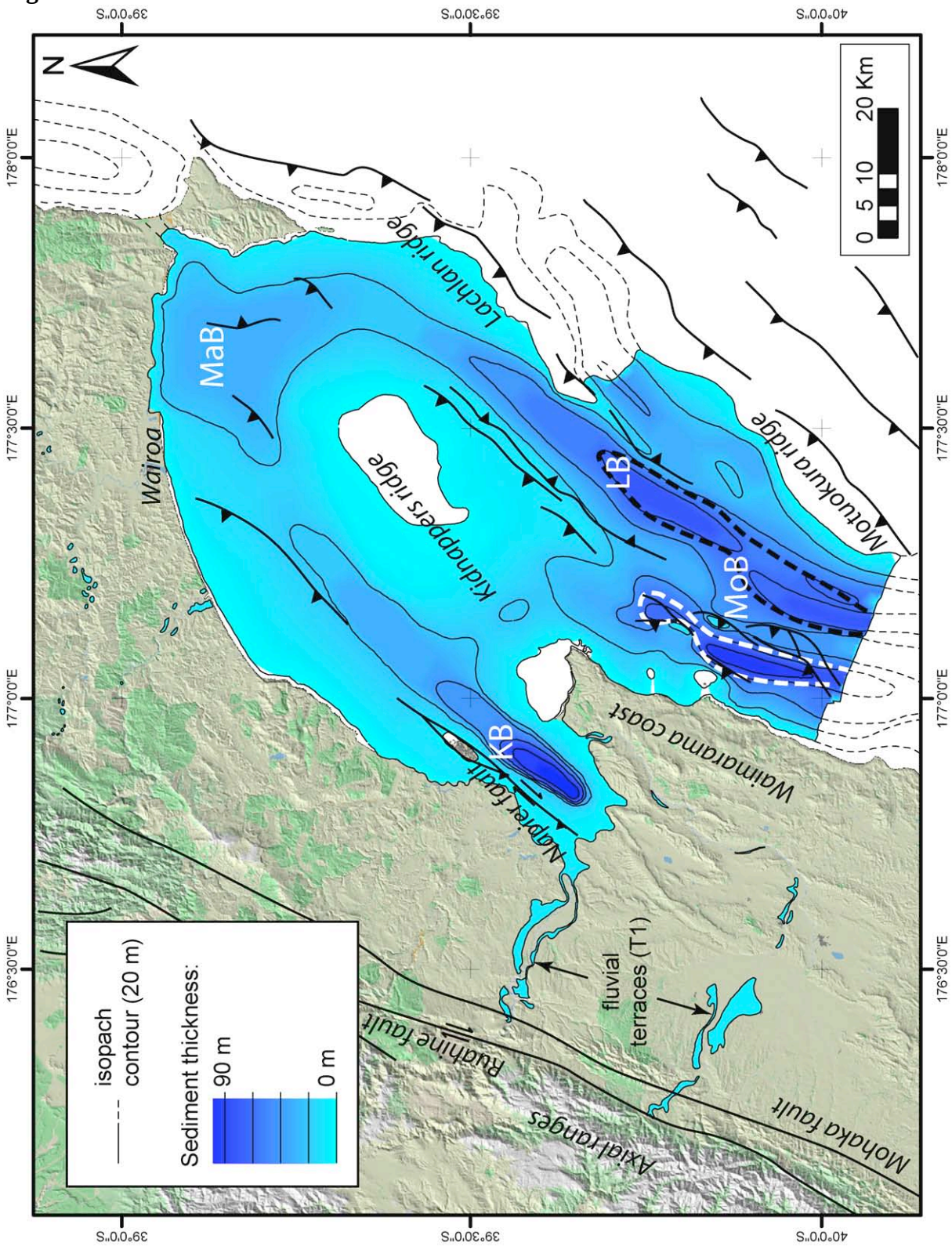
N
0 5 10 20 Km
Lachlan ridge
MaB
Wairoa
Kidnappers ridge
LB
Mottokura ridge
MoB
KB
Napier fault
Waimarama coast
fluvial terraces (T1)
Ruahine fault
Axial ranges
Mohaka fault
isopach contour (20 m)
Sediment thickness:
90 m
0 m
178°0'0"E
177°30'0"E
177°0'0"E
176°30'0"E
39°0'0"S
39°30'0"S
40°0'0"S

Figure 14.

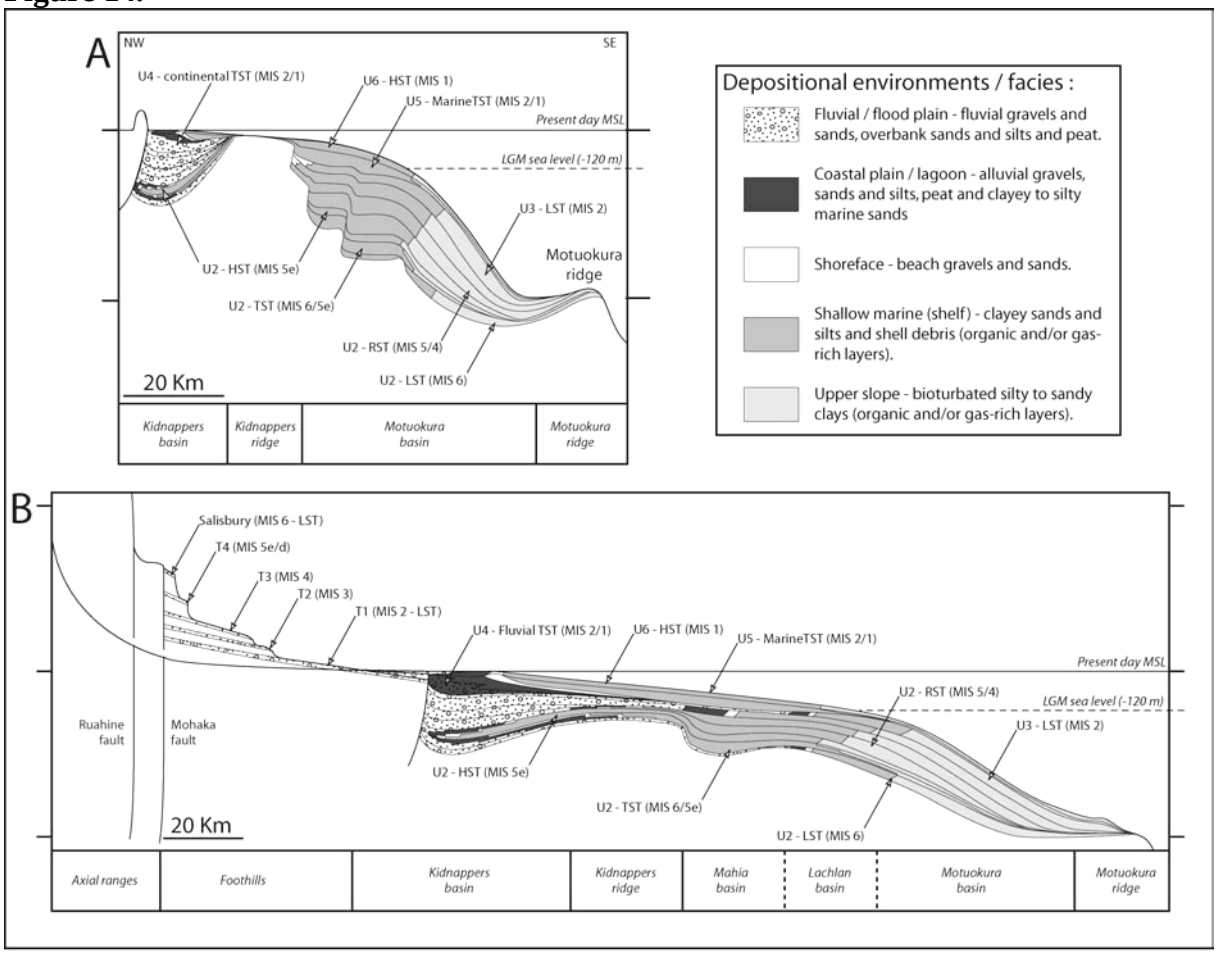
A
NW
SE
U4 - continental TST (MIS 2/1)
U6 - HST (MIS 1)
U5 - MarineTST (MIS 2/1)
Present day MSL
LGM sea level (-120 m)
U3 - LST (MIS 2)
Motuokura ridge
U2 - HST (MIS 5e)
U2 - TST (MIS 6/5e)
U2 - RST (MIS 5/4)
U2 - LST (MIS 6)
20 Km
Kidnappers basin
Kidnappers ridge
Motuokura basin
Motuokura ridge
Depositional environments / facies :
Fluvial / flood plain - fluvial gravels and sands, overbank sands and silts and peat.
Coastal plain / lagoon - alluvial gravels, sands and silts, peat and clayey to silty marine sands
Shoreface - beach gravels and sands.
Shallow marine (shelf) - clayey sands and silts and shell debris (organic and/or gas-rich layers).
Upper slope - bioturbated silty to sandy clays (organic and/or gas-rich layers).
B
Salisbury (MIS 6 - LST)
T4 (MIS 5e/d)
T3 (MIS 4)
T2 (MIS 3)
T1 (MIS 2 - LST)
U4 - Fluvial TST (MIS 2/1)
U6 - HST (MIS 1)
U5 - MarineTST (MIS 2/1)
Present day MSL
U2 - RST (MIS 5/4)
LGM sea level (-120 m)
U3 - LST (MIS 2)
Ruahine fault
Mohaka fault
U2 - HST (MIS 5e)
U2 - TST (MIS 6/5e)
U2 - LST (MIS 6)
20 Km
Axial ranges
Foothills
Kidnappers basin
Kidnappers ridge
Mahia basin
Lachlan basin
Motuokura basin
Motuokura ridge

Figure 15.

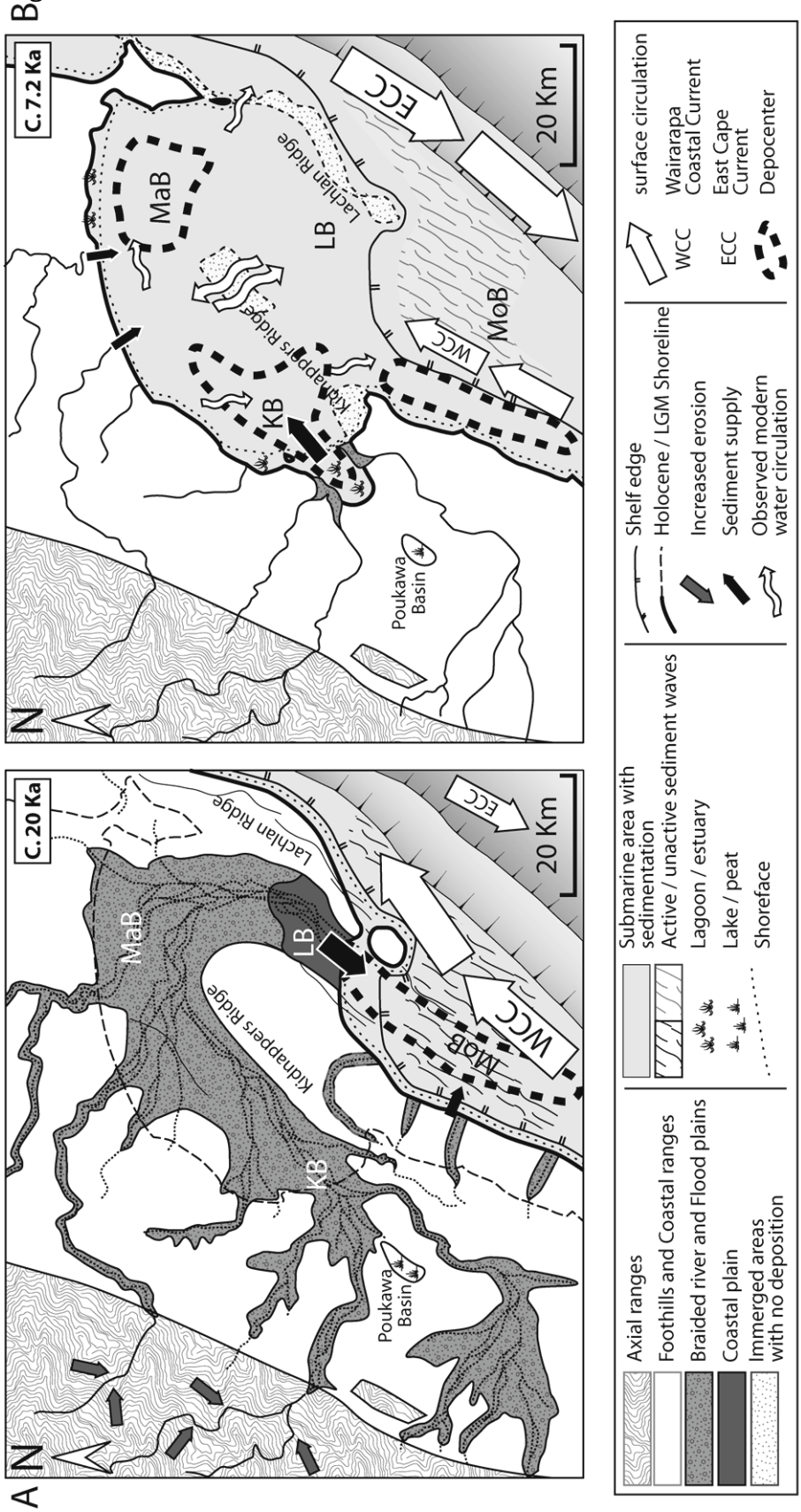
A
B
N
C.20 Ka
C.7.2 Ka
MaB
LB
KB
WCC
ECC
MøB
Lachlan Ridge
Kidnappers Ridge
Poukawa Basin
20 Km
Axial ranges
Foothills and Coastal ranges
Braided river and Flood plains
Coastal plain
Immerged areas with no deposition
Submarine area with sedimentation
Active / unactive sediment waves
Lagoon / estuary
Lake / peat
Shoreface
Shelf edge
Holocene / LGM Shoreline
Increased erosion
Sediment supply
Observed modern water circulation
surface circulation
Wairarapa Coastal Current
East Cape Current
Depocenter

Figure 16.

Chapitre 5 :

Les paramètres de contrôles de la stratigraphie et des flux sédimentaires dans les bassins avant arc :

l'exemple du bassin avant arc Pléistocène de Hawke Bay, Nouvelle Zélande.

CONTROLS ON ACTIVE FOREARC BASIN STRATIGRAPHY AND SEDIMENT FLUXES: The example of the Pleistocene Hawke Bay forearc basin, New Zealand.

Fabien PAQUET (1), Jean-Noel PROUST (1), Phil BARNES (2), Jarg PETTINGA (3)

(1) UMR Geosciences, CNRS Université de Rennes 1, Campus de Beaulieu, 35042 Rennes cedex
(2) National Institute of Water and Atmospheric Research (NIWA) Ltd, Private Bag 14-901, 301 Evans Bay Parade, Greta Point, Wellington, New Zealand
(3) Department of Geological Sciences, University of Canterbury, Private Bag 4800, Christchurch, New Zealand

Corresponding author:
Fabien Paquet
email fabien.paquet@univ-rennes1.fr;
Ph. 00 33 2 23 23 57 26;
Fax 00 33 2 23 23 61 00

1. INTRODUCTION

Forearc basins evolve in response to (i) tectonic forcing related to subduction processes (eg. plate convergence rates, flexure and geometry of the subducting slab, accretion or erosion within the subduction complex, and the partitioning and localisation of strain between the upper plate and the subduction thrust), (ii) to isostatic subsidence due to forearc sediment load (sediment fluxes) and (iii) to eustatic changes in sea level and their effect on the depositional profile (Dickinson and Seely, 1979; Dickinson, 1995; Fuller et al., 2006 ; Song and Simons, 2003). The structure and stratigraphic framework of many subduction margins are broadly understood from seismic reflection studies and field mapping, enabling previous workers to evaluate long-term changes in tectonic deformation and basin evolution (e.g., Field et al., 1989; Coulbourne and Moberley, 1977; Lewis and Hayes, 1984-2; Laursen et al., 2002; Laursen and Normack, 2003). Whilst it is clear from such studies that fore arc basin evolution is influenced by tectonic, sedimentation and climatic interactions, the stratigraphic resolution available in the basin sequence is seldom adequate to precisely quantify the relative contributions of the various drivers over an appropriate length of time spanning multiple glacio-eustatic cycles (McNeill et al., 1997; Mountney and Westbrook, 1997; Barnes et al., 2002)

The Hawke Bay forearc of the Hikurangi subduction margin in New Zealand is undergoing active tectonic deformation and sedimentation in response to convergence between the Pacific and Australian plates. The margin provides a fairly unique location for detailed, Pleistocene basin fill investigation with an extensive set of offshore and onshore correlative data available. The interpretation of this dataset provides an opportunity to present (1) a high resolution chronostratigraphic evaluation of the forearc basin fill during the last 1.1 Myrs, with the identification of different scales of the depositional sequences and their stacking patterns; (2) an estimation of the preserved sediment fluxes and denudation rates through time, and (3) the timing, style and rates of tectonic deformation. Through this analysis we are able to quantify the relative roles of tectonic deformation, climato-eustatic and isostatic forcings on the forearc basin stratigraphic pattern and morphostructural evolution, with a special emphasis on their effects on preserved sediment fluxes at different time-scales (1 Ma, 100 Ka and human scales). . These data offer new insights into primary factors controlling forarc basin evolution on active subduction margins.

2. REGIONAL SETTING

The Hawke Bay forearc domain is located along the east coast of the North Island of New Zealand (Fig. 1),where the Pacific plate subducts at a rate of about 40 mm/yr (Fig. 1). The overall morphostructure of the margin includes from trench to arc (Fig. 1 & 2) (1) an imbricate frontal wedge (accretionary wedge / prism) with several thrust-related ridges and associated slope basins, (2) an emerging coastal high that corresponds to the highest ridge of the frontal wedge, (3) a forearc domain spanning both terrestrial and marine environments in the Hawke Bay area, (4) the 1700m-high axial Ranges (structural arc) and (5) a southward propagating continental backarc rift and volcanic arc system (Taupo Volcanic Zone) – (Cole and Lewis, 1981; Lewis and Pettinga, 1993; Barnes and Mercier de Lépinay, 1997; Barnes et al., 2002; Lamarche et al., 2006; Villamor and Berryman, 2006) including the active volcanic arc (eg. Mt Ruapehu), and a proto-backarc basin (Wanganui basin - Proust et al., 2005).

The geological evolution of the subduction margin which started in the early Miocene (Balance, 1976; Pettinga, 1982; Spörli and Balance, 1989; Chanier, 1991), is complex and still debated. Some authors propose that thrust and fold tectonics occurred throughout Miocene and continued until present day Pettinga (1982); others suggest an intermediate period of extension (15 to 5 Ma) and associated subsidence due to subduction erosion (Chanier et al., 1999) or presents the extensional deformation as a result of thin-skinned

tectonics related to shallow gravitational collapse or spreading of the covering rock sequence (Barnes and Nicol, 2004). This evolution implies significant changes during Pleistocene such as the emergence and growth of the axial ranges (Beu et al., 1981, Erdman and Kelsey, 1992), inversion of extensional structures in the forearc domain (Barnes and Nicol, 2004) or the development of a margin-wide unconformity at the base of the Castelcliffian stage at 1.07 Ma (Proust and Chanier; 2004; Naish et al. 2005).

In Hawke Bay, the forearc basin fill sequence reaches up to 6000 m-thick and is characterized by Mio-Pliocene deep marine turbidites and Plio-Pleistocene shallow marine to fluvial sediments. This study concentrates on the uppermost, c.1000 meter-thick Castelcliffian-Haweran sequence (c. 0-1 Ma in age) of the forearc basin fill preserved in structurally controlled sub-basins both onshore (e.g. Ruataniwha plains) at the foot of the Axial Ranges (Ruahine range), buried beneath the present day coastal plains (eg. Heretaunga plains - Dravid and Brown, 1997) and offshore in a suite of piggy back sub-basins on the accretion prism (Lewis 1971; Barnes et al., 2002; Barnes and Nicol, 2004; Paquet et al., in prep). The lower part of this sequence (c. 1 Ma to c. 0.5 Ma) is very well exposed along coastal cliffs in southern Hawke Bay where it represents the 450 m-thick, shallow marine and fluvial, north-west dipping (c. 10°) deposits of the Kidnappers group (Kingma, 1971; Shane et al., 1996; Proust and Chanier, 2004). This section together with the Wanganui-type section (e.g. Fleming, 1953; Kamp and Turner, 1990; Naish and Kamp, 1997; Naish et al., 1998; Naish et al., 2005) in the back arc domain, provides one of the most complete calibrated sequence stratigraphies for the last 1Ma climatic and sea-level variations (Proust and Chanier, 2004). Some studies in Hawke Bay basin provided fairly well-constrained stratigraphic framework for the Late Pleistocene (Lewis, 1971; 1973; 1974), the last 100 Kyrs sequence (Paquet et al., 2008), the Oligocene to recent (Barnes et al., 2002) and the Cretaceous to Neogene intervals (Field et al., 1997). However, the coverage of Pleistocene (Castelcliffian-Haweran) stratigraphy is not described with enough resolution over the whole forearc domain to undertake a comprehensive study that encompass the continuum of the climatic and tectonic controls on three-dimensional sediment fills

3. DATA and METHOD

An extensive set of offshore and onshore data was used in this study to describe and quantify sediment deposition, vertical displacements on tectonic structures and sediment fluxes. The core of the dataset is a dense grid of marine seismic surveys including Multichannel, 3.5 KHz

and boomer data of various origins (see details on Fig. 3) that cover a large part of the forearc domain. Several age-calibrated cores, dredges and wells including six recently acquired giant piston cores from Marion-Dufresne survey (Proust et al., 2006) complete the set of data in the marine domain (Fig. 3 – Appendix 1). Onshore seismic data, coupled with well, boreholes, sedimentological section and geological mapping complement the information over the terrestrial environments in the Heretaunga Plains (Fig. 3 – Appendix 1).

Geological mapping undertaken in this study focused on the Pleistocene (c. 1.0 Ma to c. 0.5 Ma) terrestrial-shallow marine Kidnappers Group (Kingma, 1971) that lies on the western limb of the accretion wedge, in the coastal area of southern Hawke's Bay (Fig. 3 – Appendix 2). A geological map, based on ours and other workers results (e.g. Kingma, 1971; Kamp, 1978, Shane et al., 1996; Proust & Chanier, 2004), covers up a 34 km2 area between Cape Kidnappers and the Maraetotara River. Two 250 m-long onshore boreholes at Tollemache and Awatoto (Dravid and Brown, 1997) were re-interpreted as part of this study. In addition the exploration well Whakatu-1 (Ozolins and Francis, 2000), penetrated the Pleistocene deposits below the Heretaunga plains (Fig. 3 – Appendix 1).

The evaluation of the Pleistocene sequence stacking patterns in Hawke Bay is based on the recognition of 100 Kyr-type depositional sequences, the upper most of which is well exposed, and is the subject of a detailed presentation elsewhere (Paquet et al., submitted paper). Key bounding surfaces, together with the seismic units, facies and systems tracts, are well documented in the youngest sequence (Paquet el al., in prep). Transgressive surfaces (TS) were used as key-bounding unconformities to trace geometries at depth and over the whole basin. These surfaces have little diachroneity relative to the time span of each sequence (c.10 Ka over c.100 ka sequence duration). The seismic interpretation is validated by correlations to wells, cores, dredges and to the onshore Kidnappers group, that provide age and sedimentary facies calibrations. These results are extended onto the whole onshore domain in the Heretaunga Plains where seismic data and boreholes are available. The onshore-offshore stratigraphy is then correlated to the O18 eustatic curve (Lisiecki and Raymo, 2005) to complement the detailed age control on depositional sequences and bounding surfaces.

Isopach maps were developed for each 100-40 Kyrs sequence by measuring two-way-travel reflection time intervals between bounding unconformities, and digitized on GIS software. The preserved volumes of sediments were calculated for each sequence after converting isochors time values to thickness values by using an average internal velocity estimated from well logs and migration velocities. Porosity values for each sequence estimated from their average lithology and burial depth were compacted to 0%, converted to mass assuming a 2.7

g/cm3 average grain density, and finally converted into sediment fluxes (Mt/yr) by dividing the total sediment mass preserved into each sequence (Gt) by the overall duration of each sequence (Kyrs). Preserved sediment volumes into each sequence are compared to each other and also to the present day sediment flux (Hicks and Shankar, 2003). In the latter, we used an average porosity value of 20% (estimated porosity of the sediment in the drainage area, Field et al., 2005 and references herein) to compare sediment volumes deposited in the offshore to eroded volumes onshore. We estimated the uncertainties on values of both volumes and masses to be not more than ± 30%.

The identification of fault activity and vertical displacement rates were achieved using the key markers surfaces and their assigned ages. Errors on vertical displacement rates are minor (± 30%) as they depend on a well-constrained chronostratigraphic scheme and time-depth conversion.

4. RESULTS

The Pleistocene sediments in the Hawke's Bay region are mostly preserved offshore in the forearc domain and upper trench-slope of the imbricate frontal wedge within four structurally controlled basins (Motuokura, Lachlan, Mahia and Kidnappers basins), and in a smaller proportion, in the onshore foothills of the axial ranges (western Ruataniwha plains) (Fig. 1).. The forearc/upper trench-slope area extends from the coastal plains (Heretaunga plains), the shelf and the upper slope to water depth of 500 m at the toe of the late Pleistocene, lowstand wedge.

In the following section, we successively present (1) the stratigraphy, through the detailed sediment architecture of the uppermost 100Kyrs depositional sequence expanded at depth and in the different sub-basins in a complex stack of depositional sequences, (2) the age calibration and groundtruthing of seismic sequences by using wells, cores, and outcrops, (3) the correlation to the OIS and eustatic curve, (4) the major tectonic structures timing and displacements rates and (5) the isopach maps and estimation of preserved sediments volume and fluxes.

Results of seismic interpretations are illustrated in details along three key seismic profiles (Lines 05CM# 29, 41 and 3 – see Fig. 3 for location) located respectively (1) in the upper trench-slope basin (Motuokura basin – Fig. 4 and 5), (2) in the transition between the upper trench-slope and the shelf (from the Motuokura basin toward the Lachlan basin – Fig. 6) and (3) over the Hawke Bay shelf (from the Lachlan basin to the Mahia-Kidnappers basins – Fig.

7). Seismic interpretations are presented on series of profiles that cover most of the Hawke Bay forearc domain.

4.1 Stratigraphy

On the regional seismic section, the reflections are truncated by three major unconformities that build up three large scale megasequences (M1 to M3). In detail however, the megasequences are comprised of a set of eleven small scale sequences (Seq1 to Seq 11) bounded by 12 major unconformities (S1 to S12) overlain by the postglacial mud wedge (Seq0).

4.1.1 Sediment architecture of the uppermost depositional sequence:

The shallowest part of the seismic sections in Hawke Bay exhibits a well-defined seismic unit up to 400 ms TWTT-thick, characterized by a substantial prograding succession of seaward stepping sediment packages (Fig. 4) (see details of the description of this unit in Paquet et al., 2008). The seismic unit is bounded below by an onlap and downlap surface (S2) and above by a truncation or conformable surface (S1) on the shelf and slope respectively.

Five seismic facies are differentiated on seismic profiles (Fs1 to Fs5) (Fig. 4a). Fs1 forms the bulk of, and, the thickest part of an individual seaward stepping seismic package. Fs1 exhibits reflections with a regular sub-parallel configuration and good continuity that pass progressively to a sub-parallel, wavy seismic facies configuration (Fs2) in a basinward direction, and reflection free configuration (Fs3) in a landward direction (Fig. 4a). Towards the top of the seismic unit, in the uppermost and seaward most sediment package, Fs1 passes to chaotic high amplitude reflector configurations (Fs4) (Fig. 4a) and then to wavy, parallel and highly continuous reflections (Fs5) (Fig. 4a). According to Paquet et al. (2008), Fs1 corresponds to shelf edge marine environments; Fs2 is interpreted as clayey and silty deep slope marine deposits and Fs3 as sandy to silty marine shelf sediments. Fs4 coincides with marine sandy deposits of near shore environment and Fs5 is an equivalent of Fs1 with specific wavy undulations related to S-type upslope migrating sediment waves (see figure 7 in Paquet et al., in prep)..

The two unconformities S1 and S2 are characterized by a sharp, high amplitude reflection horizon that is easily traced over most of the forearc domain. S1 correlates with the last post-glacial (c.10 Kyrs) transgressive surface and S2 corresponds to the penultimate post-glacial (c. 130 Kyrs) transgressive surface (Paquet et al., 2008). These transgressive surfaces are easily traced across the seismic sections (e.g., Fig. 5). Following the example of Embry

(1993) and earlier work on Hawke Bay stratigraphy (Barnes et al., 2002), these surfaces are used as the reference bounding surfaces of the elementary building blocks that forms the framework of the sequence stacking pattern of the basin fill.

The basal sediment package corresponds to the Transgressive System Tract (TST). The following set of seaward stepping packages compose the bulk of the highstand systems tract comprised of prograding lens-shaped units bounded below by a downlap surface and above by a toplap surfaces of local extend. Seaward stepping sediment packages may correspond respectively to the regressive (RST) (Fig. 4) or forced regressive systems tracts (FRST) as witnessed by the presence of toplap terminations in the Lachlan basin (Fig. 6). These packages are lying on a marine regressive surface of erosion (RS). The seaward-most package corresponds to the Lowstand System tract (LST) bounded below by the sequence boundary (SB). On the shelf, the latter corresponds to the last channelized surface (fluvial depositional environment) that develops along basin axis below the TS. At the rim of the sub-basins, it is truncated by the overlying TS (Fig. 6 and 7) and below the shelf edge, it becomes conformable. The overlying Transgressive System Tract (TST) corresponds to the post-LGM mud wedge that covers most of Hawke Bay. This latter is not considered as part of the elementary sequence (Seq1) and is referred here as Seq0. As discussed below, it represents only part of a full sea level-cycle sedimentary sequence.

Comparable successions of systems tracts were recognized all around the seismic grid for the uppermost four sequences but were more difficult to identify in the deepest parts of the seismic sections due to the loss of resolution. However the TS bounding surfaces (S1 to S12) of the elementary sequences can be easily identified and form the basis of defining eleven sequences (Seq1 to Seq11) in the Motuokura basin between the southern Hawkes Bay coast and the Motuokura ridge (Fig. 5). These sequences exhibit similar (1) size/thickness, (2) amplitude of landward and seaward stepping of sediment packages, (3) internal reflector configurations and (4) seismic facies changes and then stacking pattern characteristics.

4.1.2 Stacking patterns of the depositional sequences

In the Motuokura basin, the stacking pattern of the eleven sequences stacking pattern exhibits an overall remarkable retrogradational geometry (or architecture) that develops on a concave up erosion unconformity at the base of the Pleistocene basin fill (Fig. 5). In detail however, this basal unconformity is made up of a series of coincident, overlapping erosion surfaces. Each surface developed at the landward end of the depositional sequences, and is overlain by

shallow marine and coastal plain sediments. The surface is therefore strongly diachronous, and formed partly as a result of wave abrasion and subaerial erosion (Fig. 5, 6 and 7).
Two to Three regional megasequences have been identified on seismic data and are described below.

The uppermost megasequence (M1) reaches a maximum thickness of c. 1.3 s TWT (c. 1150 m @ 1750 m/s). It is bounded below and above by S5 and S1 respectively and comprises four sequences (Seq1 to Seq4, eg. Fig. 5). The sequences exhibit typical lens-shape, shelf-edge clinoforms up to c. 250 meter-height relief and c. 0.3s to 0.4s-thick. Each sequence of M1 exhibits mostly seaward stepping lens-shaped sediment packages that define internal progradational clinoforms of a prominant shelf edge (Fig. 5). The seismic facies and their distribution within both the sequences and internal sediment packages are similar to Seq1 (Fig. 5). This implies that the ranges of sedimentary facies, depositional environments are equivalent between sequences and evolve from shallow marine sandy-silty deposits against the basal unconformity to deep marine silty clays toward the Motuokura ridge with sediment waves-like features at the shelf edge. This is illustrated by high amplitude reflections that grade basinward into weak reflectivity (Fig 5). This is consistent with lateral variation from shoreface and inner shelf deposits to shelf and slope muddy sequences. This also implies that M1 sequences developed under the same bathymetric conditions within the Motuokura basin during the overall retrogradation. The landward migration during M1 reaches c. 25% of the total migration of the megasequences.
The growth of tectonic structures beneath the shelf and upper slope has influenced the overall geometry of the megasequence. M1 is folded and faulted across the Waimarama thrust fault system and thins out on the western flank of the Motuokura ridge. The latter represents a tectonic growth sequence reflecting sedimentation contemporaneous with thrust faulting and uplift of the Motuokura Ridge. Sedimentary sequences exhibit gentle, concave up, bending (synform) migrating progressively eastward. The maximum of synform-bending of each sequence broadly corresponds to the location(s) of the following sequence(s) depocenter(s) (Fig. 5 and 10). The relative thickening and decrease of the slope at the base of the clinoforms build up the present day flat morphology of the Motuokura trough.
The middle megasequence (M2) reaches a maximum thickness of c. 0.7 s TWT (c. 630 m @ 1800 m/s). It is bounded below and above by S 9 and S 5 respectively, and comprises four sequences (Seq5 to Seq8, Fig. 5). The sequences exhibit pronounced lens-shape clinoforms up to c. 250 meter-height relief (c. 0.1s to c. 0.3s-thick) that thin out rapidly on the western flank

of the Motuokura ridge. M2 is thinner than M1, with thinner sequences but build up prominent shelf edge morphology (Fig. 5) and trough-like morphology at the base of clinoforms. Despite the loss of resolution in data, it remains possible to identify seismic facies that are equivalent to those seen in M1 with similar relative distribution within each sequence (Fig. 5). From this we infer that the sequences and their internal sedimentary facies formed in a similar environment to those in megasequence 1.

M2 sequences are tilted 3° to the WNW on the western flank (hangingwall sequence) of the Motuokura ridge. Compared to M1, the rate of overall retrogradation of the sequences decreases, with little landward shifts of the shelf edge margin and extension of the transgressive surfaces over the Cenozoic substratum. The landward migration of the LST shelf edge during M2 reaches less than 10% of the total lateral migration.

The lower megasequence (M3), reaches a maximum thickness c. 0.6 s TWT (c. 570 m@ 1900 m/s). It is bounded below and above by S12 and S9 respectively and comprises up to three sequences (Seq9 to Seq11, Fig.5). Sequences exhibit lens-shape clinoforms that are less pronounced than those from M1 and M2 sequences, with less than c. 100 meter-height (c. 0.1 to c. 0.2 s TWT). They show little thickness variation and poorly developed shelf edge morphology. The presence of shelf edge morphology is suspected downslope, west of the ridge in the northern part of the basin (05CM28 & 27– Fig. 8), and east of the ridge in the southernmost part (05CM30 – Fig. 8) but remains faint along the profile 05CM29 (Fig. 5). The facies identification and distribution in the sequences is more speculative due to the loss of resolution in data. Nevertheless the distribution appears broadly similar to those of M1 and M2. The sequence is inferred to include shallow marine facies against the basal unconformity and deeper marine strata basinward within each sequence.. The landward migration of the LST shelf edge during M3 reaches less than 10% of the total migration.

M3 sequences are tilted to the WNW, on the western flank of the Motuokura ridge, with dip values up to c. 4°. Normal bending faulting resulting from flexural extension dissects the sequences along the Motuokura ridge anticline axis (eg. lines 05CM 29 and 30) but the diminished signature of growth faulting in the sequence geometry implies that most of deformation occurred largely after the deposition of M3.

To the west, below the present day Hawke's Bay shelf, the eleven depositional sequences "onlap" the composite basal unconformity of the Pleistocene/Castelcliffian basin fill with its typical overall fault-controlled retrogradational stacking pattern (05CM03 – Fig. 6 & 7). M2

and M3 megasequences merge together and wedge out laterally along the unconformity at mid-shelf position. M1 is largely distributed laterally over S5 unconformity and thicken in local sub-basins (Lachlan, Mahia and Kidnappers basins, Fig. 6, 7, 8 & 9) individualized between the main thrust fault ridges (Fig. 8). Evidence of channels between Fs3 and Fs4 on seismic data, in most of sequences over the present day shelf is in accordance with fluvial channel deposits interbedded with shallow marine and shelf deposits. This similarity between sequences M1, M2 and M3 implies that the bathymetric range and depositional environments were similar as sequences developed during the general retrogradation.

4.2 Correlations and age calibration

Offshore and onshore stratigraphy have been tied to wells and cores distributed throughout the bay and to the Pleistocene Kidnappers Group that outcrops in the Coastal Ranges, west of Cape Kidnappers (Location on fig. 2). These correlations aims (1) to validate of the seismic facies and sequence stratigraphy interpretation, and (2) to calibrate in age the sedimentary record and to the Pleistocene stratigraphic chart (Gradstein et al., 2004a, 2004b). The latter is also correlated to the New Zealand biostratigraphic stages and substages (Naish et al., 1998; Carter and Naish, 1998). Results are summarised on figure 10 that revised the stratigraphy proposed by Barnes et al. (2002) within the Lachlan Basin.

Megasequence 1:

M1 seismic sequences were tied to (1) several dated cores and dredges and to one exploration well (Hawke Bay-1) in the marine realm (Heffer et al., 1976; Strong et al., 1989; Barnes et al., 1991; Proust et al., 2006; Shane, personnal communication) and (2) to two testbores (Awatoto & Tollemache) (Dravid and Brown, 1997) and one exploration well (Whakatu-1) in the Heretaunga plains (Ozolins and Francis, 2000) (see details on Fig. 10). The results show that Seq1, 2 and 3 developed mainly during Haweran stage (0.34 Ma to present day). Therefore, Seq4 is older than Haweran and constitutes the last Castelcliffian sequence.

Lithological calibrations confirm the seismic facies interpretations of Seq1 (Paquet et al, 2008) and consequently of most M1 sequences. The sediments evolve from an alternance of fluvial, flood plain and shallow marine deposits (gravels to silty sands in Awatoto, Tollemache and Whakatu wells - Dravid and Brown, 1997; Ozolins and Francis, 2000) to deep offshore marine deposits (silty clays in piston cores within the Motuokura basin – Barnes et al., 1991; Proust et al., 2006).

Megasequence 2-3:

M2-3 Seismic sequences were tied to cores and dredges in the marine realm (Strong et al, 1989; Proust et al., 2006) and (2) to the Pleistocene Kidnappers group exposed along the coastal cliff of the southern Hawke Bay (Proust and Chanier, 2004; and reference therein). MD06 piston cores indicate that Seq6 is probably older than 0.5 Ma (Proust et al., 2006). Six sequences identified on seismic data (Seq11 to Seq6) were tied to the six depositional sequences previously identified by Proust and Chanier (2004) in the Kidnappers group, by using very high resolution boomer survey (GSR05301),). The base of Seq11 (S12) ties to the base of the Kidnappers group that is marked by the presence of the Potaka tephra dated at 1.0±0.1 Ma (Shane, 1994; Shane et al., 1996) (Fig. 10). The last sequence (Seq6) correlates to the Te Awanga beds formation that is older than 0.46 Ma (Beu and Pillans, 1987; Bowen et al., 1998). This latter result is compatible with results obtain offshore for Seq6 (Fig. 10). These correlations show that M2-3 developed during the Castelcliffian stage from 1.0±0.1 Ma to c. 0.5 Ma or c. 0.34 Ma. The major unconformities identified offshore as transgressive surfaces with wave abrasion on high resolution boomer lines correlate somewhere between the top of the major gravel beds and the maximum flooding surfaces identified by Proust and Chanier (2004) (Fig. 10). The presence of dated tephras (eg. Rabbit Gully ignimbrite – c. 0.88 Ma) within the Kidnappers group section (Shane, 1994; Shane et al., 1996) help in the age calibration of the M2-3 sequences (Fig. 10).

Lithological calibrations of M2-3 sequences using available samples confirm the seismic facies interpretations. Fluvial to shallow marine deposits are recognized in the Kidnappers group and form most of the basin fill of the inner parts of Hawke Bay. Facies evolve seaward to deep marine sediments as revealed by MD06-2995 and 2996 piston cores (Proust et al., 2006).

4.3 Correlation to eustasy curve and Oxygen Isotope Stratigraphy (OIS):

Correlations of the sequence stratigraphy to the oxygen isotope stratigraphy and eustasy curve (Shackelton et al., 1990; Lisiecki and Raymo, 2005) have been undertaken in order to verify the possible control of eustasy on the sequence development and to refine the age calibration of the seismic stratigraphy. The correlations are based on direct correlation of (1) the dated horizons, (2) the relative sea level curve derived from depositional environments variations and (3) the stratigraphic features (surface, system tract) identified on seismic data, to the OIS and eustasy curve (Fig. 9). The international and New Zealand stratigraphic stages and substages (Naish et al., 1998) as well as magnetostratigraphic stages and substages equivalence (Shackelton et al., 1995; Gradstein et al., 2004a) are indicated (Fig. 10).

S 12 (base of Seq 11 and M3) developed between OIS 32 (c. 1.1 Ma) and OIS 31 (c. 1.07) that correspond to the base of Castelcliffian biostratigraphic stage. It also corresponds to the base of the magnetostratigraphic Jaramillo Subchron (c. 1.072 Ma). S 9 (base of Seq 8 and M2) developed between OIS 20 (c. 0.79 Ma) and OIS 19 (c. 0.77 Ma), that corresponds to the Okehuan-Putikian substage boundary at c. 0.78 Ma and to the Matuyama-Burnhes magnetostratigraphic stage boundary (c. 0.781 Ma). TS 5 (base of Seq 4 and M1) developed between OIS 12 (c. 0.43 Ma) and OIS 11 (c. 0.41 Ma). S 4 (base of Seq 3) developed between OIS 10 (c. 0.34 Ma) and OIS 9 (c. 0.33 Ma), that corresponds to the top of Castelcliffian / base of Haweran (c. 0.34 Ma). S 2 (base of Seq 1) developed between OIS 6 (c. 0.135 Ma) and OIS 5 (c. 0.125 Ma), that corresponds to the Middle-Late Pleistocene Boundary at c. 0.126 (Fig. 10). These results are in agreement with recent studies led on the Hawke's Bay Pleistocene basin fill (Barnes et al., 2002; Proust and Chanier, 2004). In addition, lithological data obtain from wells and cores confirm the interpretations of seismic facies. Major sea level rise over the last 1.1 Myr correlate to the eleven 100 Ka-type depositional sequences transgressive surfaces (S1é to S1) well documented on the seismic sections (Fig. 5 to 7). The depositional sequence internal organisation correlates fairly well also to the more subtle 20 Ka and 40 Ka eustatic variations (Fig. 10). Correlations of the seismic stratigraphy to dated sections, wells and cores and to the age-calibrated eustasy/OIS curve provides a high-resolution lithological and chronological control on depositional sequence development within the forearc domain for the Castelcliffian and Haweran stages (c. 1.07 Ma to Present).

4.4 Spatial migration of basin depocenters through time

The extensive stratigraphic dataset over most of the Hawkes Bay forearc basin together with the very high chronostratigraphic resolution allows us to evaluate the temporal and spatial distribution of each depositional sequence preserved in three dimensions. Twelve isopach maps are presented on figure 11 that show the extent of the eleven 100-40Kyrs depositional sequence (Seq1 to Seq11) and the last transgressive/early highstand postglacial wedge (Seq0).. The lateral extent of preserved sequence boundaries (Fig. 11) is roughly constant for Seq11 to Seq5 (c. 2600 ± 300 km²) and widens significantly from Seq4 to Seq1 (c. 4000 km² to c. 5300 km²). The post-glacial sequence boundary (Seq0) is preserved over the widest (c. 5800 km²) area, covering most of the marine and coastal parts of the forearc domain.

Thinning of sequences is particularly noticeable over growing thrust ridges, where uplift inhibits deposition, whilst enhancing erosion on the shelf during successive marine transgressions. The broad scale distribution of sediment confirms the presence of distinct

depocenters (Kidnappers, Mahia, Lachlan basins on the shelf, and Motuokura basin on the slope) that progressively shift in position through time.

In the Motuokura basin, where depositional sequences are well preserved, the individual sequences exhibit elongated-shape depocenters striking subparallel to the fault structures (c. N 50°). The maximum thickness of these depocenters ranges from c. 110 m (Seq8 and Seq6) to c. 350 m (Seq1) and correspond to the vertical stacking of the LST shelf edge clinoforms. This corresponds to mean sedimentation rates of up to c. 3.2 mm.yr-1. From Seq11 to Seq1, depocenters migrate landward over 20 km. The maximum landward migration occurs along S9 (c. 0.78 Ma) and S5 (c. 0.43 Ma) and correspond to the retrogradational "upward" shifts of sediment observed between M3, M2 and M1 (Fig. 5). The overall landward migration / retrogradation of sequence depocenters in the Motuokura basin (c. 20 km),during the last 1.1 Ma occurred with an approximate rate of 18.2 mm.yr-1 along a N270° direction.

Because of the importance of erosion, the reconstruction of depocenters migration through time on the shelf is more complex than in the Motuokura basin. The depocenters are variously distributed along distinct narrow corridors between structures.

It shows an overall arcward migration of sediment that includes in detail the following steps: the westward migration of the Lachlan I and Mahia basins (S12 to S6, c. 1.07 to c. 0.50 Ma), the development of the Kidnapper Basin to the east of Napier-Wairoa ridge (Seq7, c. 0.71 to c. 0.62 Ma), the merging of the Lachlan I and Kidnappers Basins (Seq6 to Seq5, c. 0.62 to c. 0.43 Ma) together with the deepening of the Mahia Basin.

The basin geometries developed from S5 to S1 (c. 0.43 to c. 0.13 Ma) (Fig. 11) reveals renewal of subsidence in the Lachlan basin (Lachlan II basin stage) and a junction of the Motuokura, Lachlan II, Mahia, Kidnappers and Heretaunga basin in a broad arched string of subsidence around the tectonic ridges. In detail however, Mahia basin migrates 15 km to the North, Kidnappers basin stretches along the Napier-Wairoa ridge and migrates 40 km to the SW when subsidence increases between in the Lachlan and Kidnapper ridges (Fig. 11) and sediment onlap the northern end of the Lachlan basin II (Figure 8b and c). The arched geometry is then sealed by postglacial muds.

4.5 Sediment budget

Sediment volumes and masses preserved in Hawkes Bay forearc basin are estimated from isopach maps presented on figure 12. To compare sequence volumes and masses to each other and, sediment volumes and masses preserved in the basin, to sediment volumes and masses eroded onshore, all volumes were compacted to 0% of porosity. Error estimates have been

determined by evaluating the maximum and minimum values of each parameter that are used in the sediment budget calculation (i.e. velocity ±50m/s; surface ±1ms; area ±200km^2; porosity ±5%; sequence duration ±10ka). Mean porosity values are estimated for each sequence with an error of ±5%. These values vary from 55±5% for Seq0 to 32±5% for Seq11.

The bulk estimated volumes of sediment preserved in the eleven depositional sequences reaches 2515±346 km^3. This volume corresponds to 1533±340 km3 of sediment at 0% of porosity and a total mass of 4140±960 Gt. Volumes, masses and lateral extent of surfaces exhibit similar evolution trends through time with more voluminous (heavier) and extensive younger sequences than older ones (Fig. 12). Seq1 is 252±44 km^3 in volume (680±130 Gt) whereas Seq11 reaches only 100±21 km^3 (270±55 Gt). The evolution through time of sediment volumes and masses shows a regular increase that comprises two main periods (Fig. 12). The first period (Seq11 to Seq5) exhibits very little increase in preserved sediment masses (270±55 Gt to 316±75 Gt). The second period (Seq4 to Seq1) shows a drastic increase in sediment masses from 443±101 Gt to 680±130 Gt (Seq.1).

Preserved sediment fluxes (Mt.yr-1) are estimated for each sequence by dividing the sediment mass (Gt) by the duration of each sequence (kyr). Errors on mass accumulation rates vary from ±22% to ±36% so values have to be understood with care. Preserved sediment flux increases regularly through time and parallels the trend in sediment volumes and masses (Fig. 12) as sequence duration is almost constant (98 ± 17 kyr), except for Seq0 (15±1 ka). Two periods are recognized: the first period (Seq11 to Seq5 – M 2 & 3) exhibits very little increase of sediment fluxes from 2.5±0.8 Mt.yr-1 to 3.2±0.9 Mt.yr-1. The second period (Seq4 to Seq1 – M1) starts with a sharp increase in Seq4 with 4.9±1.4 Mt.yr-1 (Fig. 12) followed by a slight and probably insignificant decrease in Seq3 (4.6±1.2 Mt.yr-1), and a constant rise again until Seq 1 (6.2±1.4 Mt .yr-1). Sediment fluxes for the last c. 1.1 Ma averages 3.8±1.0Mt.yr-1.

If the extent of the present day Hawke Bay drainage basin (c. 14,300 km²) is representative for the last 1.1 Ma (stable hydrographical network, reference), the minimum preserved sediment yield of the drainage basin varies from 164±55 (Seq10) to 432±95 t.km-².yr-1 (Seq1). It reaches a maximum value of 536±150 t.km-².yr-1 during the last post-glacial period. Preserved sediment yield for the last c. 1.1 Ma averages 265±70 t.km-².yr-1. Assuming a constant mean drainage area of c. 14,300 km² for the last 1 Ma, the mean erosion rate estimated from preserved volumes for this period is of the order of c. 0.12 mm.yr-1. The incremental erosion rates would have changed from c. 0.08 mm.yr-1 during M2-3 to c. 0.2 mm.yr-1 by the end of M1 (c. 0.25 mm.yr-1 for Seq0). Considering the uncertainties in the

preserved sediment flux estimations and the more or less speculative assumptions (eg. drainage area, % of preservation, rock density), sediment yield and erosion rate values are mostly indicative.

In terms of erosion over the whole Hawke Bay drainage basin during the last 1 Ma, considering a mean porosity value of 20% for source rocks (Field et al, 2005) the eroded material estimated from preserved sediments reaches a volume of c. 1850 km3. This result is very close to the broad estimation of c. 2170 km3 of eroded material calculated by subtracting the present day topography to the present day shape of the c. 1 Ma paleotopography (estimated from mapping and several previous work; eg. Kingma, 1962; Smale et al., 1978; Beu et al., 1987; Pillans, 1986; Shane 1994; Browne, 2004). Uncertainty concerning the estimation of eroded material volume is difficult to assess as remnants of the c. 1 Ma paleotopography are scace. Considering a putative error of ± 30% (2170 ± 650 km3) this implies that the volume of deposited sediments preserved in the basin account for 65 to 100 % of the estimated volume of eroded material during the last 1 Ma.

The long-term sediment budget (1.1 Ma) in the Hawke Bay basin shows two distinctive phases. The first period that lasts until c.430 Kyrs (S5) exhibits an apparent stability in sediment fluxes (c. 2.5 Mt.yr-1). The second period that starts after c.430 Kyrs, shows a significant increase in sediment fluxes (from c. 3 Mt.yr-1 to c. 6 Mt.yr-1). The transition between the two phases coincides approximately with development of a major unconformity (S5) that bounds the two megasequences (M1 and M2-3) identified on seismic profiles.

4.6 Timing and displacement along the main tectonic structures

This study complements the detailed structural maps presented in Barnes et al (2002) and Barnes and Nicol (2004). A set of active thrust faults and ridges bound the main sediment depocenters: the Motuokura basin between the Motuokura ridge and the Kairakau-Waimarama Thrust Complex; the Lachlan basin between the Lachlan and Kidnappers ridges; the Mahia basin between the Lachlan and Napier-Wairoa ridges and the Kidnappers basin between the Kidnappers and the Napier-Wairoa ridges (Fig. 13).

In these basins, the eleven depositional sequences are deformed by active thrust faults and folds. These structures reflect the regional shortening of this part of the upper plate above the subduction zone during the last 1.1 Ma (Fig. 4 to 8).

In addition to the primary contractional structures, scarce extensional structures are present. These correspond to (1) bending moment normal faults associated with growing anticline, e.g., on the Motuokura Ridge (Fig. 5 and 8h), Lachlan Ridge (Fig. 8f) and the Kidnappers ridges (Fig. 8b), (2) shallow gravitational collapse of the uplifting Waimarama coast (Pettinga, 1982; Pettinga, 1985; Pettinga, 2004) and, (3) Late Pleistocene, SE dipping normal faults with dextral strike slip component in the coastal Kidnappers group exposures (Hull, 1985; Cashman and Kelsey, 1990 – Appendice 2).

We consider the timing of activity and vertical rates of deformation associated with the major tectonic structures using the twelve transgressive surfaces (S12 to S1) as deformation markers (Fig. 13). A set of cross margin transects were selected trough the main active ridges at places where preservation of sequences on both sides of tectonic structures allows vertical displacement measurements (Fig. 13). Structural timing of a series of thrust faults along NW-SE transect (05CM28), within the Motuokura, basin is detailed on figure 14.

Although the purpose here is not to undertake a detailed analysis of the tectonic structures and their plate boundary significance, several important observations can be made with respect to the spatial and temporal variability in activity of the major faults.:

1. On transect C (Fig. 13 c; Fig. 14), the initiation or cessation of fault activity tends to migrate in a landward-arcward direction.Such trend is suspected along other profiles (Fig. 13).

2. The Lachlan fault/ridge is the dominant active structure with high vertical displacement rates, up to c.3 mm.yr-1, throughout the last 1.1 Myrs. This structure and the other faults within the Lachlan basin area are reactivated normal faults (Barnes et al., 2002; Barnes and Nicol, 2004). In the southern Lachlan basin (Fig. 13 d) the onset of activity of back-thrusts (LS, LB1E, LB1W and KFS (Kidnappers Fault South); see caption of figure 13 for details) occurs in relay (one set up when the other ceases) after the cessation of the activity on the main thrust (the Kidnappers ridge) which implies a fault connection at depth as proposed by Barnes and Nicol (2004).

3. The Motuokura fault ridge initiated in the North at c. 1.1 Ma and propagated southward with a continuous activity until present day. Accelerations are noticeable at c. 0.8 Ma and c. 0.43 Ma (S 9 and S5) (Fig. 13 b and c). The mean displacement rate reaches c. 1 mm.yr-1 in its central part (Fig. 13).

4. The Kidnappers ridge is wider and more developed in the South (figure 8 f and g) than in the North (Figure 8 b to d). It is the predominant structure on the shelf area that was active since Late Miocene – Early Pliocene (Barnes and Nicol, 2004). Its mean vertical displacement

rate measured in the north estimated from the new sequence stratigraphy is c. 1 mm.yr-1 Late Pleistocene and Holocene uplift rate estimates, based on height of marine terraces, in the southern part of the ridge (Cape Kidnappers area) provide values up to c.1 mm.yr-1 and 2 mm.yr-1, respectively (Hull, 1985; Hull, 1987). The last activation of the ridge started probably in the Mid Pleistocene (c. S5).

5. The Napier-Wairoa ridge complexe is a succession of faults and folds, forming a structural high along the western boundary of the Kidnapper basin. The wedging out of Mid-Late Pleistocene sequences along the ridge (Fig. 8 a to e) shows that the structure had several periods of activity during the mid-Pleistocene. Recent activity of the ridge is attested by the rupture of the Napier fault that resulted in the Ms = 7.8 Hawke's Bay earthquake in 1931 (Hull, 1990).

Four major long-lasting Pleistocene active structural ridges (Napier-Wairoa, Kidnappers Lachlan and Motuokura) bound the main depocenters of the Hawke Bay forearc basin fill. These ridges developed grow up at a rate that may encompass 3 mm.yr-1 with a progressive displacement of the tectonic activity in a landward (arcward) direction through time.

This trend is accommodated by the overall retrogradational stacking pattern of depositional sequences in the basins where faults are progressively sealed by 100 Kyr-type sequence depocenters (e.g. see cessation of fault activity W8b, W8 and W7 when 100 Kyr-type sequence depocenter developed right above the fault location – Fig. 14). Landward activity migration rates estimate from these latter faults give values of 22,5 ± 2 mm.yr-1. This value is comparable to the c. 18.2 mm.yr-1 of landward migration of depocenters.

This structural analysis provides a rough approximation of the fault activity through time. Extensive structural work is needed to fully understand the tectonic deformation and fault interactions in the area.

5. DISCUSSION

This section discusses the respective role of eustasy, tectonic deformation and sediment fluxes that control the sediment architecture of the Hawkes Bay basin with a special emphasis on the significance of changes in long term sediment fluxes with respect to observed present day fluxes.

5.1-Eustatic, tectonic and isostatic controls on the stratigraphic pattern

The Pleistocene stratigraphic architecture in the Hawke Bay forearc basin is comprised of three megasequences (M1, M2, M3) bounded by two region wide unconformities (S5, S9). These megasequences are composed of a set of 11 sequences bounded by 12 major unconformities (S12 to S1).

Groundtruthing and age-dating of these elementary sequences through their correlation to wells, cores, and onland exposures shows that the major transgressive surfaces (TS) and sequence boundaries (SB) of the sequences correlate to global eustatic sea level rises and falls (Fig.9). Therefore, climatically-driven eustasy appears to be the predominant parameter that controls the c. 100kyrs cyclicity in the sedimentary basin. This result confirms the conclusions of previous studies on the Pleistocene forearc (Proust and Chanier, 2004; Paquet et al., 2008) and back-arc basins (eg. Lewis 1973 ; Naish et al., 1998; Saul et al., 1999; Burger et al., 2002; Barnes et al., 2002; Proust et al., 2005). In the Motuokura basin, the sequences exhibit characteristic geometry with pronounced shelf edges from c. 780 ka (S9 – Seq8). This period corresponds to the most significant change of the Mid Pleistocene Transition (MPT), that is the demise of predominantly 40 kyr-type glacio-eustasy and the onset of major 100 Kyr-type cycles (Head and Gibbard, 2005; Murray-Wallace, 2007 and references therein). It is therefore possible that the building of pronounced paleo-shelf edges results partly from the change in the amplitude of sea-level changes.

However, excepting the high amplitude 100 kyr sea-level, the long term, net absolute mean sea-level did not change more than 30m during the Pleistocene. This 30m change in sea-level cannot account for the accommodation space required to accumulate locally up to 1 km of sediment in the Motuokura Basin (Fig. 5 and 10) and to produce tens of kilometres of onlap along the slope and shelf in the overall retrogradational stacking pattern of sequences. The basal unconformity to the 11 sequences in the Motuokura Basin developed as a composite feature with diachronous erosion occurring at shelf depths. The presence of this surface now at a depth of more than 1 km beneath the seafloor indicates long term subsidence of the basin at a rate of about 1 mm/yr. The retrogradtional architecture reflects the progressive basin subsidence and landward roll-back of the shelf break through timeis pattern can however be fairly well explain by tectonically induced lateral changes in subsidence regime in the basin. Some hypothesis based on observation in other Neogene forearc basins around the world may explain this landward migration of sequences:

(1) a local thrust-related uplift of the Motuokura Ridge superimposed on the regional subsidence of the margin (offshore the east coast of Honshu Island in Japan, von Huene and Arthur, (1982); North Canterbury, New Zealand, Barnes (1995, 1996))

(2) a progressive subsidence due to subduction erosion and superimposed episodes of compressional deformation of the outer part of the forearc (Valparaiso forearc basin, subduction of the Juan de Fuca Ridge and seamounts, Laursen et al., 2002);

(3) a growth of the accretion prism against a seaward dipping backstop that would generate the upward and landward growth of the major thrusts (northern Chilean Arica and Iquique basins and Colombian forearc basins, Coulbourn and Moberly, 1977, and Mountney and Westbrook, 1997, respectively).

Nevertheless, application of these models to the Hawke Bay forearc domain must be undertaken with care. Regional tectonic erosion responsible of potential regional subsidence is not attested in that area (Beanland et al, 1998; Nicol and Wallace, 2007). The basins where the landward migration occurs are not systematically intercalated between a growing accretionary prism and a backstop (e.g. Motuokura and Lachlan basins). Landward migrations and the retrogradational trend vary in direction and amplitude between basins. This is not compatible with the effects of subducted seamounts that would result in a similar amplitude and direction migration and would reflect the plate convergence motion. In addition, while subducted seamounts infer migrating subsidence and gravitational collapses such as those identified by Pettinga (1980, 1982, 2004) along the Waimarama coast, they would have deeply affected the Cenozoic succession and created large-scale instability along their trails (re-entrant), as observed and detailed at the northern end of the Hikurangi margin (Ruatoria avalanche) by Lewis et al. (1998), Collot et al. (2001) and Lewis et al. (2004), or modelled by Dominguez et al. (1998). Such evidences have not been found in seismic and bathymetric data in offshore Hawke Bay yet.

The landward/arcward migration is visible in most sub-basins of the whole Hikurangi forearc domain, but also in the Wanganui proto-back-arc basin since c. 1.35 Ma (Proust et al., 2005). Therefore, sequence depocenters tend to migrate arcward during the Pleistocene

The major active structures in the Hawke Bay forearc domain during the Pleistocene (Fig. 13), are the Motuokura, the Lachlan and the Kidnappers ridges that bound the major sediment depocenters observed over Hawke Bay. These growing structures do not produce any significant relief on the shelf seafloor, source of along slope gravity processes, but create, at depth, progressive deformation structures (Fig. 2 & 8) and relative subsidence at the origin of the sub-basins (eg. Motuokura, Lachlan, Mahia and Kidnappers basins). In detail, however,

the vertical growth of these major seaward verging ridges generates successive landward tilting of the hanging wall sequences , and influences the landward migration of sequence depocenters. Nevertheless, the tectonically-controlled tilting may not be sufficient to entirely trigger this landward migration of sediments because displacement rates along the major thrusts during the last 1.1 Ma are too low to explain the measured c. 20 km of observed landward migration. The migration of depocenters locally corresponds to the progressive sealing of successive thrusts faults (Fig. 14) and a landward shift in fault activity. This suggests a possible relationship between sediment loading and fault activity. The lowering and cessation of fault activity occurred when a sequence depocenter developed right above the fault location (Fig. 14) and migration speed of both tectonic activity and depocenter migration are almost similar in the Motuokura basin (c. 22.5 and c. 18.2 mm.yr-1 respectively). This process induces a progressive landward-arcward propagation of deformation and depocenter location in an overall retrogradational pattern that implies a close relationship between tectonic deformation and sedimentation. The landward-arcward migration of sedimentation is visible in most sub-basins of the whole Hikurangi forearc domain, but also in the Wanganui proto-back-arc basin since c. 1.35 Ma (Proust et al., 2005). Therefore, sequence depocenters tend to migrate arcward during the Pleistocene all over the Hikurangi margin. The uncertainty remains however, whether the arcward sequence of structure development influence the landward migration, or if the sediment loading influence the fault development. The effect of sedimentation rates (isostasy) has to be considered as a key parameter in the basin development as explored by Barrier et al. (2002). Thus, as observed in the Motuokura basin, the synform-bending of each sequence occurs below the next sequence depocenters (Fig. 5). This implies that the sediment load associated to one sequence depocenter is sufficient to bend the previous sequence(s) as well as the whole Pleistocène fill may bend the underlying substratum including Mio-Pliocene series. This latter show indeed evidences of extensional deformation characterized by small-scale normal fault networks (Fig. 5) that develop below the Pleistocene basin fill. This feature is often encountered on seismic data below the Pleistocene basins in Hawke Bay and in other places in the Hikurangi margin, along the east coast of North Island. Thus, even if the initiation of the normal faulting occurred prior to the Pleistocene, the existence of the normal fault network may have weakened the substratum and potentially favour the Pleistocene sequence bending and consequently, the retrogradational trend. Therefore we assume that isostasy due to the sediment load, along with the regional stability of the thrust wedge and the local structurally controlled uplift and subsidence, plays an important role in the basin evolution and the development of the retrogradational trend

observed in the stratigraphic record. Nonetheless the prominent unconformities of broad lateral extend like surfaces S9 and S5 at megasequences boundaries, that mark important retrogradational shifts, could reasonably be the record of major, basin-wide to margin-wide reactivations of thrusts or onset of regional uplift events related to deeper seated geodynamical processes within the thrust wedge (Fig. 8) that partly control the longer term stratigraphic pattern. Finally, we assume that the location and activity of major structures influence the location and evolution of sedimentary basins over the Hawke Bay forearc domain, and that the isostasy, created by the basin fill (sedimentation rates up to c. 3.2 mm.yr-1 in the Motuokura basin), influences retroactively the tectonic activity and consequently, both the development (arcward migration) of the basin and the overall morphostructural evolution.

5.2-Tectonic and climatic controls on sediment fluxes

The flat and ramp morphology, the bathymetry (shelf and upper-slope) and the active relative subsidence of the Hawke Bay forearc domain offer an efficient trap for sediments as evidenced by comparison between broad eroded and deposited volume estimations (see section 4.4). This section aims to explain the observed variations in long-term preserved sediment fluxes (PSF) and to compare them to the present day flux estimations.

The analysis of the evolution through time of sediment volumes, masses and fluxes in the basin points to the existence of two distinct phases for the last 1.1 Ma. The first phase, from c. 1.1 Myrs to c. 430 Kyrs, shows a nearly constant value of sediment fluxes of c. 2.5 Mt.yr-1. The second phase from c. 430 Kyrs to present day, exhibits a significant and constant increase of sediment flux up to c. 6.2 Mt.yr-1. This represents a 250% increase during the last 430 Kyrs. Such a drastic increase of PSF in the basin are often attributed to important changes in climate or tectonic deformation (Molnar and England, 1990; Allen and Densmore, 2000).

5.2.1-Climatic influence

An attentive look at the Pleistocene climato-eustatic curve (018 record – e.g. Lisiecki and Raymo, 2005) does not reveal any evidence of significant change around 430 Ka that can directly explain the increase in PSF values. The only documented important long term climatic change that could account for the PSF increase is the Mid Pleistocene Transition (MPT) (Pillans, 2003; Head and Gibbard, 2005). The MPT is characterized by the shift from 41 ka obliquity-forced (early Pleistocene) to 100 ka precessionaly-forced climate cycles

(Milankovitch, 1941; Berger, 1978). The transition progressively emplaced from c. 1.0-0.9 Ma with an important amplification at c. 0.78 Ma and finished at c. 0.6-0.5 Ma. It has been punctuated by several events that lead to the pronounced Mid-Late Pleistocene 100 Ka-type climatic variations (Head and Gibbard, 2005, and reference therein). Nevertheless, a significant delay of at least 100 Ka exists between the MPT emplacement and the increase of PSF. Existence of such a lag time in the response of the Hawke Bay drainage system to the Pleistocene climate forcing is not compatible with (1) recent observations that reveal rapid response of the system to abrupt climate variations such as rapid sediment flux increase responsible of fill terrace formation during Late Pleistocene climate degradations (Litchfield and Berryman, 2005), the increase of terrigenous mass accumulation rates in deep slope basins (piston core MD97-2121; Fig. 3) during the last glacial maximum (Carter and Manighetti, 2006) and the increase of sediment fluxes calculated from preserved sediment volumes at the LGM termination (Paquet et al., 2008); or with (2) results from modelling that indicate that short transfer subsystems (< 300 km) such as the Hawke Bay rivers, respond instantaneously to climate variations (Castelltort et al., 2003).

Therefore, we assume that the cause of the important PSF increase observed in the Hawke Bay forearc basin is not directly related to any more or less synchronous Pleistocene climate change.

5.2.2-Tectonic influence

The increase in sediment fluxes occurs above the major 430 ka unconformity (S5, Fig. 8). This unconformity corresponds to the boundary between megasequences M2-3 and M1 characterized by a drastic landward shift of 100Kyr depositional sequences and arcward migration of depocenters location. This migration coincides with the change of configuration of the forearc domain (Fig. 11) due to the rejuvenated uplift of the major existing ridges (e.g. Lachlan, Kidnappers and Motuokura ridges).

-Intrabasinal “cannibalism”

As a result of changes in activity of the major faults and the overall shape of the basin, the main depocenters of M2-3 sequences (e.g. in the Lachlan Basin I) are incorporated into the newly uplifting Kidnappers ridge and deeply eroded as they progressively reach the surface whereas M1 sequences developed in newly forming or subsiding sub-basins of the forearc domain (Kidnappers, Mahia, Lachlan II, Motuokura) (Fig 8 and 11). The constant rise of the volume of preserved sediment during the last 430 Ka can be interpreted as the result of the erosion of the older part of the M1 sequences together with the recycling of the older M2-3

into the younger M1 sequences. Because of this probable sediment “cannibalism”, the highest values of preserved sediment fluxes observed after 430Kyrs probably overestimate the sediment supply whereas the lowest values of preserved sediment fluxes measured before 430kyrs may underestimate the sediment supply to the basin. An approximate of the real sediment supply from source areas is probably close to the mean preserved sediment fluxes for the whole 1.1 Ma evaluated at c. 3.8 Mt.yr-1.

- Uplift and denudation of the ranges

The axial ranges correspond to the structural elevation that separate the forearc domain from the volcanic arc and back-arc domain. Their uplift history is complex with several phases of emersion since the onset of subduction 25 Myrs ago (Kamp et al., 2002; Browne, 2004). The last of these growth phases reportedly commenced during early Pleistocene (c. 1.5 Ma) as evidenced by the presence of shallow marine deposits on top of the range (Smale et al., 1978; Beu et al., 1981; Erdman and Kelsey, 1992). The potential increase in sediment supply observed on the Preserved Sediment Fluxes PSF curve at c. 430 ka should normally be accompanied by changes in the geometry of source areas (eg. mean elevation, relief) leading to higher denudation rates (Ahnert, 1970; Pinet and Souriau, 1988, Milliman and Syvitski, 1992). Such increase in mean denudation rate from c. 0.1 mm.yr-1 (M2-3) up to c. 0.2 mm.yr-1 (M1-Seq1) during the last c. 1.1 Ma has not been documented yet. Evidence of increase of uplift in Hawke Bay catchments would be the change of sedimentation conditions observed in the Makaroro Pleistocene section (Raub, 1985; Shane, 1994; Paquet et al, 2008) located at the range front, west of the Ruataniwha Plains in southern Hawke Bay drainage basin (Fig. 2). Sedimentation evolves from fluvial-flood plain deposits (silts, sands and gravels) at c. 1.63 Ma to mostly fluvial channel and fan deposits (gravels) at the top of the section during late Pleistocene. This change may results from an increase of uplift and erosion rates in the axial ranges with the occurrences of landslides (Hovius et al. 1998, Montgomery and Brandon, 2002). Despite the poor age control on the Makaroro section, it appears that the shift occurred during the Mid Pleistocene above the Potaka tephra (after c. 1.0 Ma) and below the top of the section (late Pleistocene, Paquet et al., 2008).

Since the beginning of the Late Pleistocene, the whole Ruataniwha plains have been experienced uplift that increases towards the axial ranges (Litchfield and Berryman, 2006; Paquet et al., 2008). Another additional source of sediments that may develop around c. 430 ka would be the uplifting coastal ranges. The northern part of the coastal ranges may have grown significantly and synchronously with the Pleistocene uplift phase of both the Kidnappers ridge and Elsthorpe anticline during M1 development. This is evidenced by the

westward tilt and the folding of the M2-3 sequences in the Kidnappers Group (Fig. 18 and Appendix 2). The growth of the southern part of the coastal ranges in the Hawke Bay drainage basin is not as well constrained. However, the presence of small patches of Castelcliffian fluvial deposits on top of the ranges (Kingma, 1962) indicates that most of the uplift occurred after c. 1 Ma.

Increasing uplift during Pleistocene within both the coastal ranges and the foothill domains would have resulted in the occurrences of landslides. Such events are documented and mapped in these areas: the deep-seated Kahuranaki Klippe and Kaiwhakapiripiri Range landslides within the coastal ranges (Spörli and Pettinga, 1980; Pettinga 1980, 1982, 2004); several deep-seated landslides along the Esk river in the foothills (Leith, 2003); and a multitude of smaller slides within the Kidnappers Group (this study - Appendix 2). Additional age calibrations are therefore needed to test the hypothesis that proposes uplift of the coastal ranges as a possible contributor to the post M2-3 PSF increase.

Finally, considering the significant erosion that affects the M2-3 sequences, we believe that most of the increase of preserved sediment fluxes at c. 430 ka is a consequence of the contemporaneous changes in the overall forearc basin configuration and in its preservation ability. Further work is needed, on the timing and amplitude of both the uplift and erosion of the ranges, to involve any increase of sediment supply as a cause of the 250 % preserved sediment flux increase at c. 430 ka.

-Tectonic impact on climatic evidences

As discussed above, tectonic deformation is the main factor that controls the record of the long-term preserved sediment fluxes in the Hawke Bay forearc basin and it tends to overwhelm the influence of climate and eustasy on the preserved sediment flux record. Thus the variations in PSF determined from sediment budget are directly proportional to the erosion-preservation ratio. This fact implies that potential records of sediment flux changes through time related to former tectonic and/or climatic causes may have been erased from the preserved sediment flux signal by the last tectonic deformation phase (c. 430 Ka to present day). Therefore, it remains possible (and likely) that climate variations, such as the Mid Pleistocene Transition (MPT), have had significant influence on the long-term sediment flux in Hawke Bay but no evidence is visible anymore on PSF. A possible evidence of long-term sediment flux variation due to the MPT climatic forcing is the progressive building of prominent shelf edges in the set of depositional sequences of M2 and M1 megasequences, within the Motuokura basin (Fig. 5 and 8). This feature developed after S9 (c. 780 Ka) which corresponds indeed to the major phase of the MPT (Head and Gibbard, 2005 and references

therein) with the establishment of major 100 Kyr-type climate fluctuations. Thus the Motuokura basin, as it mostly corresponds to the ultimate sink of the Hawke Bay forearc domain with negligible cannibalism and recycling, is probably the best site for studying the effects of climate variations and especially the MPT on both the sediment flux and the stratigraphic pattern.

5.3-Alternative controls on sediment fluxes

5.3.1-The influence of human settlement

The mean long-term sediment flux value of c. 3.8 Mt.yr-1 (yield: c. 265 t.km-2.yr-1) for the last 1.1 Myrs, is at least three times lower than the present day suspended sediment flux estimation of Hicks and a (2003) at the outlet of Hawke Bay rivers that reaches c. 12 Mt.yr-1 (yield: c. 840 t.km-².yr-1) This difference of 300% between the long and short terms values is in agreement with recent studies of post-glacial deposits in the Waipaoa river-Poverty shelf system, immediately north of Hawke Bay (Foster and Carter, 1997; Orpin et al., 2006; Gomez et al., 2007) where estimated sediment discharge, deduced accumulation rates at MD97-2122 piston core (Poverty Bay shelf), varies from 2 to 4 Mt.yr-1 before European settlement and increase by 400 %, with values up to c. 16 Mt.yr-1 after the dramatic deforestation of the low-relief and headwaters areas and beginning of modern agricultural practices (Gomez et al., 2007). In addition, the potential internal storage of sediments in floodplains has been reduced in the small Hawke Bay floodplains and coastal plains (eg. Ruataniwha and Heretaunga plains) as they have been modified by the building of stopbanks along Ngaruroro and Tukituki rivers. Therefore we assume that the historical increase of the sediment flux of c. 300% is the consequence of the deforestation and the land use (mainly sheep grazing) and land management.

5.3.2-The influence of time scales on sediment fluxes appraisal in Hawke Bay

The estimation of preserved sediment fluxes and their variations during the last c. 1.1 Ma are provided in this study with an incremental resolution of c. 100 Ka (depositional sequence). The increase of the PSF from c. 430 Ka is associated to (1) the increase in tectonic activity, uplift and consecutive erosion and (2) the changes of structural pattern and paleogeographic configurations (cannibalism and recycling). In a recent study of the Hawke Bay late Pleistocene sequence, Paquet et al. (in prep) show that for a 100 Ka time-scale, with a resolution of c. 10 Ka, the PSF, variations of PSF result from Pleistocene abrupt and dramatic climate variations (c. 3.8 Mt.yr-1 for interglacial conditions and c. 4.3 Mt.yr-1 LGM-

Holocene). These observations imply that in an active forearc basin context, long-term (0.5 Ma and over) and short-term (100 Ka and below) changes in sediment fluxes exhibit preferentially, and respectively, the tectonic and climatic influences.

The present day sediment flux estimations in Hawke Bay are 300 % higher than the maximum value for Pleistocene. Agricultural development generally results in a significant increase of denudation and would consecutively increase the sediment fluxes (Syvitski et al., 2005; Wilkinson and McElroy, 2007; Sommerfield and Wheatcroft, 2007). However this observation is counterbalanced by (1) short-term sediment flux measurements that may also underestimate the long-term fluxes (even in anthropized context) as they do not record the rare catastrophic erosion events that deliver most of the sediment discharge (Kirchner et al., 2001; Farnsworth and Milliman, 2007) or (2) the time gap between the increase of denudation and the increase in sediment flux to ocean due to temporary storage of sediments close to the source (tributary rivers, fans…) or within alluvial floodplains and coastal plains (Métivier and Gaudemer, 1999; Phillips, 2003). The geologic and geomorphic characteristics of the river catchments (drainage area, uplift, elevation, relief, slope, lithology of the bedrock…) appear to be critical, with this respect, in their sensitivity to environmental changes including anthropogenic changes (Ahnert, 1970; Pinet and Souriau, 1988; Milliman and Syvitski, 1992; Hovius et al., 1998; Montgomery and Brandon, 2002; Binnie et al., 2007).

Hawke Bay is very responsive to the human deforestation, land use and land management due to the high topography and sharp relief of the drainage basin, the soft, highly erodible substratum lithology (eg. Cenozoic marine siltstones), the changing climatic conditions with high rainfall magnitude and frequencies and the fluvial network configuration. Such conditions were described for the neighbouring Waipaoa river system (Phillips and Gomez, 2007) and for other active margins around the world such as Taiwan and Papua New Guinea, where denudation and landsliding occurs in easily erodible substratum (Hovius et al., 1998). Occurrences of catastrophic events, such as the large cyclone Bola in 1988, every c. 35 years are not required for present day sediment fluxes to encompass longer-term estimations although catastrophic events are systematically accompanied by an increase in sediment discharge (Eden and Page, 1998; Lake Tutira Drilling Group, 2007). This implies that the Hawke Bay drainage basin characteristics (eg. relief, elevation, substratum…) do not constitute any efficient threshold that could limit the increase of erosion and sediment fluxes to the ocean when climatic or anthropogenic changes modify dramatically the environmental conditions.

CONCLUSION

The interpretation of a dense grid of high resolution seismic data covering the Hawke Bay forearc domain, together with correlations to dated samples and sections, provides an opportunity to access the three-dimensional geometry of the age-calibrated stratigraphic record. Interpretations reveal the existence of four sub-basins (Motuokura, Lachlan (I & II), Mahia and Kidnappers basins) where eleven elementary depositional sequences (Seq11 to Seq1) and the overlying post-glacial (post-LGM) wedge (Seq0) developed during the Castelcliffian-Haweran stages (c. 1.1 Ma to present day). The origin of these sequences is related to the 41- to 100-Kyr periods that characterize the Pleistocene climatically controlled eustasy. The eleven depositional sequences show an overall retrogradational trend over a basin-wide diachronic composite erosion unconformity formed by the lateral succession of the 12 sequence-bounding unconformities (S12 to S1). The stacking pattern of sequences reveals the existence of one tectonically-induced major regional unconformities within the sedimentary succession (S5, c. 430 ka) that reflect phases of tectonic activity (increased vertical displacement rates). This unconformity individualize two regional megasequences (M2-3: Seq11 to Seq5 and M1: Seq4 to Seq1). Both significant changes in the tectonic activity and the rise of the Kidnappers Ridge at c. 430 ka (S5) result in a significant change in the Hawke Bay forearc domain configuration that evolves from “branching lens” to “arched string geometry. The overall retrogradation is associated to a general landward-arcward migration of both the subsidence (sequence depocenters location) and the activity of thrust faults. Such migration of the subsidence is attributed to the interplay between the tectonic activities of the thrust faults (eg. Motuokura, Lachlan and Kidnappers ridges) and the sediment-load-induced isostasy. Control on the three-dimensional geometry of the sequences allows incremental volume and preserved sediment flux (PSF) estimations for the last 1.1 Ma. Sediments preserved over the studied area, within the sub-basins, account for most (c. 85 %) of the sediment delivered by the Hawke Bay drainage basin during the last 1.1 Ma (estimated values). The evolution of the PSF shows two distinct phases: (1) a first phase characterized by almost constant fluxes (2.8±0.3 Mt.yr-1) from c. 1.1 Ma and 430 ka and (2) a second phase from c. 430 ka to Late Pleistocene characterized by an increase of PSF from c. 4.6 to c. 6.2 Mt.yr-1 (250 % of increase). These two phases are correlated to the two successive configurations of the Hawke Bay forearc domain. We infer that the evolution of PSF over 1 Myr time-scale, in the Hawke Bay forearc results from the combined effects of both the tectonically-induced change in configuration and the efficient cannibalism of the older M2-

3sequences. Therefore, PSF reflects the change in the long-term preservation potential that is mostly controlled by tectonic processes and does not systematically reflect the true sediment delivery from the drainage basin. Tectonic or climatic processes that may affect the drainage area and modify the sediment delivery are progressively erased from the PSF signal as the basin configuration changes. However, climate impact on sediment fluxes is recorded on shorter time-scale (100 kyr) as evidenced for the Late Pleistocene depositional sequence (Paquet et al., 2008). Comparison of past sediment fluxes (1 Myr to 100 kyr) to present day estimation shows an increase of c. 300 % attributed to the effects of post-European-settlement deforestation and land use. This significant increase also confirms that the geologic and geomorphologic conditions (uplift, elevation, relief) and the easily erodible substratum (marine silts) are very responsive to environmental changes. This implies that long-term climate events such as the Mid Pleistocene Transition would have had an effect on the sediment delivery as possibly illustrated by the building of prominent shelf edges in the Motuokura basin since c. 780 kyr.

Acknowledgements :

This study was funded by the CNRS-INSU, CNRS Research Department n°6118 – 'Géosciences Rennes', the University of Rennes 1, the 'Active Tectonics and Earthquake Hazards Research Program' at the University of Canterbury. French Ministry of Foreign Affairs.

NIWA for access to the extensive seismic data set and acquisition of new data, ship time..

The IPEV and Marion-Dufresne II crew for Calypso long piston-cores acquisition…

This research project was undertaken under a co-tutelle agreement between Université de Rennes 1 and University of Canterbury.

REFERENCES

Ahnert F. 1970. Functional relationships between denudation, relief and uplift in large mid-latitude drainage basins. American Journal of Science 268: 243-263.

Allen PA, Densmore AL. 2000. Sediment flux from an uplifting fault block. Basin Research 12: 367-380.

Ballance PF. 1976. Evolution of the upper Cenozoic magmatic arc and plate boundary in northern New Zealand. Earth and planetary science letters 28: 356-370.

Barnes PM, Mercier de Lépinay B. 1997. Rates and mechanics of rapid frontal accretion along the very obliquely convergent southern Hikurangi margin, New Zealand. Journal Geophysical Research 102: 24 931–24 952.

Barnes PM, Cheung KC, Smits AP, Almagor G, Read SAL, Barker PR, Froggatt P. 1991: Geotechnical analysis of the Kidnappers Slide, upper continental slope, New Zealand. Marine geotechnology 10: 159-188.

Barnes PM, Nicol A, Harrison T. 2002. Late Cenozoic evolution and earthquake potential of an active listric thrust complex above the Hikurangi subduction zone, New Zealand. Geological Society of America Bulletin 114: 1379–1405.

Barnes PM, Nicol A. 2004. Formation of an active thrust triangle zone associated with structural inversion in subducting setting, eastern New Zealand. Tectonics 23(1): TC1015.
Barrier L, Nalpas T, Gapais D, Proust JN, Cassas A, Bourquin S. 2002. Influence of syntectonic sedimentation on thrust geometry. Field examples from the Iberian Chain (Spain) and analogue modelling. Sedimentary Geology 146: 91-104.

B.C.M. Geophysics Ltd. 1989. Report on a land seismic survey on PPL38320, Hawkes Bay, New Zealand. (C89 survey). New Zealand unpublished open-file petroleum report 1522. Ministry of Economic Development, Wellington.

Beanland S, Melhuish A, Nicol A, Ravens J. 1998. Structure and deformation history of the inner forearc region, Hikurangi subduction margin, New Zealand. New Zealand Journal of Geology and Geophysics 41: 325–342.

Berger A. 1978. Long-term variations of daily insolation and Quaternary climatic changes. Journal Atmospheric Science 35: 1379-1405.

Beu AG, Browne GH, Grant-Taylor TL. 1981. New Chlamys delicatula localities in the central North Island and uplift of the Ruahine Range. New Zealand Journal of Geology and Geophysics 24: 127-132.

Beu AG, Pillans B. 1987. A review of New Zealand Pleistocene stratigraphy with emphasis on marine rocks. In Proceedings of the First International Colloquium on Quaternary Stratigraphy of Asia and Pacific Area, Osaka, 1986, Itihara M, Kamel T (eds): 250–269.

Binnie SA, Phillips WM, Summerfield MA, Fifield LK. 2007. Tectonic uplift, threshold hillslopes, and denudation rates in a developing mountain range. Geology 35: 743-746.

Bowen DQ, Pillans B, Sykes GA, Beu AG, Edwards AR, Kamp PJJ, Hull AG. 1998. Amino acid geochronology of Pleistocene marine sediments in the Wanganui Basin: a New Zealand framework for correlation and dating. Journal of the Geological Society London 155: 439–446.

Brown, L.J., 1993, Heretaunga Plains ground water resource investigations - Flaxmere and Tollemache Orchard exploratory water wells, Institute of Geological & Nuclear Sciences Ltd Report 1993/732402-11: 24 pp.

Brown, L.J. & Gibbs, B.R., 1996, Heretaunga Plains Ground Water Resource Investigations – Awatoto Exploratory Water Well – HBRC Well No. 3699, Institute of Geological & Nuclear Sciences Ltd Report 1996/735102: 93 pp.

Browne GH. 2004. Late Neogene sedimentation adjacent to the tectonically evolving North Island axial ranges: insights from Kuripapango, western Hawke's Bay. New Zealand Journal of Geology and Geophysics 47: 663-674.

Burger RL, Fulthorpe CS, Austin Jr JA, Gulick SPS. 2002. Lower Pleistocene to present structural deformation and sequence stratigraphy of the continental shelf, offshore Eel iver Basin, northern California. Marine Geology 185: 249-281.

Carter L, Manighetti B. 2006. Glacial/interglacial control of terrigenous and biogenic fluxes in the deep ocean off a high input collisional margin: 1 139 kyr-record from New Zealand. Marine Geology 226: 307-322.

Carter RM, Naish TR. 1998a. A review of Wanganui Basin, New Zealand: global reference section for shallow marine, Plio–Pleistocene (2.5–0 Ma) cyclostratigraphy. Sedimentary Geology 122: 37-52.

Carter RM, Naish TR. 1998b. Have local stages outlived their usefulness for the New Zealand Pliocene-Pleistocene? New Zealand Journal of Geology and Geophysics 41: 271-279.

Cashman SM, Kelsey HM. 1990. Forearc uplift and extension, southern Hawke's Bay, New Zealand: Mid-Pleistocene to present. Tectonics 9: 23-44.

Castelltort S, Van Den Driessche. 2003. How plausible are high-frequency sediment supply-driven cycles in the stratigraphic record? Sedimentary Geology 157 : 3-13.

Chanier F. 1991. Le Prisme d'accrétion Hikurangi: un témoin de l'évolution géodynamique d'une marge active péripacifique (Nouvelle-Zélande). Thèse de Doctorat de l'Université des Sciences et Techniques de Lille – Flandres-Artois.

Chanier F, Ferrière J, Angelier J. 1999. Extensional deformation across an active margin, relations with subsidence, uplift and rotations: the Hikurangi subduction, New Zealand. Tectonics 18: 862–876.

Cole JW, Lewis KB (1981) Evolution of the Taupo-Hikurangi subduction system. Tectonophys 72:1–21

Collot J-Y, Delteil J, Herzer RH, Wood R, Lewis KB. 1995. Sonic imaging reveals new plate boundary structures off shore New Zealand. EOS 76: 4-5.

Collot J-Y, Delteil J, Lewis KB, Davy B, Lamarche G, Audru J-C, Barnes P, Chanier F, Chaumillon E, Lallemand S, de Lépinay BMD, Orpin AR, Pelletier B, Sosson M, Toussaint B, Uruski C. 1996. From oblique subduction to intra-continental transpression: structures of the southern Kermadec-Hikurangi margin from multibeam bathymetry, side-scan sonar and seismic reflection. Marine Geophysical Researches 18: 357–381.

Collot J-Y, Lewis KB, Lamarche G, Lallemand S. 2001. The giant Ruatoria debris avalanche on the northern Hikurangi margin, New Zealand; results of oblique seamount subduction. Journal of Geophysical Research B: Solid Earth and Planets 106: 19271-19297.

Conquest Exploration. 1988. Conquest Exploration 1988 seismic survey, AG and S lines, PPL 38321. New Zealand unpublished open-file petroleum report 2059. Ministry of Economic Development, Wellington.

Conquest Exploration Co. 1989. Hawkes Bay shallow seismic and bottom sampling 38322 New Zealand. New Zealand unpublished open-file petroleum report 1471. Ministry of Economic Development, Wellington.

Coulbourne WT, Moberley R.1977. Structural evidence of the evolution of fore-arc basins off South America. Canadian Journal of Earth Sciences 14: 102-116.

Dickinson WR. 1995. Forearc Basins. In Tectonics of Sedimentary Basins., Busby CJ, Ingersoll RV. (eds). Blackwell Science, Cambridge : 221-261.

Dickinson WR, Seely DR. 1979. Structure and stratigraphy of forearc regions. American Association of Petroleum Geologists Bulletin 63: 2-31.

Dominguez S, Lallemand SE, Malavieille J, von Huene R. 1998. Upper plate deformation associated with seamount subduction. Tectonophysics 293: 207-224.

Dravid PN, Brown LJ. 1997. Heretaunga Plains—Groundwater study, Vol. I & II. Napier, New Zealand. Hawke's Bay Regional Council: 254 pp.

Eden DN, Page MJ.1998. Palaeoclimatic implications of a storm erosion record from late Holocene lake sediments, North Island, New Zealand. Palaeogeography Palaeoclimatology. Palaeoecology 139: 37-58.

Erdman CF, Kelsey HM. 1992. Pliocene and Pleistocene stratigraphy and tectonics, Ohara Depression and Wakarara Range, North Island, New Zealand. New Zealand Journal of Geology and Geophysics 35: 177-192.

Farnsworth KL, Milliman JD. 2003. Effects of climatic and anthropogenic change on small mountainous rivers: the Salinas River example. Global and Planetary Change 39: 53-64.

Field BD, Uruski CI and others. 1997. Cretaceous-Cenozoic geology and petroleum systems of the East Coast region, New Zealand. Institute of Geological & Nuclear Sciences Monograph 19. Institute of Geological & Nuclear SciencesLimited, Lower Hutt, New Zealand: 301pp.

Fleming CA. 1953. The geology of the Wanganui Subdivision. Bulletin of the Geological Society of New Zealand 52: 362.

Foster G, Carter L. 1997. Mud sedimentation on the continental shelf at an accretionary margin—Poverty Bay, New Zealand. New Zealand Journal of Geology and Geophysics 40, 157–173.

Geo-Prakla. 2000. Wairarapa & Hawke Bay 2D Seismic Survey – WE00 Hawke Bay. PEP 38325. New Zealand unpublished open-file petroleum report 2483. Ministry of Economic Development, Wellington.

Gomez B, Carter L, Trustrum NA. In press. A 2400 yr record of natural events and anthropogenic impacts in inter-correlated terrestrial and marine sediment cores: Waipaoa Sedimentary System, New Zealand. Geological Society of America Bulletin, doi: 10.1140/B259961.

Gradstein FM, Ogg JG, Smith AG, Agterberg FP, Bleeker W, Cooper RA, Davydov V, Gibbard P, Hinnov LA, House MR, Lourens L, Luterbacher H-P, McArthur J, Melchin MJ, Robb LJ, Shergold J, Villeneuve M, Wardlaw BR, Ali J, Brinkhuis H, Hilgen FJ, Hooker J, Howarth RJ, Knoll AH, Laskar J, Monechi S, Powell J, Plumb KA, Raffi I, Röhl U, Sanfilippo A, Schmitz B, Shackleton NJ, Shields GA, Strauss H, Van Dam J, Veizer J, van Kolfschoten Th, Wilson D. 2004a. A Geologic Time Scale 2004. Cambridge University Press, 610 pp.

Gradstein FM, Ogg JG, Smith AG, Bleeker W, Lourens LJ. 2004b. A new Geologic Time Scale, with special reference to Precambrian and Neogene. Episodes 27: 83-100.

Head MJ, Gibbard PL. 2005. Early-Middle Pleistocene transitions: an overview and recommendation for the defining boundary. In Early-Middle Pleistocene Transitions: The land-Ocean Evidence., Head MJ, Gibbard PL. (eds). Geological Society, London, Special Publications 247: 1-18.

Heffer K, Milne AD, Simpson C. 1976. BP, Shell Aquitaine and Todd Petroleum Development Ltd, Well completion report, Hawke Bay-1, Offshore east coast, North Island, New Zealand: Wellington, Ministry of Economic Development – Crown Minerals, Open-File Petroleum Report 667: 61pp.

Hicks DM, Shankar U. 2003. Sediment yield from New Zealand rivers. NIWA Chart, Miscellaneous Series 79.

Hovius N, Stark CP, Tutton MA, Abbott LD. 1998. Landslide-driven network evolution in a pre-steady-state mountain belt: Finisterre Mountains, Papua New Guinea. Geology 26: 1071-1074.

Hull AG. 1985. Late Quaternary geology of the Cape Kidnappers area, Hawkes Bay, New Zealand. MSc thesis, Victoria University, Wellington, New Zealand.

Hull AG. 1987. A late Holocene uplifted shore platform on the Kidnappers coast, North Island, New Zealand. some implications for shore platform development processes and uplift mechanism. Quaternary Research 28: 183-195.

Hull AG. 1990. Tectonics of the 1931 Hawke Bay earthquake. New Zealand Journal Geology and Geophysics 33: 309-320.

Kamp PJJ. 1978. Stratigraphy and sedimentology of conglomerates in the Pleistocene Kidnappers Group, Hawkes Bay. Unpublished MSc thesis, University of Waikato, Hamilton, New Zealand

Kamp PJJ, Turner G. 1990. Pleistocene unconformity-bounded shelf sequences (Wanganui basin, New Zealand), correlated with the global isotope record. Sedimentary Geology 68: 155-161.

Kamp PJJ, Vonk AJ, Bland KJ, Griffin AG, Hayton S, Hendy AJW, McIntyre AP, Nelson CS, Naish T. 2002. Megasequence architecture of Taranaki, Wanganui, and King Country basins and Neogene progradation of two continental margin wedges across western New Zealand. Proceedings of the New Zealand Petroleum Exploration Conference, Auckland, February 2002: 464–481.

Kingma JT. 1962. Sheet 11—Dannevirke. Geological map of New Zealand 1:250 000. Wellington, New Zealand Department of Scientific and Industrial Research.

Kingma, J.T., 1970: Sheets N134 Napier and Hastings, N135 Kidnappers (1st Ed.). Geological Map of New Zealand 1:63,360. Department of Scientific and Industrial Research, Wellington, New Zealand.

Kingma JT. 1971. Geology of the Te Aute subdivision. New Zealand Geological Survey bulletin 70: 173 pp.

Kirchner JW, Finkel RC, Riebe RC, Granger DE, Clayton JL, King JG, Megahan WF. 2001. Mountain erosion over 10 yr, 10 k.y., and 10 m.y. time scales. Geology 29: 591-594.

Lake Tutira Drilling Group. 2007. Eight thousand years of storms and droughts. Water & Atmosphere 15: 24-25.

Lamarche G, Barnes PM, Bull JM. 2006. Faulting and extension rate over the last 20,000 years in the offshore Whakatane Graben, New Zealand continental shelf. Tectonics 25: doi: 10.1029/2005TC001886.

Laursen J, Scholl DW, von Huene R. 2002. Neotectonic deformation of the central Chile margin: Deepwater forearc basin formation in response to hot spot ridge and seamount subduction. Tectonics 21: doi: 10.1029/2001TC901023.

Laursen J, Normack WR. 2003. Impact of structural and autocyclic basin-floor topography on the depositional evolution of the deep-water Valparaiso forearc basin, central Chile. Basin Research 15: 201-226.

Leith KJ. 2003. The role of deep-seated landslide in the geomorphic evolution of the Esk Valley, Hawke's Bay: An innovative approach to hazard evaluation. Unpublished MSc thesis, University of Canterbury, Christchurch, New Zealand.

Lewis KB. 1971a. Growth rate of folds using tilted wave planed surfaces: coast and continental shelf, Hawke's Bay, New Zealand. In: Collins, B. W.; Fraser, R. ed. Recent crustal movements. The Royal Society of New Zealand Bulletin 9: 225-231.

Lewis KB. 1973b. Sediments on the continental shelf and slope between Napier and Castelpoint, New Zealand. New Zealand journal of marine and freshwater research 7: 183-208.

Lewis KB. 1974. Upper Tertiary rocks from the continental shelf and slope of Southern Hawke's Bay. New Zealand journal of marine and freshwater research 8: 663-670.

Lewis SD, Hayes DE. 1984. A Geophysical Study of the Manila Trench, Luzon, Philippines 2. Fore Arc Basin Structural and Stratigraphic Evolution. Journal of Geophysical Research 89: 9196-9214.

Lewis KB, Pettinga JR. 1993. The emerging, imbricate frontal wedge of the Hikurangi margin. In: South Pacific sedimentary basins. Sedimentary Basins of the World 2, Basins of the Southwest Pacific, Ballance PF (ed.). Elsevier, Amsterdam: 225-250.

Lewis KB, Collot J-Y, Lallemand SE. 1998. The dammed Hikurangi Trough: a channel-fed trench blocked by subducting seamounts and their wake avalanches (New Zealand-France GeodyNZ Project). Basin Research 10: 441-468.

Lewis KB, Lallemand S, Carter L. 2004. Collapse in a Quaternary shelf basin off East Cape, New Zealand: evidence for passage of a subducted seamount inboard of the Ruatoria giant avalanche. New Zealand Journal of Geology and Geophysics 47 415-429.

Lisiecki LE, Raymo ME. 2005. A Pliocene-Pleistocene stack of 57 globally distributed benthic δ18O records. Paleoceanography 20: PA1003, doi:10.1029/2004PA001071.

Litchfield NJ, Berryman KR. 2005. Correlation of fluvial terraces within the Hikurangi Margin, New Zealand: Implications for climate and base level controls. Geomorphology 68: 291-313.

Litchfield NJ, Berryman KR. 2006. Relations between postglacial fluvial incision rates and uplift rates in North Island, New Zealand. Journal of Geophysical Research 111: doi:10.1029/2005JF000374.

Métivier F, Gaudemer Y.1999. Stability of output fluxes of large rivers in South and East Asia during the last 2 million years: implications on floodplain processes. Basin Research 11: 293-303.

Milankovitch MM. 1941. Kanon der Erdbestrahlung und seine Anwendung auf das Eizeitenproblem. Serbian Royal Academy Special Edition: Belgrade.

Milliman JD, Syvitski JPM. 1992. Geomorphic/tectonic control on sediment discharge to the ocean: the importance of small mountain rivers. Journal of Geology 100: 524-544.

Molnar P, England P. 1990. Late Cenozoic uplift of mountain ranges and global climate change: chicken or egg? Nature 346: 29-34.

Montgomery DR, Brandon MT. 2002. Topographic controls on erosion rates in tectonically active mountain ranges. Earth and Planetary Science Letters 201: 481-489.

Mountney NP, Westbrook GK. 1997. Quantitative analysis of Miocene to Recent forearc basin evolution along the Colombian convergent margin. Basin Research 9: 177-196.

Multiwave. 2005. 05CM 2D Seismic Survey, Offshore East Coast - North Island. New Zealand unpublished openfile petroleum report 3136. Ministry of Economic Development, Wellington.

Murray-Wallace CV. 2007. Eustatic Sea-Level Changes Glacial-Interglacial Cycles. In Encyclopedia of Quaternary Science. Elias SA (ed). Elsevier, Amsterdam: 3024-3034.

Naish T, Kamp PJJ. 1997. Sequence stratigraphy of the sixth-order (41 k.y.) Pliocene-Pleistocene cyclothems, Wanganui basin, New Zealand: A case for the regressive system tract. Geological Society of America Bulletin 109: 978-999.

Naish T, Abbott ST, Alloway BV, Beu AG, Carter RM, Edwards AR Journeaux TD, Kamp PJJ, Pillans BJ, Saul G, Woolfe KJ. 1998. Astronomical calibration of a southern hemisphere Plio-Pleistocene reference section, Wanganui basin, New Zealand. Quaternary Science Reviews 17: 695-710.

Naish TR, Field BD, Zhu H, Melhuish A, Carter RM, Abbott ST, Edwards S, Alloway BV, Wilson GS, Niessen F, Barker A, Browne GH, Maslen G. 2005. Integrated outcrop, drill core, borehale and seismic stratigraphic architecture of a cyclothemic, shallow-marine depositional system, Wanganui Basin, New Zealand. Journal of the Royal Society of New Zealand 35: 91-122.

Nees S, Jellinek T, Suhohen J, Winkler A, Helmke J, Emmermann P and Shipboard Scientific Party. 1998. Images III—IPHIS. Indian and Pacific Ocean Pleistocene and Holocene History: an images Study. Cruise MD106—Lef 1.2; RV Marion Dufresne II, Hobart (Australia)—Christchurch (New Zealand) May 6 to May 21, 1997.

Nicol A, Wallace LM. 2007. Temporal stability of deformation rates: Comparison of geological and geodetic observations, Hikurangi subduction margin, New Zealand. Earth and Planetary Science Letters 258: 397-413.

Nicol A, Mazengarb C, Chanier F, Rait G, Uruski C, Wallace L. 2007. Tectonic evolution of the Hikurangi subduction margin, New Zealand, since Oligocene. Tectonics 26: doi: 10.1029/2006TC002090.

Orpin AR, Alexander C, Carter L, Kuehl S, Walsh JP. 2006. Temporal and spatial complexity in post-glacial sedimentation on the tectonically active, Poverty Bay continental margin of New Zealand. Continental Shelf Research 26: 2205-2224.

Ozolins V, Francis D. 2000. Whakatu-1 Well Completion Report PEP 38328– Indo-Pacific Energy (NZ) Ltd: Wellington, Ministry of Economic Development – Crown Minerals, Open-File Petroleum Report 2476: 496 pp.

Paquet F, Proust J-N, Barnes PM, Pettinga JR. 2008. Late Pleistocene sedimentation in Hawke Bay, New Zealand: new insights into forearc basin morphostructural evolution. Submitted to Journal of Quaternary Science.

Pettinga JR. 1980. Geology and landslides of the eastern Te Aute District, southern Hawke's Bay. Unpublished PhD thesis, University of Auckland Library, Auckland, New Zealand.

Pettinga JR. 1982. Upper Cenozoic structural history, coastal southern Hawke's Bay, New Zealand. New Zealand journal of geology and geophysics 25: 149-19 1.

Pettinga JR, 2004. Three-stage massive gravitational collapse of the emerging imbricate frontal wedge, Hikurangi Subduction Zone, New Zealand. New Zealand Journal of Geology & Geophysics 47: 399-414.

Phillips JD. 2003. Alluvial storage and the long term stability of sediment yields. Basin Research 15: 153-163.

Phillips JD, Gomez B. 2007. Controls on sediment export from the Waipaoa River basin, New Zealand. Basin Research 19: 241-252.

Pillans B. 1986. A late Quaternary uplift map for North Island, New Zealand. In Recent crustal movements of the Pacific region, Reilly, W.l., Harford, B.E. (eds). Royal Society of New Zealand bulletin 24: 409-417.

Pillans, B. (2003). Subdividing the Pleistocene using the Matuyama-Brunhes boundary (MBB): An Australasian perspective. Quaternary Science Reviews 22, 1569–1577.

Pinet P, Souriau M. 1988. Continental erosion and large-scale relief. Tectonics 7: 563-582.

Proust J-N, Chanier F. 2004. The Pleistocene Cape Kidnappers section in New Zealand : orbitally forced controls on active margin sedimentation? Journal of Quaternary Science 19: 591-603.

Proust J-N, Lamarche G, Nodder S, Kamp PJJ. 2005. Sedimentary architecture of a Plio-Pleistocene proto-back-arc basin: Wanganui, New Zealand. Sedimentary Geology 181: 107-145.

Proust J-N, Lamarche G, Migeon S, Neil H, and Shipboard party. 2006. MD152 / MATACORE "Tectonic and climate controls on sediment budget". Les rapports de campagnes à la mer : pp. 107.

Raub ML. 1985. The neotectonic evolution of the Wakarara area, M.Sc. thesis, Auckland Univ., Auckland, New Zealand: pp. 122.

Saul G, Naish TR, Abbot ST, Carter RM.1999. Sedimentary cyclicity in the marine Pliocene-Pleistocene of the Wanganui basin (New Zealand): Sequence stratigraphic motifs characteristic of the past 2.5 m.y. Geological Society of America Bulletin 111: 524-537.

Schlumberger Geco Prakla. 1998. Seismic survey, PEP 38332, Hawkes Bay, IP332-98 lines and IP332-99 lines. New Zealand unpublished open-file petroleum report 2392. Ministry of Economic Development, Wellington.

Schlumberger Geco Prakla. 1998. Hawkes Bay seismic survey, PEP 38328, IP328-98 lines and IP328-99 lines. New Zealand unpublished open-file petroleum report 2393. Ministry of Economic Development, Wellington.

Shackleton NJ, Berger A, Peltier WR. 1990. An alternative astronomical calibration of the lower Pleistocene timescale based on ODP Site 677. Transactions Royal Society Edinburgh Earth Sciences 81: 251–261.

Shackleton NJ, Crowhurst S, Hagelberg T, Pisias N G, Schneider DA. 1995. A new late Neogene time scale: application to Leg 138 sites. In Pisias NG, Mayer LA, Janecek TR, Palmer-Julsen A, van Andel TH (eds). Proceedings of the Ocean Drilling Program Scientific Results 138:73-101.

Shane PAR. 1994. A widespread, early Pleistocene tephra (Potaka tephra, 1 Ma) in New Zealand: Character, distribution, and implications. New Zealand Journal of Geology and Geophysics 37: 25-35.

Shane PAR, Black TM, Alloway BV, Westgate JA 1996. Early to middle Pleistocene tephrochronology of North Island, New Zealand: implications for volcanism, tectonism, and paleoenvironments. Geological Society of America Bulletin 108: 915–925.

Smale D, Houghton BF, McKellar IC, Mansergh GD, Moore PR. 1978. Geology and erosion in the Ruahine Range: a reconnaissance study. In Geology and erosion in the Ruahine Range, Speden, I. (ed.). New Zealand Geologicalsurvey report G20: 7-30.

Small M, & others. 1997. Hawkes Bay seismic survey, PEP38328, IP328-97 lines. New Zealand unpublished open-file petroleum report 2299. Ministry of Economic Development, Wellington.

Sommerfield CK, Wheatcroft RA. 2007. Late Holocene sediment accumulation on the northern Californian shelf: Oceanic, fluvial, and anthropogenic influences. Geological Society of America Bulletin doi: 10.1130/B26019.1.

Spörli KB, Pettinga JR. 1980. Mount Kahuranaki, Hawkes Bay, New Zealand, A Klippe Emplaced by Gravity sliding from the Crest of the Nearby Elsthorpe Anticline. Journal of the Royal Society of New Zealand 10: 287-307.

Spörli KB, Ballance PF. 1989. Mesozoic-Cenozoic ocean floor-continent interaction and terrane configuration, southwest Pacific area around New Zealand. In. Mesozoic and Cenozoic evolution of the Pacific Ocean margins, Ben Avraham Z. (ed.). Oxford University Monograph, geology and geophysics 8: 176-190.

Strong CP, Scott GH, Edwards AR. 1989. Foraminifera and calcareous nannoplankton from Hawke's Bay sea floor samples PPL 38321 PPL 38322 PPL 38323. New Zealand unpublished openfile Petroleum Report 1470. Ministry of Economic Development, Wellington.

Sullivan D. 1990. 2D Marine Seismic Survey Acquisition Report PPL 38322, PPL 38321. New Zealand unpublished openfile Petroleum Report 1666. Ministry of Economic Development, Wellington.

Syvitski JPM, Vörösmarty CJ, Kettner AJ, Green PA. 2005. Impact of humans on the flux of terrestrial sediment to the global coastal ocean. Science 308: 376-380.

Von Huene R, Arthur MA. 1982. Sedimentation across the Japan Trench off northern Honshu Island. In Trench-ForearcGeology. Leggett JK (ed). Geological Society, London, Special Publication 10: 27-48.

Villamor P, Berryman KR. 2006. Evolution of the southern termination of the Taupo Rift, New Zealand. New Zealand Journal of Geology and Geophysics 49: 23-37.

Wilkinson BH, McElroy BJ. 2007. The impact of humans on continental erosion and sedimentation. Geological Society of America Bulletin 119: 140-156.

FIGURES CAPTIONS

Figure 1:

Tectonic setting of the active Hikurangi subduction margin. (A) Australian-Pacific plate boundary and relative motion in the New Zealand region. Light gray shading corresponds to submerged continental crust and dark gray shading represents the emergent continental crust

of the New Zealand micro-continent. (B) Arrangement of the major morphostructural elements of the Hikurangi subduction margin in the North Island including the Hikurangi Trough, the imbricate frontal wedge emergent in the coastal ranges, the Neogene forearc basin, the axial ranges and the backarc basins (See descriptions in the text). The location of both Mio-Pliocene and Pleistocene volcanic arcs reflects the progressive rotation of the margin. The dashed line A-A' corresponds to the trace of the crustal cross section. (C) Map showing the arrangement of the characteristic morphostructural elements in the Hawke's Bay region. (D) Crustal cross section A-A' modified from Beanland (1995), Begg et al. (1996) and Barnes et al. (2002) showing the structure of the central part of the subduction margin. RF: Ruahine Fault; MF: Mohaka Fault; KR: Kidnappers Ridge; LB: Lachlan Basin; LR: Lachlan Ridge; MR: Motuokura Ridge.

Figure 2:

Map showing the current Hawke's Bay onshore topography and offshore bathymetry and the main tectonic structures. The bathymetry contours (every 50 m) and illuminated digital elevation model are from Collot et al. (1994, 1995, 1996), Lewis et al. (1997) and unpublished data acquired by NIWA. The topographic illuminated digital elevation model is from the NZTopo digital elevation model (Land Information New Zealand). The dashed line limits the Hawke Bay drainage basin.

Figure 3:

Location map of seismic surveys, long piston cores and wells used for this study. Seismic profiles that appear in figures (sections) are respectively in bold solid black lines with reference to the figure number. See details of surveys in table X.

Figure 4:

Interpreted seismic profile 05CM29 detailing the elementary 100 Ka depositional sequences in the Motuokura basin. See figure 3 for location. TS 1 and 2 are labelled in open circles.

Figure 5:

Interpreted seismic profile 05CM29 showing the stacking pattern of the eleven depositional sequences in the Motuokura basin and the facies distribution in each sequence. See figure 3 for location and figure 4 for the facies interpretation legend. The twelve transgressive surfaces (TS) are labelled in open circles.

Figure 6:

Interpreted seismic profile 05CM41 showing the stacking pattern of the eleven depositional sequences from the Lachlan basin to the Motuokura basin and the facies distribution in each sequence. See figure 3 for location and figure 4 for the facies interpretation legend. The twelve transgressive surfaces (TS) are labelled in open circles.

Figure 7:

Interpreted seismic profile 05CM03 showing the stacking pattern of the eleven depositional sequences from the Kidnappers/Mahia basin to the Lachlan basin and the facies distribution in each sequence. See figure 3 for location and figure 4 for the facies interpretation legend. The twelve transgressive surfaces (TS) are labelled in open circles.

Figure 8:

Series of EW interpreted seismic profiles showing the geometry of the eleven depositional sequences. See figure 3 for location.

Figure 9:

Series of NS interpreted seismic profiles showing the geometry of the eleven depositional sequences. See figure 3 for location and figure 8 for legend.

Figure 10:

Correlation of the Hawke Bay seismic stratigraphy to marine core, well and dredge samples (Heffer et al., 1976; Strong et al., 1989; Barnes et al., 1991; Proust et al., 2006); to the onshore Awatoto testbore (Dravid and Brown, 1997; Paquet et al., 2008) and to the Kidnappers Group section (Proust and Chanier, 2004 and reference therein); to the isotope stratigraphy (δ18O) / climato-eustatic curve (Lisiecki and Raymo, 2005; Shackleton et al., 1990); to the magnetostratigraphiy scale (Gradstein et al., 2004) and to the International and New Zealand stratigraphy (ICS, 2004; Naish et al., 1998). Details on dated samples are summarized on appendix 3. RG: Rabbit Gully ignimbrite; PT: Potaka Tephra. See figure 3 for sample and section locations.

Figure 11:

Isopach maps of the eleven depositional sequences (Seq11 to Seq1) and the post-glacial wedge (Seq0) identified from seismic data interpretation. Estimated thicknesses result from approximate time-depth conversions with linear increase of the average velocity deduced from seismic data (Multiwave, 2005). The successive maps show (1) the progressive landward-arc ward migration of the sequences and associated depocenters through time and the change in the forearc configuration from "branching lens" geometry (Seq11 to Seq5) to "arched string" geometry (Seq5 to Seq1) that occurred at c. 430 ka (S5). And (2) the formation and the evolution of the sub-basins (Motuokura, Lachlan I & II, Mahia and Kidnappers basins). The main tectonic structures are visible as solid (presumed active) or dashed (presumed inactive) black lines. Age boundaries of each depositional sequence is indicative. See text for details.

Figure 12:

Diagrams showing the evolution of the preserved sequences area and preserved sediment volumes, masses and fluxes. (a) Diagram showing the preserved volume and surface estimations for each of the eleven depositional sequences and for the post-glacial wedge (Seq0). Note their joint evolution with an almost proportionality trend. (b) Diagram showing the difference between deposited volume estimations and compacted preserved sediment volumes (0% of porosity) for each of the eleven sequences and the post-glacial wedge (Seq0). (c) Diagram showing the preserved sediment fluxes within each of the eleven depositional sequences, the post-glacial wedge (Seq0) and the present day estimation (PD) from Hicks and Shankar (2003). MoB: Motuokura basin megasequences; HBB: Regional megasequences for the whole Hawke Bay forearc basin.

Figure 13:

(a) Simplified structural map of the Hawke Bay forearc domain showing the main tectonic structures and the position of the four margin-normal transects used for determining the timing and amplitude of the structure activity. (b to e): Analysis of the timing and amplitude of structural activity along four margin-normal transects during the last c. 1.1 Ma. Results for each transect are plotted on graphics that display incremental vertical displacement rates of the structures. Time increments correspond to the eleven sequences determined from the stratigraphic framework. Line width is proportional to the incremental vertical displacement rates (mm.yr-1) deduced from growth strata and vertical separations. Dashed lines, white stars

and black cross indicate respectively possible undocumented activity, inferred increase in activity and cessation of activity (See text for details). Data on the Lachlan fault (segment III) are revised values from Barnes et al. (2002) considering the new stratigraphy developed in this study.

Mo (N/C/S): Motuokura Ridge (North/Central/South); K: Kairakau Faults; W: Waimarama Faults; KFS: Kidnappers Fault South; KF: Kidnappers Fault; LB: Lachlan Basin Fault; LS: Lachlan Fault South; L: Lachlan Fault; KR: Kidnappers Ridge.

Figure 14:

Interpreted seismic profile 05CM28 corresponding to the margin-normal transect of figure 13c and showing the stacking pattern of (1) the depositional sequences in the Motuokura basin, (2) the position of the shelf edge and (3) the joint landward-arcward migration of both the depocenter location and the thrust faults activity and cessation through time. The faults are sealed when the depocenter is located above them. See figures 3 and 13 for location.

Appendix 1:

Table summarising the different surveys and data set interpreted or used in this study.

Appendix 2:

Geological map of the Cape Kidnappers area and the Kidnappers group coastal section with emphasize on onshore/offshore correlations.

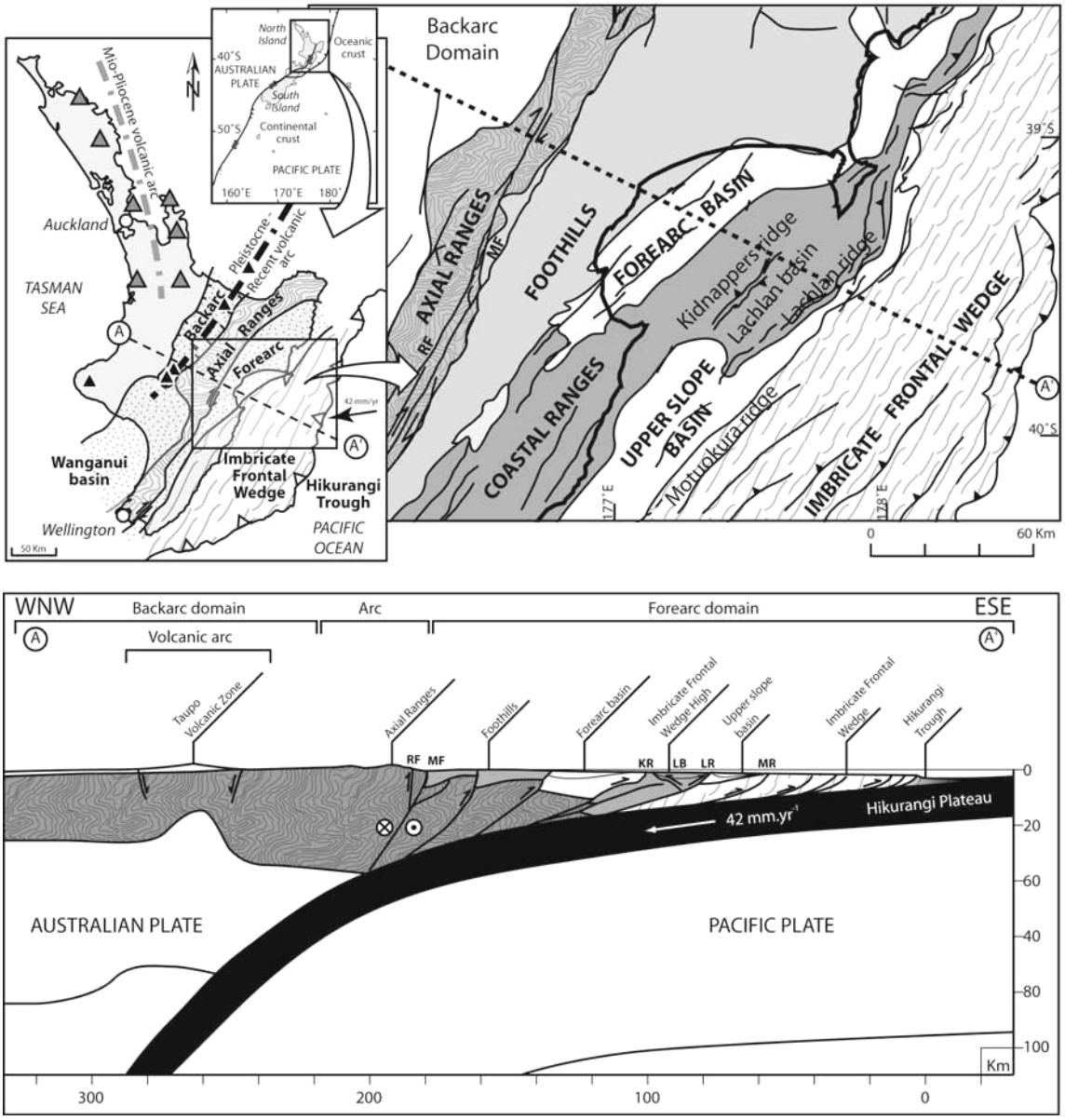
Backarc Domain
North Island
Oceanic crust
40°S
AUSTRALIAN PLATE
South Island
50°S
Continental crust
PACIFIC PLATE
160°E
170°E
180°
Mio-Pliocene volcanic arc
Auckland
TASMAN SEA
Pleistocene-Recent volcanic arc
Backarc
Axial Ranges
Forearc
42 mm/yr
Wanganui basin
Imbricate Frontal Wedge
Hikurangi Trough
Wellington
PACIFIC OCEAN
50 Km
AXIAL RANGES
MF
RF
FOOTHILLS
FOREARC BASIN
Kidnappers ridge
Lachlan basin
Lachlan ridge
COASTAL RANGES
UPPER SLOPE BASIN
Motuokura ridge
IMBRICATE FRONTAL WEDGE
39°S
40°S
177°E
178°E
0
60 Km
WNW
Backarc domain
Arc
Forearc domain
ESE
Volcanic arc
Taupo Volcanic Zone
Axial Ranges
Foothills
Forearc basin
Imbricate Frontal Wedge High
Upper slope basin
Imbricate Frontal Wedge
Hikurangi Trough
RF MF
KR
LB
LR
MR
42 mm.yr-1
Hikurangi Plateau
AUSTRALIAN PLATE
PACIFIC PLATE
0
20
60
40
80
100
Km
300
200
100
0

Figure 1.

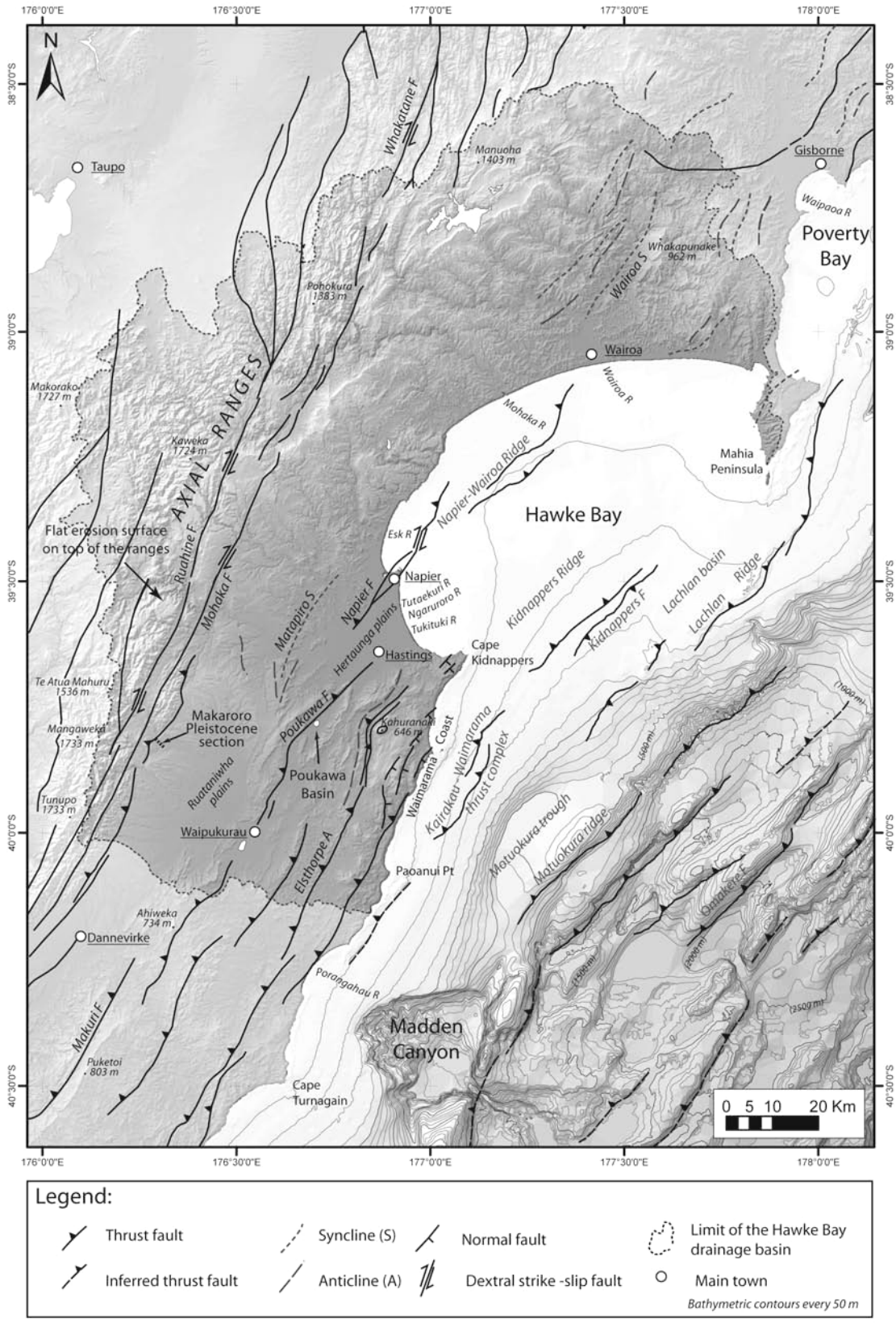
176°0'0"E
176°30'0"E
177°0'0"E
177°30'0"E
178°0'0"E
38°30'0"S
39°0'0"S
39°30'0"S
40°0'0"S
40°30'0"S
N
Taupo
Gisborne
Waipaoa R
Poverty Bay
Whakapunake 962 m
Wairoa S
Wairoa
Wairoa R
Whakatane F
Manuoha 1403 m
Pohokura 1883 m
Makorako 1727 m
Kaweka 1724 m
AXIAL RANGES
Flat erosion surface on top of the ranges
Ruahine F
Mohaka F
Mohaka R
Napier-Wairoa Ridge
Mahia Peninsula
Hawke Bay
Esk R
Napier
Napier F
Matapiro S
Tutaekuri R
Ngaruroro R
Tukituki R
Hastings
Heretaunga plains
Kidnappers Ridge
Kidnappers F
Lachlan basin
Lachlan Ridge
Cape Kidnappers
Te Atua Mahuru 1536 m
Mangaweka 1733 m
Tunupo 1733 m
Makaroro Pleistocene section
Ruataniwha plains
Poukawa F
Poukawa Basin
Kahuranaki 646 m
Waimarama - Coast
Kairakau - Waimarama thrust complex
Matuokura trough
Matuokura ridge
Omakere F
Waipukurau
Elsthorpe A
Paoanui Pt
Ahiweka 734 m
Dannevirke
Porangahau R
Makuri F
Puketoi 803 m
Madden Canyon
Cape Turnagain
0 5 10 20 Km
Legend:
Thrust fault
Inferred thrust fault
Syncline (S)
Anticline (A)
Normal fault
Dextral strike -slip fault
Limit of the Hawke Bay drainage basin
Main town
Bathymetric contours every 50 m

Figure 2.

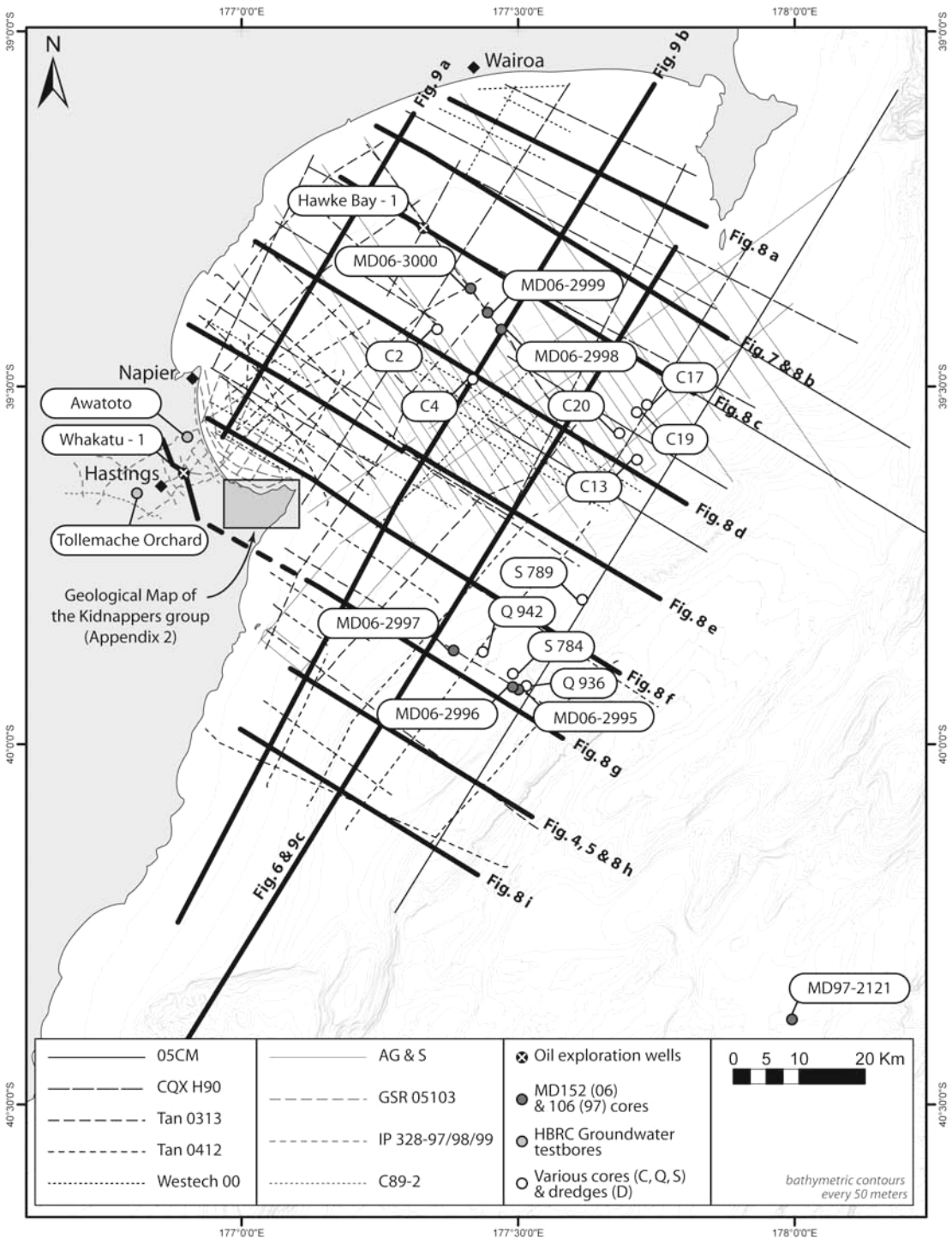
177°0'0"E
177°30'0"E
178°0'0"E
39°0'0"S
39°30'0"S
40°0'0"S
40°30'0"S
N
Wairoa
Napier
Hastings
Awatoto
Whakatu - 1
Tollemache Orchard
Geological Map of the Kidnappers group (Appendix 2)
Hawke Bay - 1
MD06-3000
MD06-2999
MD06-2998
MD06-2997
MD06-2996
MD06-2995
MD97-2121
C2
C4
C20
C17
C19
C13
S 789
Q 942
S 784
Q 936
Fig. 9 a
Fig. 9 b
Fig. 8 a
Fig. 7 & 8 b
Fig. 8 c
Fig. 8 d
Fig. 8 e
Fig. 8 f
Fig. 8 g
Fig. 4, 5 & 8 h
Fig. 8 i
Fig. 6 & 9c
05CM
CQX H90
Tan 0313
Tan 0412
Westech 00
AG & S
GSR 05103
IP 328-97/98/99
C89-2
Oil exploration wells
MD152 (06) & 106 (97) cores
HBRC Groundwater testbores
Various cores (C, Q, S) & dredges (D)
0 5 10 20 Km
bathymetric contours every 50 meters

Figure 3.

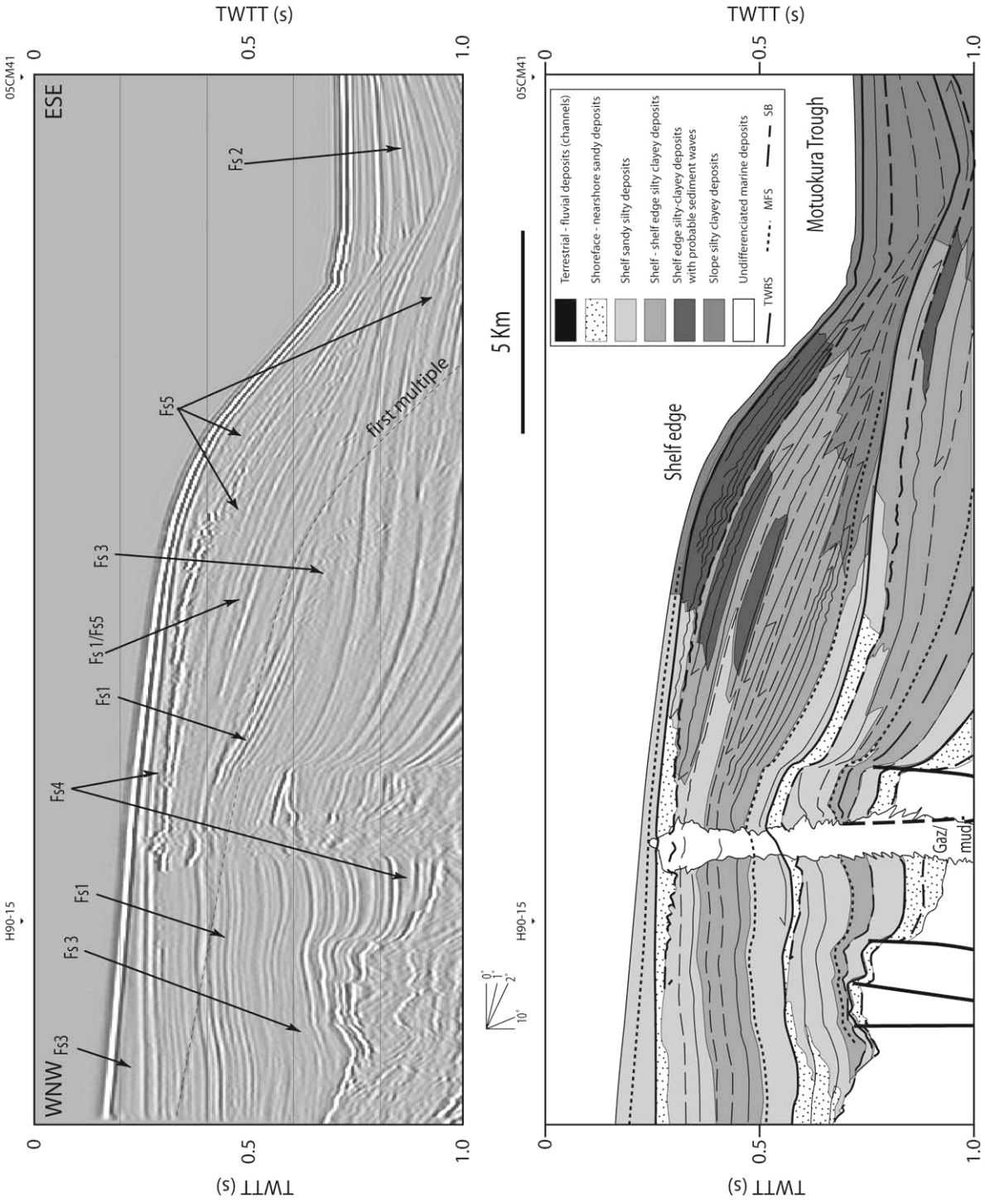
TWTT (s)
0
0.5
1.0
05CM41
H90-15
ESE
WNW
Fs 2
Fs5
first multiple
Fs 3
Fs 1/Fs5
Fs1
Fs4
Fs1
Fs 3
Fs3
5 Km
Terrestrial - fluvial deposits (channels)
Shoreface - nearshore sandy deposits
Shelf sandy silty deposits
Shelf - shelf edge silty clayey deposits
Shelf edge silty-clayey deposits with probable sediment waves
Slope silty clayey deposits
Undifferenciated marine deposits
TWRS
MFS
SB
Motuokura Trough
Shelf edge
Gaz/ mud

Figure 4.

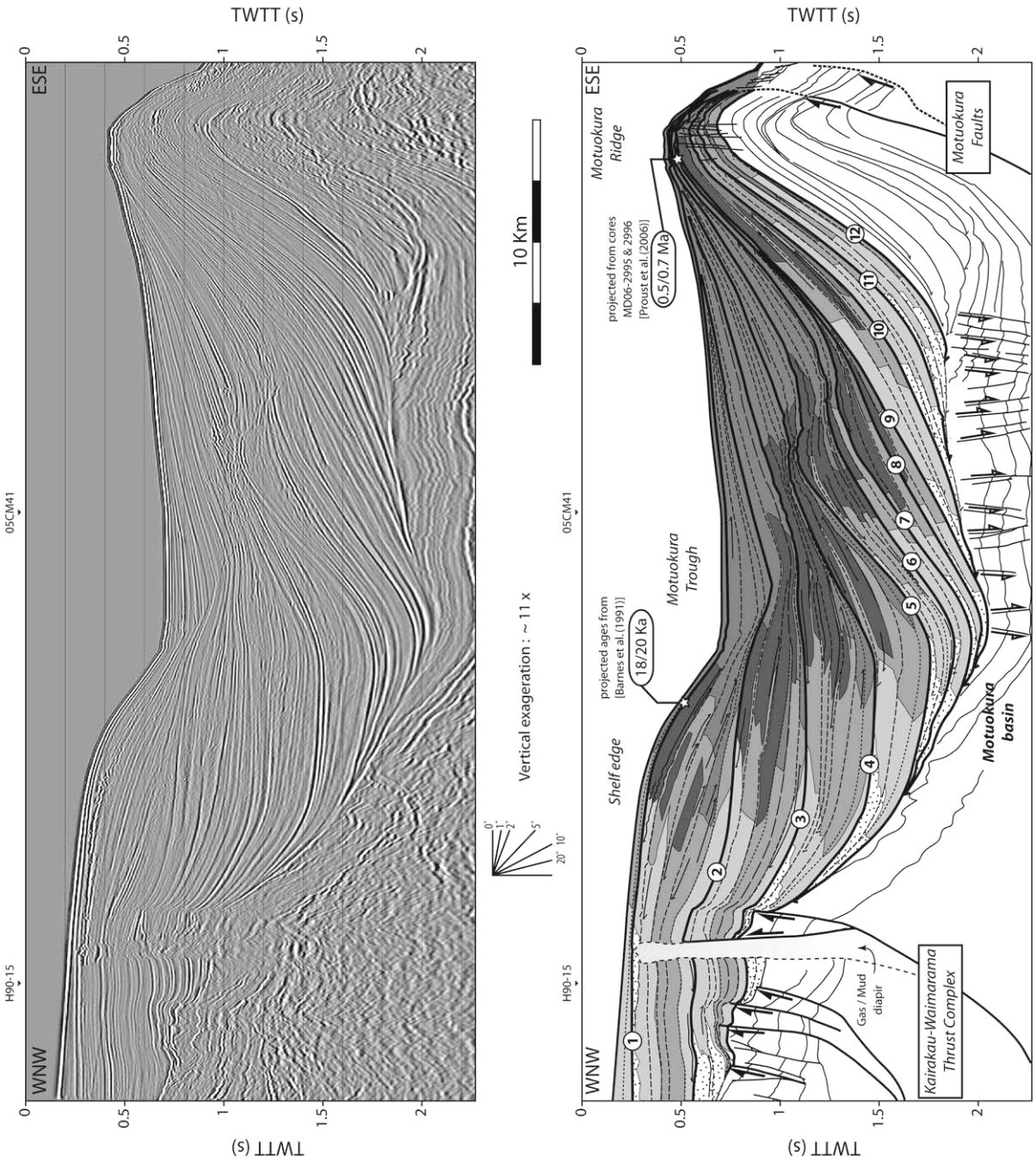
TWTT (s)
ESE
WNW
H90-15
05CM41
10 Km
Vertical exageration : ~ 11 x
0°
1°
2°
5°
20° 10°
Motuokura Ridge
projected from cores MD06-2995 & 2996 [Proust et al. (2006)]
0.5/0.7 Ma
Motuokura Faults
Motuokura Trough
projected ages from [Barnes et al. (1991)]
18/20 Ka
Shelf edge
Motuokura basin
Gas / Mud diapir
Kairakau-Waimarama Thrust Complex
1
2
3
4
5
6
7
8
9
10
11
12

Figure 5.

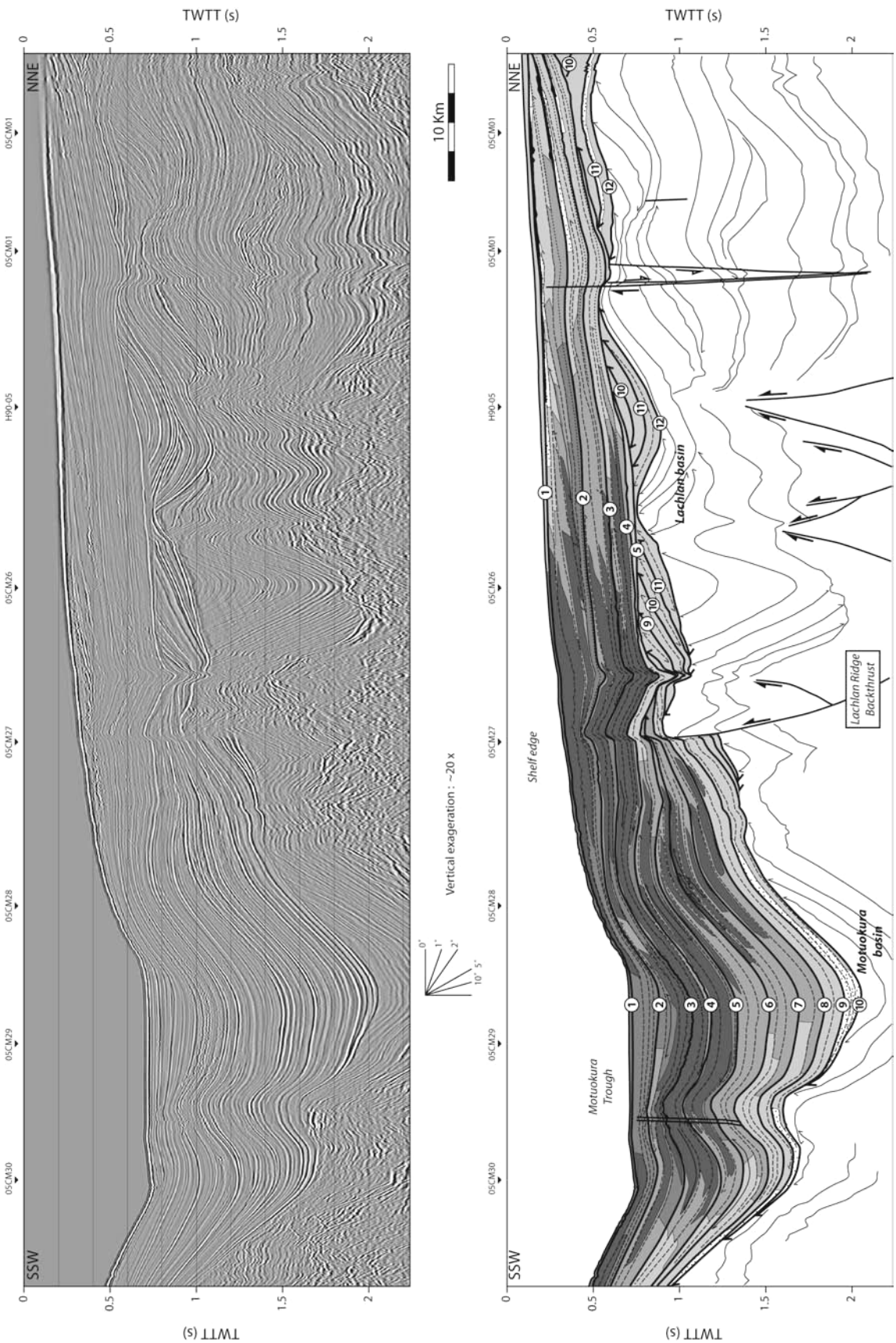
TWTT (s)
NNE
SSW
05CM30
05CM29
05CM28
05CM27
05CM26
H90-05
05CM01
05CM01
10 Km
Vertical exageration : ~20 x
Shelf edge
Motuokura Trough
Lachlan basin
Lachlan Ridge Backthrust
Motuokura basin

Figure 6.

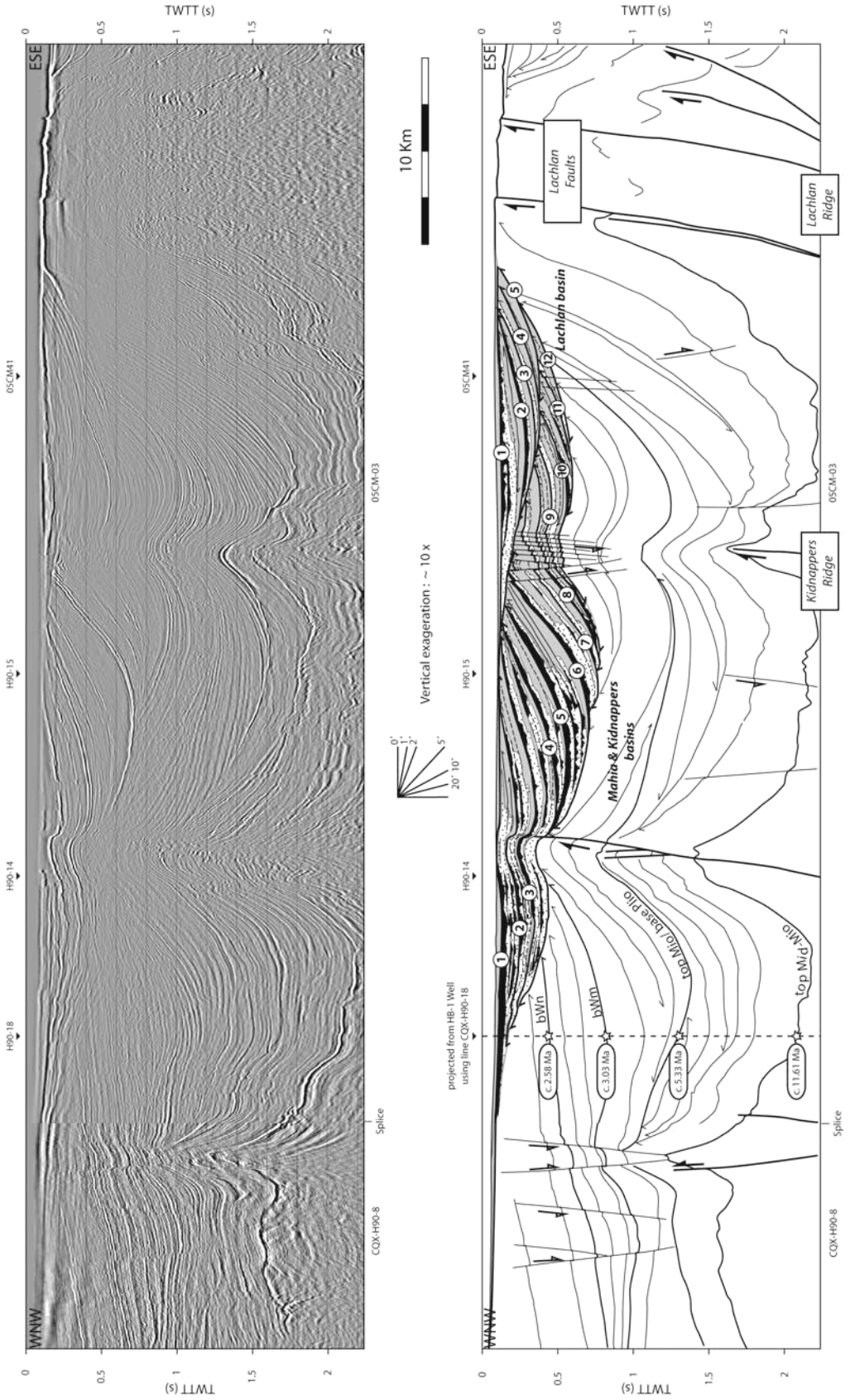
TWTT (s)
ESE
WNW
05CM41
H90-15
H90-14
H90-18
05CM-03
Splice
COX-H90-8
10 Km
Vertical exageration : ~ 10 x
Lachlan Faults
Lachlan Ridge
Lachlan basin
Mahia & Kidnappers basins
Kidnappers Ridge
projected from HB-1 Well using line COX-H90-18
bWn
bWm
top Mio/ base Plio
top Plio-Mio
c. 2.58 Ma
c. 3.03 Ma
c. 5.33 Ma
c. 11.61 Ma

Figure 7.

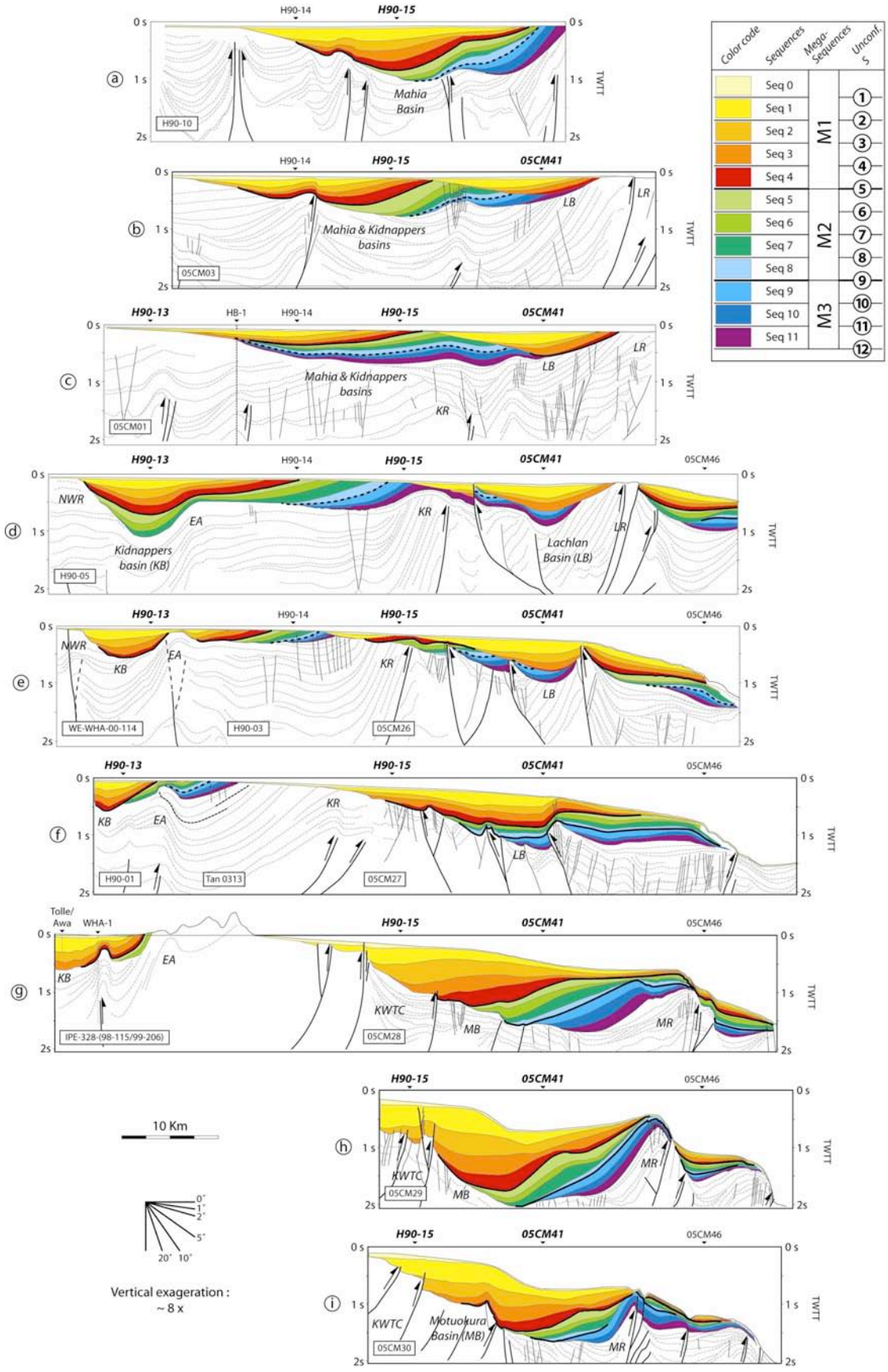
Color code
Sequences
Mega-sequences
Unconf.s
Seq 0
Seq 1
Seq 2
Seq 3
Seq 4
Seq 5
Seq 6
Seq 7
Seq 8
Seq 9
Seq 10
Seq 11
M1
M2
M3
1
2
3
4
5
6
7
8
9
10
11
12
a
H90-14
H90-15
Mahia Basin
H90-10
b
05CM41
LB
LR
Mahia & Kidnappers basins
05CM03
c
H90-13
HB-1
KR
05CM01
d
05CM46
NWR
EA
Kidnappers basin (KB)
H90-05
Lachlan Basin (LB)
e
KB
WE-WHA-00-114
H90-03
05CM26
f
H90-01
Tan 0313
05CM27
g
Tolle/ Awa
WHA-1
IPE-328-(98-115/99-206)
KWTC
MB
MR
05CM28
h
05CM29
i
Motuokura Basin (MB)
05CM30
0 s
1 s
2s
TWTT
10 Km
0°
1°
2°
5°
20°
10°
Vertical exaggeration :
~ 8 x

Figure 8.

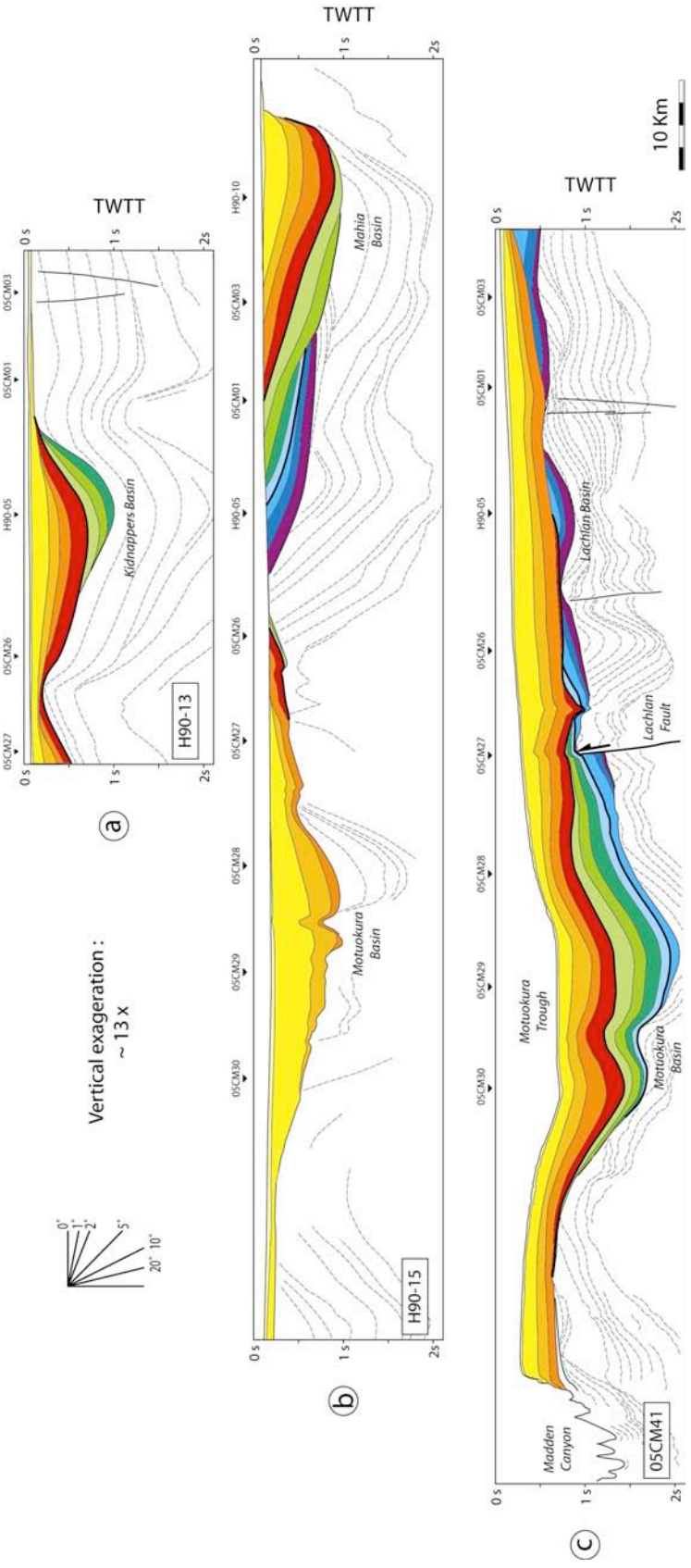
TWTT
0 s
1 s
2s
05CM03
05CM01
H90-05
05CM26
05CM27
Kidnappers Basin
H90-13
a
Vertical exageration :
~ 13 x
0°
1°
2°
5°
10°
20°
TWTT
H90-10
05CM28
05CM29
05CM30
Mahia
Basin
Motuokura
Basin
H90-15
b
10 Km
Lachlan Basin
Lachlan
Fault
Motuokura
Trough
Madden
Canyon
05CM41
c

Figure 9.

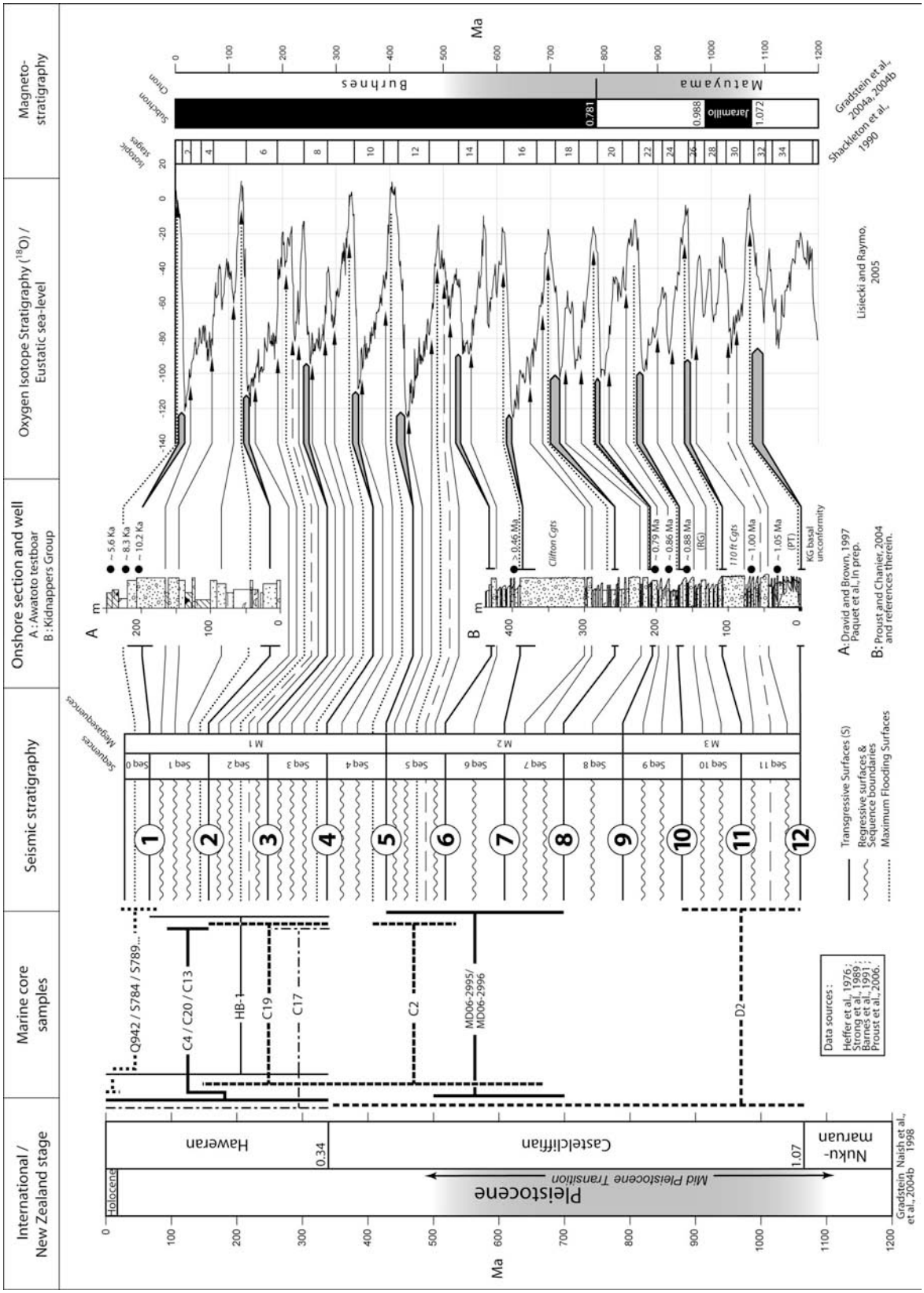
International / New Zealand stage
Marine core samples
Seismic stratigraphy
Onshore section and well
A : Awatoto testboar
B : Kidnappers Group
Oxygen Isotope Stratigraphy (^{18}O) / Eustatic sea-level
Magneto-stratigraphy
Ma
Holocene
Pleistocene
Mid Pleistocene Transition
Hawera
Castlecliffian
Nukumaruan
0.34
1.07
Gradstein, Naish et al., et al., 2004b 1998
Brunhes
Matuyama
Jaramillo
0.781
0.988
1.072
Gradstein et al., 2004a, 2004b
Shackleton et al., 1990
Lisiecki and Raymo, 2005
Isotopic stages
Subchron
Chron
~ 5.6 Ka
~ 8.3 Ka
~ 10.2 Ka
~ 0.46 Ma
Clifton Cgts
~ 0.79 Ma
~ 0.86 Ma
~ 0.88 Ma
(RG)
110 ft Cgts
~ 1.00 Ma
~ 1.05 Ma
(PT)
KG basal unconformity
A: Dravid and Brown, 1997
Paquet et al., In prep.
B: Proust and Chanier, 2004
and references therein.
Megasequences
Sequences
M1
M2
M3
Seq 0
Seq 1
Seq 2
Seq 3
Seq 4
Seq 5
Seq 6
Seq 7
Seq 8
Seq 9
Seq 10
Seq 11
Transgressive Surfaces (S)
Regressive surfaces & Sequence boundaries
Maximum Flooding Surfaces
Q942 / S784 / S789...
C4 / C20 / C13
HB-1
C19
C17
C2
MD06-2995/ MD06-2996
D2
Data sources :
Heffer et al., 1976 ;
Strong et al., 1989 ;
Barnes et al., 1991 ;
Proust et al., 2006.

Figure 10.

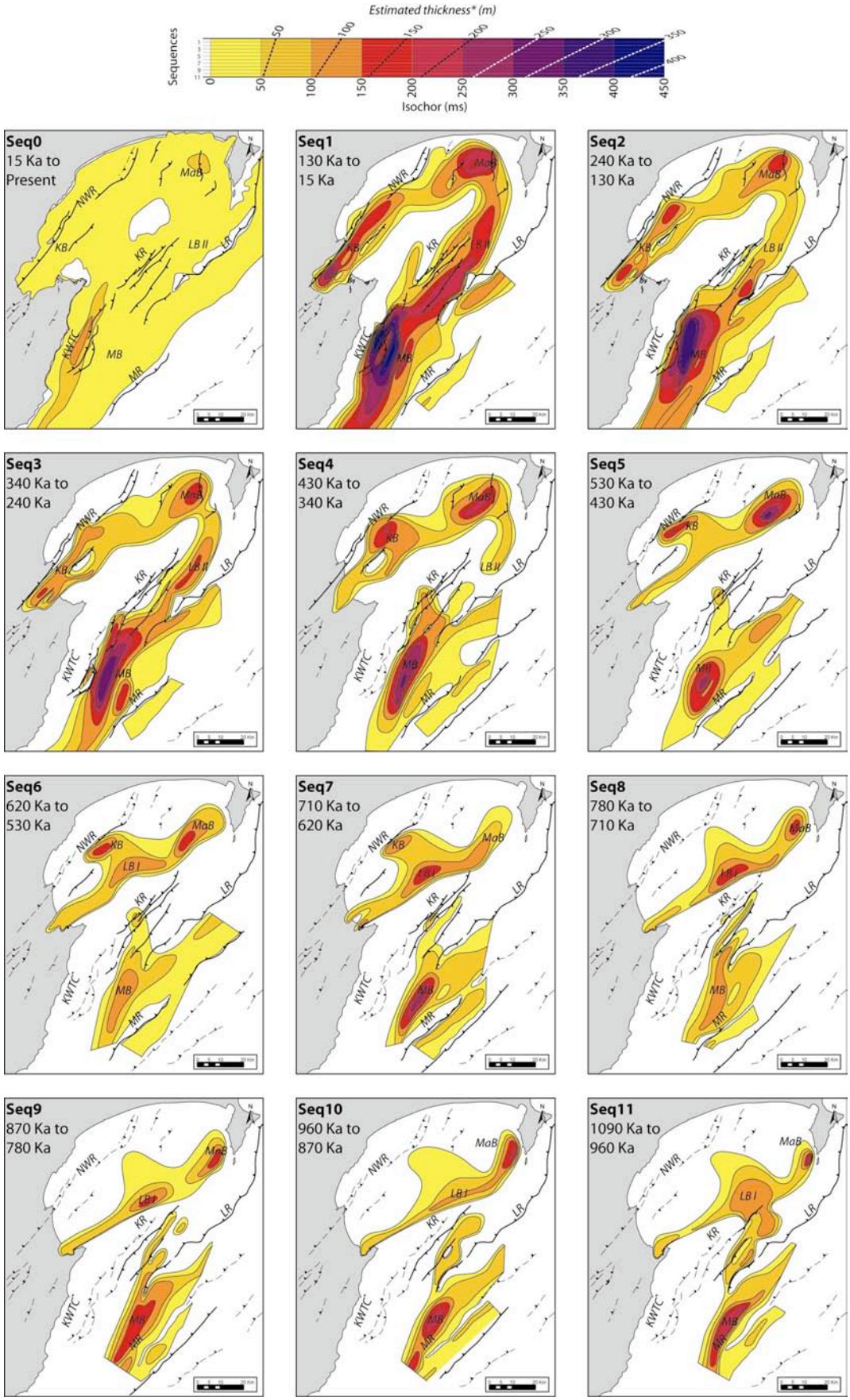
Estimated thickness* (m)
Sequences
0
50
100
150
200
250
300
350
400
450
Isochor (ms)
Seq0
15 Ka to
Present
Seq1
130 Ka to
15 Ka
Seq2
240 Ka to
130 Ka
Seq3
340 Ka to
240 Ka
Seq4
430 Ka to
340 Ka
Seq5
530 Ka to
430 Ka
Seq6
620 Ka to
530 Ka
Seq7
710 Ka to
620 Ka
Seq8
780 Ka to
710 Ka
Seq9
870 Ka to
780 Ka
Seq10
960 Ka to
870 Ka
Seq11
1090 Ka to
960 Ka
MaB
NWR
KB
KR
LB II
LB I
LB
KWTC
MB
MR

Figure 11.

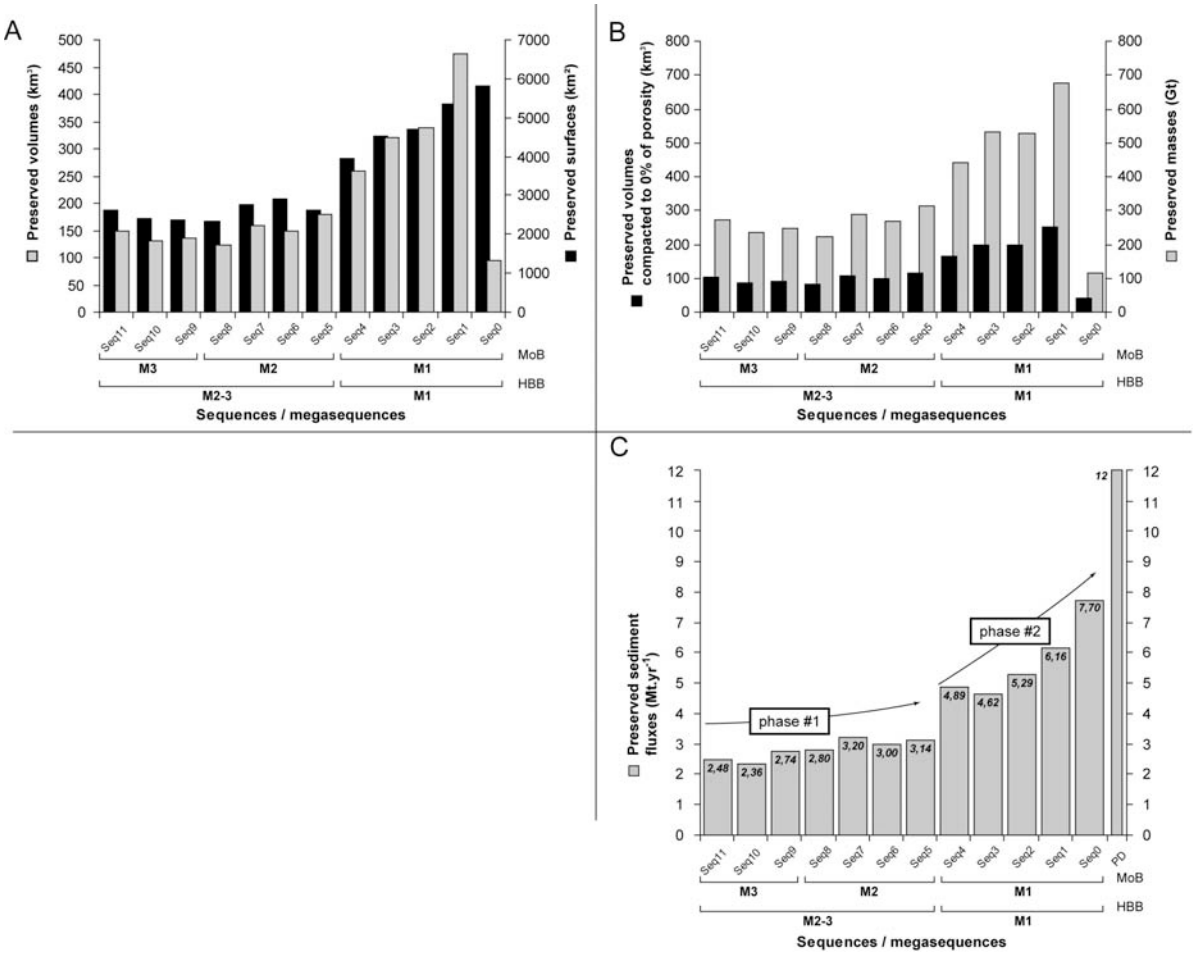
A
Preserved volumes (km³)
Preserved surfaces (km²)
Seq11 Seq10 Seq9 Seq8 Seq7 Seq6 Seq5 Seq4 Seq3 Seq2 Seq1 Seq0
MoB
M3 M2 M1
HBB
M2-3 M1
Sequences / megasequences
B
Preserved volumes compacted to 0% of porosity (km³)
Preserved masses (Gt)
Seq11 Seq10 Seq9 Seq8 Seq7 Seq6 Seq5 Seq4 Seq3 Seq2 Seq1 Seq0
MoB
M3 M2 M1
HBB
M2-3 M1
Sequences / megasequences
C
Preserved sediment fluxes (Mt.yr⁻¹)
phase #1
phase #2
2,48 2,36 2,74 2,80 3,20 3,00 3,14 4,89 4,62 5,29 6,16 7,70 12
Seq11 Seq10 Seq9 Seq8 Seq7 Seq6 Seq5 Seq4 Seq3 Seq2 Seq1 Seq0 PD
MoB
M3 M2 M1
HBB
M2-3 M1
Sequences / megasequences

Figure 12.

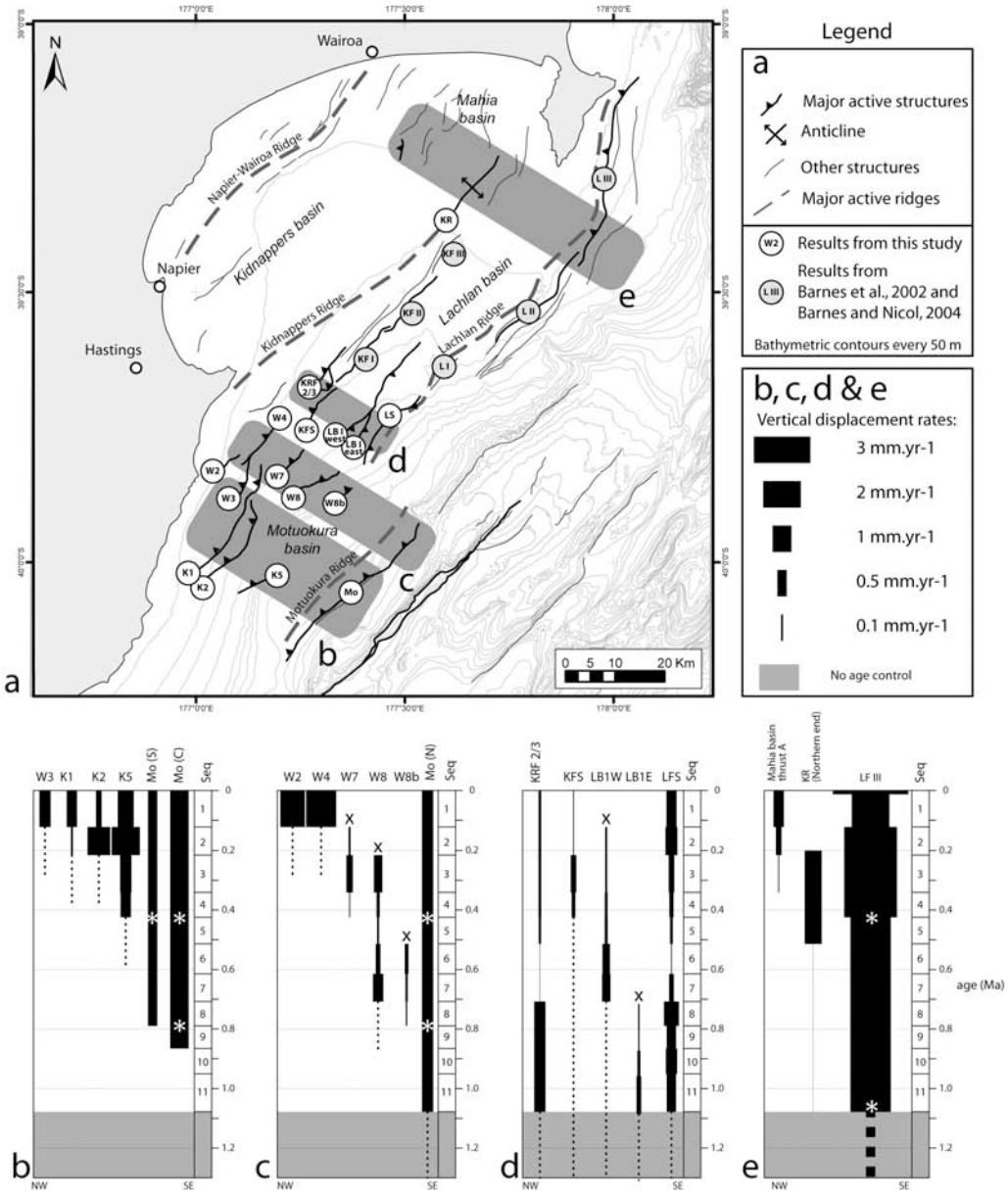
Legend
a
Major active structures
Anticline
Other structures
Major active ridges
Results from this study
Results from Barnes et al., 2002 and Barnes and Nicol, 2004
Bathymetric contours every 50 m
b, c, d & e
Vertical displacement rates:
3 mm.yr-1
2 mm.yr-1
1 mm.yr-1
0.5 mm.yr-1
0.1 mm.yr-1
No age control
Wairoa
Napier
Hastings
Mahia basin
Napier-Wairoa Ridge
Kidnappers basin
Kidnappers Ridge
Lachlan basin
Lachlan Ridge
Motuokura basin
Motuokura Ridge
0 5 10 20 Km
W3 K1 K2 K5 Mo (S) Mo (C) Seq
W2 W4 W7 W8 W8b Mo (N) Seq
KRF 2/3 KFS LB1W LB1E LFS Seq
Mahia basin thrust A KR (Northern end) LF III Seq
age (Ma)
NW
SE

Figure 13.

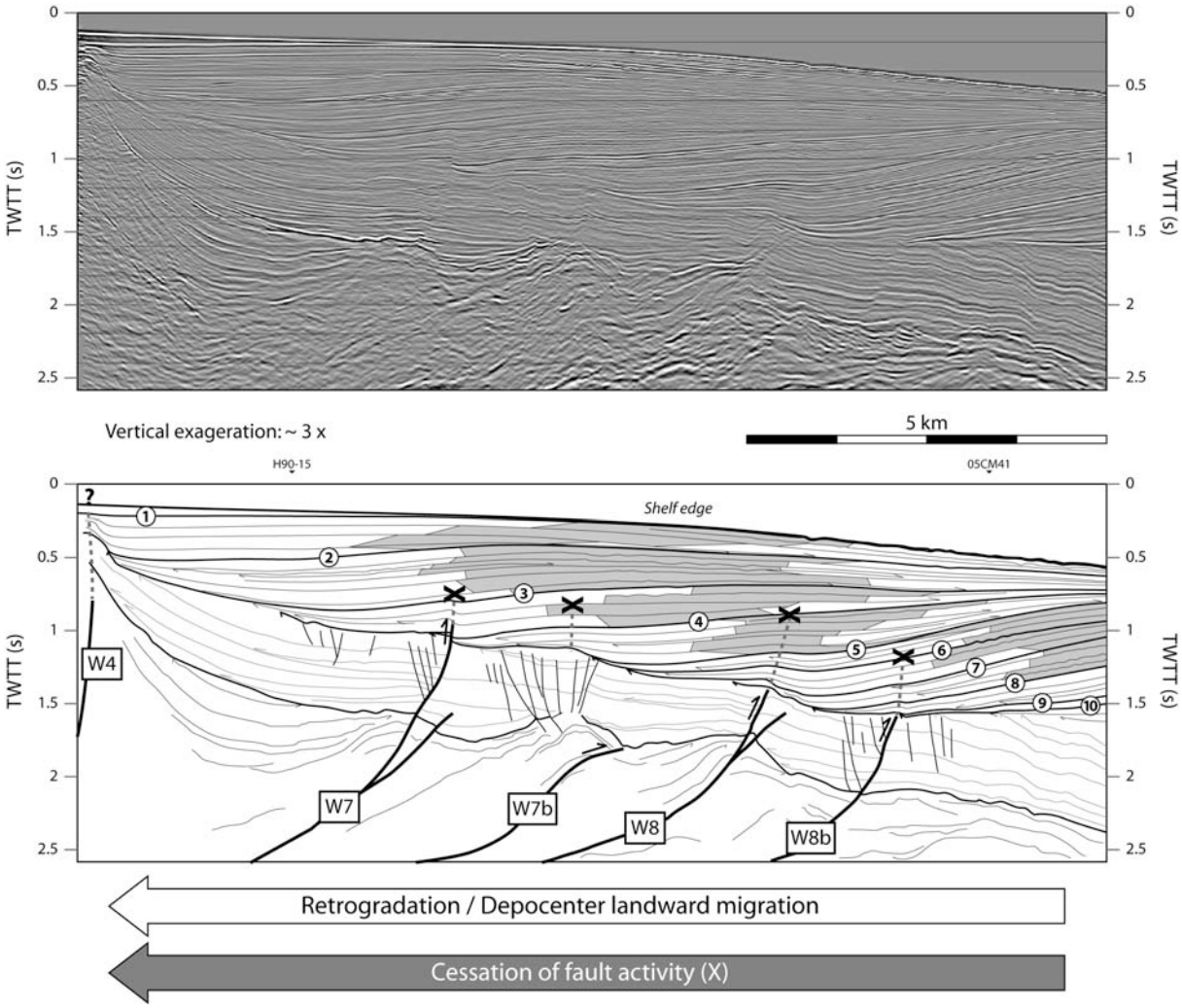
TWTT (s)
Vertical exageration: ~ 3 x
5 km
H90-15
05CM41
Shelf edge
W4
W7
W7b
W8
W8b
Retrogradation / Depocenter landward migration
Cessation of fault activity (X)

Figure 14.

Appendix 1:

Survey Name	Data type	Length (interpreted)	Operator / Country	Vessel	Year	Avaliable report (PR) or publications :
GeodyNZ	Bathymetry EM12		Ifremer / France	R/V Atalante	1993	Collot et al. (1995, 1996) ; Lewis et al. (1998)
TAN 0106	Bathymetry EM300		NIWA / NZ	R/V Tangaroa	2001	
GSR 05301	Boomer	175 km	NIWA / CNRS	Big Kahuna	2005	Paquet et al. (2008)
CQX H90	MCS (60 folds)	1000 km	NZ CQX Ltd.	M/V Western Pacific	1990	Sullivan – PR 1666 (1990)
05CM	MCS (640/960 channels)	720 km	Ministry of Economic Development / NZ	M/V Pacific Titan	2005	Multiwave – PR 3186 (2005)
WE00	MCS (240 channels)	305 km	Westech Energy NZ Ltd / NZ	M/V GECO MY	2000	Geo-Prakla – PR 2483 (2000)
TAN 0313	3.5 KHz & MCS (48 channels)	830 km	NIWA / NZ	R/V Tangaroa	2003	
TAN 0412	3.5 KHz & MCS (48 channels)	298 km	NIWA / NZ	R/V Tangaroa	2004	
CR8024	3.5 KHz	1200 km	Conquest Exploration Ltd / NZ	GRV Rapuhia	1988	Conquest Exploration - PR2059 (1988)
C89	Onshore seismic data	several tenths of km from 1 profile	Croft Exploration Ltd (NZ)	Vibrator VVCA	1989	B.C.M. Geophysics Ltd – PR 1522 (1989)
IP 328-97/98/99	Onshore seismic data	several tenths of km from 15 profiles	Indo-Pacific Energy NZ Ltd / NZ	Vibrator VVCA	1997 1998 1999	Small, Michael & others – PR 2299 (1997); Schlumberger Geco Prakla – PR 2392, PR 2393 (1998, 1999)

Apendix 1 (continued):

Survey Name	Data type	Length (interpreted)	Operator / Country	Vessel	Year	Avaliable report (PR) or publications :
MD152 / Matacore	3.5 KHz and 6 giant calypso piston cores (MD06-2995/96/97 on the upper slope and MD06-2998/99 /3000 on the shelf)	c. 100 km (core length up to c. 30 m)	IPEV / CNRS-INSU / NIWA / AWI / VIMS SIO	R/V Marion-Dufresne	2006	Proust et al. (2006)
Hawke Bay - 1	Exploration well	2372 m	BP Shell Aquitaine and Todd Petroleum development Ltd	'Glomar Tasman' drillship	1976	Heffer et al. – PR 667 (1976)
Whakatu - 1	Exploration well	1455 m	Indo-Pacific Energy NZ Ltd / NZ	Century-2, IDECO RIG	2000	Ozolins and Francis – PR 2476 (2000)
Tollemache Orchard	Groundwater testbores	257 m	HBRC – IGNS / NZ		1993	Brown (1993); Dravid and Brown (1997)
Awatoto	Groundwater testbores	254 m	HBRC – IGNS / NZ		1995	Brown and Gibbs (1996); Dravid and Brown (1997)
Unknown	Cores and dredges	6 cores (C) and 1 dredge (D)	NZ CQX Ltd	GRV/Rapuhia	1988	Strong et al. – PR 1470 (1989)
Unknown	Cores	4 cores (up to 4 m)	NZOI DSIR	GRV/ Rapuhia	1987	Barnes et al. (1991)

Appendix 2

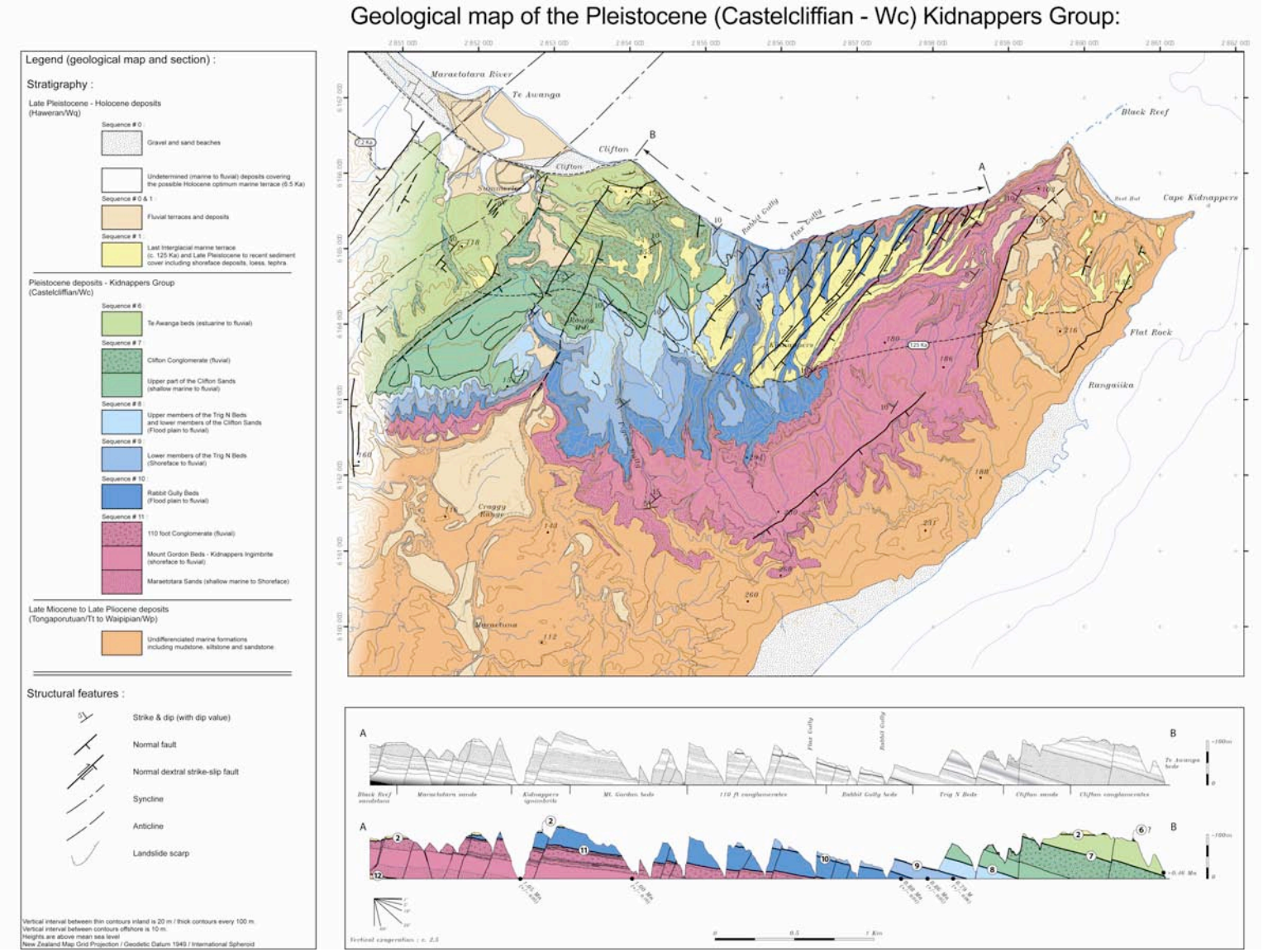
Geological map of the Pleistocene (Castelcliffian - Wc) Kidnappers Group:
Legend (geological map and section) :
Stratigraphy :
Late Pleistocene - Holocene deposits
(Haweran/Wq)
Sequence # 0 :
Gravel and sand beaches
Undetermined (marine to fluvial) deposits covering the possible Holocene optimum marine terrace (6.5 Ka)
Sequence # 0 & 1 :
Fluvial terraces and deposits
Sequence # 1 :
Last Interglacial marine terrace (c. 125 Ka) and Late Pleistocene to recent sediment cover including shoreface deposits, loess, tephra
Pleistocene deposits - Kidnappers Group
(Castelcliffian/Wc)
Sequence # 6 :
Te Awanga beds (estuarine to fluvial)
Sequence # 7 :
Clifton Conglomerate (fluvial)
Upper part of the Clifton Sands (shallow marine to fluvial)
Sequence # 8 :
Upper members of the Trig N Beds and lower members of the Clifton Sands (Flood plain to fluvial)
Sequence # 9 :
Lower members of the Trig N Beds (Shoreface to fluvial)
Sequence # 10 :
Rabbit Gully Beds (Flood plain to fluvial)
Sequence # 11 :
110 foot Conglomerate (fluvial)
Mount Gordon Beds - Kidnappers Ingimbrite (shoreface to fluvial)
Maraetotara Sands (shallow marine to Shoreface)
Late Miocene to Late Pliocene deposits
(Tongaporutuan/Tt to Waipipian/Wp)
Undifferenciated marine formations including mudstone, siltstone and sandstone
Structural features :
Strike & dip (with dip value)
Normal fault
Normal dextral strike-slip fault
Syncline
Anticline
Landslide scarp
Vertical interval between thin contours inland is 20 m / thick contours every 100 m.
Vertical interval between contours offshore is 10 m.
Heights are above mean sea level
New Zealand Map Grid Projection / Geodetic Datum 1949 / International Spheroid
Maraetotara River
Te Awanga
Clifton
Black Reef
Cape Kidnappers
Flat Rock
Rangaiika
Craggy Ridge
Maraetotara
Rabbit Gully
Flat Gully
Round Hill
A
B

Conclusions & outlooks:

-

Conclusions & perspectives :

Conclusion :

The goals of this work were the description and the quantification of the morphostructural evolution of landscape and associated sediment fluxes within an active subduction margin, from the mountains (erosion – sources) to the toe of the sedimentary system. The hawke bay forearc domain of New Zealand have been selected to undertake this study which is based on a multidisciplinary apporoach combining stratigraphy, geomorphologic and structural analyses.

The interpretation of an extensive dataset, including marine and terrestrial seismic profiles (MCS, 3.5 KHz and Boomer) covering most of the areas dominated by sedimentation, correlated to geological geomorphologic data (maps, sections, wells, cores, terraces) allow to:

- Identify and describe a 100 ka-type depositional sequence that extends from zones dominated by erosion (300 m) to the base of the sedimentary wedge (-500 m) as accurately as possible (extent, age calibration, sedimentary facies, depositional environments, volumetric partitioning), and to propose two paleogeographic reconstructions for Hawke Bay.
- Describe the detailed stratigraphy for the last c.1.1 Ma as a stacking of 11 depositional sequences grouped in 2 megasequences that show an overall retrogradational trend.
- Determine the three-dimensional geometry of sequences and to reveal the existence of structurally controlled sub-basins that evolve simultaneously with changes in the whole forearc domain structural history and with the development of the megasequence-bounding unconformity.
- Precise the structural cartography and to establish the style, the timing and the rates of deformation of the major structures.
- Quantify preserved sediment fluxes within the basin for each sequence from isopach maps and to describe their evolution at 1 Ma and 10 ka .
- Finally discuss the influence of tectonics, climate and eustasy on the stratigraphic architecture and sediment fluxes at different timescales and the consequences for the morphostructural evolution of the forearc domain.

This work presents a local interest that helps to improve our understanding of the evolution of the Hawke Bay forearc domain during the last 1.0 Ma and it also brings additional constrains that complement our knowledge of the Hikurangi margin history.

From a global point of view, this study brings qualitative and quantitative results on the behaviour of drainage – sedimentary basin system in an active forearc domain hat allow estimating the respective influence of the various control parameters (tectonic, climate, eustasy) on the **stratigraphic architecture**, the **morphostructural configuration**, and the **sediment fluxes** evolutions.

Detailed conclusions are presented according to these three themes with a special attention to local and global aspects.

- **Stratigraphic architecture:**

This work reveals the existence of 11 depositional sequences that developed during the last 1.1 Ma within the Hawke Bay forearc domain. They originate in the Pleistocene high amplitude climato-eustatic variations, with periodicities of c. 41 and c. 100 ka. Sediment packages identified within 100 ka-type sequences correlate with the c. 20 ka periodicity.

Thus this work confirms results from former studies (e.g. Proust and Chanier, 2004): the stratigraphic architecture within an actively deformed forearc basin, such as the Hawke Bay forearc basin, is strongly controlled by orbitaly-driven climato-eustasy from the scale of the elementary depositional sequence to the 1 Ma timescale.

The detailed source-to-sink study of the last 100 ka depositional sequence of the Late Pleistocene shows that fluvial aggradation occurred along the whole river profile during phases of climate degradation and sea level fall, even in uplifting areas (up to 3 mm.yr-1). These latter domains are subject to important river incision during phases of sea level rise or high. Such timing determines an unusual sediment partitioning that differs from classical models that predict fluvial incision during sea level fall and aggradation within valleys during sea level rise. Two explanations are proposed:

- Fluvial aggradation occurs when erosion increases in the mountain ranges as the vegetation cover disappears during phases of cold climate (Litchfield and Berryman, 2005).
- Fluvial aggradation is linked with the increase of aerial accommodation space in the valley due to an important lengthening of the river profile during sea level fall. This phenomenon is favoured by the flatness of the broad Hawke Bay shelf and by the sinuosity imposed to river courses by the growing Kidnappers ridge.

Both explanations are not antagonistic. It is highly probable that fluvial aggradation occurred as a result of an increase of sediment load in the river and a course lengthening.

Thus, in active margins, in areas subject to significant uplift (mm.yr-1), climate changes and their impact on eustasy and sediment fluxes can control the river behaviour (incision vs. aggradtion). Nevertheless, this control operates at short-term scales (<100 ka) and incision and aggradation depend mainly on tectonic deformation (uplift and subsidence) at long-term timescales (>100 ka).

The stacking pattern of the 100 ka-type sequences shows an important retrogradational trend that is followed by a progressive arcward migration of depositional environments and depocenters. A major composite erosive unconformity is formed by the lateral juxtaposition of the 11 sequence basal boundaries at their proximal end. The general arcward migration of sequences and the development of the basal unconformity are attributed to interactions and co-evolutions between sedimentation and deformation that result in the individualization of a 1 Ma timescale major mega-sequence within the forearc basin fill. The basal diachronic unconformity is correlated between basins in the forearc domain and even in the backarc domain (Proust et al., 2005) where it also underlies a migration of sequences toward the uplifting forearc.

The joint migration of sedimentation and tectonic deformation within a major-megasequence, from distal areas (sedimentary basins) toward proximal areas (uplifting arc and sediment sources) reveals the strong tectono-sedimentary interplays that affect the morphostructural evolution of active margins.

The development of a regional unconformity (S5) at c. 430 ka separates the 11 sequences in two megasequences. This unconformity is generated by significant contemporaneous changes in the tectonic activity along major structures and is characterized by an acceleration of the arcward migration of sequences. The origin of such tectonic change in the margin may result from (1) an increase of the tectonic accretion at the wedge fronthat is transmitted to the forearc domain, (2) the subduction of a wide submarine relief (*eg.* Hikurangi Plateau) or a seamount ridge or (3) changes in the plate coupling.

A rapid and significant change in the structural activity can be recorded in the sedimentary architecture at the 100 ka-timescale (depositional sequence) despite the strong eustasy control. The occurrence of brief phases of tectonic intensification within an active margin

remains unclear and may result from the increase of accretion or change in the plate coupling due to climatically-induced increases of sedimentation rates at the trench.

- **The basin configuration :**

The sequence geometry highlighted by isopach maps reveal (1) the extent of zones dominated by sedimentation in the forearc and (2) the significant change of configuration that occurred in the forearc domain during the last 1 Ma.

Terrigenous sediments originated from eroded mountains are transported and deposited in the forearc basin *s.s.* (Kidnappers, Mahia, Lachlan I and II sub-basins) and in the first upper-slope basins such as the Motuokura basin. This latter basin constitutes the main sediment trap of the Hawke Bay forearc basin. Therefore, it appears important to distinguish the forearc basin *s.s.* (between arc and wedge) from the forearc domain (forearc basin and upper-slope basin), at least for the Hawke Bay region. This is absolutely required for any reliable quantitative approach.

The morphology of forearc domains determines their ability to retain and preserve sediments. Deep-sea terrace basins are generally able to trap large volumes of deposits whereas higher small segmented forearc sub-basins such as Hawke Bay forearc basin re not. Sediments therefore transit over the forearc basin and are deposited in the trench-slope basins.

In addition to the general retrogradational-arcward migration trend observed on the incremental isopach maps, it is also possible to detect the change from a configuration in three sub-basins (Mahia, Lachlan I and Mouokura) to a configuration in four sub-basins (Kidnappers, Mahia, Lachlan II and Motuokura). The development of both Kidnappers and Lachlan II sub-basins in place of the Lachlan basin I is attributed to the growth of the Kidnappers tectonic ridge in the middle of the shelf. The growth of this ridge points out the lateral (north-eastward) growth of the Costal Ranges at the back of the imbricate frontal wedge. The development of this ridge results in the arched succession where the four sub-basins are connected together from proximal end (Kidnappers) to the distal end (Motuokura).
The transition between the two configurations occurred synchronously with the development of the megasequence boundary S5 at c. 430 ka.

The change of configuration observed in the Hawke Bay basin reveals the importance of tectonic deformation and structure growth in the distribution of areas dominated by erosion

or sedimentation in an active margin. It also shows the importance of a growth of the wedge on the morphostructural evolution of a forearc basin.

- **Sediment fluxes evolution and timescales:**

Sediment fluxes have been estimated from the calculation of preserved sediment volumes within the forearc domain.

At the depositional sequence scale (Late Pleistocene - 100 ka), increase of the sediment fluxes is detected around the glacial maximum (*ie.* c.18 ka). This increase is attributed to (1) an intensification of erosion in source areas (axial ranges) that follow the decrease of the vegetation cover during the climate degradation and (2) to the fluvial incision that occurred over the uplifted foothills during the postglacial period. Thus, erosion and sediment fluxes are very sensitive and reactive (short response times) to the rapid Pleistocene climate variations. This sensitiveness is attributed to (1) geomorphologic parameters (relief, drainage area) and to (2) the softness of the Hawke Bay substratum:

- Mio-Pliocene marine silts
- Density of fractures in the Mesozoic basement of the axial ranges.

It therefore appears that high amplitude and high frequency climate changes induce rapid variations of the sediment fluxes in active margin basins. This phenomenon is amplified by high topographies and steep slopes (high reliefs), large drainage areas and by tectonically fractured substratum.

At the 1 Ma timescale, sediment fluxes values estimated for each of the 11 depositional sequences show two distinct phases: (1) a phase of relative stability of fluxes c. 2.8 ± 0.3 $Mt.yr^{-1}$ between c.1.1 Ma nd c.430 ka, and (2) a phase of continuous flux increase from c. 4.6 to c. 6.2 Mt.yr-1 (250 %) between c. 430 ka et present day.

This increase from c. 430 ka is correlated to the rapid change in the morphostructural evolution (see above) that induced significant erosion of sequences deposited prior to c. 430 ka and a change of the basins of the forearc domain to preserve sediments (*eg.* contemporaneous formation of the new Kidnappers and Lachlan II sub-basins).

In an actively deformed forearc basin at the 1 Ma timescale, sediment flux values estimated from preserved sediment volumes mostly reflect the changes in the ability of the basin to preserve sediments, rather than a real variations of the sediment supply from the drainage basin.

Present day estimations of sediment fluxes are three times the mean value of preserved sediment flux determined over the last 1 Ma and twice the value estimated for the last glacial maximum. These significant differences can be explain by (1) analytical problems associated to the methodologies used to estimate past and present fluxes, by (2) the export of sediments beyond the boundary of the forearc domain, or more likely, by (3) the anthropologic impact on the land cover (deforestation, agriculture). The rapid increase of present day sediment fluxes (< 100 yrs) points out the sensitiveness of the Hawke Bay drainage basin to environmental changes (anthropologic or climatic), that is related to geomorphic (relief, drainage area, limited internal sediment storage) and geologic conditions (uplift, substratum).
Considering their morphologic and geologic characteristics, forearc domains are inclined to react quasi instantly to environmental variations (climatic or anthropologic). Thus, it is probable that an effective influence of a phenomenon, such as the Mid Pleistocene climatic transition (passage from 41 to 100 ka periodicity), on the sediment fluxes (sediment delivery) has been erased from the sedimentary record as a result of the tectonic deformation.

Outlooks :

Regional outlooks:

This study offers a detailed vision of the morphostructural evolution of the Hawke Bay forearc domain for the last 1.1 Ma (basin condiguration, preservation ability…). Nevertheless, the potential events that controlled this evolution remain unidentified or classified hierarchically. It appears that this work corresponds to a first and localized attempt that should lead to an inevitable global approach of the margin.

- Thus, it is conceivable to reproduce this type of work (stratigraphy, sediment flux quantifications) for the whole active sedimentary basins of the forearc domain, including shelf basins (eg. Poverty Bay) or slope basins. Most of the seismic and geologic data needed to undertake extensive work are readily available and/or partially interpreted.
- The comparison between the forearc and the backarc domain is unavoidable. It should provide an quantified overview of the Hikurangi margin morphostructural evolution.

From a more specific point of view, it appears that the Motuokura basin presents an exceptional sedimentary fill for the last 1.1 Ma (thickness and the resolution of the eustatic record). It gathers the ideal characteristics for undertaking a detailed study of the Mid Pleistocene Transition.

General outlooks:

This study provides values of preserved sediment fluxes, constraints on the structural activity, depositional environments, depositional sequence geometry, precise chronostratigraphic scheme, and paleogeographic variations in an active margin. These results could be uploaded in numerical stratigraphic modelling in order to test sediment flux values.

Conclusion :

L’objectif de cette étude était de décrire et de quantifier l’évolution "morphostructurale" des reliefs, et flux sédimentaires associés, sur un segment complet de marge active en subduction depuis l'apex des zones en érosion, jusqu’au pied des zones en dépôt. L'exemple choisi est le domaine avant arc de Hawke Bay en Nouvelle Zélande. Les approches employées associent des analyses stratigraphiques, géomorphologiques et structurales..

L’interprétation d’un jeu de données sismiques marines et terrestres (MCS, 3.5 KHz et Boomer), couvrant l'essentiel des zones en dépôt du bassin, corrélée au données géologiques et géomorphologiques, à terre et en mer (cartes, coupes, puits, carottes et terrasses) a permis :

- d’identifier et de décrire une séquence de dépôt type (~100 ka) depuis la zone en érosion (300 m) à la base des cortèges sédimentaire (-500 m), de façon approfondie (extension, calage chronostratigraphique, cortèges de dépôt, faciès sédimentaire, milieu de dépôt, partitionnement volumétrique) et de proposer des reconstitutions paléogéographiques montrant deux visages différents de Hawke Bay; Lesquels?
- de décrire ensuite la stratigraphie détaillée des derniers ~1.1 millions d’années en un empilement de 11 séquences de dépôt regroupées en 2 méga-séquences en rétrogradation généralisée;
- de déterminer la géométrie tridimensionnelle des séquences et de montrer l’existence de sous bassins dont l’évolution traduit un changement de configuration du domaine avant arc contemporain de la limite entre les deux méga-séquences;
- de préciser la cartographie structurale et d’établir le calendrier et les vitesses de déformation des failles majeures;
- de quantifier les flux sédimentaires préservés dans le bassin à partir de cartes d’isopaques des séquences et de décrire leur évolution à l’échelle de la séquence de dépôt et de leur emboîtement, à l’échelle du million d’années;
- Enfin, de discuter l’influence des paramètres tectonique, climatique et eustatique sur l’architecture stratigraphique de ce type de bassin, les variations de flux sédimentaires à différentes échelles de temps, et de leurs conséquences sur l’évolution morphostructurale du domaine avant arc.

Ce travail présente un intérêt local important pour améliorer notre compréhension du fonctionnement général du bassin avant arc d’Hawke Bay, sur le dernier million d’années et des contraintes supplémentaires pour amender notre connaissance du développement de la marge active d’Hikurangi. D’un point de vue plus global, cette étude apporte des résultats qualitatifs et quantitatifs sur le comportement d’un couple bassin versant – bassin sédimentaire d’un domaine de forearc actif et permet d’estimer la part respective des différents paramètres de contrôle (tectonique, climat, eustatisme…) sur l’évolution de l’architecture stratigraphique, la **configuration morphostructurale** et des **flux sédimentaires** dans ce type de bassin.

Les conclusions sont présentées suivant ces trois axes en traitant pour chacun des aspects locaux et des aspects globaux.

- **L'architecture stratigraphique :**

Ce travail a permis de mettre en évidence l'existence de 11 séquences de dépôts développées au cours du dernier 1 .1 Ma dans le domaine avant arc de Hawke Bay. L'origine de ces séquences est attribuée aux variations climato-eustatiques périodiques de fortes amplitudes à c.41 et c.100 ka qui caractérisent le Pléistocène. L'existence de cortège de dépôt d'une séquence élémentaire à 100 ka se corrèle à la cyclicité à c. 20 ka.

Ainsi, ce travail confirme les études précédentes (Proust et Chanier, 2004): l'architecture stratigraphique d'un bassin avant arc soumis à une déformation tectonique importante, tel que le bassin de Hawke Bay est fortement contrôlée par l'eustatisme depuis l'échelle de la séquence élémentaire, jusqu'à celle du million d'années.

L'étude détaillée de la dernière séquence à 100 ka, du Pléistocène supérieur, depuis les zones en érosion jusqu'à la base du cortège de bas niveau, montre que l'aggradation des rivières intervient en période de dégradation climatique et de chute importante du niveau eustatique, sur l'ensemble du profil longitudinal, y compris dans les zones soumises à la surrection (jusqu'à 3 mm.yr-1). Ces dernières zones connaissent une incision fluviatile importante lors des périodes de remontée ou de haut niveau marin eustatique. Cette observation témoigne d'un partitionnement volumétrique des sédiments spécifique, qui diffère des modèles classiques. Ces modèles prédisent en effet, une incision fluviatile en période de chute eustatique et une aggradation sédimentaire dans les vallées en période de remontée. Deux explications peuvent être proposées pour rendre compte de ces observations :

- l'aggradation fluviatile s'opère grâce à l'augmentation de l'érosion dans les chaînes axiales due à la raréfaction du couvert végétal en période glaciaire (Litchfield et Berryman, 2005).
- l'aggradation fluviatile est liée à l'augmentation de l'espace d'accommodation aérien de la rivière contemporain par allongement du profil de dépôt lors d'une chute eustatique. Ce phénomène est favorisé par la planéité de la large plateforme de Hawke Bay et par la sinuosité du tracé de la rivière imposé par la croissance de la ride de Kidnappers.

Ces deux explications ne sont pas antagonistes. Il est vraisemblable que l'aggradation fluviatile en période glaciaire, résulte à la fois de l'augmentation de la charge sédimentaire dans la rivière et de l'allongement de son cours.

Ainsi, sur les marges actives, zones où la surrection est importante (mm.yr-1,) à l'échelle de la séquence de dépôt de 100.000ans, les variations climatiques, via leur impact sur l'eustatisme et sur les flux sédimentaires, peuvent contrôler le comportement des rivières (incision vs. aggradation) . Néanmoins, si ce contrôle climatique a une influence sur le comportement des rivières à court terme (<100 ka), l'incision et l'aggradation à plus long terme (> 100 ka) sont dépendantes de la déformation tectonique et donc de la surrection et de la subsidence.

L'empilement des séquences à 100 ka montre une forte rétrogradation, qui se traduit par une migration progressive vers l'arc des environnements de dépôt et des dépocentres. Une discordance érosive composite majeure, se forme par la juxtaposition latérale des limites proximales des 11 séquences. La migration des séquences vers l'arc et le développement de la discordance basale sont attribués aux interactions et co-évolutions entre sédimentation et déformation qui donnent ainsi naissance à une « séquence de remplissage » dont la durée est de l'ordre du million d'années. Cette discordance, largement diachrone se corrèle de bassin en bassin dans l'avant arc et jusque dans le domaine arrière arc (Proust et al., 2005) où elle souligne aussi une migration des séquences vers l'arc en surrection, source des sédiments.
La migration conjointe de la sédimentation et de la déformation, au sein d'une « séquence de remplissage », depuis les zones externes (bassins sédimentaires) vers les zones internes (arc soumis à la déformation et source de sédiments), révèle les interactions tectono-sédimentaires fortes, susceptibles d'intervenir dans l'évolution morphostructurale les bassins de marges actives.

Le développement d'une surface de discontinuité majeure d'étendue régionale (S5) à c.430ka, séparant les onze séquences de dépôts en deux méga-séquences, est attribué à un changement important de l'activité tectonique des structures,.Ce changement correspond à une migration accélérée des séquences de dépôts vers l'arc dont l'origine n'est pas encore clairement identifiée. Cette origine peut être liée (1) à l'augmentation de l'accrétion tectonique dans le prisme, qui se répercuterait jusque dans l'avant arc ou bien encore (2) à la subduction d'un relief particulier (Plateau d'Hikurangi.
Une modification rapide de l'activité tectonique peut donc également s'exprimer sur l'architecture sédimentaire à l'échelle d'une séquence de dépôt élémentaire (100 ka) malgré un développement principalement contrôlé par l'eustatisme. L'occurrence de brèves phases d'intensification de la tectonique dans une marge active reste à expliquer mais

pourrait correspondre à une accrétion tectonique importante reliée à une forte accumulation de la sédimentation dans la fosse consécutive à une variations climatique forte (type Transition du Pléistocène Moyen).

- **La configuration du bassin :**

La géométrie des séquences de dépôt dans Hawke Bay, révélée par les cartes d'isopaques, montre (1) l'étendue de la zone de sédimentation active du domaine avant arc et (2) un changement profond de la configuration du bassin lors du dernier million d'années.

Les sédiments terrigènes provenant de l'érosion des reliefs en surrection sont transportés et déposés dans le bassin avant arc sensu stricto (bassins localisés sur la côte et sur la plateforme continentale – i.e. bassins de Kidnappers, Mahia et Lachlan I & II.), mais également dans le premier bassin de pente du prisme d'accrétion (bassin de Motuokura). Ce dernier constitue le piège ultime pour l'essentiel des sédiments du domaine avant arc. Il est donc important, au moins dans le cas de Hawke Bay, de distinguer le bassin avant arc sensu stricto (entre prisme et arc) et le domaine avant arc au sens large (incluant les bassins de pente), dès lors qu'il est envisagé d'entreprendre des approches quantificatives pertinentes.

La morphologie des domaines avant arc détermine leur capacité à stocker les sédiments. Un bassin de type terrasse profonde aura la capacité de stocker un grand volume de sédiment alors que pour un bassin segmenté en sous bassins, la capacité de stockage est limitée et les sédiments transiteront dans les différents sous bassins.

Dans le contexte de régression et de migration généralisée vers l'arc des sédiments, on peut observer le passage dans le détail, d'une configuration complexe avec trois sous bassins principaux (Mahia, Lachlan I et Motuokura) à une configuration en quatre sous bassins (Kidnappers, Mahia, Lachlan II et Motuokura). L'apparition des bassins de Kidnappers et Lachlan II en lieu et place du bassin de Lachlan I s'explique par la croissance de la ride tectonique de Kidnappers, au sein de ce dernier bassin. La croissance de cette ride marque la croissance latérale des chaînes côtières et par extension, du prisme d'accrétion. Il en résulte une configuration particulière « arquée » dans laquelle les quatre bassins sont connectés en série depuis le bassin de Kidnappers, jusqu'au bassin de Motuokura, en passant par ceux de Mahia et Lachlan II. La transition entre les deux phases s'opère de façon synchrone avec le développement de la limite de mégaséquence S5 vers c. 430 ka.

Ce changement de configuration dans le bassin de Hawke Bay révèle l'importance de la déformation et du développement des structures tectonique dans la distribution des zones d'érosion et de dépôt dans les bassins de marge active. Elle montre plus particulièrement l'importance de la croissance du prisme d'accrétion sur la morphostructure du bassin avant arc et la nécessité de l'appréhender en trois dimensions.

- **L'évolution des flux sédimentaires et les échelles de temps :**

Les flux sédimentaires ont été calculés à partir des estimations de volumes préservés de sédiment dans le domaine avant arc.

A l'échelle de la séquence élémentaire à 100 ka du Pléistocène supérieur, une augmentation flux sédimentaire a été détectée autour du maximum glaciaire (c. 18 ka). Cette augmentation est attribuée à l'intensification de l'érosion dans les zones sources (chaînes axiales) consécutivement à la diminution du couvert végétal lors de la dégradation climatique et à l'importante incision fluviatile, qui caractérise le piedmont en surrection la période post-glaciaire. Ainsi, concernant la dynamique érosive et les flux sédimentaire, le bassin versant de l'avant arc de Hawke Bay montre une forte sensibilité et des temps de réponse courts aux variations rapides du climat du Pléistocène. Cette rapidité et cette efficacité sont attribuées (1) aux paramètres géomorphologiques de relief (fort) et d'aire drainée (faible), et (2) à l'érodabilité du substrat rencontré dans la région Hawke Bay :

- lithologie peu résistante des dépôts marins Mio-Pliocène,
- fracturation importante du socle affleurant dans les chaînes axiales.

Il apparaît donc que les variations climatiques de fortes amplitudes et de fréquences élevées induisent des variations rapides de flux sédimentaires dans les bassins avant arc de marge active. Ce phénomène est amplifié par une topographie et un relief forts, des aires drainées faibles et des substrats peu indurés ou fracturés par la déformation.

A l'échelle du million d'années, les valeurs de flux estimées à partir des volumes préservés pour chacune des onze séquences montrent une évolution en deux phases : (1) une phase de stabilité des flux (c. 2.8 ± 0.3 Mt.yr-1) entre c. 1.1 Ma et c. 430 ka, puis (2) une phase d'augmentation continue des flux de c. 4.6 à c. 6.2 Mt.yr-1 (250 %) entre c. 430 ka et l'actuel. Cette augmentation à partir de c. 430 ka est corrélée au changement de morphostructure du bassin (voir ci-dessus). Cette modification induit une érosion importante des séquences

déposées avant c. 430 ka et un changement de la capacité du bassin à préserver les sédiments déposés dans les bassins nouvellement formés (Kidnappers et Lachlan II).

Les flux sédimentaires estimés à partir des sédiments préservés dans un bassin avant arc affecté par une déformation active reflètent essentiellement des changement dans le potentiel de préservation à long terme (1 Ma) du bassin, plutôt que des variations réelles du flux sédimentaire en provenance du bassin versant.

Les estimations des flux sédimentaires actuels sont trois fois supérieures à la valeur moyenne des flux préservés sur le dernier million d'années et deux fois supérieures à la valeur maximale estimée pour la dernière séquence (dernier maximum glaciaire). Ces différences significatives s'expliquent par (1) des problèmes analytiques inhérents aux méthodes d'estimation des flux anciens et actuels, (2) l'export des sédiments or du domaine de sédimentation avant arc ou, plus vraisemblablement, (3) l'impact de la déforestation anthropique qui intervient avec le développement de l'agriculture extensive. Cette augmentation significative et rapide (< 100 ans) montre également que les conditions géomorphologiques (relief, aire drainée, stockage interne limité) et géologiques (surrection, érodabilité du substrat) rendent le bassin versant de Hawke Bay, particulièrement réactif aux modifications environnementales avec une incidence direct sur les flux sédimentaires.

Les domaines avant arcs, de part leurs caractéristiques morphologiques et géologiques, sont enclins à réagir de façon quasi-instantanée à une variation environnementale (climatique ou anthropique). Il est alors probable qu'un phénomène telle la transition climatique du Pléistocène moyen (cyclicité passant de 41 à 100 ka) est eu une influence sur les flux sédimentaires réels, mais que la déformation tectonique postérieure ait effacé son enregistrement en terme de volumes préservés.

Perspectives :

Perspectives régionales :

Cette étude offre une vision détaillée de l'évolution morphostructurale du domaine avant arc de Hawke Bay sur le dernier 1.1 Ma (configuration des bassins, capacité de préservation…).

Il demeure que les évènements contrôlant cette évolution ne sont pas clairement identifiés ou hiérarchisés. Il apparaît donc que cette étude constitue un point départ vers une approche inévitable de la marge dans sa globalité.

- Il est ainsi envisageable de reproduire ce type d'étude (stratigraphie, quantification des flux sédimentaires) sur l'ensemble des bassins sédimentaires actifs du domaine avant arc, incluant les bassins de plateforme (eg. Poverty Bay) ou de pente. Les données sismiques et géologiques nécessaires sont déjà disponibles pour entreprendre ce type d'étude et certaines d'entre elles sont partiellement interprétées.
- La comparaison entre les domaines avant et arrière arc semble également inévitable. Elle offrirait une vision globale quantifiée de l'évolution morphostructurale de la marge Hikurangi.

D'un point de vue plus spécifique, il est apparu que le bassin de Motuokura présente un remplissage sédimentaire exceptionnel, de par son épaisseur et son enregistrement fin des variations eustatiques sur le dernier 1.1 Ma. Il revêt ainsi les caractéristiques idéales pour une étude détaillée de la transition climatique du Pléistocène moyen.

Perspectives générales :

Par son approche quantificative, cette étude fournit des valeurs de flux sédimentaires préservés, des contraintes sur l'activité des structures, les environnements de dépôt, la géométrie des séquences de dépôts, la chronostratigraphie et les variations paléogéographiques d'une zone de marge active. Ces résultats peuvent être intégrés à des modélisations stratigraphiques numériques, ce qui permettrait de tester les valeurs de flux obtenues.

Références bibliographiques :

A

Ahnert F. 1970. Functional relationships between denudation, relief and uplift in large mid-latitude drainage basins. *American Journal of Science* **268**: 243-263.

Allen PA, Densmore AL. 2000. Sediment flux from an uplifting fault block. *Basin Research* **12**: 367-380.

Alloway BV, Lowe DJ, Barrell DJA, Newnham RM, Almond PC, Augustinus PC, Bertler NAN, Carter L, Litchfield NJ, McGlone MS, Shulmeister J, Vandergoes MJ, Williams PW, NZ-INTIMATE members. 2007. Towards a climate event stratigraphy for New Zealand over the past 30 000 years (NZ-INTIMATE project). *Journal of Quaternary Science* **22**: 9-35.

Anderson RS, Repka JL, Dick GS. 1996. Explicit treatment of inheritance in dating depositional surfaces using in situ ^{10}Be and ^{26}Al. *Geology* **24**: 47-51.

Anderton PW. 1981. Structure and evolution of the south Wanganui Basin, New Zealand. *New Zealand Journal of Geology and Geophysics* **24** : 39-63.

Ansell JH, Bannister S. 1996. Shallowmorphology of the subducted Pacific plate along the Hikurangi margin, New Zealand, *Physics of the Earth and planetary Interiors* **93**: 3–20.

B

Babault J. 2004. *Dynamique de l'érosion dans une chaîne de montagnes : Influence de la sedimentation de piedmont. L'exemple des Pyrénées*. PhD thesis, Mémoires de Géosciences 112, Université de Rennes 1, Rennes: 218 pp.

Babault J, Bonnet S, Crave A, Van den Driessche. 2005a. Influence of piedmont sedimentation on erosion dynamics of an uplifting landscape: An experimental approach, *Geology, 33*, 301-304.

Babault J, Van den Driessche J, Bonnet S, Castelltort S, Crave A. 2005b. Origin of the highly elevated Pyrenean peneplain. *Tectonics* **24:** TC2010.

Babault J, Bonnet S, Van Den Driessche J, Crave A. 2007. High elevation of low-relief surfaces in mountain belts: does it equate to post-orogenic surface uplit? *Terra Nova* **19**: 272-277.

Ballance PF. 1976. Evolution of the upper Cenozoic magmatic arc and plate boundary in northern New Zealand. *Earth and planetary science letters* **28**: 356-370.

Ballance PF, Pettinga JR, Webb C. 1982. A model of the Cenozoic evolution of the northern New Zealand and adjacent areas of the southwest Pacific. *Tectonophysics* **87**: 37–48.

Barnes PM, Lewis KB. 1991. Sheet and rotational failures on a convergent margin: the Kidnappers Slide, New Zealand. *Sedimentology* **38**: 205-22 1.

Barnes PM, Cheung KC, Smits AP, Almagor G, Read SAL, Barker PR, Froggatt P. 1991: Geotechnical analysis of the Kidnappers Slide, upper continental slope, New Zealand. *Marine geotechnology* **10**: 159-188.

Barnes PM. 1996. Active folding of Pleistocene unconformities on te edge of the Australian –Pacific plate boundary zone, offshore North Canterbury, New Zealand. *Tectonics* **15**: 623-640.

Barnes PM. 1995. High-frequency sequences deposited during Quaternary sea-level cycles on a deforming continental shelf, north Canterbury, New Zealand. *Sedimentary Geology* **97**: 131-156.

Barnes PM, Mercier de Lépinay B. 1997. Rates and mechanics of rapid frontal accretion along the very obliquely convergent southern Hikurangi margin, New Zealand. *Journal Geophysical Research* **102**: 24 931–24 952.

Barnes PM, Cheung KC, Smits AP, Almagor G, Read SAL, Barker PR, Froggatt P. 1991: Geotechnical analysis of the Kidnappers Slide,

upper continental slope, New Zealand. *Marine geotechnology* **10**: 159-188.

Barnes PM, Nicol A, Harrison T. 2002. Late Cenozoic evolution and earthquake potential of an active listric thrust complex above the Hikurangi subduction zone, New Zealand. *Geological Society of America Bulletin* **114**: 1379–1405.

Barnes PM, Nicol A. 2004. Formation of an active thrust triangle zone associated with structural inversion in subducting setting, eastern New Zealand. *Tectonics* **23**: TC1015.

Barrell DJA, Alloway BV, Shulmeister J, Newnham RM (eds). 2005. Towards a climate event stratigraphy for New Zealand over the past 30,000 years. *GNS Science Report* SR **2005/07**: 12 pp.

Barrier L, Nalpas T, Gapais D, Proust JN, Cassas A, Bourquin S. 2002. Influence of syntectonic sedimentation on thrust geometry. Field examples from the Iberian Chain (Spain) and analogue modelling. *Sedimentary Geology* **146**: 91-104.

B.C.M. Geophysics Ltd. 1989. Report on a land seismic survey on PPL38320, Hawkes Bay, New Zealand. (C89 survey). *New Zealand unpublished open-file petroleum report* **1522**. Ministry of Economic Development, Wellington.

Beaumont C, Fullsack P, Hamilton J. 1992. Erosional control of active compressional orogens. In *Thrust tectonics*, McClay KR (ed). Chapman & Hall, London: 1-18.

Beanland, S. 1995. The North Island dextral fault belt, Hikurangi subduction margin, New Zealand, Ph.D. thesis, Victoria Univ. of Wellington, Wellington, New Zealand.

Beanland S, Melhuish A, Nicol A, Ravens J. 1998. Structure and deformation history of the inner forearc region, Hikurangi subduction margin, New Zealand. *New Zealand Journal of Geology and Geophysics* **41**: 325–342.

Beavan J, Tregoning P, Bevis B, Kato T, Meertens C. 2002. The motion and rigidity of the Pacific Plate and implications for plate boundary deformation. *Journal of Geophysical Research* **107**: 2261, doi:10.1029/2001JB000282.

Begg JG, Mazengarb C. 1996. Geology of the Wellington area, Sheet R27, R28, part Q27, *IGNS map* **22**, scale 1:50,000: 3 sheets.

Begin ZB, Meyer DF, Shumm SA. 1981. Development of longitudinal profiles of alluvial channels in response to base-level lowering. *Earth Surface Processes and Landforms* **6**: 49-68.

Berger A. 1978. Long-term variations of daily insolation and Quaternary climatic changes. *Journal Atmospheric Science* **35**: 1379-1405.

Bernet M, Zattin M, Garver JI, Brandon MT, Vance JA. 2001. Steady-state exhumation of the European Alps. *Geology* **29**: 35-38.

Berryman K. 1993. Distribution, age, and deformation of Late Pleistocene marine terraces at Mahia Peninsula, Hikurangi Subduction Margin, New Zealand, *Tectonics* **12**: 1365– 1379.

Berryman KR, Marden M, Eden DN, Mazengarb C, Ota Y, Moriya I. 2000. Tectonic and paleoclimatic signifi cance of Quaternary river terraces of the Waipaoa River, east coast, New Zealand. *New Zealand Journal of Geology and Geophysics* **43**: 229–245.

Beu AG, Browne GH, Grant-Taylor TL. 1981. New *Chlamys delicatula* localities in the central North Island and uplift of the Ruahine Range. *New Zealand Journal of Geology and Geophysics* **24**: 127- 132.

Beu AG, Pillans B. 1987. A review of New Zealand Pleistocene stratigraphy with emphasis on marine rocks. In Proceedings *of the First International Colloquium on Quaternary Stratigraphy of Asia and Pacific Area*, Osaka, 1986, Itihara M, Kamel T (eds): 250–269.

Binnie SA, Phillips WM, Summerfield MA, Fifield LK. 2007. Tectonic uplift, threshold hillslopes, and denudation rates in a developing mountain range. *Geology* **35**: 743-746.

Blum MD, Törnquist TE. 2000. Fluvial responses to climate and sea-level change: a review and look forward. *Sedimentology* **47**: 2–48.

Bodger KL, Pettinga JR, Barnes PM. 2006. Seafloor Structural Geomorphic Evolution in Response to Seamount Subduction, Poverty Bay Indentation, New Zealand. EOS Transactions AGU **87**(52), Fall Meeting Supplement, Abstrasts T21A-0392.

Bonnet S. 2005. *Variations climatiques, soulèvements continentaux et dynamique des reliefs – Exemples naturels et apports de la modélisation expérimentale en géomorphologie*. Unpublished HDR Thesis, Université de Rennes 1, Rennes : 125 pp.

Bowen DQ, Pillans B, Sykes GA, Beu AG, Edwards AR, Kamp PJJ, Hull AG. 1998. Amino acid geochronology of Pleistocene marine sediments in the Wanganui Basin: a New Zealand framework for correlation and dating. *Journal of the Geological Society London* **155**: 439–446.

Brandon MT, Roden-Tice MK, Garver JI. 1998. Late Cenozoic exhumation of the Cascadia accretionary wedge in the Olympic Mountains, northwest Washington State, *Geological Society of America Bulletin* **110**: 985-1009.

Braun J. 2002. Quantifying the effect of recent relief changes on age-elevation relationships, *Earth Planetary Science Letters* **200**: 331-343.

Braun J, Pauselli C. 2004. Tectonic evolution of the Lachlan Fold Belt, southeastern Australia: constraints from coupled numerical models of crustal deformation and surface erosion driven by subduction of the underlying mantle, *Physics of the Earth and Planetary Interiors* **141**: 281-301.

Brook MS, Brock BW. 2005. Valley morphology and glaciation in the Tararua Range, southern North Island, New Zealand. *New Zealand Journal of Geology and Geophysics* **48**: 717-724.

Brown, L.J., 1993, Heretaunga Plains ground water resource investigations - Flaxmere and Tollemache Orchard exploratory water wells, *Institute of Geological & Nuclear Sciences Ltd Report* **1993/732402-11**: 24 pp.

Brown, L.J. & Gibbs, B.R., 1996, Heretaunga Plains Ground Water Resource Investigations – Awatoto Exploratory Water Well – HBRC Well No. 3699, *Institute of Geological & Nuclear Sciences Ltd Report* **1996/735102**: 93 pp.

Browne GH. 2004. Late Neogene sedimentation adjacent to the tectonically evolving North Island axial ranges: insights from Kuripapango, western Hawke's Bay. *New Zealand Journal of Geology and Geophysics* **47**: 663-674.

Browne GH, Naish TR, 2003. Facies development and sequence architecture of a late Quaternary fluvial-marine transition, Canterbury Plains and shelf, New Zealand: implications for forced regressive deposits. *Sedimentary Geology* **158**: 57–86.

Burbank DW, Leland J, Fielding EJ, Anderson RS, Brozovic N, Reid MR, Duncan C. 1996. Bedrock incision, rock uplift and threshold hillslopes in the northwestern Himalayas. *Nature* **379**: 505-510.

Buret Ch, Chanier F, Ferrière J, Proust JN. 1997. Individualization of a forearc basin during the active margin evolution: Hikurangi subduction margin, New Zealand. *Comptes Rendus Académie Sciences Paris* **325**: 615–621.

Burger RL, Fulthorpe CS, Austin Jr JA, Gulick SPS. 2002. Lower Pleistocene to present structural deformation and sequence stratigraphy of the continental shelf, offshore Eel iver Basin, northern California. *Marine Geology* **185**: 249-281.

C

Carretier S, Lucazeau F. 2005. How does alluvial sedimentation at range fronts modify the erosional dynamics of mountain catchments. *Basin Research* **17**: 361-381.

Carter JA. 2002. Phytolith analysis and paleoenvironmental reconstruction from Lake

Poukawa core, Hawkes Bay, New Zealand. *Global and Planetary Change* **33**: 257– 267.

Carter L. 1974. Sedimentation in Hawke Bay off Hastings. *NZOI Oceanographic Summary* **3**: 8 pp.

Carter L, 2001. Currents of change: the ocean flow in a changing world. *Water and Atmosphere* **9**: 15-17 http://www.niwa.co.nz/pubs/wa/09-4/

Carter L, Heath RA. 1975. Role of mean circulation, tides and waves in the transport of bottom sediment on the New Zealand continental shelf. *New Zealand Journal of Marine and Freshwater Research* **9**: 423-428.

Carter L, Lewis KB. 1976. Subsurface structure and its influence on nearshore sedimentation off southern Hawkes Bay. *NZOI Records* **3**(5): 33-40.

Carter L, Garlick RD, Sutton P, Chiswell S, Oien NA, Stanton BR. 1998. Ocean Circulation New Zealand. *NIWA Chart Miscellaneous Series* **76**.

Carter L, Manighetti B. 2006. Glacial/interglacial control of terrigenous and biogenic fluxes in the deep ocean off a high input collisional margin: 1 139 kyr-record from New Zealand. *Marine Geology* **226**: 307-322.

Carter RM, Naish TR. 1998a. A review of Wanganui Basin, New Zealand: global reference section for shallow marine, Plio–Pleistocene (2.5–0 Ma) cyclostratigraphy. *Sedimentary Geology* **122**: 37-52.

Carter RM, Naish TR. 1998b. Have local stages outlived their usefulness for the New Zealand Pliocene-Pleistocene? *New Zealand Journal of Geology and Geophysics* **41**: 271-279.

Carter RM, McCave IN, Richter C, Carter L, et al. 1999. Southwest Pacific Gateways, Sites 1119-1125. *Proceedings of Ocean Drilling Program, Initial Reports* **181**: 1-112.

Cashman SM, Kelsey HM. 1990. Forearc uplift and extension, southern Hawke's Bay, New Zealand: Mid-Pleistocene to present. *Tectonics* **9**: 23-44.

Cashman SM, Kelsey HM, Erdman CF, Cutten HNC, Berryman KB. 1992. A structural transect and analysis of strain partitioning across the forearc of the Hikurangi subduction zone, southern Hawke's Bay, North Island, New Zealand. *Tectonics* **11**: 242-257.

Castelltort S, Van Den Driessche. 2003. How plausible are high-frequency sediment supply-driven cycles in the stratigraphic record? *Sedimentary Geology* **157** : 3-13.

Catuneanu O. 2006. *Principles of sequence stratigraphy*. Elsevier Science: Amsterdam; 386.

Chanier F. 1991. *Le Prisme d'accrétion Hikurangi: un témoin de l'évolution géodynamique d'une marge active péripacifique (Nouvelle-Zélande).* Thèse de Doctorat de l'Université des Sciences et Techniques de Lille – Flandres-Artois.

Chanier F, Ferrière J, Angelier J. 1992. Extension et érosion tectonique dans un prisme d'accrétion: l'exemple du prisme Hikurangi (Nouvelle Zélande). *Compte Rendus de l'Académie des Sciences Paris* **315**: série II, 741–747.

Chanier F, Ferrière J, Angelier J. 1999. Extensional deformation across an active margin, relations with subsidence, uplift and rotations: the Hikurangi subduction, New Zealand. *Tectonics* **18**: 862–876.

Chiswell SM. 2000. The Wairarapa Coastal Current. *New Zealand Journal of Marine and Freshwater Research* **34**: 303-315.

Christie-Blick N, Driscoll NW. 1995. Sequence stratigraphy. *Annual Review of Earth and Planetary Sciences* **23**: 451-478.

Cochran U, Zachariasen J, Mildenhall D, Hayward B, Southall K, Hollis C, Barker P, Wallace L, Alloway B, Wilson K. 2006. Paleoecological insights into subduction zone earthquake occurrence, eastern North Island, New Zealand. *GSA Bulletin*, **118**: 1051-1074.

Cole JW, Lewis KB (1981) Evolution of the Taupo-Hikurangi subduction system. *Tectonophys* **72**:1–21

Collier REL, Leeder MR, Trout M, Ferentinos G, Lyberis E, Papatheodorous G. 2000. High sediment yields and cool, wet winters: rest of past glacial paleoclimates in the northern Mediterranean. *Geology* **28**: 999-1002.

Collot J-Y, Delteil J, Herzer RH, Wood R, Lewis KB. 1995. Sonic imaging reveals new plate boundary structures off shore New Zealand. *EOS* **76**: 4-5.

Collot J-Y, Delteil J, Lewis KB, Davy B, Lamarche G, Audru J-C, Barnes P, Chanier F, Chaumillon E, Lallemand S, de Lépinay BMD, Orpin AR, Pelletier B, Sosson M, Toussaint B, Uruski C. 1996. From oblique subduction to intra-continental transpression: structures of the southern Kermadec-Hikurangi margin from multibeam bathymetry, side-scan sonar and seismic reflection. *Marine Geophysical Researches* **18**: 357–381.

Collot J-Y, Lewis KB, Lamarche G, Lallemand S. 2001. The giant Ruatoria debris avalanche on the northern Hikurangi margin, New Zealand; results of oblique seamount subduction. *Journal of Geophysical Research B*: *Solid Earth and Planets* **106**: 19271-19297.

Conquest Exploration. 1988. Conquest Exploration 1988 seismic survey, AG and S lines, PPL 38321. *New Zealand unpublished open-file petroleum report* **2059**. Ministry of Economic Development, Wellington.

Conquest Exploration Co. 1989. Hawkes Bay shallow seismic and bottom sampling 38322 New Zealand. *New Zealand unpublished open-file petroleum report* **1471**. Ministry of Economic Development, Wellington.

Cooke PJ., Campbell NS. 1988. Micropalaeontology and climatic implications of the latest Quaternary section at DSDP Site 594, Southeast New Zealand. *Geological Society of New Zealand Miscellaneous Publication* **41a**: 55 pp.

Coulbourne WT, Moberley R.1977. Structural evidence of the evolution of fore-arc basins off South America. *Canadian Journal of Earth Sciences* **14**: 102-116.

D

Dadson, S.J., et al. 2003. Links between erosion, runoff variability and seidmicity in the Taiwan orogen. *Nature*, **426**: 648-651.

Dadson, S.J., et al. 2004. Earthquake-triggered increase in sediment delivery from an active mountain belt. *Geology* **32**: 733-736.

Dalrymple M, Prosser J Williams B. 1998. A dynamic systems approach to the regional controls on deposition and architecture of alluvial sequences, illustrated in the statfjord formation (United Kingdom, northern North Sea). In Shanley KW, McCabe PJ, Relative Role of Eustasy, Climate, and Tectonism in Continental Rocks. *Special Publication* **59**, Society Economic Paleontologists Mineralogists: Tulsa, OK; 65-81.

Davis WM. 1889. The rivers and valleys of Pennsylvania. *National Geographic Magazine* **1**: 183-253.

Dickinson WR. 1995. Forearc Basins. In *Tectonics of Sedimentary Basins*., Busby CJ, Ingersoll RV. (eds). Blackwell Science, Cambridge : 221-261.

Dickinson WR, Seely DR. 1979. Structure and stratigraphy of forearc regions. *American Association of Petroleum Geologists Bulletin* **63**: 2-31.

Dominguez S, Lallemand SE, Malavieille J, von Huene R. 1998. Upper plate deformation associated with seamount subduction. *Tectonophysics* **293**: 207-224.

Dravid PN, Brown LJ. 1997. *Heretaunga Plains—Groundwater study, Vol. I & II*. Napier, New Zealand. Hawke's Bay Regional Council: 254 pp.

Dymond JR, Ausseil AG, Shepherd JD, Buettner L. 2006. Validation of a region-wide model of landslide susceptibility in the Manawatu–Wanganui region of New Zealand. *Geomorphology* **74**: 70-79.

E

Eden DN, Page MJ.1998. Palaeoclimatic implications of a storm erosion record from late Holocene lake sediments, North Island, New Zealand. *Palaeogeography Palaeoclimatology. Palaeoecology* **139**: 37-58.

Einsele G. 1992. Sedimentary Basins – Evolution, Facies and Sediment Budget. Springer Verlag, Berlin: 628 pp.

Erdman CF, Kelsey HM. 1992. Pliocene and Pleistocene stratigraphy and tectonics, Ohara Depression and Wakarara Range, North Island, New Zealand. *New Zealand Journal of Geology and Geophysics* **35**: 177-192.

Ehlers TA, Farley KA. 2003. Apatite (U-Th)/He thermochronomotry: methods and applications in tectonic and surface processe. *Earth and Planetary Science Letters* **206**: 1-14.

F

Farley KA, Rusmore ME, Bogue SW. 2001. Post-10Ma uplift and exhumation of the northern Coast Mountains, British Columbia. *Geology* **29**: 97-192.

Farnsworth KL, Milliman JD. 2003. Effects of climatic and anthropogenic change on small mountainous rivers: the Salinas River example. *Global and Planetary Change* **39**: 53-64.

Field, BD, et al. 1989. Cretaceous and Cenozoic sedimentary basin and geological evolution of the Canterbury region, South Island, New Zealand. *IGNS Geological Bulletin, Sedimentary basin research* **2**: 94 pp.

Field BD, Uruski CI, et al. 1997. Cretaceous-Cenozoic geology and petroleum systems of the East Coast region, New Zealand. *Institute of Geological & Nuclear Sciences Monograph* **19**. Institute of Geological & Nuclear SciencesLimited, Lower Hutt, New Zealand: 301pp.

Fisk HN. 1944. Geological investigation of the alluvial valley of the lower Mississippi River: Mississippi River Commission, Vicksburg.

Fitzgerald PG, Stump E, Redfield TF. 1993. Late Cenozoic uplift of Denali and its relation to relative plate motion and fault morphology. *Science* **259**: 497-499.

Fleming CA. 1953. The geology of the Wanganui Subdivision. *Bulletin of the Geological Society of New Zealand* **52**: 362.

Foster G, Carter L. 1997. Mud sedimentation on the continental shelf at an accretionary margin—Poverty Bay, New Zealand. *New Zealand Journal of Geology and Geophysics* **40**, 157–173.

Francis RICC. 1985. An alternative water circulation pattern for Hawke Bay, New Zealand. *New Zealand Journal of Marine and Freshwater Research* **19**: 399-404.

Francis DA. 1993. Report on the geology of the Waimarama – Kidnappers area, Hawke's Bay adjacent to offshore PPL38321. Wellington, Ministry of Economic Development – Crown Minerals, Open-File *Petroleum Report* **1926**: 46pp.

Francis DA. 2002. Prospects and leads in PEP38332, Hawke's Bay East Coast Basin, NZ. Wellington, Ministry of Economic Development – Crown Minerals, Open-File *Petroleum Report* **3114**: 11pp.

Francis DA. 2002. Prospects and leads in PEP38332, Hawke's Bay East Coast Basin, NZ. Wellington, Ministry of Economic Development – Crown Minerals, Open-File *Petroleum Report* **3114**: 11pp.

Francis DA, Bennett D, Courteney S. 2004. Advances in understanding of onshore East Coast Basin structure, stratigraphic thikness and hydrocarbon generation. *New Zealand Petroleum Conference Proceedings* **2004**: 20pp

Froggatt PC, Rogers GM. 1990. Tephrostratigraphy of high altitude peat bogs along the axial ranges, North Island, New Zealand. *New Zealand Journal of Geology and Geophysics* **33**: 111–125.

Fuller CW, Willett SD, Brandon MT. 2006. Formation of forearc basins and their influence

on subduction zone earthquakes. *Geology* **34**: 65-68.

G

Gallagher K. 1995. Evolving temperature histories from apatite fission-track data. *Earth and Planetary Science Letters* **136** : 421–435.

Galy A, France-Lanord C. 2001. Higher erosion rates in the Himalaya: geochemical constraints on riverine flux. *Geology* **29**: 23-26.

Geo-Prakla. 2000. Wairarapa & Hawke Bay 2D Seismic Survey – WE00 Hawke Bay. PEP 38325. *New Zealand unpublished open-file petroleum report* **2483**. Ministry of Economic Development, Wellington.

Gibb JG. 1986. A New Zealand regional Holocene eustatic sea-level curve and its application for determination of vertical tectonic movements. In Reilly, W.I., and Harford, B.E., eds., Recent crustal movements of the Pacific region: Wellington, *Bulletin of Royal Society of New Zealand* **24**: 377–395.

Gomez B, Filipelli G, Carter L, Trustrum N. 2001. *Recent sedimentation on an actively subsiding shelf: Hikurangi subduction margin, North Island, New Zealand*. In: MARGINS Chapman Conference, Puerto Rico, June 2001.

Gomez B, Carter L, Trustrum NA. 2007. 2400 yr record of natural events and anthropogenic impacts in inter-correlated terrestrial and marine sediment cores: Waipaoa Sedimentary System, New Zealand. *Geological Society of America Bulletin*, doi: 10.1140/B259961.

Gradstein FM, Ogg JG, Smith AG, Agterberg FP, Bleeker W, Cooper RA, Davydov V, Gibbard P, Hinnov LA, House MR, Lourens L, Luterbacher H-P, McArthur J, Melchin MJ, Robb LJ, Shergold J, Villeneuve M, Wardlaw BR, Ali J, Brinkhuis H, Hilgen FJ, Hooker J, Howarth RJ, Knoll AH, Laskar J, Monechi S, Powell J, Plumb KA, Raffi I, Röhl U, Sanfilippo A, Schmitz B, Shackleton NJ, Shields GA, Strauss H, Van Dam J, Veizer J, van Kolfschoten Th, Wilson D. 2004a. *A Geologic Time Scale 2004*. Cambridge University Press, 610 pp.

Gradstein FM, Ogg JG, Smith AG, Bleeker W, Lourens LJ. 2004b. A new Geologic Time Scale, with special reference to Precambrian and Neogene. *Episodes* **27**: 83-100.

Granger DE. 2007. Landscape Evolution. In *Encyclopedia of Quaternary Science*, Elias SA (ed). Elsevier, Amsterdam: 445-452.

Grant-Taylor TL. 1978. The geology and structure of the Ruataniwha Plains. *In:* Speden, I. *ed.* Geology and erosion in the Ruahine Range. *New Zealand Geological Survey report* **G20**: 31-51.

Gunnell Y. 1998. Present, past and potential denudation rates: is there a link? Tentative evidence from fission-track data, river sediment loads and terrain analysis in the South Indian shield. *Geomorphology* **25**: 135-153.

H

Harmsen FJ. 1985. Lithostratigraphy of Pliocene strata, central and southern Hawke's Bay, New Zealand. *New Zealand journal of geology and geophysics* **28**: 413 -433.

Harper MA, Collen J. 2002. Glaciations, interglaciations and reworked microfossils in Poukawa Basin, New Zealand. *Global and Planetary Change* **33**: 43–256.

Hack JT. 1960. Interpretation of erosional topography in humid temerate regions. *American Journal of Science* **258**: 80-97.

Hayward B, Grenfell HR, Sabaa AT, Carter R, Cochran U, Lipps JH, Shane PR, Morley M. 2006. Micropaleontological evidence of large earthquakes in the past 7200 years in southern Hawke's Bay, New Zealand. *Quaternary Science Reviews* **25**: 1186-1207.

Hay WW, Sloan JL, Wold CN. 1988. Mass/age distribution and composition of sediments on the ocean floor and the global rate of sediment subduction. *Journal of Geophysical Research* **93**: 14,933-14,940.

Head MJ, Gibbard PL. 2005. Early-Middle Pleistocene transitions: an overview and recommendation for the defining boundary. In *Early-Middle Pleistocene Transitions: The land-Ocean Evidence*., Head MJ, Gibbard PL. (eds). Geological Society, London, Special Publications **247**: 1-18.

Heffer K, Milne AD, Simpson C. 1976. BP, Shell Aquitaine and Todd Petroleum Development Ltd, Well completion report, Hawke Bay-1, Offshore east coast, North Island, New Zealand: Wellington, Ministry of Economic Development – Crown Minerals, Open-File *Petroleum Report* **667**: 61pp.

Heuret A, Lallemand S. 2003. Upper plate absolute motion and slab-anchor force control on back-arc deformation ; Abstract AGU-EUG-EGS Joint Assembly, Nice, April 2003.

Hicks DM, Shankar U. 2003. Sediment yield from New Zealand rivers. *NIWA Chart, Miscellaneous Series* **79**.

Hoernle K, Hauff F, Werner R, Mortimer N. 2004. New insights into the origin of the Hikurangi oceanic plateau, EOS Transactions of the American Geophysical Union **85**: 401-416.

Hoffman PF, Grotzinger JP. 1993. Orographic precipitation, erosional unloading, and tectonic style. *Geology **21***: 195-198.

Hovius N, Stark CP, Allen PA. 1997. Sediment flux from a mountain belt derived by landslide mapping. *Geology* **25**: 231-234.

Hovius N, Stark CP, Tutton MA, Abbott LD. 1998. Landslide-driven network evolution in a pre-steady-state mountain belt: Finisterre Mountains, Papua New Guinea. *Geology* **26**: 1071-1074.

Howard AD, Kerby G. 1983. Channel changes in badlands. *Geological Society of America Bulletin* **94**: 739-752.

Hull AG. 1985. *Late Quaternary geology of the Cape Kidnappers area, Hawkes Bay, New Zealand*. MSc thesis, Victoria University, Wellington, New Zealand.

Hull AG. 1986. Pre-A.D. 1931 tectonic subsidence of Ahuriri Lagoon, Napier, Hawkes Bay, New Zealand. *New Zealand Journal of Geology and Geophysics* **29**: 75-82.

Hull AG. 1987. A late Holocene uplifted shore platform on the Kidnappers coast, North Island, New Zealand. some implications for shore platform development processes and uplift mechanism. *Quaternary Research* **28**: 183-195.

Hull AG. 1990. Tectonics of the 1931 Hawke Bay earthquake. *New Zealand Journal Geology and Geophysics* **33**: 309-320.

Huntington E. 1907. Some characteristics of the glacial period in non-glaciated regions. *Geological Society of America Bulletin* **18**: 351-388.

I

Imbrie J, Hays JD, Martinson DG, McIntyre A, Mix AC, Morley JJ, Pisias NG, Prell WL, Shackleton NJ, 1984. The orbital theory of Pleistocene climate: support from a revised chronology of the marine $\delta\ ^{18}O$ record. In: Berger A, Imbrie J, Hays J, Kukla G, Saltzman B. (Eds.), Milankovitch and climate. Reidel Publishing Company, Dordrecht, pp. 269-305.

J

Jervey MT. 1988. Quantitative geological modeling of siliciclastic rock sequences and their seismic expression. In Sea-level Changes—An Integrated Approach, Wilgus CK, Hastings BS, Kendall ChStCG, Posamentier HW, Ross CA, Van Wagoner JC (eds). Special Publication 42, Society Economic Paleontologists Mineralogists: Tulsa, OK: 47-69.

Jiongxin X .2005. Precipitation–vegetation coupling and its influence on erosion on the Loess Plateau, China. *Catena* **64**: 103- 116.

K

Kamp PJJ. 1978. *Stratigraphy and sedimentology of conglomerates in the Pleistocene Kidnappers Group, Hawkes Bay*. Unpublished MSc thesis, University of Waikato, Hamilton, New Zealand

Kamp PJJ. 1990. Kidnappers Group (middle Pleistocene), Hawke Bay.*Geological Society of New Zealand miscellaneous publication* **50B**: 105-118.

Kamp PJJ. 1999. Tracking crustal processes by FT thermochronology in a forearc high (Hikurangi margin, New Zealand) involving Cretaceous subduction termination and mid-Cenozoic subduction initiation. *Tectonophysics* **307**: 313-343.

Kamp PJJ, Turner G. 1990. Pleistocene unconformity-bounded shelf sequences (Wanganui basin, New Zealand), correlated with the global isotope record. *Sedimentary Geology* **68**: 155-161.

Kamp PJJ, Vonk AJ, Bland KJ, Griffin AG, Hayton S, Hendy AJW, McIntyre AP, Nelson CS, Naish T. 2002. Megasequence architecture of Taranaki, Wanganui, and King Country basins and Neogene progradation of two continental margin wedges across western New Zealand. *Proceedings of the New Zealand Petroleum Exploration Conference*, Auckland, February 2002: 464–481.

Kamp PJJ, Vonk AJ, Bland KJ, Hansen RJ, Handy AJW, McIntyre AP, Ngatai M, Cartwright SJ, Hayton S, Nelson CS. 2004. Neogene stratigraphic architecture and tectonic evolution of Wanganui, King Country, and eastern Taranaki Basins, New Zealand. *New Zealand Journal of Geology and Geophysics* **47**: 625–644.

Katz HR, Leask B. 1990. The South Wanganui Basin—a neglected hydrocarbon prospect. Petroleum exploration in New Zealand News, Wellington, New Zealand, pp. 19–25.

Kettner AJ, Gomez B, Syvitski JPM. 2007. Modeling suspended sediment discharge from the Waipaoa River system, New Zealand: The last 3000 years: *Water Resources Research* **43**: doi: 10.1029/2006WR005570.

King PR. 2000. Tectonic reconstruction of New Zealand: 40 Ma to present. *New Zealand Journal of Geology and Geophysics* **43**: 611-638.

Kingma JT, 1958. Geology of the Wakarara Range, central Hawke's Bay. *New Zealand Journal of Geology and Geophysics* **1**, 76-91.

Kingma JT. 1962. Sheet **11**—Dannevirke. Geological map of New Zealand 1:250 000. Wellington, New Zealand Department of Scientific and Industrial Research.

Kingma, J.T., 1970: Sheets **N134** Napier and Hastings, N135 Kidnappers (1st Ed.). Geological Map of New Zealand 1:63,360. Department of Scientific and Industrial Research, Wellington, New Zealand.

Kingma JT. 1971. Geology of the Te Aute subdivision. *New Zealand Geological Survey bulletin* **70**: 173 pp.

Kirchner JW, Finkel RC, Riebe RC, Granger DE, Clayton JL, King JG, Megahan WF. 2001. Mountain erosion over 10 yr, 10 k.y., and 10 m.y. time scales. *Geology* **29**: 591-594.

Koons PO. 1990. Two-sided orogen: Collision and erosion from the sandbox to the Southern Alps, New Zealand. *Geology* **18**: 679-682.

Koons P0. 1994. Three-dimensional critical wedges: Tectonics and topography in oblique collisional orogens. ***Journal of Geophysical Research* 99**: ***12301-12315.***

Kvenvolden KA. 1988. Hydrocarbon gas in sediments of the Pacific Ocean. *Geo-marine Letters* **8**: 179-187.

L

Lague D, Davy P, Crave A. 2000. Estimating uplift rate and erodibility from the area-slope relationship: examples from Brittany (France) and numerical modelling, *Physics and Chemistry of the Earth* **25**: 543-548.

Lague D, Davy P. 2003. Constraints on the long-term colluvial erosion law by analysing slope-area relationships at various tectonic

uplift rates in the Siwaliks Hills (Nepal), *Journal of Geophysical Research* **108**: doi:10.1029/2002JB001893

Lake Tutira Drilling Group. 2007. Eight thousand years of storms and droughts. *Water & Atmosphere* **15**: 24-25.

Lallemand S, Huchon P, Jolivet L, Prouteau G. 2005. Convergence lithosphérique. *Société Géologique de France*. Vuibert, Paris: 182 pp.

Lallemand S, Heuret A, Boutelier D. 2003. Control of slab dip on upper plate strain regime in subduction zones. Abstract AGU-EUG-EGS Joint Assembly, Nice, April 2003.

Lamarche G, Collot JY, Garlick R, de Lange W. 2002. Submarine avalanche volume calculations, a prerequisite to tsunami modelling: the example of the Ruatoria debris avalanche. EGS General Assembly, Abstract, Nice, France.

Lamarche G, Proust JN, Nodder SD. 2005. Long-term slip rates and fault interactions under low contractional strain, South Wanganui Basin, New Zealand. *Tectonics* **24**: TC4004 [doi:10.1029/2004TC001699].

Lamarche G, Barnes PM, Bull JM. 2006. Faulting and extension rate over the last 20,000 years in the offshore Whakatane Graben, New Zealand continental shelf. *Tectonics* **25**: doi: 10.1029/2005TC001886.

Lamb SH. 1988. Tectonic rotations about vertical axes during the last 4 Ma in part of the New Zealand plate-boundary zone. *Journal of structural Geology* **10**:, 874 – 893.

Lamothe L. 1918. Les anciennes nappes alluviales et lignes de rivages du bassin de la Somme et leurs rapports avec celles de la Méditerranée occidentale. *Bulletin de la Société géologique de France* **18**: 3-58.

Langbein WB, Schumm SA. 1958. Yield of sediment in relation to mean annual precipitation. *Transactions of the American Geophysical Union* **47**: 1076-1084.

Laursen J, Scholl DW, von Huene R. 2002. Neotectonic deformation of the central Chile margin: Deepwater forearc basin formation in response to hot spot ridge and seamount subduction. *Tectonics* **21**: doi: 10.1029/2001TC901023.

Laursen J, Normack WR. 2003. Impact of structural and autocyclic basin-floor topography on the depositional evolution of the deep-water Valparaiso forearc basin, central Chile. *Basin Research* **15**: 201-226.

Leckie DA. 1994. Canterbury Plains, New Zealand – Implications for sequence stratigraphic models. *American Association of Petroleum Geologists Bulletin* **78**: 1240-1252.

Lee HJ, Syvitski JPM, Parker G, Orange D, Locat J, Hutton EWH, Imram J. 2002. Distinguishing sediment waves from slope failure deposits: field examples, including the 'Humboldt Slide', and modelling results. *Marine Geology* **192**: 79-104.

Leith KJ. 2003. The role of deep-seated landslide in the geomorphic evolution of the Esk Valley, Hawke's Bay: An innovative approach to hazard evaluation. *Unpublished MSc thesis*, University of Canterbury, Christchurch, New Zealand.

Letetrel C. 2006. Quantification et modélisation numérique de la dynamique du flux sédimentaire dans le bassin de Wanganui, Nouvelle-Zélande, au plio-pléistocène. Mémoires de Master 2 2005-2006, non publié, Géosciences Rennes, Rennes : 24 pp.

Lewis KB. 1971a. Growth rate of folds using tilted wave planed surfaces: coast and continental shelf, Hawke's Bay, New Zealand. *In*: Collins, B. W.; Fraser, R. *ed*. Recent crustal movements. *The Royal Society of New Zealand Bulletin* **9**: 225-231.

Lewis KB. 1971b. Slumping on a continental slope inclined at *l°-4°*. *Sedimentology* **16**: 97-110.

Lewis KB. 1973a. Erosion and deposition on a tilting continental shelf during Quaternary oscillations of sea level. *New Zealand journal of geology and geophysics* **16**: 281-301.

Lewis KB. 1973b. Sediments on the continental shelf and slope between Napier and Castelpoint, New Zealand. *New Zealand*

journal of marine and freshwater research **7**: 183-208.

Lewis KB. 1974. Upper Tertiary rocks from the continental shelf and slope of Southern Hawke's Bay. *New Zealand journal of marine and freshwater research* **8**: 663-670.

Lewis KB. 1980. Quaternary sedimentation on the Hikurangi oblique-subduction and transform margin, New Zealand. In *Sedimentation in obliqueslip mobile zone*, Ballance, P.F., Reading, H.G. (eds). Special publication International Association of Sedimentologists **4**: 171-189.

Lewis KB, Bennett DJ. 1985. Structural pattern on the Hikurangi Margin: an interpretation of new seismic data. in *New seismic profiles, cores, and dated rocks from the Hikurangi margin, New Zealand*, Lewis, K.B. (comp). New Zealand Oceanographic Institute field report **22**. Division of Marine and Freshwater Science, Department of Scientific and Industrial Research, Wellington.

Lewis SD, Hayes DE. 1984. A Geophysical Study of the Manila Trench, Luzon, Philippines 2. Fore Arc Basin Structural and Stratigraphic Evolution. *Journal of Geophysical Research* **89**: 9196-9214.

Lewis KB, Pettinga JR. 1993. The emerging, imbricate frontal wedge of the Hikurangi margin. *In*: South Pacific sedimentary basins. *Sedimentary Basins of the World 2, Basins of the Southwest Pacific*, Ballance PF (ed.). Elsevier, Amsterdam: 225-250.

Lewis KB, Pantin HM. 2002. Channel-axis, overbank and drift sediment waves in the southern Hikurangi Trough, New Zealand. *Marine Geology* **192**: 123–151.

Lewis KB, Collot J-Y, Davy BW, Delteil L, Lallemand SE, Uruski CI & GeodyNZ team. 1997. North Hikurangi GeodyNZ swath maps: depth, texture and geological interpretation. *NIWA chart miscellaneous series* **72**. National Institute of Water and Atmospheric Research, Wellington.

Lewis KB, Collot J-Y, Lallemand SE. 1998. The dammed Hikurangi Trough: a channel-fed trench blocked by subducting seamounts and their wake avalanches (New Zealand-France GeodyNZ Project). *Basin Research* **10**: 441-468.

Lewis KB, Lallemand S, Carter L. 2004. Collapse in a Quaternary shelf basin off East Cape, New Zealand: evidence for passage of a subducted seamount inboard of the Ruatoria giant avalanche. *New Zealand Journal of Geology and Geophysics* **47** 415-429.

Li YH. 1976. Denudation of Taiwan island since the Pliocene epoch. *Geology* **4**: 105-107.

Lillie AR. 1953. The geology of the Dannevirke Subdivision. *New Zealand Geological Survey Bulletin* **46**.

LINZ (Land Information New Zealand). 2000. 25-m Digital Elevation Model based on NZMS260 Digital 20-m contours (scale 1:50,000). Published by Land Information New Zealand, Lambton Quay, Wellington. Crown Copyright reserved.

Lisiecki LE, Raymo ME. 2005. A Pliocene-Pleistocene stack of 57 globally distributed benthic $\delta^{18}O$ records. *Paleoceanography* **20**: PA1003, doi:10.1029/2004PA001071.

Litchfield N. 2003. Maps, stratigraphic logs and age control data for river terraces in the eastern North Island. *Institute of Geological and Nuclear Sciences Science Report* **31**: 102 pp.

Litchfield NJ, Berryman KR. 2005. Correlation of fluvial terraces within the Hikurangi Margin, New Zealand: Implications for climate and base level controls. *Geomorphology* **68**: 291-313.

Litchfield NJ, Berryman KR. 2006. Relations between postglacial fluvial incision rates and uplift rates in North Island, New Zealand. *Journal of Geophysical Research* **111**: doi:10.1029/2005JF000374.

Litchfield N, Rieser U. 2005. OSL age constraints for fluvial aggradation terraces and loess in the eastern North Island, New Zealand, *New Zealand Journal of Geology and Geophysics* **48**: 581-589.

Loget N, Davy P, Van Den Driessche J. 2006. Mesoscale fluvial erosion parameters deduced from modeling the Mediterranean sea level drop during the Messinian (late Miocene). *Journal Geophysical Research* **111**: doi:10.1029/2005JF000387.

Lowe DJ, Newnham RM, Ward CM. 1999. Stratigraphy and chronology of a 15 ka sequence of multi-sourced silicic tephras in a montane peat bog in eastern North Island, New Zealand. *New Zealand Journal of Geology and Geophysics* **42**: 565-579.

M

Marutani T, Kasai M, Reid LM, Trustrum NA. 1999. Influence of storm-related sediment storage on the sediment delivery from tributary catchments in the upper Waipaoa River, New Zealand. *Earth Surface Processes and Landforms* **24**: 881–896.

McArthur JL, Shepherd MJ. 1990. Late Quaternary glaciation of Mt Ruapehu, North Island, New Zealand. *Journal of The Royal Society of New Zealand* **20**: 287-296.

McGlone MS. 2001. A late Quaternary pollen record from marine core P69, southeastern North Island, New Zealand. *New Zealand Journal of Geology and Geophysics* **44**: 69-77.

McGlone MS. 2002. The late Quaternary peat, vegetation and climate history of the Southern Oceanic Islands of New Zealand. *Quaternary Science Reviews* **21**: 683-707.

McGlone MS, Howorth R, Pullar WA. 1984. Late Pleistocene stratigraphy, vegetation and climate of the Bay of Plenty and Gisborne regions, New Zealand. *New Zealand Journal of Geology and Geophysics* **27**: 327-350.

McLea WL. 1990. Palynology of the Pohehe Swamp, northwest Wairarapa, New Zealand: a study of climatic and vegetation changes during the last 41 000 years. *Journal of the Royal Society of New Zealand* **20**: 205-220.

McNeill LC, Piper KA, Goldfinger C, Klum LD, Yeats RS. 1997. Listric normal faulting on the Cascadia continental margin. *Journal of Geophysical Research* **102**: 12,123-12,138.

Métivier F, Gaudemer FY, Tapponnier P, Meyer B. 1998. Northeastward growth of the Tibet plateau deduced from mass balanced reconstruction of two depositional areas: the Qaidan and Hexi Corridor basins, China. *Tectonics,* **17**: 823-842.

Métivier F, Gaudemer Y.1999. Stability of output fluxes of large rivers in South and East Asia during the last 2 million years: implications on floodplain processes. *Basin Research* **11**: 293-303.

Miall AD. 1991. Stratigraphic sequences and their chronostratigraphic correlation. *Journal of Sedimentary Petrology* **61**: 497-505.

Milankovitch MM. 1941. *Kanon der Erdbestrahlung und seine Anwendung auf das Eizeitenproblem*. Serbian Royal Academy Special Edition: Belgrade.

Milliman JD, Syvitski JPM. 1992. Geomorphic/tectonic control on sediment discharge to the ocean: the importance of small mountain rivers. *Journal of Geology* **100**: 524-544.

Milne JDG. 1973a. *Upper Quaternary geology of the Rangitikei Drainage Basin, North Island, New Zealand*. Unpublished PhD thesis, Massey University, Palmerston North.

Milne JDG. 1973b. Map and sections of river terraces in the Rangitikei Basin, North Island, New Zealand. *New Zealand Soil Survey Report* **4**, Department of Scientific and Industrial Research, Wellington, New Zealand.

Mitchum JR, Vail PR, Thompson S. 1977. Seismic Stratigraphy and Global Changes of Sea level, Part 2: The Depositional Sequence as a Basic Unit Stratigraphic Analysis. In *Seismic Stratigraphy – applications to hydrocarbon exploration*, Payton E (Ed). American Association of Petroleum Geologist Memoir **26**: 53-62.

Mitchum JR, Vail PR, Sangree JB. 1977. Seismic Stratigraphy and Global Changes of Sea Level, Part 6: Stratigraphic Interpretation of Seismic Reflection Patterns. In Depositional

Sequences. In *Seismic Stratigraphy – applications to hydrocarbon exploration*, Payton E (Ed). American Association of Petroleum Geologist Memoir **26**: 117-133.

Moberly R, Shepherd GL, Coulbourn WT. 1982. Forearc and other basins, continental margin of northern and southern Peru and adjacent Ecuador and Chile. In *Trench-Forearc Geology*. Leggett JK (ed). Special Publication of the Geological Society **10**: 171-189.

Molnar P. 2001. Climate change, flooding in arid environments, and erosion rates, *Geology*, **29**: 1071-1074.

Molnar P. 2004. Late Cenozoic increase in accumulation rates of terrestial sediment: how might climate change have affected erosion rates? *Annual Review of Earth and Planetary Sciences* **32**: 67-89.

Molnar P, England P. 1990. Late Cenozoic uplift of mountain ranges and global climate change: chicken or egg? *Nature* **346**: 29-34.

Montgomery DR, Brandon MT. 2002. Topographic controls on erosion rates in tectonically active mountain ranges. *Earth and Planetary Science Letters* **201**: 481-489.

Mountney NP, Westbrook GK. 1997. Quantitative analysis of Miocene to Recent forearc basin evolution along the Colombian convergent margin. *Basin Research* **9**: 177-196.

Multiwave. 2005. 05CM 2D Seismic Survey, Offshore East Coast - North Island. New Zealand unpublished openfile petroleum report 3136. Ministry of Economic Development, Wellington.

Murray-Wallace CV. 2007. Sea Level Studies - Eustatic Sea-Level Changes Glacial-Interglacial Cycles. In *Encyclopedia of Quaternary Science*. Elias SA (ed). Elsevier, Amsterdam: 3024-3034.

N

Naish T, Kamp PJJ. 1997. Sequence stratigraphy of the sixth-order (41 k.y.) Pliocene-Pleistocene cyclothems, Wanganui basin, New Zealand: A case for the regressive system tract. *Geological Society of America Bulletin* **109**: 978-999.

Naish T, Abbott ST, Alloway BV, Beu AG, Carter RM, Edwards AR Journeaux TD, Kamp PJJ, Pillans BJ, Saul G, Woolfe KJ. 1998. Astronomical calibration of a southern hemisphere Plio-Pleistocene reference section, Wanganui basin, New Zealand. *Quaternary Science Reviews* **17**: 695-710.

Naish TR, Field BD, Zhu H, Melhuish A, Carter RM, Abbott ST, Edwards S, Alloway BV, Wilson GS, Niessen F, Barker A, Browne GH, Maslen G. 2005. Integrated outcrop, drill core, borehale and seismic stratigraphic architecture of a cyclothemic, shallow-marine depositional system, Wanganui Basin, New Zealand. *Journal of the Royal Society of New Zealand* **35**: 91-122.

Nees S, Jellinek T, Suhohen J, Winkler A, Helmke J, Emmermann P and Shipboard Scientific Party. 1998. Images III—IPHIS. Indian and Pacific Ocean Pleistocene and Holocene History: an images Study. Cruise MD106—Lef 1.2; RV Marion Dufresne II, Hobart (Australia)—Christchurch (New Zealand) May 6 to May 21, 1997.

Nelson CS, Hendy CH, Jarrett GR, Cuthbertson AM. 1985. Near-synchroneity of New Zealand alpine glaciations and Northern Hemisphere continental glaciations during the past 750 kyr. *Nature* **318**: 361-363.

Newnham RM, Lowe DJ, Williams PW. 1999. Quaternary environmental change in New Zealand: a review. *Progress in Physical Geography* **23**: 567-610.

Newnham RM, Lowe DJ. 2000. Fine–resolution pollen record oflate-glacia l climate reversal from New Zealand. *Geology* **28**: 759-762.

Newnham RM, Eden DN, Lowe DJ, Hendy CH. 2003. Rerewhakaaitu Tephra, a land-sea marker for the last termination in New Zealand with implications for global climatic change. *Quaternary Science Reviews* **22**: 289–308.

Nicol A, Wallace LM. 2007. Temporal stability of deformation rates: Comparison of geological and geodetic observations, Hikurangi subduction margin, New Zealand. *Earth and Planetary Science Letters* **258**: 397-413.

Nicol A, Mazengarb C, Chanier F, Rait G, Uruski C, Wallace L. 2007. Tectonic evolution of the Hikurangi subduction margin, New Zealand, since Oligocene. *Tectonics* **26**: doi: 10.1029/2006TC002090.

Norris, JR, Cooper AF. 1997. Erosional control on the structural evolution of a transpressional thrust complex on the Alpine Faults, New Zealand. *Journal of Structural Geology* **19**: 1323–1342.

O

Okamura Y, Blum P. 1993. Seismic stratigraphy of Quaternary stacked progradational sequences in the southwest Japan forearc: an example of fourth-order sequences in an active margin, Sequence Stratigraphy and Facies Associations. *International Association of Sedimentologists, Special Publication* **18**: 213-232.

Okuda M, Shulmeister J, Flenley JR. 2002. Vegetation changes and their climatic implications for the late Pleistocene at Lake Poukawa, Hawkes Bay. *Global and Planetary Change* **33**: 269-282.

Orpin AR, Alexander C, Carter L, Kuehl S, Walsh JP. 2006. Temporal and spatial complexity in post-glacial sedimentation on the tectonically active, Poverty Bay continental margin of New Zealand. *Continental Shelf Research* **26**: 2205-2224.

Ozolins V, Francis D. 2000. Whakatu-1 Well Completion Report PEP 38328– Indo-Pacific Energy (NZ) Ltd: Wellington, Ministry of Economic Development – Crown Minerals, Open-File *Petroleum Report* **2476**: 496 pp.

P

Pantin HM. 1963. Submarine morphology east of North Island, New Zealand. *New Zealand Department of Scientific and Industrial Research Bulletin* **149**: 9-42.

Pantin HM. 1966. Sedimentation in Hawke Bay. *New Zealand Department of Scientific and Industrial Research bulletin* **171**: 70 pp.

Paquet F, Proust J-N, Barnes PM, Pettinga JR. 2008. Late Pleistocene sedimentation in Hawke Bay, New Zealand: new insights into forearc basin morphostructural evolution. Submitted to *Journal of Quaternary Science*.

Pavlis TL, Hamburger W, Pavlis GL. 1997. Erosional processes as a control on the structural evolution of an actively deforming fold and thrust belt; an example from the Pamir–Tien Shan region, Central Asia. *Tectonics* **16** : 810–822.

Payton CE. 1977. *Seismic Stratigraphy – applications to hydrocarbon exploration*. American Association of Petroleum Geologist Memoir **26**: 516 pp.

Pazzaglia FJ, Brandon MT. 1996. Macrogeomorphic evolution of the post-Triassic Appalachian mountains determined by deconvolution of the offshore basin sedimentary record. *Basin Research* **8**: 255-278.

Penck A, Brückner E. 1909. Die Alpen im Eiszeitalter. Tauchnitz, Leipzig.

Perg LA, Anderson RS, Finkel RC. 2001. Use of a new 10Be and 26Al inventory method to date marine terraces, California, USA, *Geology* **29**: 879-882.

Pettinga JR. 1980. Geology and landslides of the eastern Te Aute District, southern Hawke's Bay. *Unpublished PhD thesis*, University of Auckland Library, Auckland, New Zealand.

Pettinga JR. 1982. Upper Cenozoic structural history, coastal southern Hawke's Bay, New Zealand. *New Zealand journal of geology and geophysics* **25**: 149-19 1.

Pettinga JR. 1985. Seismic evidence of the offshore extension of the Kairakau-Waimarama regional slump, Hikurangi

Margin. In *New seismic profiles, cores, and dated rocks from the Hikurangi margin, New Zealand*, Lewis, K.B. (comp) New Zealand Oceanographic Institute field report **22**. Division of Marine and Freshwater Science, Department of Scientific and Industrial Research, Wellington.

Pettinga JR, 2004. Three-stage massive gravitational collapse of the emerging imbricate frontal wedge, Hikurangi Subduction Zone, New Zealand. *New Zealand Journal of Geology & Geophysics* **47**: 399-414.

Phillips JD. 2003. Alluvial storage and the long term stability of sediment yields. *Basin Research* **15**: 153-163.

Phillips JD, Gomez B. 2007. Controls on sediment export from the Waipaoa River basin, New Zealand. *Basin Research* **19**: 241-252.

Pillans B. 1986. A late Quaternary uplift map for North Island, New Zealand. In *Recent crustal movements of the Pacific region*, Reilly, W.l., Harford, B.E. (eds). Royal Society of New Zealand bulletin **24**: 409-417.

Pillans B. 1994. Direct marine–terrestrial correlations, Wanganui Basin, New Zealand: the last 1 million years. *Quaternary Science Reviews* **13**: 189-200.

Pillans B. 2003. Subdividing the Pleistocene using the Matuyama-Brunhes boundary (MBB): An Australasian perspective. Quaternary Science Reviews 22, 1569–1577.

Pillans B. 2007. Quaternary Stratigraphy – Overview. In *Encyclopedia of Quaternary Science*. Elias SA (ed). Elsevier, Amsterdam: 2785-2802.

Pillans B, McGlone M, Palmer A, Mildenhall D, Alloway B, Berger G. 1993. The Last Glacial Maximum in central and southern North Island, New Zealand: a paleoenvironmental reconstruction using Kawakawa Tephra Formation as a chronostratigraphic marker. *Palaeogeography Palaeoclimatology Palaeoecology* **101**: 283-304.

Pinet P, Souriau M. 1988. Continental erosion and large-scale relief. *Tectonics* **7**: 563-582.

Posamentier HW, Jervey MT, Vail PR. 1988. Eustatic controls on clastic deposition I-Conceptual framework. In *Sea-level Changes—an Integrated Approach*, Special Publication 42, Wilgus CK, Hastings BS, Kendall ChStCG, Posamentier HW, Ross CA, Van Wagoner JC (eds). Society Economic Paleontologists Mineralogists: Tulsa, OK; 109-124.

Posamentier HW, Vail PR. 1988. Eustatic controls on clastic deposition II-Sequence and systems tract models. In *Sea-level Changes—an Integrated Approach*, Wilgus CK, Hastings BS, Kendall ChStCG, Posamentier HW, Ross CA, Van Wagoner JC (eds). Special Publication 42, Society Economic Paleontologists Mineralogists: Tulsa, OK; 125-154.

Posamentier HW, Allen GP, James DP, Tesson M. 1992. Forced regressions in a sequence stratigraphic framework: concepts, examples and exploration significance. *American Association of Petroleum Geologists Bulletin* **76**: 1687-1709.

Powell JW. 1875. Exploration of the Colorado River of the west and its tributaries. Government Printing office. Washington DC.

Proust J-N, Chanier F. 2004. The Pleistocene Cape Kidnappers section in New Zealand : orbitally forced controls on active margin sedimentation? *Journal of Quaternary Science* **19**: 591-603.

Proust J-N, Lamarche G, Nodder S, Kamp PJJ. 2005. Sedimentary architecture of a Plio-Pleistocene proto-back-arc basin: Wanganui, New Zealand. *Sedimentary Geology* **181**: 107-145.

Proust J-N, Lamarche G, Migeon S, Neil H, and Shipboard party. 2006. MD152 / MATACORE "Tectonic and climate controls on sediment budget". *Les rapports de campagnes à la mer* : pp. 107.

Pulford A, Stern T. 2004. Pliocene exhumation and landscape evolution of central North Island, New Zealand: the role of the upper mantle. *Journal of Geophysical Research*

(Earth Surface) **109**: F01016 [doi:10.1029/2003JF000046].

R

Ranero CR, von Huene R, Weinrebe W, Reichert C. 2006. Tectonic Processes along the Chile Convergent Margin. In *The Andes – Active subduction orogeny*, Oncken O, Chong G, Franz G, Giese P, Götze H-J, Ramos VA, Strecker MR, Wigger P (eds). Springer-Verlag, Berlin, Heidelberg.

Raub ML. 1985. *The neotectonic evolution of the Wakarara area*, M.Sc. thesis, Auckland Univ., Auckland, New Zealand: pp. 122.

Rea DK. 1993. Geologic Records in Deep Sea Muds. *Geological Society of America Today* **3**: 205-209.

Ridgway NM. 1960. Surface water movements in Hawke Bay, New Zealand. *New Zealand journal of Geology and Geophysics* **3** (2): 253-261.

Ridgway NM. 1962. Nearshore surface currents in southern Hawke Bay, New Zealand. *New Zealand journal of Geology and Geophysics* **5**: 545-66.

Ridgway NM, Stanton BR. 1969. Some hydrological features of Hawke Bay and nearby shelf waters. *New Zealand journal of marine and freshwater research* **3**: 545-559.

Rohais S. 2007. Architecture stratigraphique et flux sédimentaires sur la marge sud du golfe de Corinthe (Grèce): Analyse de terrain, modélisations expérimentales et numériques. Mémoires de thèse - *Mémoires de Géosciences Rennes* **124** : 381 pp.

Rohling EJ, Fenton M, Jorissen FJ, Bertrand P, Gansen G, Caulet JP. 1998. Magnitude of the sea level lowstand of the past 500,000 yr. *Nature* **394**: 162-165.

Roksandi'c M M. 1978. Seismic Facies Analysis Concepts. *Geophysical Prospecting* **26**: 383-398.

S

Sangree JB, Widmier JM. 1977. Seismic Stratigraphy and Global Changes of Sea Level, Part 9: Seismic Interpretation of Clastic Depositional Facies. In *Seismic Stratigraphy – applications to hydrocarbon exploration*, Payton E (Ed). American Association of Petroleum Geologist Memoir **26**: 117-133.

Saul G, Naish TR, Abbot ST, Carter RM.1999. Sedimentary cyclicity in the marine Pliocene-Pleistocene of the Wanganui basin (New Zealand): Sequence stratigraphic motifs characteristic of the past 2.5 m.y. *Geological Society of America Bulletin* **111**: 524-537.

Schlumberger Geco Prakla. 1998. Seismic survey, PEP 38332, Hawkes Bay, IP332-98 lines and IP332-99 lines. *New Zealand unpublished open-file petroleum report* **2392**. Ministry of Economic Development, Wellington.

Schlumberger Geco Prakla. 1998. Hawkes Bay seismic survey, PEP 38328, IP328-98 lines and IP328-99 lines. *New Zealand unpublished open-file petroleum report* **2393**. Ministry of Economic Development, Wellington.

Shackleton NJ, Berger A, Peltier WR. 1990. An alternative astronomical calibration of the lower Pleistocene timescale based on ODP Site 677. *Transactions Royal Society Edinburgh Earth Sciences* **81**: 251–261.

Shackleton NJ, Crowhurst S, Hagelberg T, Pisias N G, Schneider DA. 1995. A new late Neogene time scale: application to Leg 138 sites. In Pisias NG, Mayer LA, Janecek TR, Palmer-Julsen A, van Andel TH (eds). *Proceedings of the Ocean Drilling Program Scientific Results* **138**:73-101.

Shane PAR. 1994. A widespread, early Pleistocene tephra (Potaka tephra, 1 Ma) in New Zealand: Character, distribution, and implications. *New Zealand Journal of Geology and Geophysics* **37**: 25-35.

Shane PAR, Black TM, Alloway BV, Westgate JA 1996. Early to middle Pleistocene tephrochronology of North Island, New Zealand: implications for volcanism,

tectonism, and paleoenvironments. *Geological Society of America Bulletin* **108**: 915–925.

Shane P, Sandiford A. 2003. Paleovegetation of marine isotope stages 4 and 3 in Northern New Zealand and the age of the widespreade Rotoehu tephra. *Quaternary Research* **59**: 420-429.

Sheriff RB. 1980: *Seismic Stratigraphy*. IHRDC, Boston: 227pp.

Shulmeister J, Shane P, Lian OB, Okuda M, Carter JA, Harper M, Dickinson WW, Augustinus P, Heijnis H. 2001. A long late-Quaternary record from Lake Poukawa, Hawkes Bay, New Zealand. *Palaeogeography Palaeoclimatology Palaeoecology* **176**: 81–107.

Shulmeister J, Goodwin I, Renwick J, Harle K, Armand L, McGlone MS, Cook E, Dodson J, Hesse PP, Mayewski P, Curran M. 2004. The Southern Hemispher westerlies in the Australasian sector over the last glacial cycle: a synthesis. *Quaternary International* **118-119**: 23-53.

Shumm SA. 1993. River Response to Baselevel Change: Implications for Sequence Stratigraphy. *The journal of Geology* **101**: 279-294.

Shroder JF Jr, Bishop MP. 2000. Unroofing of the Nanga Parbat Himalaya, In *Tectonics of the Nanga Parbat Syntaxis and the western Himalaya*. Khan MA, et al., (eds). Geological Society of London Special Publication **170**: 163–179.

Smale D, Houghton BF, McKellar IC, Mansergh GD, Moore PR. 1978. Geology and erosion in the Ruahine Range: a reconnaissance study. In *Geology and erosion in the Ruahine Range*, Speden, I. (ed.). *New Zealand Geologicalsurvey report* **G20**: 7-30.

Small M, & others. 1997. Hawkes Bay seismic survey, PEP38328, IP328-97 lines. *New Zealand unpublished open-file petroleum report* **2299**. Ministry of Economic Development, Wellington.

Snyder NP, Whipple KX, Tucker GE, Merritts DJ. 2000. Landscape response to tectonic forcing: Digital elevation model analysis of stream profiles in the Mendocino triple junction region, northern California. *Geological Society of America Bulletin* **112**: 1250-1263.

Soldati M, Corsini A, Pasuto A. 2004. Landslides and climate change in the Italian Dolomites since the late glacial. *Catena* **55**: 141-161.

Sommerfield CK, Wheatcroft RA. 2007. Late Holocene sediment accumulation on the northern Californian shelf: Oceanic, fluvial, and anthropogenic influences. *Geological Society of America Bulletin* doi: 10.1130/B26019.1.

Song TRA, Simons M. 2003. Large trench-parallel gravity variations predict seismogenic behavior in subduction zones. *Science* **301**: 630-633.

Spörli KB, Pettinga JR. 1980. Mount Kahuranaki, Hawkes Bay, New Zealand, A Klippe Emplaced by Gravity sliding from the Crest of the Nearby Elsthorpe Anticline. *Journal of the Royal Society of New Zealand* **10**: 287-307.

Spörli KB, Ballance PF. 1989. Mesozoic-Cenozoic ocean floor-continent interaction and terrane configuration, southwest Pacific area around New Zealand. In. *Mesozoic and Cenozoic evolution of the Pacific Ocean margins*, Ben Avraham Z. (ed.). Oxford University Monograph, geology and geophysics **8**: 176-190.

Stern T, Davey F. 1989. Crustal structure and origin for basins formed behind the Hikurangi subduction zone of New Zealand. In: Price, R.A. (Ed.), *Origin and Evolution of Sedimentary Basins and their Energy and Mineral Resources.* American Geophysical Union Monograph **48**: 73– 86.

Stern TA, Quinlan GM, Holt E. 1992. Basin formation behind an active subduction zone: three-dimensional flexural modelling of Wanganui Basin, New Zealand. *Basin Research* **4**: 197–214.

Strahler AH, Strahler AN. 1992. *Modern physical geography*. John Wiley & Sons, New York, 638 pp.

Strong CP, Scott GH, Edwards AR. 1989. Foraminifera and calcareous nannoplankton from Hawke's Bay sea floor samples PPL 38321 PPL 38322 PPL 38323. New Zealand unpublished openfile *Petroleum Report* **1470**. Ministry of Economic Development, Wellington.

Strong N, Paola C. 2006. Fluvial Landscapes and Stratigraphy in a Flume. *The Sedimentary Record* **4**: 4-8.

Suggate RP. 1961. Rock-strati graphic names for the South Island schists and undifferentiated sediments of the New Zealand geosyncline. *New Zealand Journal of Geology and Geophysics* **4**: 392-399.

Suggate RP. 1990. Late Pliocene and Quaternary glaciations of New Zealand. *Quaternary Science Review* **9**: 175–197.

Sullivan D. 1990. 2D Marine Seismic Survey Acquisition Report PPL 38322, PPL 38321. New Zealand unpublished openfile *Petroleum Report* **1666**. Ministry of Economic Development, Wellington.

Summerfield MA. 1985. Plate tectonics and landscape development on the African continent. In *Tectonics Geomorphology*, Morisawa M, Hack J (Eds). Allen and Unwin, Boston: 27-51.

Summerfild MA. 1991. *Global Geomorphology, Longman Group*, Burnt Mill: 537 pp.

Summerfield MA, Hulton NJ. 1994. Natural controls of fluvial denudation rates in major world drainage basins, *Journal of Geophysical. Research*, **99**: 13,871-13,883.

Syvitski JPM, Shaw J. 1995. Sedimentology and geomorphology of fjords. In *Geomorphology and sedimentology of estuaries*. Perillo GME (ed), Developments in sedimentology **53**. Amsterdam, Elsevier. p. 113–178.

Syvitski JPM, Vörösmarty CJ, Kettner AJ, Green PA. 2005. Impact of humans on the flux of terrestrial sediment to the global coastal ocean. *Science* **308**: 376-380.

Syvitski JPM, Milliman JD. 2007. Geology, Geography, and Humans Battle for Dominance over the Delivery of Fluvial Sediment to the Coastal Ocean. *Journal of Geology* **115**: 1-19.

T

Talling PJ. 1998. How and where do incised valleys form if sea level remains above the shelf edge? *Geology* **26**: 87-90.

Taylor B. 2006. Tne single largest oceanic plateau: Ontong Java-Manihiki-Hikurangi. *Earth and Planetary Science Letters* **241**: 372-380.

Tiedemann R, Sarnthein M, Shackelton NJ. 1994. Astronomical time scale for the Pliocene Atlantic $\delta\ ^{18}O$ and dust flux records of Ocean Drilling Program Site 659. *Paleoceanography* **9**: 619-638.

Tippett JM, Kamp PJJ. 1993. Fission track analysis of the Late Cenozoic vertical kinematics of continental Pacific crust, South Island, New Zealand. *Journal of Geophysical Research* **98**: 16119-16148.

U

Uyeda S, Kanamori H. 1979. Back-arc opening and the mode of subduction. *Journal of Geophysical Research* **84**: 1049-1061.

V

Vail PR, Mitchum JR, Todd RG, Widmier JM, Thompson S, Sangree JB, Bubb JN, Hatlelid WG. 1977. Seismic Stratigraphy and Global Changes of Sea Level. In Depositional Sequences. In *Seismic Stratigraphy – applications to hydrocarbon exploration*, Payton E (Ed). American Association of Petroleum Geologist Memoir **26**: 49-212.

Van der Lingen GJ, Pettinga JR. 1980. The Makara Basin: a Miocene slope-basin along

the New Zealand sector of the Australian-Pacific obliquely convergent plate boundary. In *Sedimentation in oblique strike-slip mobile zones*, Ballance PF, Reading HG (eds). Special publication of the International Association of Sedimentologists: 191-215.

Van Wagoner JC, Posamentier HW, Mitchum RM, Vail PR, Sarg JF, Loutit TS, Hardenbol J, 1988. An overview of fundamentals of sequence stratigraphy and Key definitions. *In Sea-level Changes—an Integrated Approach*, Wilgus CK, Hastings BS, Kendall ChStCG, Posamentier HW, Ross CA, Van Wagoner JC (eds). Special Publication **42**, Society Economic Paleontologists Mineralogists: Tulsa, OK; 39-45.

Van Wagoner JC, Mitchum RM, Campion KM, Rahmanian VD, 1990: Siliciclastic Sequence Stratigraphy in Well Logs, Cores and Outcrops: Concepts for high resolution Correlation of Time and Facies. American Association of Petroleum Geologists Methods in Exploration Series **7**, Tulsa: 55 pp.

von Blanckenburg, 2005von Blanckenburg, F., 2005 The control mechanisms of erosion and weathering at basin scale from cosmogenic nuclides in river sediment, *Earth and Planetary Science Letters* **237** : 462-479.

von Huene R, Arthur MA. 1982. Sedimentation across the Japan Trench off northern Honshu Island. In *Trench-ForearcGeology*. Leggett JK (ed). Geological Society, London, Special Publication **10**: 27-48.

Vörösmarty C, Meybeck M, Fekete B Sharma K, Green P, Syvitski JPM. 2003. Anthropogenic sediment retention: major global-scale impact of registered impoundments. *Global Planetary Change* **39**: 169-190.

Villamor P, Berryman KR. 2001. A late Quaternary extension rate in the Taupo Volcanic Zone, New Zealand, derived from fault slip data. *New Zealand Journal of Geology and Geophysics* **44**: 243–269.

Villamor P, Berryman KR. 2006. Evolution of the southern termination of the Taupo Rift, New Zealand. *New Zealand Journal of Geology and Geophysics* **49**: 23-37.

W

Waelbroeck C, Labeyrie L, Michel E, Duplessy JC, McManus JF, Lambeck K, Balbon E, Labracherie M. 2002. Sea-level and deep water temperature changes derived from benhic foraminifera isotopic records. *Quaternary Science Reviews* **21**: 295-305.

Walcott RI. 1987. Geodetic strain and the deformation history of the North Island of New Zealand during the late Cenozoic. *Philosophical Transaction Royal Society London* **A321**: 163–181.

Walford HL, White NJ, Sydow JC. 2005. solid sediment load history of the Zambezi Delta. *Earth an d Planetary Science Letters* **238**: 49-63.

Wallace LM, Beavan J, McCaffrey R, Darby D. 2004. Subduction zone coupling and tectonic block rotations in the North Island New Zealand. *Journal of Geophysical Research* **109**: doi:10.1029/2004JB003241.

Wegener A. 1912. Die Entstehung der Kontinente. Dr. Petermanns A Mitteilungen aus Justus Perthes' Geographischer Anstalt **58**: 185-195; 253-256; 305-309.

Wheeler HE. 1964. Baselevel, lithostratigraphic surface, and time stratigraphy. *Geological Society of America Bulletin* **75**: 599-610.

WilkinsonBH. 2005. Humans as geologic agents: A deep-time perspective: *Geology* **33**: 161-164.

Wilkinson BH, McElroy BJ. 2007. The impact of humans on continental erosion and sedimentation. *Geological Society of America Bulletin* **119**: 140-156.

Willett S, Beaumont C, Fullsack P. 1993. Mechanical model of doubly vergent compressional orogens, *Geology* **21**: 371-374.

Wood R, Davy B. 1994. The Hikurangi Plateau. *Marine Geology* **118**: 153-173.

Woolfe KJ, Larcombe P, Naish T, Purdon RG. 1998. Lowstand rivers need not incise the shelf: an example from the Great Barrier Reef, Australia, with implications for sequence stratigraphic models. *Geology* **26**: 75–78.

Wright IC, Lewis KB. 1991. Seafloor sampling as a window to deeper structure along offshore accretionary systems: an example from offshore East Coast, North Island, New Zealand. *Proceedings of 1991 New Zealand Oil Exploration Conference* **1**: 101-109.

Wynn RB, Stow DAV, 2002. Classification and characterisation of deep-water sediment waves. *Marine Geology* **192** 7–22.

Z

Zachos J, Pagani M, Sloan L, Thomas E, Billups K. 2001. trends, rhythms and aberrations in global climate 65 Ma to present. *Science* **292**: 686-693.

Zaitlin BA, Dalrymple RW, Boyd R. 1994. The stratigraphic organisation of incised valley systems associated with relative sea-level change. Soc. Econ. Paleont. Miner., Spec. Publ. **51**, 391p.

Zeitler PK, Meltzer AS, Koons PO, Craw D, Hallet B, Chamberlain CP, Kidd WSF, Park SK, Seeber L, Bishop M, Shroder J. 2001. Erosion, Himalayan geodynamics, and the geomorphology of metamorphism. *Geological Society of America Today* **11**: 4-9.

Zhang P, Molnar P, Downs WR. 2001. Increased sedimentation rates and grain sizes 2-4 Myr ago due to the influence of climate change on erosion rates. *Nature* **410**: 891-897.